The Evolution and Population Genetics of Hydrothermal Vent Megafauna from the Scotia Sea

by

Christopher Nicolai Roterman
Somerville College

Thesis submitted in partial fulfilment
of the requirements for the degree of
Doctor of Philosophy

University of Oxford
Department of Zoology

October 2013

OSS Student No. 178674

This thesis is dedicated to
my beloved family and friends

‘Nothing has such power to broaden the mind as the ability to investigate systematically and truly all that comes under thy observation in life’ – Marcus Aurelius

‘There is much pleasure to be gained from useless knowledge’ – Bertrand Russell

‘You can never turn your back on the ocean’ – Rip Torn

‘If in doubt, paddle out’ – Nat Young

Acknowledgements

Firstly and most importantly, I would like to thank Alex Rogers, Jon Copley, Katrin Linse and Paul Tyler for their supervision during my DPhil research.

In particular, I'd like to thank Alex Rogers for his role as my principal supervisor and for ensuring the funding of my project as well as much of the planning. I thank Alex, Jon and Katrin for their unswerving encouragement, both in an academic as well as a personal capacity. Jon took a chance on me in my interview and has been key in helping me communicate my science to a wider audience, whilst Katrin has provided me with crucial insights into marine fieldwork and was indispensable in helping me with the vent limpets. Paul Tyler has been instrumental in inspiring me to pursuing a path in deep-sea biology research and was a beacon of calm and inspiration during the trials and tribulations of the JC055 expedition to the Bransfield Strait, when the ROV *ISIS* was badly damaged. As the principal scientist and architect of the ChEsSO consortium, Paul was the heart and soul of this research program and without him; vents in the Southern Ocean would remain elusive.

Prior to my enrolment as a DPhil student, I owe a debt of gratitude to Dan Jones and Andrew Gates for giving me the chance to perform solo ROV survey work on rigs in the Norwegian Sea and the Faroe-Shetland Channel, which was a huge factor in my getting this DPhil opportunity.

I wish to thank those teachers who saw potential in me in my early life when others did not, in particular David Elleray, my housemaster who gave me the chance for a first-rate education and Michael Thain, my biology teacher who sparked my interest in evolution. He took me under his wing and in his spare time, coached me in philosophy and the arts of critical thinking.

I'm indebted to many of my fellow research colleagues for their input and advice, not least Philipp Boersch-Supan, who is a polymathic font of scientific knowledge, as well as Leigh Marsh and Jeff Hawkes, who have been great fieldwork companions. My fellow colleagues and housemates Michelle Taylor and Tom Hart deserve special mention for effectively being my mentors throughout my DPhil. They both trained me up in the practical skills required for population genetics and phylogenetics despite their busy schedules, but also knew when I needed feeding, cheering up or a shoulder to lean on. Tom deserves special mention, for had he not encouraged me to explore next-generation sequencing methods to speed up the development of microsatellite markers, the scope of my project would have been far narrower. Likewise, had Michelle not encouraged me to contact taxonomists around the world, my chapter on yeti crab evolution might never have got off the drawing board.

Of those taxonomists and other biologists around the world that have helped me, I would like to make special mention of Kareen Schnabel, Shane Ahyong, Enrique Macpherson, Sammy de Grave and Andrew Thurber in particular, not just for generously providing squat lobster tissue when needed, but also for their friendly advice and encouragement.

Most of the material I have been working with was sampled from the deep sea and I would like to pay homage to the professionalism of the maritime crews of the Royal Research Ship *James Cook* and the technical crews of ROV *ISIS* and *KIEL 6000* who worked in the most challenging conditions in the roughest oceanic regions in the world.

My research would not have been possible were it not for the following Natural Environment Research Council (NERC) grants:

1. The ChEsSO (Chemosynthetic Ecosystems of the Southern Oceans) consortium grant, NE/DO1249X/1, which also provided my studentship income.

2. Benthic Biodiversity of Seamounts in the Southwest Indian Ocean grant NE/F005504/1

3. Biogeography and Ecology of the First Known Deep-Sea Hydrothermal Vent Site on the Ultraslow-Spreading Southwest Indian Ridge NE/H012087/1

Lastly and most importantly, I'd like to thank those closest to me for their love, patience and reassurance. My parents, including David and Kerstin, who have supported me in every way possible over the years, kept faith with me after university and were there to help me emotionally and financially when I embarked on my path as a research scientist. Likewise, my brother and sister, who have offered nothing but positivity and encouragement. They have been indispensable in bolstering my confidence during bleak times. I thank my friends the world over, but especially Adriano, who first got me in the water all those years ago and who has been an example to me of how to get the most out of life, as well as Pete and Leiza Bladd-Symms, Bligh Gibson, Olly Toop and Dog Boy for reminding me that there is a life outside science. In addition, I cannot forget my other surfing buddies in the Witterings (and beyond) for getting me out into the waves even when the conditions were rough and unappetising. I always felt better for it. Lastly, I want to thank Vanessa Lovenburg for letting me into her world of hilarity and madness and for being my sanctuary during the most testing of times.

Declaration

I hereby declare that the work presented in this thesis was conducted by myself under the supervision of Professor Alex D. Rogers, as well as Dr Katrin Linse, Dr Jon Copley and Professor Paul Tyler, with the exception of those instances where the contribution of others has been specifically acknowledged. I have clearly indicated the presence of all material and information I have quoted, paraphrased or referenced from other sources, including any diagrams, charts, tables or graphs.

Chapters 2 and 4 are based on published research papers lead authored by myself. The contributions of the co-authors are as follows:

The ChEsSO (Chemosynthetic Ecosystems of the Southern Ocean) consortium program, of which my research is a part, was originally devised by Paul Tyler and the plan for a population genetics study utilizing microsatellite markers was the creation of Alex Rogers. Paul Tyler, Alex Rogers and Jon Copley were responsible for securing the funding for this research. Jon Copley, Katrin Linse and Alex Rogers assisted in the collection and initial preparation of tissue aboard the Royal Research Ship *James Cook* during the expedition JC042 to the Scotia Sea. Katrin Linse facilitated in the procurement of Roche 454 sequences for *Lepetodrilus* sp. and all co-authors contributed to the editing of the paper manuscripts and provided invaluable advice and mentoring in their preparation.

I hereby confirm that this thesis has not been submitted for any other qualification or degree at this university or any other institution.

Christopher Nicolai Roterman

October 2013

OSS Student No. 178674

Abstract

This project used a variety of genetic markers to investigate the evolution and population genetics of hydrothermal vent fauna that were recovered from the Scotia Sea, in the Atlantic sector of the Southern Ocean.

The origins of one of these species, an undescribed species of *Kiwa* sp. found on the East Scotia Ridge (ESR) and its constituent family Kiwaidae, a group of vent and seep-associated decapod squat lobsters (infraorder Anomura) was investigated using a concatenated nine-gene dataset and key divergences were dated using fossil calibrations. These results confirm earlier research showing Kiwaidae reside in the superfamily Chirostyloidea, but form a monophyletic clade with the non-chemosynthetic family Chirostylidae and not Eumunididae. Chirostyloid families diverged in the Cretaceous, although extant Kiwaidae radiated in the Eocene, consistent with many other chemosynthetic taxa that appear recently derived. The basal tree position of Pacific species (and the Alaska location of a likely stem-lineage kiwaid fossil) suggests kiwaids originated in the East Pacific. Within a Southern Hemisphere clade, the divergence between the southeastern Pacific *K. hirsuta* and a non-Pacific lineage (*Kiwa* sp. ESR and Southwest Indian Ridge kiwaids) is no earlier than 25.9 Ma, consistent with a spread from the Pacific into the Scotia Sea and beyond via now-extinct active ridge connections or mediated by a Miocene onset of the Antarctic Circumpolar Current (ACC) through a newly-opened Drake Passage.

This project also investigated the population genetics of three undescribed species found at two vent fields ~ 440 km apart at either end of the ESR: *Kiwa* sp., a peltospirid gastropod and *Lepetodrilus* sp. limpets. Lepetodrilus sp. was also found at the Kemp Caldera, a submerged part of the South Sandwich Islands (SSI). Analyses of cytochrome c oxidase subunit 1 (COI) as well as microsatellite loci developed from Roche 454 sequence libraries revealed no differentiation along the ESR for all three species consistent with panmixia, or the dominance of non-equilibrium processes between vent field colonies within a metapopulation, possibly enhanced further by cold-induced arrested larval development. Despite apparent connectivity along the ESR, both COI and microsatellites revealed differentiation between ESR limpets and Kemp Caldera limpets ~ 95 km to the east, possibly owing to the hydrographic isolation of the caldera. Both COI and microsatellite diversity patterns were consistent with recent (< 1 Ma) demographic expansions for all three species (although the influence of selection sweeps on COI cannot be discounted); a pattern observed worldwide at vent communities and may reflect demographic instability over time as a consequence of the stochastic birth and death of vent colonies within a metapopulation. Different COI bottleneck ages between the three species (excluding the influence of possible selection) as well as the absence of kiwaids and peltospirids at Kemp, have been attributed to differences in life history, in particular larval morphology and presumed dispersal strategy.

These results highlight the role of larval dispersal of vent fauna along active spreading ridges, both in maintaining vent metapopulations across vent colonies prone to stochastic birth and extinction in the short term, but also in the spread of taxa globally and the formation of biogeographic provinces. The likelihood that the three species presented here exist at vents east of the ESR and SSI, prompts further exploration along ridges in the South Atlantic, in order to investigate the effect of the ACC in enhancing gene flow and delineating biogeographic provinces.

List of Tables

List of Figures

CHAPTER 1

Introduction to the Biogeography & Evolution of Hydrothermal Vent Megafauna

1.1 Deep-sea Chemosynthetic Ecosystems

1.1.1 Hydrothermal Vents

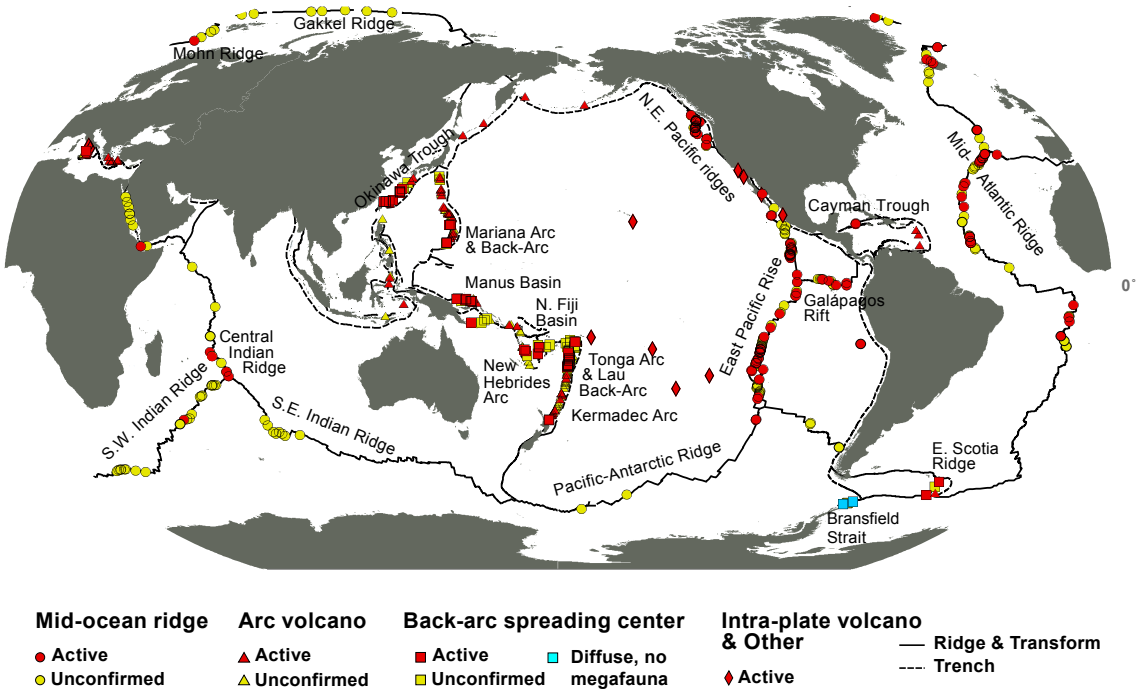

Figure 1.1. Updated version of 2010 InterRidge map produced at the Woods Hole Oceanographic Institute showing the confirmed and unconfirmed location of hydrothermal vents around the world.

1.1.1.1 Early Discoveries in the East Pacific & Atlantic Oceans

In 1976 a series of submersible dives over the Galapagos Rift (GAR), an oceanic spreading ridge in the East Pacific, yielded proof of warm fluid venting from the sea floor. These hydrothermal vents - springs of geothermally heated water - hosted an astonishing biomass of creatures living around the warm (up to 17 ˚C) effluent (Corliss et al. 1979). The deep sea had been generally considered food limited, with only a tiny fraction (< 1%) of the food generated from primary production in surface waters reaching the abyssal plains (Van Dover 2000).

Subsequent exploration suggested that these vents were the product of seawater percolating deep into the ocean crust (generally along the spreading axis of a mid-ocean ridge), which came into close contact with the axial magma chamber. Here, the water reacted with the surrounding rock at temperatures in excess of 350 ˚C (Van Dover 2000), resulting in its enrichment in hydrogen sulphide (H_2S), methane, manganese, iron, barium, zinc and copper and the loss of dissolved oxygen and magnesium. This hot, anoxic, buoyant water then emerged at the sea floor (Van Dover 2000).

These high-biomass communities appeared to be sustained by the primary production of bacteria that oxidised H_2S emanating from the vent fluid to fix carbon from carbon dioxide (CO_2) dissolved in ambient seawater (Jannasch and Wirsen 1979; Karl et al. 1980). Subsequent analyses of the siboglinid vestimentiferan tubeworm *Riftia pachyptila* (Fig. 1.2A) and the giant vesicomyid clam *Clayptogena magnifica* revealed that these animals lacked functional guts and housed chemosynthetic bacteria internally, indicative of a possible symbiotic relationship (Jones 1980; Felbeck 1981; Rau 1981; Cavanaugh 1983; Terwilliger et al. 1983; Stahl et al. 1984).

After this initial discovery, vents were subsequently found on the adjacent East Pacific Rise (EPR) (Spiess et al. 1980; Hekinian et al. 1983; Lonsdale and Becker 1985; Renard et al. 1985), which hosted similar fauna dominated by vestimentiferan tubeworms (either *Riftia pachyptila, Tevnia jerichonana* or *Oasisia alvinae*), the alvinellid polychaete, *Alvinella pompejana*, giant vesicomyid clams of the *Calyptogena* genus and large bathymodiolid mussels, (*Bathymodiolus thermophilus*). These vents typically boasted tall (> 5 m), columnar, black or white ‘smoker’ sulphide chimneys. The black ‘smoke’ consisted of metallic sulphides precipitating out of solution as the ~ 380 ˚C vent effluent rapidly cooled in contact with ambient seawater. White smoker chimneys indicated a cooler vent fluid (100-300 ˚C) where silica, anhydrite and barite precipitated as white particles. These chimneys, characteristic of many hydrothermal vents,

were the product of the deposition of those precipitates (Van Dover 2000).

The first vents to be discovered on ridges not contiguous with the EPR were those in the Northeastern Pacific. Communities on the Juan de Fuca Ridge were superficially similar to those at the EPR and the GAR (Normark et al. 1982; Normark et al. 1983; Tunnicliffe et al. 1986) with tubeworms and alvinellid polychaetes visually dominant, but with different genera (*Ridgeia* and *Paralvinella* respectively). *Calyptogena* clams were present, but mussels absent (Van Dover 2000). Further discoveries on the Explorer and Gorda Ridges revealed similar communities (Tunnicliffe et al. 1986; Rona et al. 1990; Desbruyeres and Segonzac 1997; Johnson et al. 2006).

Beyond the Pacific, the first vents on the slow-spreading (10-50 mm yr. $^{-1}$; Van Dover 2000) Mid-Atlantic Ridge (MAR) were discovered in 1985, (TAG site; Rona et al. 1986). Here and at other similar sites, dense swarms of alvinocaridid shrimp consisting of two species *Rimicaris exoculata* and *Chorocaris chacei* (Williams and Rona 1986) visually dominated. Tubeworms and clams were absent (although, *Ectenagena* spp. clams have since been found at the Logachev site (Gebruk et al. 1997; Gebruk et al. 2000). Bathymodiolid mussels were present as in the Pacific, although different species (Van Dover 2000).

1.1.1.2 Beyond the East Pacific & Atlantic

Since these initial discoveries in the late 1970s and 1980s, there has been a remarkable expansion of vent exploration globally resulting in a vast improvement in our knowledge of the biogeography of vent-endemic fauna. Below, the major vent sites and regions discovered beyond the tropical East Pacific and Atlantic, have been summarised.

Caribbean & Arctic

The deepest vents yet found (4,960 m depth), populated by a new species of alvinocaridid shrimp *Rimicaris hybisae* (Nye et al. 2012) have been recently found on the mid-Cayman spreading centre (Fig. 1.2B), a 110 km-long ultra-slow spreading ridge within the Cayman Trough (Connelly et al. 2012). The communities are similar to those in the Atlantic, which is perhaps unsurprising given the proximity of these two waters. In contrast, despite being connected to the North Atlantic, vents in the Arctic on the Mohn and Knipovich ridges (71˚ N and 73˚ N respectively) (Pedersen et al. 2010; Schander et al. 2010) bear no resemblance to those communities, being dominated by rissoid gastropods, a moniliferan siboglinid polychaete worm, *Sclerolinum contortum*, a new genus of amphipod and a polychaete of the *Nicomache* genus, *N. lokii* (Kongsrud and Rapp 2012).

West & South Pacific

Exploration of the western Pacific has yielded a host of vents in a series of isolated back-arc spreading centres. The Manus, Fiji and Lau back-arc basins (Galkin 1992; Desbruyeres et al. 1994; Desbruyeres 2006) are dominated by gastropods, (e.g., *Ifremeria nautilei*) stalked neolepadine barnacles (*Volcanolepas* sp.; Perez-Losada et al. 2008) (Fig. 1.2D), bathymodiolid mussels and vesicomyid tubeworms. The alvinocaridid shrimp, *Chorocaris vandoverae* has also been found at the nearby Mariana Trough (Hessler and Lonsdale 1991; Van Dover 2000). Within the last decade, stalked barnacles, mussels and alvinocaridid shrimp have been found on the Brothers Seamount near New Zealand (Buckeridge 2000; Von Cosel and Marshall 2003; Webber 2004; Perez-Losada et al. 2008; Ahyong 2009).

Vents explored on the Pacific-Antarctic Ridge (P-AR) south of Easter Island are the most southerly yet reported (38˚ S) in the Pacific (Macpherson et al. 2005; Southward 2005). Here, the stalked barnacle, *Volcanolepas parensis* (Southward 2005) dominates (no tubeworms), as well as buccinid gastropods and a new species (and family) of anomuran crab, *Kiwa hirsuta* (Kiwaidae) known as the "yeti crab" (Macpherson et al. 2005).

Indian Ocean

Since 2000, vents have been surveyed on the Central Indian Ridge (CIR) and the Southwest Indian Ridge (SWIR) (Hashimoto et al. 2001; Copley 2011; Nakamura et al. 2012). They host a new species of *Rimicaris* shrimp; *R. kairei* (Hashimoto et al. 2001; Van Dover et al. 2001; Watanabe and Hashimoto 2002) as well as neolepadine stalked barnacles, bathymodiolid mussels and gastropods (including one sporting iron scales; Yao et al. 2010). Although similar in many ways to the CIR, the SWIR differs slightly in also hosting yeti crabs and a large, distinctive smooth-shelled peltospiroid gastropod (Fig. 1.2C).

Southern Ocean

Vents in the Southern Ocean have only recently been investigated with communities discovered in the Scotia Sea. Vents on the East Scotia Ridge, an isolated back-arc spreading system, house yeti crabs, neolepadine barnacles, peltospiroid gastropods and *Lepetodrilus* limpets, but no vestimentiferan tubeworms, vesicomyid clams, bathymodiolid mussels, or alvinocaridid shrimps (Rogers et al. 2012). Another site nearby within a submerged caldera, adjacent to the Kemp Seamount, lacks yeti crabs and peltospiroid gastropods and is dominated by pycnogonid sea spiders, *Pyropelta* gastropods, vesicomyid clams and the same species of *Lepetodrilus* limpets as those on the ESR limpets (Katrin Linse manuscript in preparation). The new research presented here in this thesis is the product of these discoveries in the Scotia Sea, part of the

ChEsSO (Chemosynthetic Ecosystems of the Southern Ocean) consortium. More details relating to these discoveries will follow at the end of this chapter.

1.1.1.3 Summary

As this section summarising the discovery of vent communities worldwide makes clear, the vast majority of these discoveries have been in tropical, equatorial regions. Only the recent discoveries in the Arctic and the Scotia Sea have extended exploration to high latitudes, although the Scotia Sea discoveries represent only a tiny fraction of the ridges likely to host vent communities in the Southern Ocean (sections of the southern MAR, the American-Antarctic Ridge, the SWIR, the P-AR). Other regions also remain unexplored, such as the Chile Rise and the Southeast Indian Ridge and the discovery of communities at all these areas, as well as on seamounts will be crucial understanding the global biogeography of vent communities (see section 1.3).

1.1.2 Cognate Ecosystems

Whilst the emphasis of this thesis is on hydrothermal vent biogeography and connectivity, it is necessary to briefly introduce other cognate ecosystems that support similar taxa with close evolutionary ties.

The fauna found at hydrocarbon seeps are remarkably similar to those at vents, at least at the level of genus and family. Vestimentiferan tubeworms (*Lamellibrachia* spp.) vesicomyid clams and bathymodiolid mussels are commonly present, where water enriched in methane and other hydrocarbons seeps out on, or at the base of continental slopes at ambient or close to ambient temperatures (Van Dover 2000). Broadly speaking, this water is the product of percolation

through organic-rich sediments where methane is produced by anaerobic bacterial degradation. The methane in the water drives the microbial reduction of sulphate from seawater to form sulphides (Paull et al. 1985; Chanton et al. 1991; Martens et al. 1991), which support the bacterial communities on which the megafauna depend. Seeps have been found worldwide, both on passive continental margins (e.g., Brooks et al. 1984; Paull et al. 1995; Cordes et al. 2007; Levin et al. 2009) as well as on active margins (e.g., Suess et al. 1985; Hashimoto et al. 1995; Sibuet and Olu 1998; Sellanes et al. 2008; Baco et al. 2010; Levin et al. 2012).

Chemosynthetic bacteria-harbouring vesicomyid clams, mytilid mussels and gastropods have also been found thriving on the oil-rich bones of whale carcasses (Smith and Kukert 1989). H_2S is generated from the anaerobic breakdown of lipids in the bone, which in turn is utilised by the chemosynthetic bacteria (Smith and Baco 2003). Whale falls have been found in the Pacific (Naganuma et al. 1996; Smith and Baco 1998), the Southern Ocean (Amon et al. 2013) and the North Sea (Glover et al. 2005) or experimentally sunk, e.g. off California (Smith et al. 2002). Recently a new genus of siboglinid worm, *Osedax* was discovered (Rouse et al. 2004) embedded in whale bones, which uses root-like structures housing heterotrophic bacteria, which aerobically break down the bone lipids (Goffredi et al. 2005). Since this initial discovery, *Osedax* has been found on whalebones in the Atlantic, the Pacific and the Southern Ocean (Vrijenhoek et al. 2009; Amon et al. 2013).

Despite the similarities in community assemblage between vents, seeps and organic falls (e.g., whale carcasses), there are few cases of species overlap. The tubeworm *Escarpia spicata* has been found at seeps and whale falls off southern California as well as hydrothermal vents in the Guaymas basin (Olu et al. 2010) although this may be due to the proximity of these ecosystems and the fact that the Guaymas vents are found in a seep-like sedimented setting. The lack of species overlap may be due differences in setting: most vents fields tend to be surrounded by basalt rock and vent animals must often tolerate rapid temperature fluctuations. Vents have

generally been found on mid-ocean ridges and seamounts and therefore may also be relatively isolated from continental slopes where seep communities tend to be found (Van Dover 2000).

Seeps are generally considered to be very long-lived and stable compared to vent sites (Vrijenhoek 2010): it is estimated that some seep areas have been active for at least a thousand years and perhaps throughout the Pleistocene (Powell et al. 1998). The longevity of vents on mid-ocean ridges appears determined by ridge spreading rates, with short-lived vents (~ decades) found on fast-spreading ridges, e.g., the EPR and vent fields on slow-spreading ridges lasting much longer (thousands of years) e.g. the MAR, although vent activity at long-lived sites may fluctuate with dormant episodes (Lalou et al. 1993; Van Dover 2000). Vents are also vulnerable to eruptive episodes that can wipe out whole communities in an instant (Haymon et al. 1993). The presumed stability of seep communities in comparison to vent habitats has led to the idea that seeps may have been the evolutionary 'launch pad' for (possibly multiple) radiations into vent habitats (Hecker 1985) (to be examined in the following section). This idea may also account for the fact that compared to vent communities globally, seep communities appear largely the same around the world (similar genera), perhaps suggesting that these communities are more stable and less prone to extinctions, therefore providing sufficient time for the same groups to spread around the world.

The similarity of whale-fall fauna to vent and seep fauna, along with the estimated prevalence of whale carcasses on the seafloor (12-30 km nearest neighbour distances; Smith and Baco 2003) prompted Smith et al. (1989) to suggest that whale falls may provide dispersal stepping stones for vent/seep fauna throughout the oceans; supported by the discovery of clams on whale falls that are commonly found at vents (Baco et al. 1999) in the East Pacific. However, apart from that instance, evidence is generally lacking for this theory.

1.2 Origins

1.2.1 Ancient or Recent?

The discovery of 'primitive' fauna at vents, such as the neolepadine stalked barnacles (Newman 1979) as well as fossils resembling tubeworms, bivalves and gastropods in sulphide Silurian deposits (roughly 430 Ma) (Campbell 2006) led to the hypothesis that modern vent and seep fauna are 'living fossils' (Newman 1985; Tunnicliffe 1992; Tunnicliffe and Fowler 1996). A food source uncoupled from photosynthetic production could have protected these animals from extinction events affecting other marine animals. The alternative hypothesis is that chemosynthetically associated metazoans are not invulnerable to extinctions (e.g., anoxic episodes in the deep sea) that have affected other metazoans (Rogers 2000; Vrijenhoek 2013), with taxa repeatedly radiating into these habitats after extinction events. Analogous morphology similar to that of fossils arises owing to the unique selection pressures of these environments (Hickman 1984; Little et al. 1998; Little and Vrijenhoek 2003; Kiel and Dando 2009; Vrijenhoek 2013). Molecular phylogenetic work in recent years has contributed hugely to the antiquity debate, as well as helping to infer how taxa became vent-endemic.

1.2.1.1 Inferences from Molecular Phylogenetic Tree Topologies

Phylogenetic analyses of chemosynthetic habitat-associated siboglinid worms using 28S ribosomal rRNA and cytochrome oxidase c subunit I (COI) genes, indicates that seep vestimentiferan tubeworms are basal to a vent clade (Williams et al. 1993; Black et al. 1998). This is the best evidence yet consistent with a seep-to-vent evolutionary progression (Hecker 1985). A similar but weaker pattern has been found with vesicomyid clams, using only COI

(Peek et al. 1997; Decker et al. 2012). An early 18S rRNA phylogeny of bathymodioline mussels indicated that vent taxa were the most derived (Distel et al. 2000), but more recent analyses with more species and genes indicate that some seep, and organic fall clades are derived rather than basal (Jones et al. 2006; Samadi et al. 2007; Lorion et al. 2010). The tree topology of neolepadine barnacles, based on 18S, 28S and H3 (Histone 3) indicates that the seep-endemic *Ashinkailepas seepiophila* splits basally with a vent clade (Perez-Losada et al. 2008), consistent with this hypothesis, although this phylogeny only included a few chemosynthetic species. In contrast, a COI phylogeny of alvinocaridid shrimps shows no clear geographic or habitat pattern at all (Shank et al. 1999).

1.2.1.2 Divergence Date Estimates

The reliability of divergence date estimates are dependent on whether or not there is a good fossil record for calibration, how many genes are used in the phylogeny or whether realistic substitution rates for key genes can be found. A complication with using substitution rates (often estimated from the divergence of geminate species by a dated vicariance event; Lessios 2008) is that some fast-evolving genes may be ineffective in estimating the date of old divergences owing to the saturation of synonymous substitutions resulting in a gross underestimation of the true divergence date (Vrijenhoek 2013). Ideally therefore, multiple gene datasets should be cross-referenced for accuracy. Nevertheless, despite these potential pitfalls, attempts to estimate the radiation of extant crown taxa have resulted in a relatively consistent picture across the board.

Dates for the last common ancestor of vent and seep endemic vestimentiferan tubeworms are 50-126 Ma based on COI and 18S substitution rates (Black et al. 1998; Halanych et al. 1998; Chevaldonne et al. 2002; Hurtado 2002; Vrijenhoek 2013). These ages seem to rule out the

likelihood that Palaeozoic tube-like fossils are vestimentifera (Little and Vrijenhoek 2003; Kiel and Dando 2009). Vesicomyid clams radiated 21-43 Ma (COI rates) (Peek et al. 1997), in agreement with the oldest uncontroversial vesicomyid fossil (*Calyptogena chinookensis* 45 Ma) (Vrijenhoek 2013). Likewise, bathymodiolines split from non-chemosynthetic taxa 20-94 Ma (18S rates) (Distel et al. 2000; Little and Vrijenhoek 2003), again consistent with the Cenozoic appearance of bathymodiolines in the fossil record (Campbell 2006).

Neomphaline and lepetodrillid gastropods, found exclusively at deep-sea chemosynthetic sites suggests they radiated ~ 59 Ma and 54 Ma respectively (conservative COI rates) (Vrijenhoek 2013) and analyses of seven genes indicates that abyssocryssoids gastropods radiated in the mid-to-late Cretaceous (Johnson et al. 2010), although the fossil record appears to extend further back to the late Jurassic (Kaim and Kelly 2009).

Vent and seep crustaceans also appear recently derived. Alvinocaridid shrimp radiated 20-49 Ma (COI rates) (Shank et al. 1999; Vrijenhoek 2013) and bythograeid crabs, no earlier than 49 Ma (Vrijenhoek 2013). Fossil calibrations indicate that neolepadine and neoverrucid stalked barnacles date to the early Cretaceous and Cenozoic respectively (Perez-Losada et al. 2008).

1.2.2 Conclusions

Close examination of the fossil record and recent phylogenetic analyses of vent/seep fauna appears to challenge Newman's (1985) "Refugia" hypothesis: whilst there are Palaeozoic and early Mesozoic fossils resembling modern fauna, molecular phylogenetic analyses suggests that crown taxa of extant fauna date from the Cretaceous onwards, with the majority dating to the Cenozoic.

In three cases there is some molecular evidence consistent with a possible evolution from seeps to vents (vestimentiferan tubeworms, vesicomyid clams and neolepadine barnacles) and some fossil evidence also indicates a greater antiquity for seep fauna over vent fauna (Kiel and Little 2006; Schweitzer and Feldmann 2008). However, more thorough phylogenies will be needed to see if the seep-to-vent hypothesis stands across a range of taxa.

Given the recent origins of vent and seep, it seems likely that these environments are not immune from global and regional extinction events. Vrijenhoek (2013) suggests, given the radiation of many taxa from the Eocene onwards that anoxic/suboxic events in the deep sea during the Palaeocene-Eocene Thermal Maximum (PETM) wiped out much of the earlier diversity, paving the way for radiations (or re-radiations), an idea promulgated for the deep-sea fauna in general in earlier publications (e.g. Rogers, 2000). Whether or not this was the case, the idea that chemosynthetic fauna diversity may be ancient now appears untenable.

1.3 Vent Biogeography

As the first section of this literature review revealed, hydrothermal vent communities are regionally distinct. Vents in the tropical East Pacific, for example are visually dominated by vestimentiferan tubeworms, alvinellid polychaete worms, bathymodiolid mussels and vesicomyid clams, whereas alvinocaridid shrimp dominate in place of tubeworms in much of the Atlantic. Different regions with similar taxa and community structure have therefore been designated as biogeographic provinces.

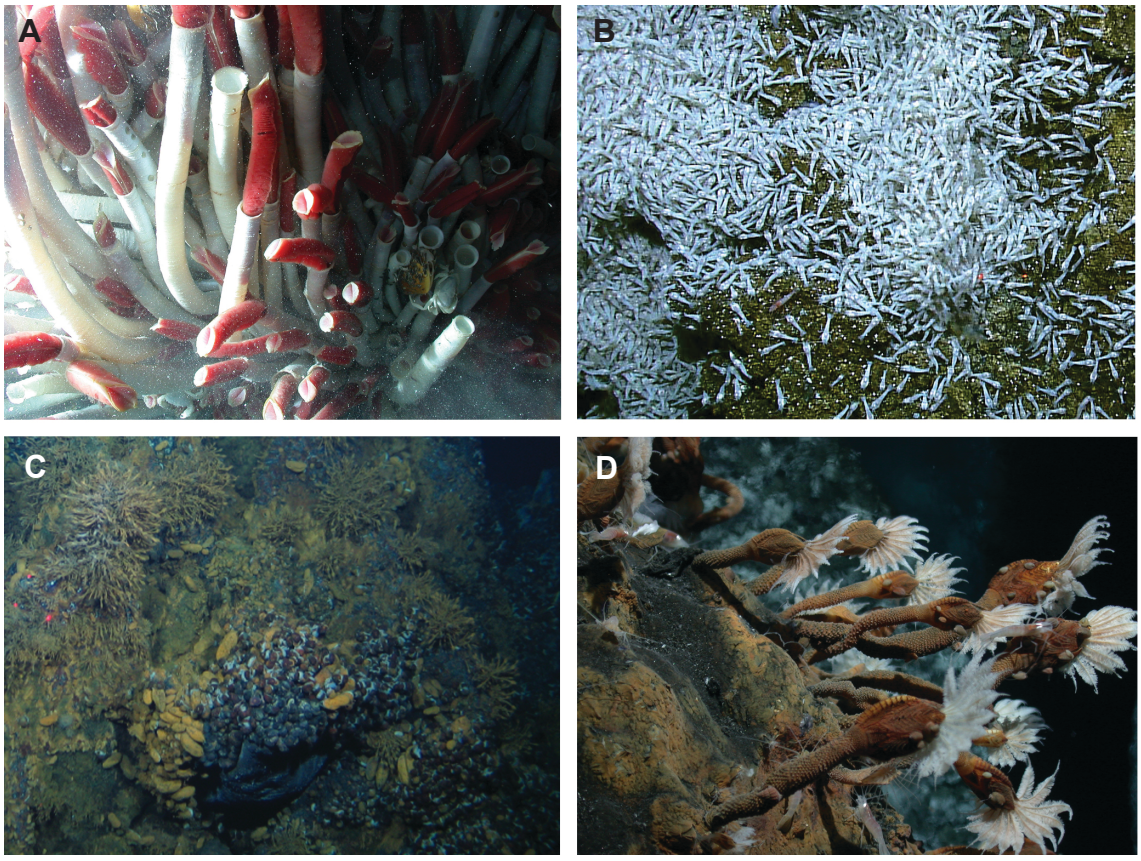

Figure 1.2. Photographs of dominant vent fauna in different regions: Giant tubeworms, which are dominant in the tropical East Pacific (A), *Rimicaris* shrimp, which are numerically dominant in the Atlantic (B), aggregations of gastropods, molluscs and stalked barnacles, typical of vents in the Indian Ocean (C) and dense stands of stalked barnacles, which are commonly found at vents in the SW Pacific (D). Photos courtesy of Vicki Ferrini (A), the National Oceanographic and Atmospheric Administration (B), JC 67 cruise using ROV *ISIS* (Copley 2011) and Charles Fisher (D).

Depending on the author cited, the number and delineation of these provinces varies (Tunnicliffe 1991; Tunnicliffe and Fowler 1996; Tunnicliffe et al. 1998; Van Dover 2000; Van Dover et al. 2002; Ramirez-Llodra et al. 2007; Bachraty et al. 2009; Rogers et al. 2012). Some have designated the entire EPR and GAR as a single province (Van Dover et al. 2002; Ramirez-Llodra et al. 2007), whereas others have separated the northern and southern EPR around the equator (Bachraty et al. 2009; Rogers et al. 2012) (Fig. 1.3). Some refer to a single West Pacific province (Tunnicliffe 1991; Tunnicliffe and Fowler 1996; Tunnicliffe et al. 1998; Van Dover 2000; Van Dover et al. 2002; Ramirez-Llodra et al. 2007) whereas Bachraty et al. (2009) separates it into a northern and southern province, with the Indian Ocean vent sites as part of a southwest Pacific province. Rogers et al. (2012) suggested that the West Pacific could be split into four provinces (Fig. 1.3B). Van Dover et al. (2002) and others (Tyler et al. 2002; Ramirez-Llodra et al. 2007) refer to two Atlantic provinces; a shallow Azores (Lucky Strike and Menez Gwen) and a deep Atlantic, but others do not (Desbruyeres 2006; Bachraty et al. 2009; Rogers et al. 2012). None have included the Arctic communities yet, although these communities are entirely different from vents found elsewhere. The causes for the discrepancies in province delineation, examined below, reveal some of the inherent pitfalls with the creation of boundaries that may in fact be artificial.

Firstly, the dispersal capabilities of vent taxa vary considerably (Tyler and Young 2003) and there is no reason to assume that geographical ranges across taxa should be similar. A hydrographic or topographic feature may be a dispersal filter for some but not other species, as is the case across the Equator and Easter Microplate on the EPR (Hurtado et al. 2004; Plouviez et al. 2009; Plouviez et al. 2010). Therefore, there may be no clear delineation between provinces. But for the conspicuous presence of *Rimicaris* on the CIR, many Indian Ocean taxa appear West Pacific in provenance. A qualitative approach may therefore assign these vents to their own province (Van Dover et al. 2002), whilst a quantitative approach may not (Bachraty et al. 2009).

Secondly, these methods are only as effective as the present extent of vent discovery: aside from the relatively isolated ESR (Rogers et al. 2012) nothing is yet published of the vents in the Southern Ocean, or of high latitude vent communities in the South Atlantic, the Chile Rise or the P-AR. It may be that the distinction between the western and eastern Pacific fauna will become less obvious with greater exploration of the South Pacific. Recently, the EPR has been separated into a northern and southern province (NEPR and SEPR), separated by the equator (Bachraty et al. 2009; Rogers et al. 2012), but a different analysis of vent-species lists along the East Pacific Rise, suggests that the southern part of the SEPR represents a transition zone between the NEPR, the P-AR and the back-arc systems of the West Pacific (Matabos et al. 2011).

Thirdly, systematic methods for site comparison have compared lists of vent 'endemic' species (Desbruyeres 2006; Bachraty et al. 2009; Rogers et al. 2012), but, the status of many species described as such may reflect the disproportionately large sampling effort at vents compared to the vast oceanic abyssal plains. Rogers et al. (2012) suggest that using species and rank abundance may go some way to minimising this shortcoming. Furthermore, other factors thought to influence biogeography of hydrothermal vent fauna, e.g., depth, current strength/direction and ridge topography have not been included in these analyses. It remains to be seen if such a quantitative approach can be useful without finding a way to incorporate these variables, which are implicitly considered in qualitative analyses.

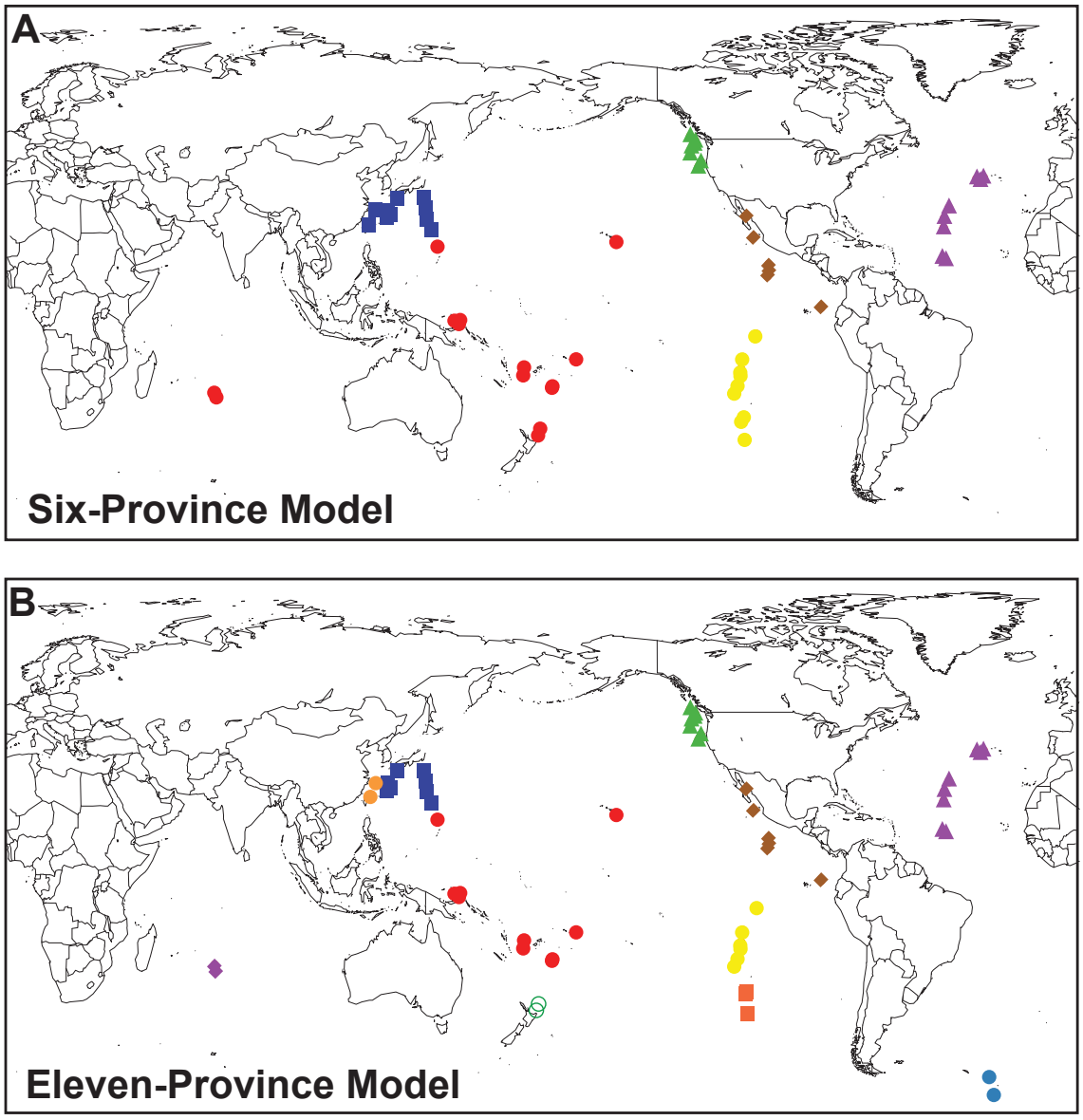

Figure 1.3. Results of geographically constrained clustering using multivariate regression trees modified from two different analyses: a six-province model produced by Bachraty et al. (2009) and an eleven-province model produced by Rogers et al. (2012) after the discovery of vents on the East Scotia Ridge.

1.3.1 Understanding Vent Biogeography

The discovery of similar, yet distinct vent communities between the Northeast Pacific ridges and the EPR and GAR has led Verena Tunnicliffe and others to propose these differences can be accounted for by ridge evolution throughout the Cenozoic: the Pacific-Farallon Ridge began to be subducted under the N. American plate ~ 28 Ma, cutting off the Northern portion, which

became the Northeast Pacific ridges, from the southern portion, which became the EPR and GAR (Tunnicliffe 1991; Tunnicliffe and Fowler 1996; Fowler and Tunnicliffe 1997; Tunnicliffe et al. 1998) (Fig. 1.4) and a Mantel test of matrix comparison of species lists at vents in the East Pacific shows vent fauna are more closely related to each other by along-ridge distance, rather than the shortest seafloor distance.

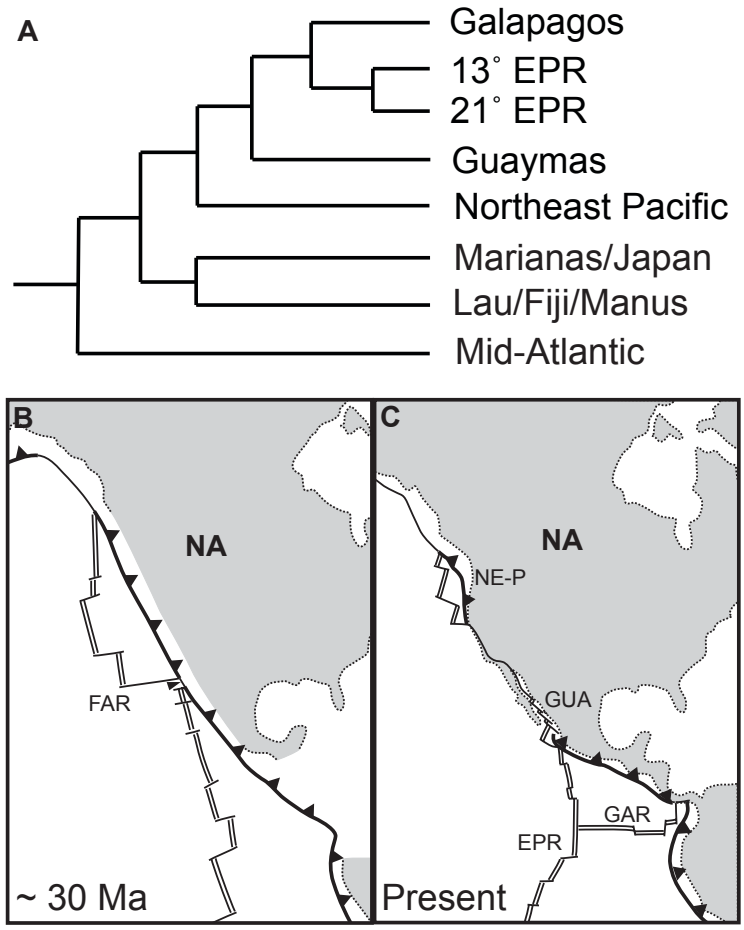

Figure 1.4. Cladogram modified from Tunnicliffe & Fowler (1996) showing species similarity across different ridges (A), with a simplified schematic from Schellart et al. (2010) showing the subduction of the Pacific-Farallon ridge (PAC-FAR) under the North American Plate (NA) within the last ~ 30 million years (B – C) separating the tropical East Pacific ridges (East Pacific Rise = EPR, Galapagos Rift = GAR, Guaymas Basin = GUA) from the Northeast Pacific Ridges (NE-P). Grey indicates continental plate, double lines are spreading ridges and thick lines with triangles indicate subduction zones.

Tunnicliffe and Fowler have made three key predictions relating to this theory (Tunnicliffe and Fowler 1996; Fowler and Tunnicliffe 1997):

1. The South Atlantic vent fauna will be much like the North Atlantic vent fauna, given the continuous ridge connection.
2. An examination of the Southern Ocean would reveal whether there had been Cenozoic flow of Pacific vent fauna since the opening of the Drake Passage.
3. The Indian Ocean vents should exhibit a mixture of Pacific and Atlantic vent fauna mediated by a ridge system that connects the southern Atlantic to the Indian Ocean and then into the Pacific.

The lack of exploration of southern Atlantic vents on the MAR means the first prediction has yet to be addressed. However, the recent exploration of the ESR in the Atlantic sector of the Southern Ocean (Rogers et al. 2012) revealed a community in which three of the dominant undescribed species (*Kiwa* sp., *Vulcanolepas* sp. and a peltospirid gastropod) appear to have a Pacific affinity, consistent with the second prediction. The third prediction has been addressed with the discovery of vents in the Indian Ocean (Hashimoto et al. 2001; Van Dover et al. 2001) showing a mix of Pacific and Atlantic fauna.

Tunnicliffe's vicariance hypothesis has been challenged, however. Shank et al. (1999) estimated that alvinocaridids radiated < 20 Ma with a worldwide distribution of *Alvinocaris*, when most ridges were as they are today. In the case of mussels, the genus *Bathymodiolus* is distributed worldwide on seeps and vents suggesting that their apparent high dispersal capability 'swamps' the imprint of vicariant events in their distribution globally (Tyler et al. 2002).

More recently it has been suggested that other factors, such as larval dispersal modes in different taxa, the present and past pattern of ocean currents, depth and temperatures must also

be important in shaping the present distribution of vent and seep fauna (Tyler et al. 2002; Van Dover et al. 2002; Tyler and Young 2003). Van Dover et al. (2002) suggested that if there is a similarity in fauna between the EPR, the ESR and southern reaches of the MAR, then it could suggest that the flow of the Antarctic Circumpolar Current in the Southern Ocean may be more important than vicariance along ridges in this region, although a similarity between EPR and ESR fauna could also be explained by the past connection of ridges through the Drake Passage (Breitsprecher and Thorkelson 2009). The investigation of the southern reaches of the MAR may resolve this in the future. Regardless, the fact that the Southern Ocean directly connects into three other oceans necessitates the prioritisation of exploration in this part of the world.

Recently, mesoscale eddies have been mooted as a mechanism for transporting larvae over large distances from vents on the EPR (Adams et al. 2011). To date, no vent bathymodiolines have been found at latitudes greater than 38˚ and this pattern may be the product of historical vicariance or there may be a latitudinal limit to these mussels owing to their planktotrophic mode of larval dispersal. This was suggested by Rogers et al. (2012) where it was noted that the Southern Ocean in general has a dearth of planktotrophic larvae, perhaps owing to the environmental conditions and extreme seasonality characteristic of high latitudes (Pearse et al. 1991).

1.3.2 Dispersal & Connectivity at Vents

Research into aspects of life history may be equally important in making sense of vent biogeography around the world. Larval dispersal of vent fauna is ultimately dependent on several factors that researchers have attempted to understand, both biotic (metabolic capacity, larval anatomy, buoyancy, behaviour and mortality rate) and abiotic (deep-water currents, topographical barriers, distance between sites and suitability of habitat) (Ramirez-Llodra et al. 2007). Much of the research into dispersal capability has been conducted by the capture of

larvae in the field, experimenting on larvae in the laboratory or assessing gene flow between populations using molecular tools or by simulating dispersal using computer modelling.

1.3.2.1 Modes of Dispersal

Perhaps surprisingly, given the dispersal challenges facing vent fauna, their modes of reproduction and dispersal generally exhibit taxonomic constraint (Tyler and Young 1999). Contrary to initial expectations, the majority of vent larvae captured in pumps around vents, or cultured in the laboratory, are lecithotrophic (non-feeding with a yolk sac), with the exception of bathymodiolines mussels and alvinocaridid shrimps which may produce planktotrophic larvae, (Copley et al. 1998; Allen et al. 2001; Tyler and Young 2003). Planktotrophy is considered an optimal strategy for long-distance dispersal in deep-sea fauna as feeding larvae can travel large distances sustained by plankton in the photic zone (Gage and Tyler 1992). The prevalence of lecithotrophy in vent fauna is odds with this presumption (Tyler and Young 1999). However, bottom currents can often be rectified by mid-ocean ridge topography (Vrijenhoek 2010) and a dispersal strategy that ensures larvae are retained close to the sea floor could enhance connectivity along the ridge axis, especially when surface currents do not align with the ridge (Vrijenhoek 2010). Tyler and Young (1999) also mention that many mid-ocean ridges are found in oligotrophic regions of the world's oceans, where the production of planktotrophy could be disadvantageous if sustenance in the photic zone is lacking.

Lecithotrophy

The morphology of lecithotrophic vent larvae and their eggs is variable, with some fauna producing relatively small eggs (~ 100 μm wide) with neutrally buoyant larvae, e.g., *Lamellibrachia* and *Escarpia* spp. and which can survive up to 38 days in the laboratory (Young

et al. 1996; Van Dover 2000; Marsh et al. 2001), to large eggs (> 200 µm wide) with negatively buoyant larvae, e.g., the polychaete *Alvinella pompejana* (Pradillon et al. 2001). *Kiwa puravida*, the seep-dwelling yeti crab, has very large eggs (> 1 mm diameter) (Thurber et al. 2011). Pradillon et al. (2001) found evidence for delayed metamorphosis with *A. pompejana* larvae in cold water (2 ˚C), suggesting that the real dispersal capability may be in excess of estimates based on physiology and laboratory experiments in the frigid deep sea. This fact may be particularly important in polar waters and could explain why the Southern Ocean has fewer planktotrophic organisms than in other oceans (Pearse et al. 1991).

Planktotrophy

There is evidence of planktotrophy in the post-larval phase of *Rimicaris exoculata*, as their energy stores (wax esters) appear photosynthetically derived (Copley et al. 1998; Allen et al. 2001). This, along with laboratory experiments on *Mirocaris fortunata* larvae indicating an ability to climb the water column up to the thermocline (~ 200 m depth) suggests a high dispersal capability (postlarvae have been found more than 100 km from their likely natal vent sites; Herring and Dixon 1998). The eggs of the bathymodioline mussel *Bathymodiolus childressi* are also small compared to lecithotrophic taxa (~ 69 µm) and yield free-swimming larvae with mouths also suggestive of planktotrophy (Arellano and Young 2009).

1.3.2.2 Realised Dispersal Capability of Larvae

Little is known about the realised dispersal capability of vent larvae, but a myriad of intrinsic (e.g., lecithotrophy, planktotrophy) and extrinsic (e.g., currents, topography) factors must combine to determine just how far larvae can travel in the deep sea. For example, an estimate for larval dispersal of *R. pachyptila* is ~ 100 km (Marsh et al. 2001) based on a 38-day larval lifespan and the measured current regime at vent sites on the EPR.

The size and nature of the buoyant plume at vent sites may also be a factor in dispersal. Mullineaux et al. (1995) found evidence that *Calyptogena* larvae were found in the plume above a vent on the Juan de Fuca Ridge but not outside the plume. Work with high-volume pumps above and around vents on the EPR suggests that larval concentrations exponentially decrease with height above the vent, but not so with lateral distance, indicating that even with these shallower axial valleys, larvae are significantly retained within the valley, as expected given the prevalence of lecithotrophy (Mullineaux et al. 2005).

As just implied, the propensity for larval retention along a ridge could be strongly affected by the ridge axis topology, which relates to the spreading rate and underlying geology at the ridge in question. The slow-spreading MAR is typical in having deep, axial valleys, which may improve retention, compared to fast-spreading ridges which have shallow axial valleys or axial highs, where larvae could easily be lost off axis (Tyler and Young 2003).

There was also substantial discontinuity in the abundance of different larvae at vent communities over time, which raises the possibility of pulses of larval transport relating to spawning and flow patterns (Mullineaux et al. 2005). More recently, an eruption at 9˚ 50’ N in 2006 (the second observed at this site) on the EPR resulted in complete defaunation, but the new community that subsequently arose was different in species composition, with the settlement of *Ctenopelta porifera* gastropods, only known at vents 300 km away and the loss of some other species (Mullineaux et al. 2010). Mesoscale eddies may have played a part in transporting these distant larvae at the expense of local recruitment (Adams et al. 2011), highlighting both the importance that local recruitment of larvae play in maintaining a community structure at a vent, but also the importance of the local current regime in maintaining vent community structure.

1.4 Population Genetics

1.4.1 Connectivity

1.4.1.1 Simple Models

A key part of understanding the biogeography of hydrothermal vent fauna is in the use of population genetics to estimate the nature of connectivity between vent colonies. Vent fields can be conceptualised as islands of high biomass surrounded by deserts of low biomass (Vrijenhoek 2010) and on mid-ocean ridges, population and species ranges are determined by the biotic and abiotic factors listed in the previous section.

Historically, two basic models of connectivity, the Island Model (Wright 1932; Slatkin 1993) and the Stepping-Stone or Isolation-by-Distance (IBD) model (Wright 1943; Kimura and Weiss 1964) have been used to conceptualise connectivity of vent fauna. In essence, vent animals with limited dispersal capability, e.g., those with lecithotrophic larvae, which might be only able to reach adjacent or nearby vents are expected to conform to a stepping-stone or IBD model. This is because when dispersal occurs between neighbouring islands, the correlation in genetic similarity should decrease with increasing distance between vents along a ridge (Vrijenhoek 1997). In contrast, the Island Model describes a situation where dispersing larvae are drawn from a well-mixed pool of migrants, which might describe species with high dispersal capability, such as those with long-lasting planktotrophic larvae (Vrijenhoek 1997).

In population genetics, Sewell Wright's F_{ST} (Wright 1950) (or variants thereof) has been the most common tool used to ascertain population structure (differentiation) by looking at the

overall variance in allele frequencies amongst all populations (F_{IT}) and then partitioning this variance to that between populations (F_{ST}), a measure of genetically effective migration, and that within populations (F_{IS}), resulting from inbreeding. F_{ST} is inversely proportional to the historical rate of gene flow or N_m, (the estimated mean number of migrants exchanged between 'islands' per generation), assuming that the two populations are at drift-migration equilibrium. Much of the population genetics literature on vent populations has been dedicated over last three decades to seeing if species conform to either of the two models above. F_{ST} has also been used to try to identify key topographical and hydrographic features that may subdivide species at larger scales, e.g., between ridge segment separated by transform faults that prevent gene flow for a given species, providing insights into how life history can affect dispersal capacity (Vrijenhoek 1997).

Allozymes

The earliest population studies for vent fauna involved the use of allozymes (allelic variants of enzymes, visualised by separation on gel electrophoresis plates). Early allozyme assessments of gene flow between vestimentiferans at vents along the EPR suggested only a small degree of genetic differentiation over several thousand kilometres of ridge (Bucklin 1988; Black et al. 1994; Southward et al. 1996; Black et al. 1998). A weak IBD effect was also seen in *Alvinella pompejana*, where there was increasing genetic divergence at higher geographic scales (between vent sites, ridge segments and between ridges) along the East Pacific ridges, but *Alvinella grasslei,* a more widespread species, did not show increased divergence between ridge segments, but did between whole ridges (Jollivet et al. 1995). However, *Calyptogena magnifica* appeared undifferentiated along the EPR (Karl et al. 1996).

Something approximating the Island Model was considered possible for fauna with

planktotrophic larvae, owing to the presumed superior dispersal capability: the most comprehensive allozyme study on *Bathymodiolus thermophilus* found no evidence of genetic differentiation between sites (Craddock et al. 1995). More recent allozyme and mitochondrial studies however, have revealed strong genetic differentiation across regions of the (SEPR) (Won et al. 2003; Plouviez et al. 2009), areas not previously covered. The Island model may therefore hold in some regions and scales, but not across the entire EPR. Two studies on *Rimicaris exoculata* compared allozyme frequencies between populations separated by several hundred km and revealed no significant variance in allozyme frequencies (Creasey et al. 1996; Shank et al. 1998), indicative of a large dispersal capability.

Despite the low cost of obtaining allozyme data, there are some possible disadvantages with this approach, such as the small number of loci available for study, hidden sequence variation not expressed in protein structure or functioning and environmental influence and selection on protein expression (Parker et al. 1998), although the influence of selection can be turned into an opportunity to investigate the influence of environment on the selection of functional enzymes at vents. Nevertheless, there has been a shift to using sequence data over the past two decades.

Sequence data

The first detailed population study on vent fauna working exclusively with the mtDNA gene COI (Hurtado et al. 2004), investigated the gene flow of three tubeworm species (*R. pachyptila*, *T. jerichonana* and *O. alvinae*) and two polychaete worm species (*Alvinella pompejana* and *Branchipolynoe symmytilida*) along East Pacific vents from 27˚ N to 32˚ S. None of these species appeared to conform to the Island Model along this ~ 7,000 km stretch of mid-ocean ridge. A weak IBD signal was visible for *T. jerichonana* and for *O. alvinae*, but not for the other species. They identified several dispersal filters or barriers to one or more of these taxa, such as the Rivera Fracture zone, the equatorial region, where a strong, eastward bottom current exists

and the Easter Microplate region, but not all species were affected by all of these potential barriers. A similar study looking at seven species from 21˚ N to 21˚ S along the EPR revealed similar results (Plouviez et al. 2009), with weak to non-existent IBD within ridge segments, punctuated by dramatic apparent breaks in gene flow (large F_{ST}).

Perhaps the most convincing example of an IBD effect is with the lecithotrophic *R. pachyptila*, over 7,000 km of the EPR (Coykendall et al. 2011). However, this study showed that below distances of ~ 1,000 km, there were no apparent genetic differences between vent fields, indicating either that at such scales there is high connectivity between sites, or that the markers used are not sufficiently fast-evolving to reveal small-scale differences.

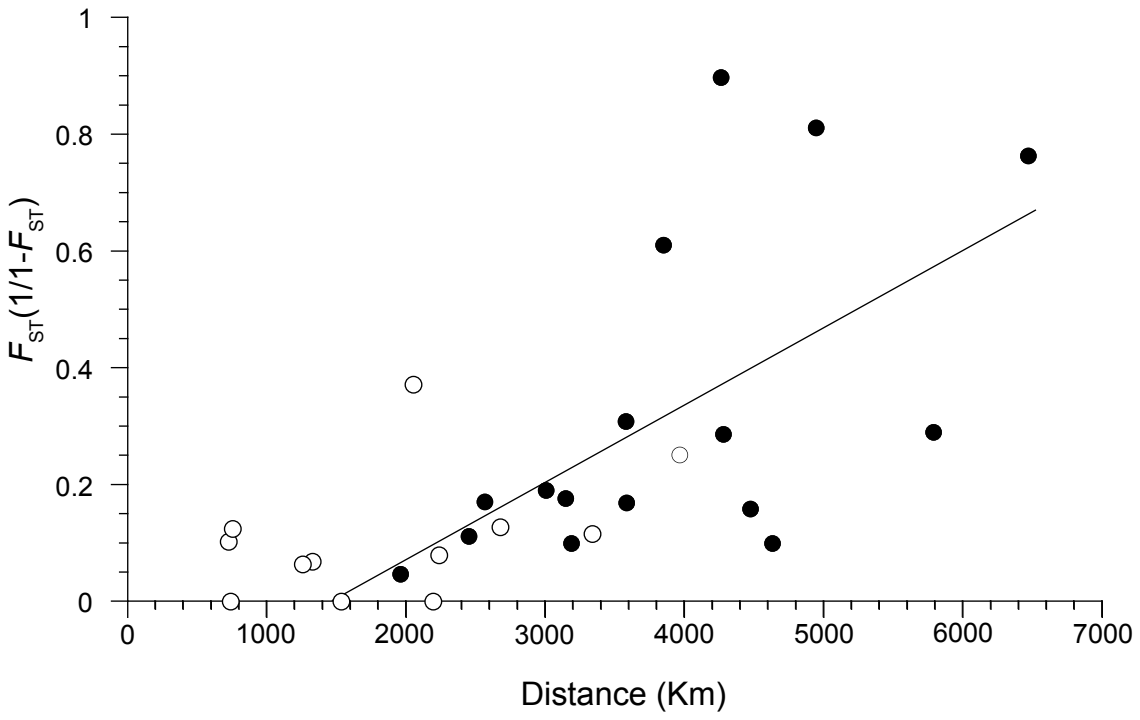

Figure 1.5. Correlation of genetic differentiation of *Riftia pachyptila*, with geographic distances among eight sample localities on the East Pacific Rise (EPR), from Coykendall et al. (2011). Black dots denote contrasts between populations from the northern and southern EPR 'clusters'. White dots denote contrasts within clusters.

Nuclear genotyping markers

Ideally, a multilocus approach with nuclear markers should add statistical power to inferences about connectivity between vent colonies (Vrijenhoek 2010). This is especially true when examining demography, which will be discussed later. Recently, more multilocus genetic markers have been employed to look at connectivity at smaller scales. AFLP markers (differences in restriction fragment lengths caused by single nucleotide polymorphisms (SNPs) or insertions/deletions) for example, revealed more structure than had previously been found with *R. pachyptila*, showing again, strong differentiation across the equatorial EPR (Shank and Halanych 2007).

In the last few years, microsatellite markers have also been used. These are short tandem repeats, (repeating motifs of di, tri, tetra etc. nucleotides), which, because of copy errors can differ in the number of repeats and therefore length. Microsatellites are useful because they have high mutation rates (between 10^{-2} and 10^{-5} per gamete per generation) compared to genes, which means they vary greatly between individuals within a population (Page and Holmes 1998).

Over the last seven years or so, suites of markers have been developed (Daguin and Jollivet 2005; Fusaro et al. 2008; Cabezas et al. 2009; Thaler et al. 2010; Schultz et al. 2011; Teixeira et al. 2012a; Jacobson et al. 2013) and in the last two years, two papers (Thaler et al. 2011; Teixeira et al. 2012b) and one doctoral thesis (Fusaro 2008) have been published. Thaler et al. (2011), working on the West Pacific vent gastropod *Ifremeria nautilei* revealed differentiation between those at vents in Manus basin and those in the Lau and North Fiji basins using F_{ST} and a clustering approach using software called STRUCTURE (Pritchard et al. 2000). This algorithm assigns individuals to groups assuming loci are at Hardy-Weinberg Equilibrium (maintenance of constant allele frequencies because of a lack of mutation, migration or selection in a large randomly mating population - HWE) within each population and estimates the population of origin for each individual from the observed genotypes. Teixeira et al. (2012)

showed, with both F_{ST} and STRUCTURE that across ~ 6,500 km of the Atlantic, vent colonies of *Rimicaris exoculata*, the vent shrimp with planktotrophic larvae, were un-differentiated. Fusaro (2008) investigated gene flow between populations of *R. pachyptila* along the NEPR and GAR, which revealed a weak IBD effect using both F_{ST} and STRUCTURE.

Coalescent–based approach

The use of the STRUCTURE algorithm with microsatellite data offers a new approach in addition to classic F_{ST}, which comes with certain assumptions, e.g., that populations are equal in size, are at drift-migration-mutation equilibrium and that migration is symmetrical (Beerli 2004). STRUCTURE offers a complimentary method to assess differentiation between vent colonies without these assumptions, as it is essentially a clustering tool, although some simulations suggest this approach is less effective with populations that do not conform to the Island Model (Evanno et al. 2005). A limitation of both F_{ST} and clustering approaches like STRUCTURE is that they cannot provide information about directionality of gene flow.

The last decade has seen the growing use of genealogy samplers that use a coalescent approach (Kingman 2000). Coalescence is the tracing back of two lineages to a common ancestral haplotype/allele at a particular time. Coalescent theory relates the patterns of common ancestry (genealogy branching patterns) within a sample, to the size, structure and history of the overall population (Kuhner 2009). Genealogy sampling methods estimate parameters of the coalescent process that has given rise to a particular genealogical tree. This approach provides a framework in which to model recombination, migration, selection, and demographic change over time (Rosenberg and Nordborg 2002).

Migrate-n & IM

Two software packages in particular have been used in vent population genetics recently to explore asymmetrical gene flow and historical vicariance.

Migrate-n (Beerli 2004; Beerli 2006) considers multiple populations using a stable-population model. It estimates θ (mutation rate-scaled effective population size) for each population and bi-directional historical migration rates M (mutation rate-scaled migration rate per generation) within a maximum likelihood (ML) or Bayesian inference (BI) computational framework. Recently, this approach has been used to infer migration rates between three colonies of *Rimicaris exoculata* on the MAR and found that migration rates were large and equal in both directions, consistent with the inference of panmixia (Teixeira et al. 2012b). A limitation of this approach is that Migrate-n assumes populations have been demographically stable for ~ $4N$ generations and that the populations have not recently diverged. If these assumptions are violated, (see section on demography) the size of θ can be affected and if two populations are recently diverged with no contemporary gene flow then the size of M will be inflated (Lemey et al. 2009). However, while the magnitude of θ and M are affected when these assumptions are violated, simulated data indicates that gene flow directionality is robust (Beerli 2010).

The Isolation with Migration (IM) approach (Hey 2010) considers cases in which two populations have recently diverged from a common ancestor. They estimate θ for each population and for the common ancestor, as well as the divergence time and bidirectional M among the daughter populations. This has the advantage of relaxing the assumptions that the populations have been stable over time, or that similar allele frequencies between the two populations are solely the result of migration and not also common ancestry. A downside in

contrast to Migrate-n however, is that only pairwise population comparisons can be done unless the splitting history of the populations is known (Hey 2010).

This approach has been used on divergent limpets across transform faults in the Northeast Pacific (Johnson et al. 2006) where they were able to show, using COI the nuclear DNA intron *Pgm-i* and allozymes that *Lepetodrilus fucensis* formed a cryptic species complex across the Blanco Transform Fault (BTF) with a weak net southward gene flow after the two populations had diverged. Similar methods have been employed for *Ridgeia piscesae* spanning the BTF (Young et al. 2008), using COI and multilocus allozyme data, inferring net southerly gene flow, consistent with modelled current flow. Thaler et al. (2011) were able to show with IM that *Ifremeria nautilei* gastropods in the Manus were reproductively isolated from those in the Lau and North Fiji basins for > 100,000 years.

The ability to model asymmetric gene flow between multiple populations allows researchers to explore models of connectivity other than IBD and the Island Model. For example, it might be possible, in conjunction with demographic analyses and directional gene flow estimates to infer a source-sink dynamic, whereby a stable population supplies larvae to less stable populations as appears the case between northern and southern populations of *Alvinella pompeyana* on the EPR (Plouviez et al. 2010). Another scenario that has not yet been observed in vent species, but has been found in isopods in the Southern Ocean is a unidirectional version of the stepping-stone scenario (Leese et al. 2010), whereby currents of the Southern Ocean prohibit gene flow in a westerly direction. This scenario may be particularly applicable to vent populations living along mid-ocean ridges bathed in the Antarctic Circumpolar Current, e.g., on parts of the SWIR and P-AR.

Metapopulations

Since their discovery hydrothermal vent ecosystems have been conceptualised as ephemeral habitats, with individual vent fields or colonies going extinct and new ones appearing nearby. From an ecological perspective, therefore, populations spanning several colonies can be conceived of as metapopulations (Vrijenhoek 1997), whereby the population as a whole is dominated by non-equilibrium conditions. That is to say that the demes (sub-populations) within the metapopulation are not at drift-migration equilibrium with each other, with consequences for the diversity and demography of the metapopulation as a whole (Juniper and Tunnicliffe 1997; Vrijenhoek 1997; Vrijenhoek 2010).

Strictly speaking, a metapopulation is "a population of populations" where the local populations undergo extinction, birth and/or recolonization (Levins 1969; Smedbol et al. 2002). In this sense, hydrothermal vent populations fit the metapopulation definition because senescent and nascent vent fields have been observed (Vrijenhoek 1997) as well as eruptive events (Haymon et al. 1993; Mullineaux et al. 2010). In order for a population to be accurately described as a metapopulation, a key requirement is that it must be subdivided into discrete sub-populations, although there is some debate about whether or not these sub-populations must be prone to regular extinctions or merely large demographic fluctuations (e.g., Smedbol et al. 2002; Kritzer and Sale 2004).

Given the presumed stochastic birth and death of vent fields, combined with the theorised limited dispersal capacity of most vent fauna (lecithotrophic larvae), the expectation was that if the metapopulation model held, one should expect to find clear population subdivision and an IBD effect along mid-ocean ridges (Jollivet et al. 1995; Vrijenhoek 1997; Jollivet et al. 1999; Audzijonyte and Vrijenhoek 2010). However the results of molecular studies over the last two

decades have been far from unequivocal, with only six of 14 species studied along the EPR showing a clear IBD effect and the rest showing some form of regional subdivision to a certain extent (Vrijenhoek 2010), or in the case of *Rimicaris exoculata* along 7,100 km of the MAR, no subdivision at all (Teixeira et al. 2012b). Even in the case of *Riftia pachyptila* on the EPR, which shows a clear IBD effect over ~ 7,000 km of ridge (Coykendall et al. 2011), there were no significant pairwise F_{ST} values below ~ 1,000 km distance, suggesting that many vent fields were receiving larvae from a well-mixed pool at scales smaller than 1,000 km.

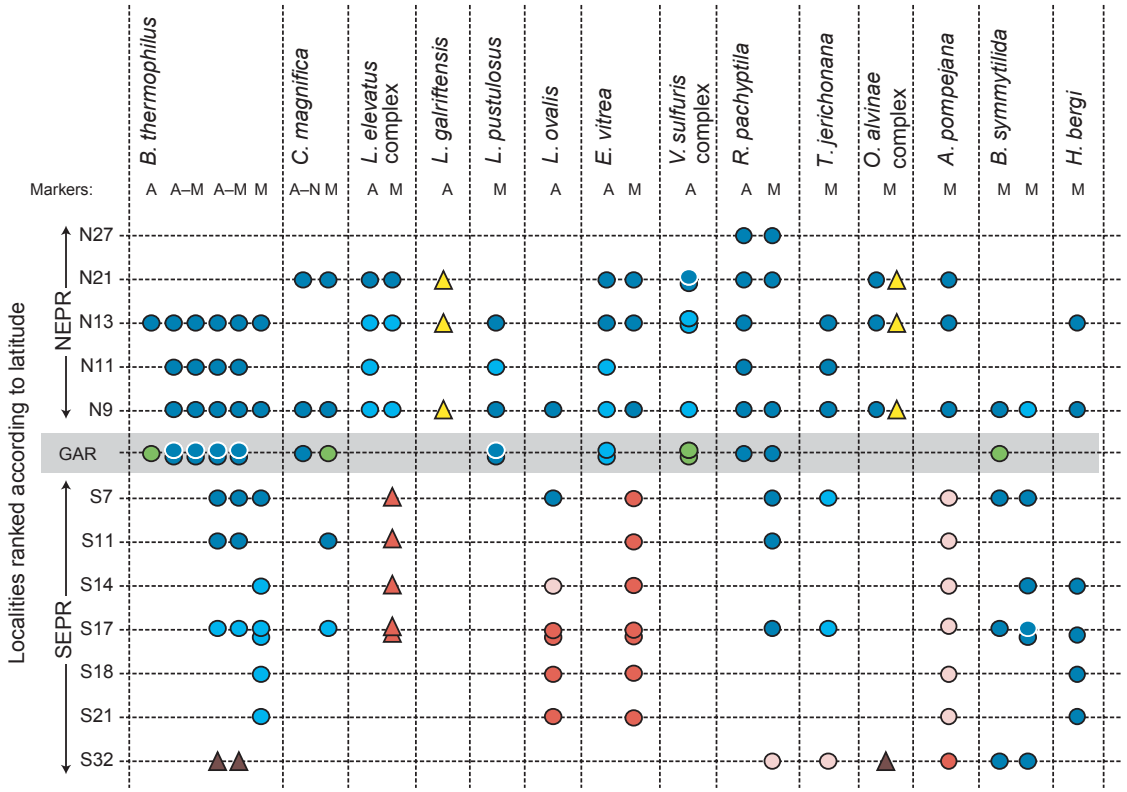

Figure 1.6. Simplified version of the same figure from Vrijenhoek (2010) summarizing molecular studies showing regional differentiation of several species along the northern East Pacific Rise (NEPR), the southern East Pacific Rise (SEPR) and the Galapagos Rift (GAR). Genetic markers are (A) allozymes, (M) mtDNA and (N) nuclear DNA. Hyphenated letters denote studies with more than one type of marker – e.g., A-M is a study using both allozymes and mtDNA. Green dots denote significantly divergent GAR samples. Blue vs. red dots indicate major partitions along the EPR (shades of blue and red indicate subpopulations within each partition). Triangles indicate putative cryptic species. Species featured are *Bathymodiolus thermophilus* mussels, *Calyptogena magnifica* clams, the limpets of the genus *Lepetodrilus* as well as *Eulepetopsis vitrea*, the amphipod *Ventiella sulphuris*, the siboglinid tubeworms *Riftia pachyptila*, *Tevnia jerichonana* and *Oasisia alvinae*, the terrebellid polychaete worm Alvinella *pompejana*, the scale worm *Branchipolynoe symmytilida* and the bristle worm *Hesiolyra bergi*.

On the face of it therefore, the metapopulation model may not be applicable for all vent species on all ridges. In the case of *R. exoculata*, the combination of planktotrophic dispersal (Teixeira et al. 2012b) as well as the inferred greater temporal stability of vent fields (Van Dover 2000) on slow-spreading ridges may render much of the MAR effectively one population, with vent fields as discrete habitat patches receiving larvae from a well-mixed pool (the Island Model).

However, there are reasons to suspect that population genetics studies have underestimated the degree of true subdivision for many species along ridges. Firstly, simulated data indicate that the failure to detect a strong IBD effect may be the consequence of weak statistical power resulting from low sampling effort (too few loci or locations sampled) (Audzijonyte and Vrijenhoek 2010).

Alternatively, the relative genetic homogeneity along stretches of ridge may be the consequence of the failure of colonies to attain drift-migration equilibrium (Jollivet et al. 1999). Jollivet et al. (1999) were able to devise a model variant to the classic metapopulation model that was fitted to the life history of *Alvinella pompeyana*. In their model, the continuous birth and death of vent fields affects the equilibrium between gene flow and drift resulting in a situation where the time required to balance these forces is never attained, leading to fluctuations in F_{ST} because of stochastic changes in inter-patch distances which in turn affect migration rates. These shifting zones of venting along the ridge would counterbalance differentiation of sub-populations.

The study by Jollivet et al. (1999) demonstrated what had already been theorised, which is that where new colonies are recruited from locally-sourced migrants (propagule-pool model; Slatkin 1977), genetic differentiation between demes will be depressed relative to the expectations of the Wright's (1943) Island Model, as colonization in effect enhances gene flow. If metapopulation demes have insufficient time to attain migration-drift equilibrium (as may be expected in dynamic environments such as hydrothermal vents), then it should be very difficult to detect an IBD pattern (Slatkin 1993).

Consequently, there is a problem with attempting to define the boundaries of sub-populations that may not be in drift-migration equilibrium using F_{ST}, which implicitly they are at drift-migration equilibrium. For example, a vent field that had recently been colonised by a nearby vent field, but with very limited subsequent gene flow between them (equivalent to a recent local range expansion) could appear relatively homogeneous and as Jollivet et al. (1999) point out, the time necessary for these two populations to diverge owing to drift may be far longer than the lifespan of the vent field.

Whether or not a metapopulation model is the best way to characterise a population along a mid-ocean ridge may very much depend not just on the geographic scale or the dispersal capability of the species in question, or the presence of topographical barriers along the ridge, but also the longevity and birth/death rate of vent fields along the ridge, which is believed to be the consequence of mid-ocean ridge spreading rate (Vrijenhoek 2010). The fast-spreading SEPR has vent fields that may exist for only a couple decades and eruptive events that may span large portions of the ridge at a time (Van Dover 2000) and it may be that here it is appropriate to apply a non-equilibrium metapopulation framework, even if the genetic evidence for subdivision and IBD isn't very strong. This framework may be less applicable to populations on the more slow-spreading MAR, with its long-lasting vent fields that may be hundreds or thousands of years old (Van Dover 2000).

Alternatively, species with a high potential dispersal living along slow spreading ridges with more long-lived vent fields may be considered metapopulations, but only when observed at a sufficiently large scale, e.g., at the scale of a whole ridge, as even large-scale features like massive transform faults may fail to present a barrier to gene flow. With such species, owing to non-equilibrium dynamics, little or no differentiation could be possible at very large scales (several thousand kilometres), as is the case with *Rimicaris exoculata* on the Mid-Atlantic

Ridge (Teixeira et al. 2012b). In such a case, panmixia may therefore be illusory. In contrast, species with a limited potential dispersal capacity may have metapopulations confined to a few or only a single ridge segment owing to ridge offsets, for example, with little or no differentiation at smaller scales owing to the non-equilibrium processes detailed above. Hierarchical subdivision (Wright 1950) has already been suggested for some species in the tropical East Pacific (Vrijenhoek 2010), although it hasn't been explicitly put forward yet that lack of differentiation within these subdivisions is the consequence of metapopulation non-equilibrium dynamics.

If such non-equilibrium processes are dominant for species with limited dispersal capability, then one would expect that at the scale of the ridge segment (or a few ridge segments), there should be little or no differentiation and then a 'jump' in differentiation between these subdivisions where gaps in the ridge are too large for regular gene flow, which is exactly what is observed using microsatellite markers with the tubeworm *Riftia pachyptila* on the EPR (Fusaro 2008), although true panmixia (Island Model) at such scales cannot be discounted. Until more accurate estimates of the real dispersal potential of these animals, are determined the metapopulation framework remains theoretical. As Vrijenhoek (2010) has already intimated, however, the pattern of recent demographic change observed in the DNA sequences of many vent fauna around the globe, could be indicative of vent ephemerality and the resultant non-equilibrium processes.

1.4.2 Diversity & Demographics

By the end of the 1990s, certain patterns of allozyme diversity became apparent:

1) Vent fauna, despite the exceptional densities, appeared to have lower diversity compared to other deepsea fauna (Creasey and Rogers 1999).

2) Populations of common vent species on the EPR appeared more diverse than those that were less common (Vrijenhoek 1997).

Both papers suggested that the general ephemerality of vents compared to other deep sea habitats may be a cause of depressed diversity in allozymes because population turnover should theoretically decrease genetic variability, both owing to allele loss as populations go extinct and because repeated founding of new populations by just a few individuals induces multiple bottlenecks. They suggested that species more common at vents would be less likely to be affected by bottlenecks caused by colony extinctions and hence would maintain a higher capacity for diversity. This was shown to be the case with *R. pachyptila*, which exhibited higher allozyme average heterozygosity than *T. jerichonana* and *O. alvinella*, perhaps owing to its greater prevalence on EPR vents (Creasey and Rogers 1999).

Working in a metapopulation framework, Vrijenhoek (1997) suggested the following factors should be key in determining the diversity in vent fauna:

1. Site occupancy and the density of vents: the more colonies within reachable distance of each other, the larger the size of the metapopulation, leading to greater diversity.
2. Ephemerality of vents: vents that are short-lived will reduce the number of generations at any one vent site and hence the number of larvae that can disperse from that location, thus lowering the size of the metapopulation and increasing the possibility of genetic bottlenecks as at any one time, the number of potential colonies may fluctuate more dramatically.
3. Dispersal capacity of the larvae: species with limited dispersal capacity are likely to have smaller more isolated populations. 'Super dispersers' should be able to maintain metapopulations across large gaps in the ridge.

4. Ridge characteristics: ridges such as the Mid-Atlantic Ridge have deep axial valleys that help to constrain larval transport along the ridge axis, which may extend the reach of the propagules owing to high retention.

Vrijenhoek (2010) has since compiled mitochondrial data and plotted haplotype diversity against vent site occupancy of species on the EPR and found a clear relationship whereby high site occupancy corresponds to higher diversity. He also noted that as the SEPR has faster spreading rates with theoretically shorter-lived vents, populations should hold less diversity than their counterparts on the NEPR, and this has been confirmed for *Riftia pachyptila* with mtDNA and three nuclear loci (Coykendall et al. 2011). A recent mtDNA study on *R. exoculata* reveals high haplotype diversity ranges across colonies (0.69-0.82) (Teixeira et al. 2010) and given the reports of vast numbers of vent shrimp around chimneys, and the impressive dispersal capability of *R. exoculata* combined with the presumed temporal stability of vent fields at slow-spreading ridges, such high levels of diversity are not surprising.

The case for the general ephemerality of vents depressing allelic diversity in vent fauna is bolstered by the common presence of mtDNA star-like haplotype networks (visual representations of haplotype relatedness and numerical dominance in populations; Posada and Crandall 2001), which, along with significantly negative Tajima's *D*, Fu's *F*s and also mismatch distributions (summary statistics showing deviations from neutrality) possibly signal 'recent' population expansions for vent species (Hurtado et al. 2004; Young et al. 2008; Plouviez et al. 2009; Plouviez et al. 2010; Teixeira et al. 2010). All of these measures, in their own way illustrate or measure the excess of low frequency allelic variants in the population (i.e., the number of low frequency allelic variants relative to the expected number in a population at HWE with neutral loci) (Tajima 1989; Fu and Li 1993; Harpending 1994; Fu 1996).

One problem with using single locus sequence data to infer demographics is the possibility of selective sweep, which reduce diversity giving the appearance of recent demographic

bottlenecks. A way around this is to use multiple unlinked loci, or by looking at mtDNA in multiple co-living species (Plouviez et al. 2009; Plouviez et al. 2010). Plouviez et al. (2009) examined seven species along the EPR and they were able to show that all seven species appeared to show evidence of a recent bottleneck, making a selective sweep less likely. Interestingly, this population expansion signature was mainly in the SEPR populations. The same SEPR expansion signature was shown again but this time with the addition of three nuclear genes for one species, *Alvinella pompejana* (Plouviez et al. 2010). This pattern fits with the expectations of Vrijenhoek (1997) that the greater degree of ephemerality of SEPR vents has probably resulted in more intense population fluctuations. Furthermore, the multigene analysis on *A. pompejana* showed a consistently lower diversity for those sampled on the SEPR compared to the NEPR (Plouviez et al. 2010) as per the expectations of Vrijenhoek (1997).

1.4.3 Large Gaps

In reviewing these population genetics studies, it becomes clear that there are huge gaps in sampling effort that inhibit efforts to draw general inferences about these ecosystems. The vast majority of studies to date have been on East Pacific vents, where ridge spreading rates are considered fast, but there are few studies from slow and medium spreading ridges. This biased coverage is likely a result of the costs of exploring ridge systems that are more remote and the fact that there is more information regarding the geology, topography and hydrography of the EPR, GAR and Northeast Pacific ridges over others making them model systems for population genetics. There is also a strong bias towards population studies in equatorial and subtropical regions, owing to the challenges involved in conducting deepsea operations in the generally rougher seas of the higher latitudes as mentioned by Macpherson et al. (2005).

In terms of taxa, no population genetics has been done on vent crustaceans other than *Rimicaris*

exoculata i.e., bythograeid crabs, anomuran crabs, stalked barnacles or other alvinellid shrimp. Neither has any work been published on neomphaline gastropods, pycnogonids, or cnidaria.

1.4.4 New Methods

The broad trend in deepsea population genetics has been from an allozyme multilocus approach to DNA sequence data, in particular, single locus mtDNA. The gains made by resolving allelic differences down to the level of nucleotide differences have been offset by the downsides of using only a single locus and some have avoided this by simultaneously analysing mtDNA in a group of cohabiting species, e.g., Plouviez et al. (2009) or to combine mtDNA sequence data with nuclear sequence markers (Plouviez et al. 2010; Coykendall et al. 2011).

Microsatellites have been used widely in population genetics, but in vent ecology, few studies have been published owing to the time and cost associated with the development of clonal libraries. Next generation sequencing methods, however, have reduced the cost of microsatellite development considerably in the last two years (Abdelkrim et al. 2009).

In the field of population genetics there now is a growing tendency to use single nucleotide polymorphisms (SNPs) as multilocus markers. The advantages over microsatellites are that the mutation model is better understood (Brito and Edwards 2009), there is less subjectivity in scoring and crucially, the comparatively slower mutation rates of sequence data reduces the likelihood of homoplasy (Brito and Edwards 2009). The disadvantage is that in order to find unlinked candidate SNP sites, large portions of the genome must be sequenced for at least two individuals, and unlike microsatellites, owing to the largely binary nature of SNPs a great deal more loci must be found in order to get significant data from population studies (Brito and Edwards 2009). Recently, the potential cost of finding and genotyping SNPs them has been greatly reduced with the advent of Restriction-site Associated DNA Sequencing

(RADSequencing) (Davey and Blaxter 2010), which combines enzyme fragmentation of the genome with high-throughput sequencing (e.g., Illumina) to create a large number of SNP markers (thousands).

1.5 Overall Conclusions

The aim of this literature review has been to compile a brief history of the discovery of chemosynthetic ecosystems, with a focus on deep-sea hydrothermal vent communities. In particular the focus of this review has been to investigate how molecular genetic techniques have been used to answer key questions relating to the ecology and evolutionary history of the inhabitants of hydrothermal vents. In some cases, molecular studies have helped develop a consistent picture that has challenged old notions, such as the presumed antiquity of vent and seep fauna and their isolation from past extinction events in the deep sea. However, in other cases, molecular techniques have failed to provide a clear-cut picture, e.g., relating larval morphology and dispersal strategy to the patterns of connectivity across topographical and hydrographic features on the EPR, or tallying a theorized metapopulation model with observed patterns of isolation by distance (or lack thereof).

Part of this failure results from the 'patchy coverage' of population genetics studies at sites that have been discovered. Even in the East Pacific, where the most detailed population studies have been conducted, there are large sampling gaps. We still know very little about the life history of many vent taxa, from mean generation time and behaviour, to basic larval morphology and longevity. Few sites have been repeatedly visited or continuously studied owing to the extreme cost of expeditions and few experiments have been conducted in the laboratory owing to the challenges of keeping specimens alive.

Population genetics has shown that different species are affected in differing ways by the same geological structures and currents and the necessary addition of a historical dimension when addressing questions of biogeography is problematic when so little is known of the geological and hydrographical past. It is likely that the relative importance of tectonic movements and

hydrography in shaping global patterns of vent biogeography will depend on the timescales involved, the dispersal capabilities of the animals in question, the successional stage at which they inhabit the site and the range of biotic and abiotic conditions necessary for their survival (e.g. the ability to colonise both vents and seeps).

The largest gaps in our knowledge are still geographical, with vast stretches of mid-ocean ridge remaining unexplored, such as the SE Indian Ridge, the P-AR, the Chile Rise the American-Antarctic ridge and most of the southern MAR. Seamounts remain largely ignored, despite the possibility that they could be important stepping-stones in the dispersal and biogeography of vent taxa.

Until these regions are reached, our understanding of the global biogeography of chemosynthetic ecosystems will remain incomplete. Nevertheless, since vents were discovered on the Galapagos Ridge 33 years ago, scientific endeavours - and molecular genetics especially - has revealed much about the evolutionary origins, ecology of these exotic ecosystems.

1.6 ChEsSO, Project Aims & Contribution

1.6.1 Discoveries in the Scotia Sea

In January 2010, an expedition to the Scotia Sea (JC042) aboard the Royal Research Ship *James Cook* sampled hydrothermal vents above the E2 and E9 ridge segments on the East Scotia Ridge (ESR) and the nearby Kemp Caldera. This was second of four expeditions that were part of the ChEsSO consortium (Chemosynthetic Ecosystems of the Southern Ocean) designed to find and sample the chemosynthetic ecosystems in this part of the world (Rogers 2010; Rogers et al. 2012).

The research presented in this thesis is the product of the JC042 expedition in which a host of new species were discovered, indicating that the ESR vents are representative of a new biogeographic province (Rogers et al. 2012). These discoveries, in particular the collection of numerous specimens of new, undescribed species of kiwaid yeti crab, peltospirid gastropods and lepetodrillid limpets collected at both E2 and E9 vents (and also at Kemp, in the case of the limpets) allowed the phylogenetics and population genetics (connectivity and demography) of these species in the Scotia Sea to be examined.

1.6.2 Phylogenetics

Chapter 2 explores the phylogeography of the chemosynthetic-associated yeti crabs (Kiwaidae). The discovery of the first non-Pacific species of this family in the Scotia Sea appears to match the prediction (Tunnicliffe and Fowler 1996; Fowler and Tunnicliffe 1997) that vents in the Atlantic sector of the Southern Ocean should host some species with a Pacific provenance

owing to the Cenozoic opening of the Drake Passage. By incorporating all known kiwaids and using a multi-gene dataset, this chapters aims to use phylogenetic tree topology and fossil-calibrated divergence dates to see if the presence of kiwaids on the ESR is the consequence of vicariance relating to the opening of the Drake Passage. At the same time, by estimating the age of the crown taxon, it is possible to contribute to the debate concerning the antiquity of vent and seep-endemic megafauna and to provide insights as to how and where this distinctive clade evolved from its non-chemosynthetic relatives.

1.6.3 Population Genetics

Chapters 3-5 are concerned with the population genetics of the three species mentioned above. This work is principally interested in characterising the degree of connectivity and patterns of diversity for species living at the first sampled vents in the Southern Ocean, thus adding to the sum knowledge of the population genetics of vent megafauna globally. However, owing to the limited number of sample sites, this study is in effect a primer for future studies that will examine connectivity and diversity between these sites and others in the Southern Ocean, such as potential sites on the American-Antarctic Ridge and the SWIR.

This study offers the opportunity to compare and contrast levels of connectivity of three species with very different larval characteristics along a stretch of medium-spreading ridge similar in scale to a single ridge segment on the fast-spreading EPR, the most studied vent region in the world. Furthermore, this is the first study examining the connectivity and diversity of species inhabiting vents surrounded by ambient temperatures close to or below 0 ˚C (Rogers et al. 2012). The patterns of connectivity and diversity of the new kiwaid species are of particular interest because initial reports of its larval morphology suggest that this animal exhibits the most direct, lecithotrophic development yet encountered in a vent species (Sven Thatje et al.

manuscript in preparation), indicative of poor range of dispersal.

Chapter 3 investigates connectivity and diversity using the mtDNA marker, COI. This work is built upon with the development (Chapter 4) and implementation (Chapter 5) of a suite of microsatellite markers. These theoretically neutral and fast evolving markers have only been used rarely (see earlier) in vent studies, but such rapid-evolving markers may be particularly useful in assessing subdivision within vent metapopulations on ridges.

It is hoped therefore that this body of work will contribute to the field of hydrothermal vent ecology and biogeography by examining the likely key processes, both ancient, e.g., ridge evolution and vicariance and recent e.g., ocean currents, temperature and larval morphology influencing connectivity, involved in shaping the first communities discovered in the Southern Ocean and perhaps to attain general insights that may be applied to the field as a whole.

CHAPTER 2

The Biogeography & Phylogeny of Kiwaidae with Notes on Chirostyloidea

2.1 Abstract

The phylogeny of the superfamily Chirostyloidea (Decapoda: Anomura) has been poorly understood owing to limited taxon sampling and discordance between different genes. Here, a nine-gene dataset across 15 chirostyloids is presented, including the yeti crabs (Kiwaidae), to improve the resolution of phylogenetic affinities within and between the different families and to date key divergences using fossil calibrations. This study supports the monophyly of Chirostyloidea and within this, a basal split between Eumunididae and a Kiwaidae-Chirostylidae clade. All three families originated in the mid-Cretaceous but extant kiwaids and most chirostylids radiated from the Eocene onwards. Within Kiwaidae there is a basal split between the Northern Hemisphere seep-endemic *Kiwa puravida* and a Southern Hemisphere vent clade comprising *Kiwa hirsuta* and *Kiwa* spp. found on the East Scotia and South West Indian ridges. Although these results are consistent with a seep-to-vent evolutionary trajectory, the recent discovery of a kiwaid closely related to *K. puravida* at vents on the EPR raises the possibility that the common ancestor of extant kiwaids could have been vent-endemic. A divergence date estimate of 13.4-25.9 Ma between the Pacific and non-Pacific lineages is consistent with Kiwaidae spreading into the Atlantic sector of the Southern Ocean via the newly opened Drake Passage. The recent radiation of Kiwaidae adds to the list of chemosynthetic fauna that appear to have diversified after the Paleocene/Eocene Thermal Maximum, a period of possibly widespread anoxia/dysoxia in deep-sea basins.

2.2 Introduction

2.2.1 Anomura

The Anomura, an infraorder of decapod crustaceans comprising a diversity of forms, such as the squat lobsters, hermit, king, mole, coconut, hairy stone and porcelain crabs has been subjected to major taxonomic revisions in recent years (Morrison et al. 2002; Ahyong and O'Meally 2004; Perez-Losada et al. 2004; Macpherson et al. 2005; Ahyong et al. 2009; Bracken et al. 2009; Lemaitre and McLaughlin 2009; Toon et al. 2009; Schnabel et al. 2011a; Tsang et al. 2011). This is especially true for squat lobsters (Anomura with a proportionally elongated abdomen only partially folded under the thorax), which used to be grouped together along with porcelain crabs (Porcellanidae) in the superfamily Galatheoidea (Ahyong et al. 2011). Over the last five years however, morphological re-examinations and molecular phylogenetics have revealed that the squat lobster form probably evolved independently at least twice within Anomura (Lemaitre and McLaughlin 2009; Ahyong et al. 2010; Schnabel and Ahyong 2011; Schnabel et al. 2011a; Tsang et al. 2011). One of these groups, Galathoidea (Ahyong et al. 2010) now only comprises the squat lobster families Galatheidae, Munididae, Munidopsidae and Porcellanidae. The other clade comprises the freshwater squat lobster superfamily Aegloidea, the marine squat lobster Chirostyloidea and the crab-like Lomisoidea (represented by one species, *Lomis hirta*, the hairy stone crab) (Tsang et al. 2011). These two groups are each independently related to separate crab-like and hermit crab groups (Paguroidea), thus revealing the exceptional scope of morphological diversity within Anomura and the capacity for the convergent evolution of certain body shapes within Decapoda (Tsang et al. 2011).

2.2.2 Chirostyloidea

One of these squat lobster clades, the recently erected superfamily Chirostyloidea, (Schnabel and Ahyong 2011) is particularly enigmatic, owing to the paucity of species that have been sequenced. Until recently, the majority of the genera (*Chirostylus*, *Gastroptychus*, *Uroptychus*, *Uroptychodes*, *Hapaloptyx*, *Eumunida* and *Pseudomunida*) in this superfamily were placed in the family Chirostylidae (Ahyong et al. 2011). However, the discovery of the hairy 'yeti crab' *Kiwa hirsuta* (Macpherson et al. 2005) and the subsequent creation of a new family - Kiwaidae - concomitant with morphological and molecular phylogenetic studies (Schnabel et al. 2011a; Tsang et al. 2011), prompted the creation of a superfamily to house these genera, which were split into three families: Chirostylidae (*Chirostylus*, *Gastroptychus*, *Uroptychus*, *Uroptychodes*, *Hapaloptyx*) Eumunididae (*Eumunida* and *Pseudomunida*) and thirdly, Kiwaidae, represented by one genus, *Kiwa* (Schnabel and Ahyong 2011).

The phylogenetic relationship between chirostyloid families is still unclear, however. Analyses of rRNA ribosomal genes and morphological characters within anomura indicated that *Kiwa*, *Eumunida* and *Pseudomunida* formed a weakly supported paraphyletic clade along with the other chirostylid genera, but nodal support was insufficient for strong assertions (Schnabel et al. 2011a). Tsang et al. (2011) utilised five nuclear protein-coding genes across Anomura and found strong nodal support for a eumunidid-kiwaid clade as sister to Chirostylidae in the main chirostylid clade. This study was limited to some extent by using only three species to represent the chirostyloid families. Nevertheless, kiwaids and eumunidids do appear to share some morphological characters to the exclusion of Chirostylidae, most notably the shared presence of supraocular spines (Fig. 2.1), an epipod bearing maxilliped 1 and a distally annulated flagellum on the exopod (Ahyong et al. 2011; Schnabel and Ahyong 2011).

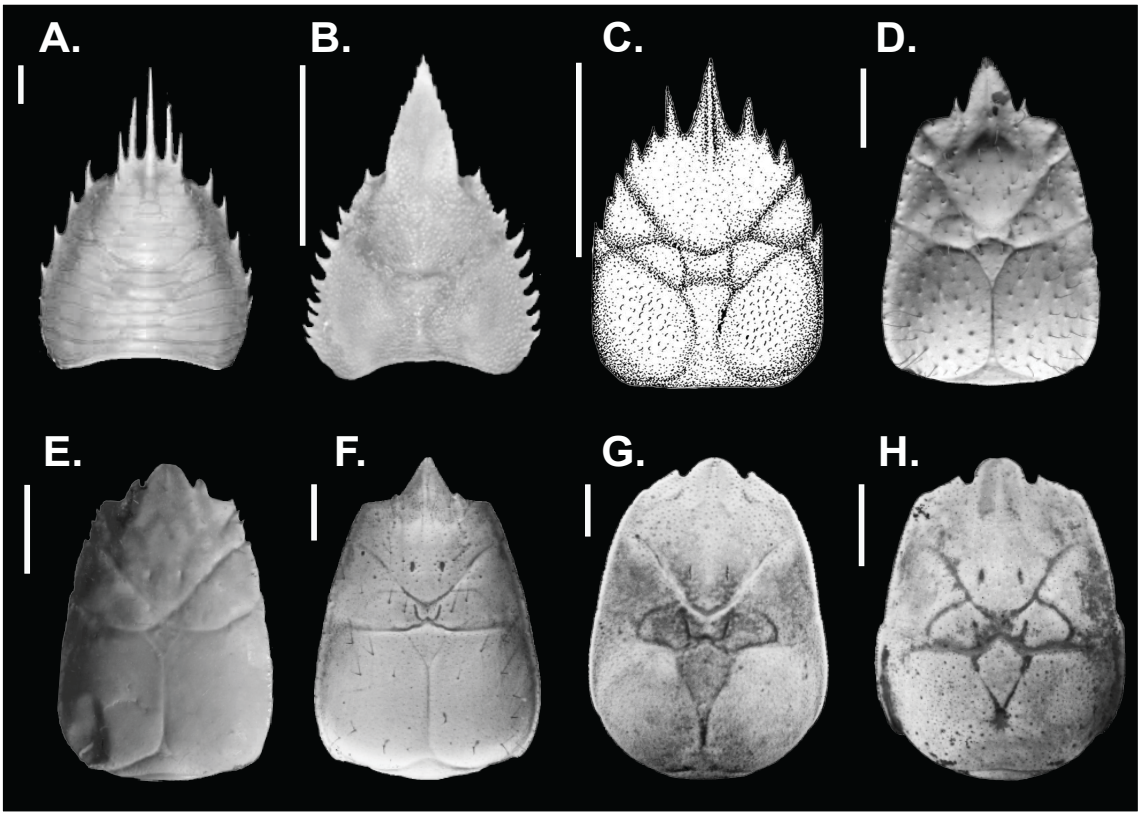

Figure 2.1. Modified photographs and illustrations of extant and extinct Chirostyloid carapaces: A) *Eumunida australis* (Eumunididae) modified from Schnabel and Ahyong (2011) B) *Uroptychus naso* (Chirostylidae) from Poore and Andreakis (2011) C) Fossil chirostyloid *Pristinaspina gelasina* from Schweitzer and Feldmann (2000) D) *Kiwa puravida* (Kiwaidae) from Thurber et al. (2011) E) Recently-discovered kiwaid collected from vents on the East Pacific Rise (Wang et al. 2013), not included in the genetic analyses of this study (image is courtesy of Xinming Liu) F) *Kiwa hirsuta* (Kiwaidae) from Macpherson et al. (2005) G) *Kiwa* sp. ESR, original photograph H) *Kiwa* sp. SWIR, original photograph. Supraocular spines either side of the rostrum are present on specimens A, D, E, F, G, H. White scale bars = 1 cm.

2.2.3 Chirostylidae & Eumunididae

Within Chirostylidae, the results of Schnabel et al. (2011) indicated that the species-rich *Uroptychus* genus might be polyphyletic, with the recently created *Uroptychodes* (Baba 2004) genus nested within. *Gastroptychus* a coral-associated genus characterised by long, slender appendages may in fact comprise two groups, as previously suggested based on morphology of the sternal plastron (Baba 2005); with one group as *Gastroptychus sensu stricto*, herein called *Gastroptychus* s.s. and a second group also nested within the *Uroptychus* clade. Within

Eumunididae, there appears to be strong morphological evidence of monophyly and although Schnabel et al. (2011) failed to generate a monophyletic clade of eumunidids using rRNA, recent molecular work using COI supports the monophyly of Eumunididae (Ahyong et al. 2011).

2.2.4 Kiwaidae

2.2.4.1 Described Species

The third chirostyloid family, Kiwaidae, is found exclusively in deep-sea chemosynthetic ecosystems, the only anomuran family known to be so and incorporates two recently described species of the genus *Kiwa* (Macpherson et al. 2005; Thurber et al. 2011). *Kiwa hirsuta*, found adjacent to hydrothermal vents on the Pacific Antarctic Ridge (P-AR) (Fig. 2.2B), was sufficiently divergent morphologically from other squat lobsters, owing to its distinctively elongated, setae-covered chelae and regionalised carapace (Fig. 2.1F), that a new family was immediately proposed (Macpherson et al. 2005). Such are the dramatic morphological differences between this clade and other anomura that a superfamily, Kiwaoidea, was briefly suggested (McLaughlin et al. 2007) until molecular work definitively placed *Kiwa hirsuta* along with the chirostylids and eumunidids in a new clade, the Chirostyloidea (Schnabel and Ahyong 2011; Schnabel et al. 2011a; Tsang et al. 2011).

It was speculated, based on the profusion of chemosynthetic filamentous bacteria found amongst the setae (Goffredi et al. 2008; Goffredi 2010), that yeti crabs may be partly reliant on farming these bacteria as a source of nutrition (Macpherson et al. 2005). This hypothesis was confirmed with the discovery of a second species in 2006 at cold seeps on the Pacific continental slope off Costa Rica (Fig. 2.2A), where isotope analyses established the principle

diet was of epibiotic bacteria, which are scraped off the setae by a specialised third maxilliped 'comb'. The second species of Kiwa to be discovered, *Kiwa puravida*, is remarkably similar in form to *K. hirsuta* and cytochrome c oxidase sub-unit I (COI) and rRNA 18S sequences have confirmed their close affinity (Thurber et al. 2011).

2.2.4.2 Recent Discoveries

A third species, currently being described (Sven Thatje et al. manuscript in preparation), was discovered in 2010 in the Atlantic sector of the Southern Ocean at vents on the East Scotia Ridge (ESR) as far south as 60˚ S (Fig. 2.2C). Unlike the two Pacific species, they have proportionally much shorter chelae, presenting a more anterior-posteriorly 'compressed' form, with the majority of the bacteria-growing setae concentrated on the ventral surface of the body rather than on the appendages. Despite the differences in morphology, rRNA sequences confirmed that *Kiwa* sp. ESR was closely related to *K. hirsuta* (6.45% divergence for 16S) (Rogers et al. 2012). In December 2011, a very similar kiwaid to *Kiwa* sp. ESR was discovered at the Dragon hydrothermal vent field on the Southwest Indian Ridge (SWIR) (Fig 2.2D) and initial COI analyses of six individuals revealed them to be ~ 3.6% divergent from all haplotypes of the ESR *Kiwas* (unpublished results). This level of divergence suggests that they could be separate species, based on a recent assessment of intra-specific and intra-generic divergence within Decapoda (da Silva et al. 2011) and interestingly, a similar level of divergence has also been found between species of a newly discovered genus of peltospirid gastropod found at the ESR and SWIR vents (4.4 %) (Chen et al. in submission).

Since the completion of the research presented here and its subsequent publication (see Appendix), there has come to light the mention of yeti crabs sampled at hydrothermal vents on the East Pacific Rise (EPR) at the junction between the EPR and the Galapagos Rift (GAR) on

the southern end of the Galapagos Microplate at depths of ~ 1600 m (Wang et al. 2013) (Fig. 2.2F). These yeti crabs appear superficially to resemble *K. hirsuta* and *K. puravida* with elongated setae-covered chelae (Fig. 2.2) and carapace markings (Fig. 2.1), in particular the overall shape, more 'serrated' rim and the prominent supraocular spines may hint at a close affinity to *Kiwa puravida* as do the proportions of the pereopods (walking legs) and the more sparse covering of setae (Fig. 2.2). The implications of this discovery will be discussed later in this chapter, including preliminary genetics reports from the author of the description (Xinming Liu, Third Institute of Oceanography, Xiamen, China).

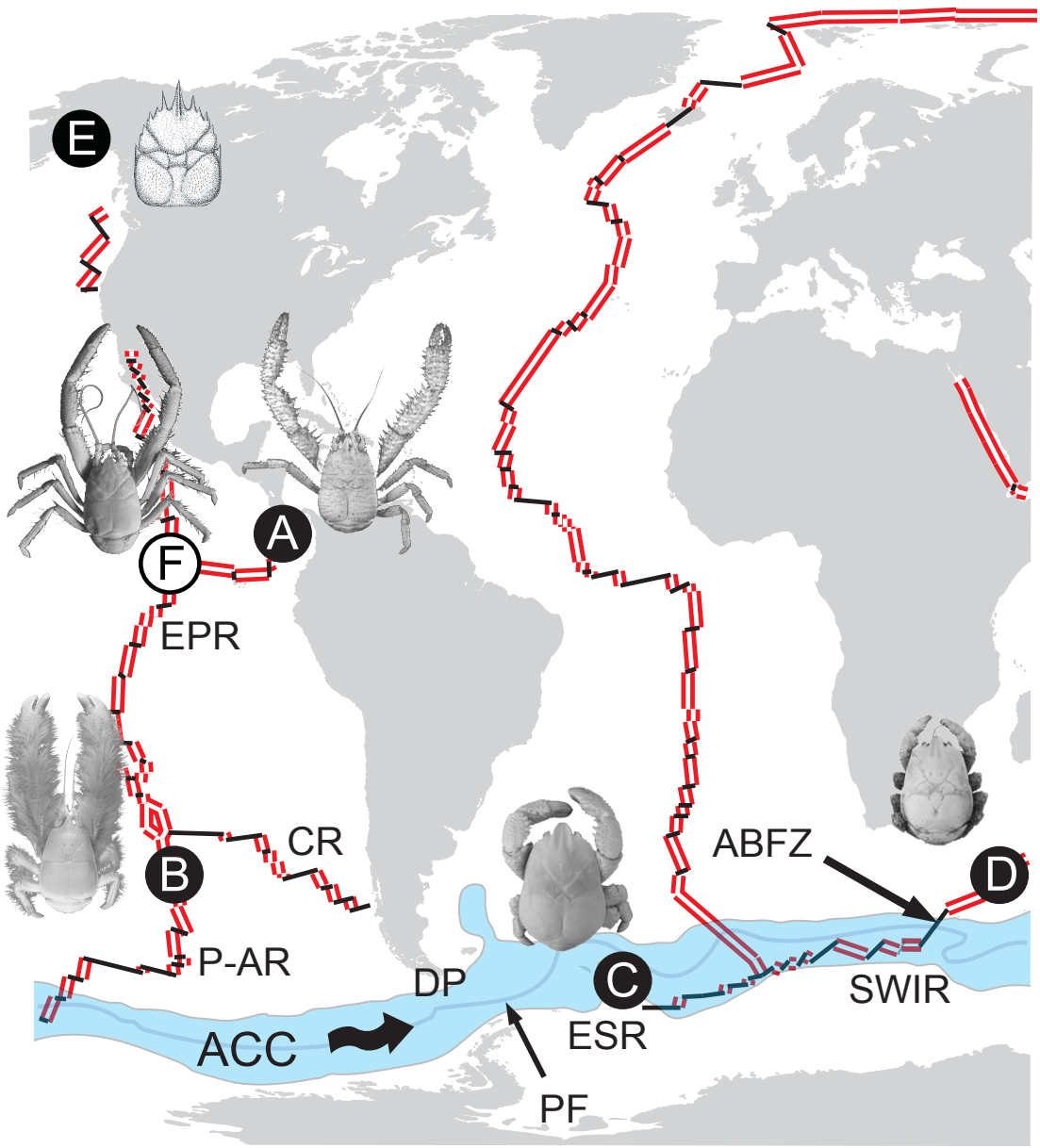

Figure 2.2. Map schematic showing locations of kiwaids, each with representative image, (A = *Kiwa puravida*, B = *Kiwa hirsuta* C = *Kiwa* sp. ESR, D = *Kiwa* sp. SWIR), as well as the location of the fossil *Pristinaspina gelasina* (E) and the putative kiwaid collected by a Chinese expedition (F) (Wang et al. 2013) in relation to mid ocean ridges (MORs) and the Antarctic Circumpolar Current (ACC). Double lines denote actively spreading MOR segments, single black lines representing intervening faults and fracture zones. Land shapes and ridge positions are modified from the NASA Digital Tectonic Activity Map (DTAM) (Lowman et al. 1999). Spreading ridge abbreviations are as follows: EPR = East Pacific Rise, P-AR = Pacific-Antarctic Ridge, CR = Chile Rise, ESR = East Scotia Ridge, SWIR = South West Indian Ridge, ABFZ = Andrew Bain Fracture Zone. Shaded area labeled ACC = Antarctic Circumpolar Current as defined by the Subantarctic Front to the north and the Southern Antarctic Circumpolar Current front to the south. PF = Polar Front. Wavy arrows illustrate direction of the ACC. DP denotes the Drake Passage. Photographs of *Kiwa puravida* and *Kiwa hirsuta*, courtesy of Shane Ahyong from Thurber et al. (2011) and Macpherson et al. (2005) respectively. Photograph of the putative kiwaid is courtesy of Xinming Liu.

2.2.5 Chirostyloid Fossil Record

The nature and timing of chirostyloid evolution is still unresolved. Details of chirostyloid fossils are lacking, in contrast to the galatheoids, for which there are many fossils dating back to the early Jurassic (Ahyong et al. 2011). Presently, there exists only one fossil attributed to the superfamily - *Pristinaspina gelasina* - a fossil recovered from upper-Cretaceous (Cenomanian to Maastrichtian) silica dominated deposits in Alaska (Schweitzer and Feldmann 2000). Originally thought to be a chirostylid, the distinctive carapace regionalisation characteristic of Kiwaidae (see Fig. 2.1) along with a broad medially carinate rostrum and supraorbital spines suggests that this animal is possibly a stem-lineage kiwaid (Schnabel and Ahyong 2011). However, as there are no early eumunidid or chirostylid fossils to compare with, the possibility that *P. gelasina* is really a stem-lineage chirostyloid cannot be ruled out at this stage. The matrix in which the fossil is encased indicates that the animal was buried in a deep-water muddy continental slope environment at present-day latitude, which is quite different from either the chemosynthetic environments of present day Kiwaidae or the deep-water coral habitats that many chirostylids and eumunidids are believed to be associated with (Baba 2005). Regrettably, the fossil was found in talus at the base of an exposed deposit, and therefore cannot be more accurately dated beyond the age range of the entire deposit ~ 99.6-65.5 Ma. Ahyong et al. (2011) have suggested that the Pacific location of the fossil, along with the present day location of *K. hirsuta* and *K. puravida* indicates the family has an eastern Pacific origin and posited that Kiwaidae might have originated in the Southern Hemisphere at high latitudes, with Aegloidea, a sister taxon of Chirostyloidea (Tsang et al. 2011) originating in the Northern hemisphere, based on a fossil, *Protaegla miniscula* found in Mexico (Feldmann et al. 1998). A hypothesised high-latitude origin for both families reflects a review of decapod fossils indicating that many taxa originated at high latitudes (Feldmann and Schweitzer 2006).

2.2.6 Study Aims

This study aims to resolve phylogenetic uncertainties in the Chirostyloidea and in particular, Kiwaidae, by analysing a concatenated nine-gene ribosomal and protein-coding DNA sequence dataset in order to:

1) Confirm the monophyly of Chirostyloidea and test the monophyly of Kiwaidae-Eumunididae

2) Investigate polyphyly within Chirostylidae

3) Reveal the internal phylogeny of the chemosynthetic clade Kiwaidae

4) Date the key divergences in Chirostyloidea and

5) Relate divergences in Kiwaidae to past tectonic and oceanographic events.

2.3 Methods

2.3.1 Taxon Sampling & Rationale

As many genera as possible from within Chirostyloidea have been included to avoid the incomplete taxon sampling of previous studies. Only the monotypic *Pseudomunida* and *Hapaloptyx* genera in Eumunididae and Chirostylidae, respectively, have not been included owing to tissue rarity. Non-chirostyloid anomurans in this study have been carefully chosen to provide fossil calibrations for estimating divergences within Chirostyloidea. Detailed justification for these fossil calibrations is included later in this section.

In total, 23 taxa were included in this study, featuring 15 chirostyloids, six other anomurans and two brachyurans (true crabs) as outgroups. Of the chirostyloids, nine specimens are chirostylids, two are eumunidids and four are kiwaids. Table 2.1 lists GenBank accession numbers and references for all loci. New sequences have been deposited in GenBank under the numbers KF051278-KF051401.

Table 2.1. Classification, sampling locations or provenance and voucher ID of the species and GenBank accession numbers of genes used in this study. 'X' denotes missing data. GenBank accession numbers in bold are new sequences from this study.

	Taxon	Sampling Origin / Provenance	Voucher ID (s)	16S	18S	28S	COI	NaK	Enolase	AK	GAPDH	PEPCK
BRACHYURA	*Eriocheir japonicus/sinensis*	China, Japan	Unv / MSLKHC-EjapHK	FJ455507	GU362670	GU362671	FJ455507	EU427132	GU382951	GU382901	GU383000	EU427201
	Callinectes sapidus	NW Atlantic	Unvouchered	NC006281	AY743951	X	NC006281	AF327439	AY522936	EU329140	AY522946	X
HIPPOIDEA												
Hippidae	*Hippa adactyla*	Indian Ocean	OUMNH 2004-03-0003	**KF051307**	**KF051278**	**KF051291**	X	GU383042	GU382914	GU382867	GU382964	GU383009
GALATHEOIDEA												
Munididae	*Munida spinosa*	JC 66 Cruise, SW Indian Ocean	Unvouchered	**KF051309**	**KF051280**	**KF051293**	**KF051391**	**KF051350**	**KF051364**	**KF051378**	**KF051336**	**KF051322**
Munidopsidae	*Shinkaia crosnieri*	Taiwan	Unv / NTOU A01106	EU420129	K. Chu	EU831285	EU420129	GU383061	GU382942	GU382892	GU382991	GU383028
Munidopsidae	*Munidopsis cf. serricornis*	JC 66 Cruise, SW Indian Ocean	Unvouchered	**KF051308**	**KF051279**	**KF051292**	X	**KF051349**	**KF051363**	**KF051377**	**KF051335**	**KF051321**
LOMISOIDEA												
Lomisidae	*Lomis hirta*	South Australia	Unv / KAClohi / NTOU A00840	AF436052	AF436013	AF435993	AY595672	EU427118	GU382917	GU382870	GU382967	EU427187
AEGLOIDEA												
Aeglidae	*Aegla alacalufi*	South America	KACa 1144, 798, 0090 / Unv	FJ472207	EU920958	AY595958	FJ471841	GU383035	GU382903	GU382856	GU382953	GU383002
CHIROSTYLOIDEA												
Chirostylidae	*Chirostylus* aff. *stellaris*	Tin-Yam Chan, NTU, Taiwan	NTOU A01347	**KF051311**	**KF051282**	**KF051295**	**KF051392**	**KF051352**	**KF051366**	**KF051380**	**KF051338**	**KF051324**
Chirostylidae	*Gastroptychus formosus*	E. Macpherson (CEAB) NW Spain	Unvouchered	**KF051312**	**KF051283**	**KF051296**	**KF051393**	**KF051353**	**KF051367**	**KF051381**	**KF051339**	**KF051325**
Chirostylidae	*Gastroptychus rogeri*	K. Schnabel (NIWA) New Zealand	NIWA 14598	**KF051313**	HQ380285	**KF051297**	**KF051394**	**KF051354**	**KF051368**	**KF051382**	**KF051340**	**KF051326**
Chirostylidae	*Gastroptychus* sp. 3804	JC 66 Cruise, SW Indian Ocean	Unvouchered	**KF051314**	**KF051284**	**KF051298**	**KF051395**	**KF051355**	**KF051369**	**KF051383**	**KF051341**	**KF051327**
Chirostylidae	*Uroptychodes grandirostris*	Taiwan	NTOU A01103	X	**KF051288**	**KF051303**	X	GU383067	GU382948	GU382898	GU382997	GU383034
Chirostylidae	*Uroptychus rubrovittatus*	NW Spain	Unvouchered	**KF051316**	**KF051285**	**KF051300**	**KF051397**	**KF051357**	**KF051371**	**KF051385**	**KF051343**	**KF051329**
Chirostylidae	*Uroptychus scambus*	K. Schnabel (NIWA) New Zealand	NIWA 10198	**KF051315**	EU821553	**KF051299**	**KF051396**	**KF051356**	**KF051370**	**KF051384**	**KF051342**	**KF051328**
Chirostylidae	*Uroptychus* sp. 3730	JC 66 Cruise, SW Indian Ocean	Unvouchered	X	**KF051286**	**KF051301**	**KF051398**	**KF051358**	**KF051372**	**KF051386**	**KF051344**	**KF051330**
Chirostylidae	*Uroptychus* sp. 3836	JC 66 Cruise, SW Indian Ocean	Unvouchered	**KF051317**	**KF051287**	**KF051302**	**KF051399**	**KF051359**	**KF051373**	**KF051387**	**KF051345**	**KF051331**
Eumunidae	*Eumunida funambulus*	Taiwan	KC3100 / NTOU A01104	EU920922	EU920957	EU920984	X	GU383041	GU382913	GU382866	GU382963	GU383008
Eumunidae	*Eumunida picta*	C. Morrison (USGS) NW Atlantic	Unv / MNHN:N1880	**KF051310**	**KF051281**	**KF051294**	EU243558	**KF051351**	**KF051365**	**KF051379**	**KF051337**	**KF051323**
Kiwaidae	*Kiwa hirsuta*	Pacific Antarctic Ridge	MNHN-Ga5310	EU831286	EU920942	U831284	Joe Jones	GU383044	GU382916	GU382869	GU382966	GU383011
Kiwaidae	*Kiwa puravida*	A. Thurber (OSU) Costa Rica	Unvouchered	**KF051318**	JN367460	**KF051304**	JN383822	**KF051360**	**KF051374**	**KF051388**	**KF051346**	**KF051332**
Kiwaidae	*Kiwa* sp. ESR	JC 42 Cruise, East Scotia Ridge	Unvouchered	**KF051319**	**KF051289**	**KF051305**	**KF051400**	**KF051361**	**KF051375**	**KF051389**	**KF051347**	**KF051333**
Kiwaidae	*Kiwa* sp. SWIR	JC 67 Cruise, SW Indian Ocean	Unvouchered	**KF051320**	**KF051290**	**KF051306**	**KF051401**	**KF051362**	**KF051376**	**KF051390**	**KF051348**	**KF051334**

Nearly half of the new sequences generated in this study came from specimens collected on two cruises aboard the Royal Research Ship (RRS) *James Cook*. The ChEsSO consortium (Chemosynthetic EcoSystems of the Southern Ocean) cruise JC 42 to hydrothermal vents on the East Scotia Ridge, in the Scotia Sea yielded tissue of the kiwaid, *Kiwa* sp. ESR (Rogers 2010). Cruise JC 66/67 to the South West Indian Ridge and surrounding seamounts, yielded specimens of another kiwaid, provisionally called here *Kiwa* SWIR, which was also found on hydrothermal vents (Copley 2011). On the surrounding seamounts, specimens of *Munida spinosa*, a *Munidopsis* in the *serricornis* complex, a *Gastroptychus* with morphological affinities to the group including *G. novaezelandiae* (Baba 2005), and three unidentified species of *Uroptychus* were also collected (see Table 2.1). Tissue samples from *Gastroptychus rogeri* and *Uroptychus scambus* were donated from the collections of the National Institute of Water and Atmospheric Research of New Zealand (NIWA), courtesy of Kareen Schnabel and tissue samples of *Chirostylus* aff. *stellaris* and *Uroptychodes grandirostris* were donated from the National Taiwan University (NTU), courtesy of Tin-Yam Chan. From Europe, a tissue sample of *Hippa adactyla* was donated by The Oxford University Museum of Natural History (OUMNH) courtesy of Sammy De Grave and tissue samples of *Uroptychus rubrovittatus* and *Gastroptychus formosus* were donated by Enrique Macpherson of Centro de Estudios Avanzados de Blanes (CSIC). Cheryl Morrison, of the U.S. Geological Survey, at the Leetown Science Center, donated tissue of *Eumunida picta*. The remaining sequences were taken from Genbank (Table 2.1).

2.3.2 Molecular Methods

2.3.2.1 DNA Extraction & Molecular Marker Choice

Total genomic DNA was extracted from pereopods, pleopods or antennae using the Qiagen DNeasy® Blood and Tissue Kit (Cat. 69506) following the manufacturer's instructions or, in cases where tissue quantities were very small, a CTAB DNA extraction protocol (Doyle and Dickson 1987). Nine gene sequence regions were selected in this study: fragments of the ribosomal rRNA genes, 16S (~ 500 bp), 18S (~ 1900 bp) and 28S (~ 300 bp) as well as ~ 500 bp fragments of the protein-coding genes cytochrome c oxidase subunit 1 (COI), arginine kinase (AK), enolase, glyceraldehyde 3-phosphate dehydrogenase (GAPDH), sodium potassium ATPase α subunit (NaK), and phosphoenolpyruvate carboxykinase (PEPCK). Of these genes, two are mitochondrial (16S and COI).

The reasons for choosing these markers are threefold:

1. These are the markers that have been used most in phylogenetic studies on Anomura, which meant that taxa could be included in this study for which there was no tissue available in this study.
2. The two most recent papers on this topic (Schnabel et al. 2011a; Tsang et al. 2011) focused on either protein-coding genes or rRNA ribosomal genes. Both types of markers have advantages and disadvantages. Protein-coding genes are very easy to align, but are constrained by the functionality of the gene, increasing the likelihood that there may have been multiple silent mutations in redundant codon positions, thus reducing the probability that the same base pair at a given locus is homologous between

two species. rRNA ribosomal genes are also functionally constrained in that they must fold into a three-dimensional shape, but there are regions of the gene that are highly variable where there can be large insertions and deletions without destroying functionality. These insertions and deletions make alignment rather difficult, which can have down-stream impacts on phylogenetic inferences. Combining these two datasets, therefore may minimize these biases.

3. COI was added to the combined gene list of Tsang et al. (2011) and Schnabel et al. (2011) as it is a commonly used barcoding gene (da Silva et al. 2011), which is good at examining recent divergences in crustaceans.

2.3.2.2 PCR & Sequencing Reactions

New Primers were designed using Geneious Pro 5.4.6 (Drummond et al. 2010) by downloading the largest possible relevant gene fragments for anomuran crustaceans and in particular, chirostyloid squat lobsters. In some cases it was possible to download whole mtDNA genomes. Alignments were created in Geneious Pro 5.4.6 and conserved regions were identified by eye. A series of primers were then designed with varying degrees of specificity (Table 2.2) on the assumption that some primers would be more effective than others, particularly with the more divergent genes, such as COI and 16S.

Table 2.2. List of primers used in this study. Newly designed primers in bold.

Gene	Primer	Sequence (5'-3')	Source
Arginine kinase	AK for a-1	CTCCCCTSTTTGAYCCCATCAT	Tsang et al. 2011
	AK for a-2	ACCCCATCATTGAGGAYTAYCA	Tsang et al. 2011
	AK for b	ATAGACGACCACTTCCTSTTCAA	Tsang et al. 2011
	AK rev 1	TGGAACTCAGTCAGACCCATRCG	Tsang et al. 2011
	AK rev 2	CCGCCCTCAGCCTCRGTGTGYTC	Tsang et al. 2011
Enolase	Enol EA1	CAGCAATCAATGTCATCAAYGGWGG	Tsang et al. 2011
	Enol EA2	AGTTGGCTATGCAGGARTTYATGAT	Tsang et al. 2011
	Enol ES1	ACTTGGTCAAATGGRTCYTCAAT	Tsang et al. 2011
	Enol ES2	ACCTGGTCGAATGGRTCYTC	Tsang et al. 2011
Glyceraldehyde 3-phosphate dehydrogenase	GAPDH F2	ATGAAGCCAGAAAACATTCCATGG	Tsang et al. 2011
	GAPDH GA	ATGGTGTATATGTTCAAGTAYGAYTC	Tsang et al. 2011
	GAPDH R	GAATAGCCTAACTCGTTGTCRTACCA	Tsang et al. 2011
	GAPDH GR	TCGCTAGATACAACATCATCYTCRGT	Tsang et al. 2011
Phosphoenolpyruvate carboxykinase	PEPCK for	GTAGGTGACGACATTGCYTGGATGAA	Tsang et al. 2008
	PEPCK for2	GCAAGACCAACCTGGCCATGATGAC	Tsang et al. 2008
	PEPCK rev	GAACCAGTTGACGTGGAAGATC	Tsang et al. 2008
	PEPCK rev3	CGGGYCTCCATGCTSAGCCARTG	Tsang et al. 2008
Sodium potassium ATPase α-subunit	NaK for-a	GTGTTCCTCATTGGTATCATTGT	Tsang et al. 2008
	NaK for-b	ATGACAGTTGCTCATATGTGGTT	Tsang et al. 2008
	NaK rev	ACCTTGATACCAGCAGATCGGCACTTGGC	Tsang et al. 2008
	NaK rev2	ATAGGGTGATCTCCAGTRACCAT	Tsang et al. 2008
Cytochrome Oxidase subunit I	LCO1490	GGTCAACAAATCATAAAGATATTGG	Folmer et al. 1994
	HCO2198	TAAACTTCAGGGTGACCAAAAAATCA	Folmer et al. 1994
	COIR1	ACNTTATATTTTATYTTYGG	Cabezas et al. 2008
	COIgalF	YGGMRCTTGAGCTGGTATAGTA	**This Study**
	COIgalR	ACCAATTGCTAGTATAGCATAAA	**This Study**
	COIchiF	DCATGAGCBGGTATAGTTGG	**This Study**
	COIchiR	AAATGYTGRTATAAAATDGGATCTC	**This Study**
	COIkiwF1	ATCATAAAGATATTGGAACWCTAT	**This Study**
	COIkiwF2	CAAATCATAAAGATATTGGAAC	**This Study**
	COIkiwR1	CAGCAGGATCAAAGAAAGAA	**This Study**
	COIkiwR2	CGATCTGTTAAAAGTATAGTAATG	**This Study**

Table 2.2 continued.

Gene	Primer	Sequence (5'-3')	Source
16S rRNA Ribosomal	16S L	CGCCTGTTTAACAAAAACAT	Ahyonh & O'Meally 2004
	16S H	CCGGTCTGAACTCAGATCACGT	Ahyonh & O'Meally 2004
	16S ChiroF	TTCTTGCCTGTTTAACAAAAAC	**This Study**
	16S ChiroR3	GGTCTGAACTCAAATCATGTAAA	**This Study**
18S rRNA Ribosomal	18e	CTGGTTGATCCTGCCAGT	Halanych et al. 1998
	18S F90	CGAATGGCTCATTAAATC	**This Study**
	18S F448	GGAGAGGGAGCCTGAGAAAC	Rogers et al. 2012
	18S F548	GGTAATTCCAGCTCCAATAG	**This Study**
	18S F896	TTAGAGTGCTCAGAGCAGGC	Rogers et al. 2012
	18S F1095	CACTAAATCATTCAATCGGTAGT	**This Study**
	18S F1265	GGCTTAATTTGACTCAACAC	**This Study**
	18S F1437	ATGGCCGTTCTTAGTTGGTG	Rogers et al. 2012
	18S F1857	TTCCCATGAACGAGGAATTC	Rogers et al. 2012
	18P	TAATGATCCTTCCGCAGGTTCACCT	Halanych et al. 1998
	18S R	CACTAAATCATTCAATCGGTAGT	**This Study**
	18S R 143	AAGGCCTCACTRAAYCATTC	**This Study**
	18S R495	CACAGACCTGTTATTGCTCA	**This Study**
	18S R498	AAGGGCATCACAGACCTGTT	Rogers et al. 2012
	18S R1074	TATCTGATCGCCTTCGAACC	Rogers et al. 2012
	18S R1106	TAAACATGCCRGCCACTC	**This Study**
	18S R1450	CGGGAGTGGGTAATTTGC	**This Study**
	18S R1536	ACGAGCTTTTTAACCGCAAC	Rogers et al. 2012
28S rRNA Ribosomal	28S-F216	CTGAATTTAAGCATATTAATTAGKGSAGG	Ahyong et al. 2009
	28S-R443	CCTCACGGTACTTGTTCGCTATCGG	Ahyong et al. 2009
	28S Chiro F	CCCTTAGTAAGTGMGACTGAA	**This Study**
	28S Chiro R	ATATTTAGCCTTAGATGGAGTTT	**This Study**

Polymerase chain reactions (PCR) were performed in 12 µl volumes, containing 0.8 µl of each primer (forward and reverse) at a concentration of 4 pmol/µl, 8 µl of Qiagen HotStarTaq Master Mix, 2 µl of DNA template (~ 10-50 ng/µl) and 0.4 µl of double-distilled water. All PCR reactions were performed on a Bio-Rad C1000 Thermal Cycler. Primers used to amplify and sequence these genes, including 15 newly designed, are listed in Table 2.2.

PCR protocols are as follows:

Initial HotStarTaq denaturation at 95 ˚C for 15 minutes, followed by 35 cycles of 94 ˚C for 1 min, 50 ˚C for 90 seconds, 72 ˚C for 1 min, and a final extension of 72 ˚C for 10 min.

In some cases template quality and quantity was insufficient in producing PCR product and a touchdown protocol was instead necessary:

Initial HotStarTaq denaturation at 95 ˚C for 15 minutes, followed by 16 cycles of 94 ˚C for 1 min, 60 ˚C for 90 seconds (decreasing by 0.5 ˚C per cycle), 72 ˚C for 1 min, and a then 35 cycles of 94 ˚C for 1 min, 46 ˚C for 90 seconds, 72 ˚C for 1 min with a final extension of 72 ˚C for 10 min.

Annealing temperatures were adjusted slightly in some cases to maximise the quality and quantity of PCR product.

The PCR products were visualised on 1% agarose gel using ethidium bromide. PCR products were then purified either using the QIAquick gel purification kits (Cat.28106) or Diffinity RapidTips (RT025-096). Sequencing reactions were performed in 10 µl volumes, containing 2.5 µl cleaned PCR product, 2 µl H_2O, 2.5 µl of 0.8 pmol/µl primer 2.5 µl BetterBuffer (or 6X Buffer) and 0.5 µl BigDye™.

The sequencing reaction protocol was as follows:

Initial denaturation at 96 ˚C for 1 minute, followed by 25 cycles of 96 ˚C for 10 seconds, 50 ˚C for 5 seconds, 60 ˚C for 4 min, and a final cool down to 4 ˚C.

Sequences were resolved using an Applied Biosystems 3100 DNA and consensus sequences were generated from forward and reverse strands using Geneious Pro 5.4.6 (Drummond et al. 2010).

2.3.2.3 Alignment

Protein-coding genes (COI, NaK, Enolase, AK, GAPDH and PEPCK) were aligned using the geneious alignment tool in Geneious Pro 5.4.6 (Drummond et al. 2010) using the progressive multiple alignment method. Aligning the ribosomal genes (16S, 28S and 18S) is more challenging owing to multiple insertions and deletions and were therefore aligned using the online version of MAFFT 6 (Katoh et al. 2009) and then adjusted by eye. MAFFT (Multiple sequence Alignment based on Fast Fourier Transform) performs better with larger datasets that are more difficult to align than other commonly used progressive method-based algorithms such as Clustal W (Katoh et al. 2009). The MAFFT L-INS-I alignment iteration strategy was considered the most optimal for these sequences according to the online version ‘auto’ setting, with the other alignment parameters set to default.

Extremely variable regions in the rRNA sequences that were difficult to align with any confidence were excised using the online version of Gblocks (Castresana 2000), hosted by the Castresana lab, Institut de Biologia Evolutiva (CSIC-UPF), Barcelona. This software is designed to eliminate highly divergent and poorly aligned regions of a DNA alignment. These

positions may not be homologous or may have been saturated by multiple substitutions and their removal will reduce the probability that incorrect phylogenetic inferences are made.

Finally, the remaining gaps in the alignment of rRNA ribosomal genes were considered to be potentially informative and were coded for, using the FastGaps software, which employs the methods of Simmons and Ochoterena (2000). The resulting gap-coding blocks were pasted to the ends of each rRNA sequence alignment to yield the final sequence dataset.

The final alignment lengths are as follows: 16S (518 bp), 18S (1681 bp), 28S (232 bp), COI (585 bp), NaK (582 bp), Enolase (339 bp), AK (600 bp), GAPDH (522 bp), PEPCK (501 bp), resulting in a concatenated total alignment of 5560 base pairs.

2.3.2.4 Partitioning & Substitution Model Choice

Many phylogenetic software packages allow for concatenated sequence datasets to be partitioned in some way, so that substitution models and rates, for example, can be assigned to each partition separately. The resultant dilemma is that there are many ways to partition a dataset, e.g., according to codon position or by gene and the more potential partitions there are, the number of possible partition combinations increases exponentially (Blair and Murphy 2011).

To avoid having to do multiple phylogenetic analyses on a shortlist of possible partition strategies, a more objective approach has been chosen which allows the simultaneous evaluation of the best partition scheme as well as the appropriate substitution model for each partition without the pitfall of the *ad hoc* approach commonly used. PartitionFinder, an open source program allows users to select partitioning schemes and substitution models using a range of information-theoretic metrics such as the Bayesian Information Criterion (BIC), Akaike

Information Criterion (AIC), and corrected AIC (AICc) (Lanfear et al. 2012). The optimal partition scheme is found using a heuristic approach, as the possible schemes from a dataset with as many as 21 possible partitions, would be astronomical. Here, the commonly used AIC was used to rank partition schemes and the partition models. The less commonly used BIC metric was also used to provide an alternative model and partition scheme as it penalises models that are 'over-parameterised' to a greater extent than AIC or AICc (Minin et al. 2003). Consequently, all downstream analyses from this point onwards were performed once for an AIC-ranked partition scheme and once for a BIC-ranked partition scheme. Optimal partitioning schemes according to the two metrics and their accompanying substitution models are shown in Table 2.3.

Table 2.3. Substitution models used in this study as determined by PartitionFinder.

Information Criterion	Partition scheme	Character set	MrBayes & Garli	Beast
AIC	Nine Partition	16S	GTR+G	GTR+G
		18S	SYM+I+G	TrNef+I+G
		28S	K80+G	K80+G
		COI 1st	SYM+I	TrNef+I
		COI 2nd	GTR+I	GTR+I
		COI 3rd	HKY+G	TrN+I+G
		Nuclear Protein 1st	GTR+I+G	GTR+I+G
		Nuclear Protein 2nd	GTR+I	GTR+I
		Nuclear Protein 3rd	GTR+G	GTR+G
BIC	Six Partition	16S	GTR+G	GTR+G
		18S - 28S	K80+I+G	TrNef+I+G
		COI 1st + 2nd	SYM+G	TrNef+G
		COI 3rd	HKY+G	TrN+I+G
		Nuclear Protein 1st + 2nd	HKY+I+G	TrN+I+G
		Nuclear Protein 3rd	GTR+G	GTR+G

2.3.3 Phylogenetic Analyses

2.3.3.1 Tree-Building Methods

Two different methods for determining phylogenies were performed in this study: maximum likelihood (ML) and Bayesian inference (BI). These two phylogenetic methods are an improvement on methods commonly used previously such as the distance method of Neighbour Joining (NJ) and the character-based Maximum parsimony (MP).

Distance methods summarise the sequence data into a matrix of pairwise distances. The best tree should have the smallest overall distance. This method can be computationally quick, but a

great deal of information is lost in compressing the data in this way. Parsimony methods, like MP map the history of gene sequences onto a tree. By assessing the plausibility of the mutations that a particular tree would require to explain the data, a score, can be assigned to each tree. This score is the minimum number of mutations that could possibly produce the data. While this method has advantages over distance methods like NJ in that the sequence data are not compressed and models of sequence evolution can be applied, this method can suffer from long-branch attraction, where sequences in two highly divergent species may be similar owing to convergent evolution (Holder and Lewis 2003).

ML improves on parsimony by being able to reconstruct the relationships between sequences that are highly divergent, or are evolving rapidly. ML seeks a tree that maximizes the probability of observing the sequence data given that tree (Hall 2004). In essence it is the probability of getting the observed data given a particular tree. The main problem is the computational burden, as algorithms that find the ML score must search through a multidimensional space of parameters and must often score the same tree hundreds of times (Holder and Lewis 2003). ML, like other methods above, assigns confidence in tree branching structure by means of nonparametric bootstrapping – a type of pseudoreplication.

BI, however, produces a probability distribution on trees (the posterior distribution) given the model of evolution, the observed sequence data, and a specification of background knowledge (the prior probability distribution). In essence, it is the probability of the tree, given the data and model. BI phylogenetics packages use a search algorithm (Markov Chain Monte Carlo – MCMC) to approximate the posterior probability and estimate the tree parameters. Confidence in the branching structure of a given tree is expressed in terms of a posterior probability (i.e. the probability that a tree is correct given model and data), which is simple to interpret, in comparison to bootstrapping methods, for which there is debate about whether bootstrap percentages can be interpreted as fully equivalent to a confidence measure (Yang and Rannala 2012). Criticisms of BI are focused on the need for a prior distribution, meaning that the

posterior distribution can be strongly influenced by the priors rather than the likelihood, especially when the data are not very informative. Also, posterior probability estimates have been shown to often overstate confidence in branching structure (Yang and Rannala 2012).

Given the ability of the ML and BI methods to incorporate more sophisticated models of evolution, and the fact that faster computers now allow intensive analyses to be performed over a period of hours rather than days or weeks, these approaches were chosen above distance and parsimony methods for this study.

ML analyses were performed using GARLI 2.0 (Zwickl 2006), with two replicate runs per partition scheme, each with 200 bootstrap pseudo-replicates to determine node support. BI for both partition schemes was performed using MrBayes 3.2 (Ronquist & Huelsenbeck, 2003). Metropolis Coupled Monte Carlo Markov Chains were run for 10 million generations in two simultaneous runs, each with four differently heated chains. Model parameters were estimated during the analysis. Convergence of the analyses was validated by the standard deviation of split frequencies and examination of the potential scale reduction factors (PSRFs) in MrBayes and by monitoring of the likelihood values over time using Tracer v1.5 (Rambaut and Drummond 2007). Topologies were sampled every 1,000 generations and the first 2,500 trees (25%) were discarded as 'burn-in'.

2.3.3.2 Topology Hypothesis Testing

Given the uncertainty regarding the affinity of Kiwaidae, Eumunididae and Chirostylidae within Chirostyloidea, three alternative *a priori* topological hypotheses were tested here using the assessment of the marginal model likelihoods using the recently proposed stepping-stone method in MrBayes 3.2 (Ronquist et al. 2012). The first hypothesis proposes a Kiwaidae-

Eumunididae clade, which is sister to Chirostylidae, whilst the second proposes Kiwaidae-Chirostylidae clade and the third proposes a Eumunididae-Chirostylidae clade as sister to Kiwaidae. The stepping-stone method has been shown to be more reliable than the commonly used comparison of the harmonic means of negative log-likelihoods (Xie et al. 2011). For each topology constraint, two simultaneous analyses were performed for 2.5 million generations, with default settings. The two runs produced very similar results (see Table 2.4), indicating the analyses were run for a sufficient number of generations.

2.3.4 Divergence Estimation

Bayesian estimation of divergence times was performed with Beast 1.7.4 (Drummond and Rambaut 2007) for the entire concatenated dataset. As with the phylogenetic analyses, all Beast analyses were performed in tandem; with one set of analyses on the AIC-ranked partition scheme and another on the BIC-ranked partition scheme. In all cases, substitution models and clock models were unlinked across the partitions.

Base frequencies were estimated for all partitions except where substitution models specified equal frequencies. Tuning parameters for the Markov chain Monte Carlo (MCMC) operators were set to auto-optimise and successive runs were tuned accordingly. Each MCMC chain commenced from a starter tree based on the topology of the phylogenetic trees created in the previous section and run for 50 million generations. Two independent runs were performed; each run was sampled every 1,000 generations and 10% of samples were removed from each run as ‘burn-in’. The runs were combined using LogCombiner v.1.7.4 to obtain a number of independent samples from the marginal posterior distribution. Effective sample size values were greater than 200 for all parameters (most were at least one order of magnitude greater) and the Beast output was visualised on Tracer v.1.5 (Rambaut & Drummond, 2007)

2.3.4.1 Fossil Calibrations

There has been to date, only one likely fossil member of the Chirostyloidea uncovered; *Pristinaspina gelasina*, which is dated from upper Cretaceous deposits in Alaska. This fossil was originally considered a chirostylid before the existence of Kiwaidae was known (Schweitzer and Feldmann 2000). Subsequent examination of its distinctive carapace markings suggest it may be a stem-lineage kiwaid, however, the lack of any definitive proto-chirostyloid fossils, in conjunction with the fact that it shares some features with Eumunididae (prominent supraocular and lateral carapace spines) raises doubts concerning its efficacy as a fossil calibration point for kiwaid divergence. *Pristinaspina* could conceivably be a stem-lineage chirostyloid, given the lack of any clear chirostylid or Eumunidid fossils. For this reason, *Pristinaspina* has not been included as a fossil calibration point in this study. However, it may be possible, based on the divergence dates between Kiwaidae and the other chirostyloids to reveal whether the age for this fossil is consistent with it being a stem-lineage kiwaid or chirostyloid. Another fossil originally assigned to Eumunididae, *Protomunida pentacantha*, has now been reevaluated and placed in the galathoid genus *Sadayosha* (Ahyong et al. 2011).

Consequently, three other fossil records were identified as calibration points on the basis of being clearly the earliest representative at a particular taxonomical level for that node. These are in reverse chronological order:

1. *Protaegla miniscula* (Aeglidae) of Albian age, 99.6-112 Ma. Earliest appearance of Aeglidae in the fossil record (Feldmann et al. 1998).
2. *Juracrista perculta* (Munididae) of Tithonian age, 145.5-150.8 Ma (Robins et al. 2012). Earliest appearance of Munididae in the fossil record.
3. *Platykotta akaina* (Platykottidae) of Norian-Rhaetian age, 199.6-216.5 Ma. Earliest appearance of an anomuran in the fossil record (Chablais et al. 2011).

The date ranges above are based on the latest dating scheme for the strata in which these fossils were discovered (Gradstein et al. 2004). In this study, an approach has been used where in the absence of information regarding the upper bound for a divergence date, an exponential prior distribution in the Beast analyses has been used as recently recommended (Ho and Phillips 2009). The fossils used as calibration points are, by nature of being clearly assigned to clades that exist after the divergences in question, an underestimation of the likely true divergence dates. Therefore only the most recent possible divergence dates can be inferred in this Beast analysis. For the above dating scheme, exponential priors shapes have been used, where the modal value (age) is the most recent possible age for the stratum containing the calibration fossil and the 97.5% quantile represents the upper age of that same stratum. This prior shape allows Beast to explore older ages for divergences if a particular fossil calibration is, relative to the other fossil calibrations, much younger than the divergence date for which it represents.

The use of *Protaegla miniscula* as a calibration for the divergence of Aeglidae and Lomisidae is justified on the grounds that both Tsang et al. (2011) and Schnabel et al. (2011), grouped them together within a monophyletic clade, based on morphological and molecular phylogenetic analyses, with the carcinised form of Lomisidae as the more derived. *Protaegla miniscula* dating from ~ 99.6-112 Ma is clearly, however, an aeglid, although one found in marine sediments, unlike the extant *Aegla* genus which is found only in South American freshwater ecosystems (Feldmann et al. 1998).

Juracrista perculta has been recently identified as a munidid and pushes the earliest occurrence of the family back from the Cretaceous into the late Jurassic (~ 145.5-150.9 Ma) (Robins et al. 2012). Although the earliest occurrence of Munidopsidae is from the mid-Jurassic (Ahyong et al. 2011), there is some disagreement concerning the basal split within the Galatheoidea. Schnabel et al. (2011) produced a tree topology with a basal split between Munidopsidae and all other Galatheoidea including Munididae, but Tsang et al. 2011 showed a basal split in the

galatheoidea between Porcellanidae and all other galathoids. Tsang et al. (2011) also considered it likely that the common ancestor of all galatheoids was squat lobster in form and therefore the earliest galathoid fossils, which have been assigned to Munidopsidae, could conceivably be stem-lineage galathoids, and not true munidopsids. This uncertainty prompts the use of the earliest munidid fossil as the calibration point for the split between the Munidopsidae and Munididae.

The choice of the late Triassic (199.6-216.5 Ma) *Platykotta akaina* as a calibration point for the most recent common ancestor (MRCA) of anomura is based simply on the fact that it is the earliest fossil assigned to the anomura and that the next available anomuran fossils in terms of antiquity are clearly galatheoid squat lobsters (Ahyong et al. 2011; Chablais et al. 2011). A comprehensive divergence study of anomura using multiple external fossil calibrations currently underway by Heather Bracken-Grissom (personal communication) suggests that the MRCA for anomura existed between 200 and 245 Ma ago, with a median age of 221 Ma, which is only marginally older than the age ranges for *Platykotta akaina*.

2.4 Results

2.4.1 Data Summary

2.4.1.1 Sequencing & Missing Data

Of the 23 sequence sets produced, 14 were complete, five were missing a single gene fragment and one (*Uroptychodes grandirostris*) was missing two gene fragments (see Table 2.1). A total of 121 new DNA sequences were obtained. PCR amplification of the mitochondrial genes was particularly difficult with tissue that was older than five years and accounted for five of the seven missing DNA sequence fragments. In total, 95.7% of the genes were successfully sequenced. Simulations of phylogenetic analyses on missing data show that ML and BI in particular, are still effective at determining true phylogenies when there is missing data, especially when the total number of characters analysed is large. In fact, even with small datasets, a total coverage of over 80% should deliver accurate results (Wiens 2006; Wiens and Moen 2008). For this reason, the less than full coverage was not considered problematic.

Partition schemes and substitution models

Two partitioning schemes (the AIC and BIC-ranked) and their accompanying substitution models, as recommended by PartitionFinder (Lanfear et al. 2012) (see Table 2.3), were used to construct two BI and two ML tree topologies. The best partition scheme based on the AIC metric was a nine-partition dataset, with the three ribosomal genes treated separately, the five nuclear protein-coding genes split three ways into first, second and third codon positions and the mitochondrial COI also split into codon positions. The best partition scheme as recommended

by the more conservative BIC metric was a six-partition dataset, similar to the AIC partition scheme, but with the nuclear ribosomal gene fragments combined (18S and 28S), and the fusing of first and second codon positions for the six protein-coding genes.

2.4.2 Phylogenetic Analyses

2.4.2.1 Topology

In both the ML and BI analyses and with both partition schemes, the branching topology of the phylogenetic trees generated was identical (Figs. 2.3 & 2.4). The key features of the tree topologies generated in this study are the monophyly of Anomura, the monophyly of Aegloidea-Lomisoidea-Chirostyloidea, the monophyly of Chirostyloidea and within it, the monophyly of Kiwaidae-Chirostylidae. In the BI analyses, both partition schemes produced nodes with posterior probabilities that were ≥ 0.98 for all nodes. In the ML analyses, all nodes had bootstrap values ≥ 60%. Across both partition schemes, 13 of the 20 nodes with bootstrap values were ≥ 99%. The nodes with weakest support in the ML analyses were the monophyly of Aegloidea-Lomisoidea (69% and 62% for the nine and six-partition schemes respectively), and the monophyly of Chirostyloidea (73% and 64% respectively). The monophyly of Kiwaidae-Chirostylidae was marginally stronger (77% and 66% respectively).

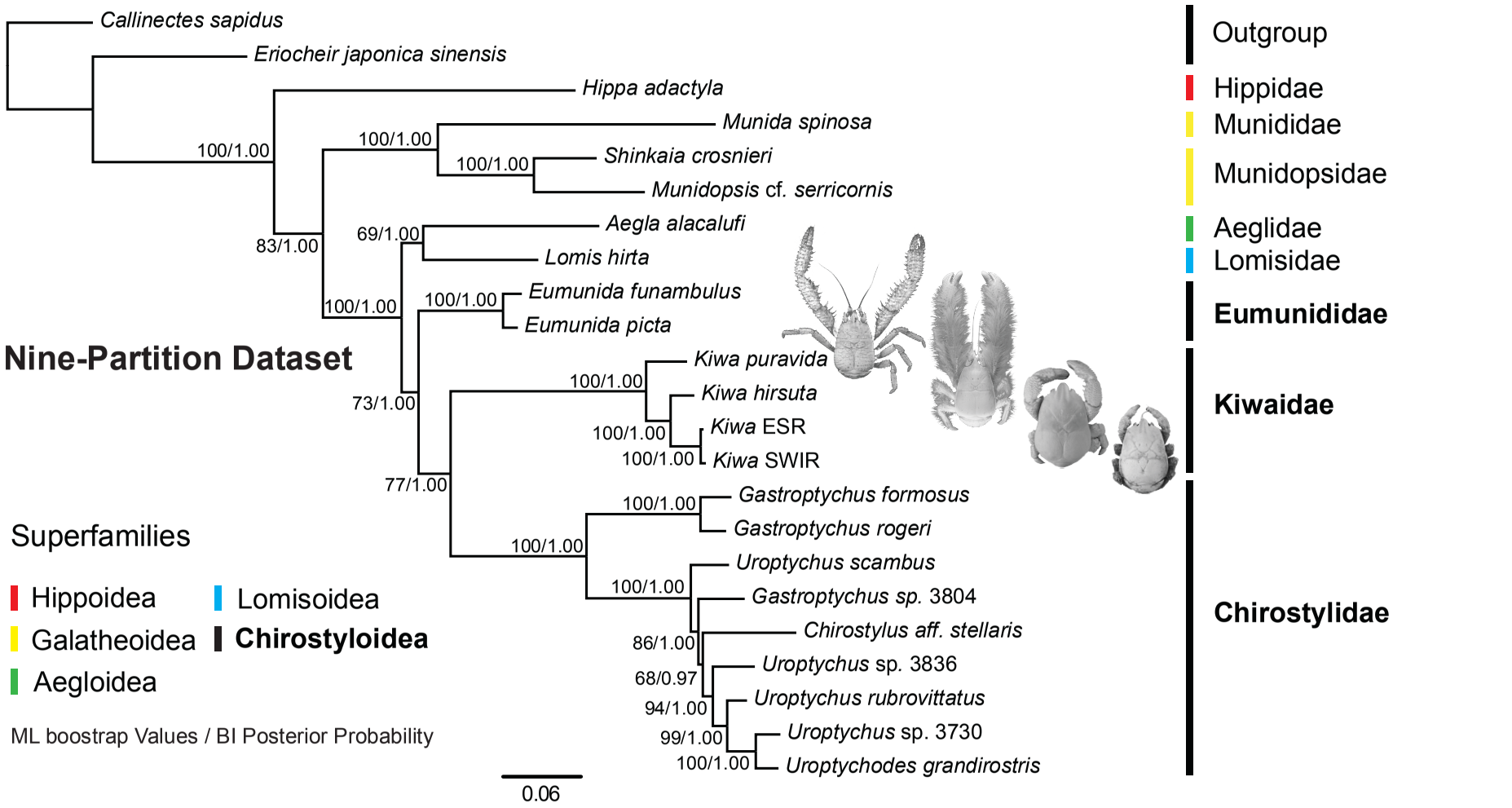

Figure 2.3. Maximum likelihood and Bayesian topology of a nine-gene concatenated dataset with nine partitions. Node support numbers represent ML bootstrap percentages and Bayesian posterior probabilities. Photographs of the four known kiwaids are superimposed next to their names. Photographs of *Kiwa puravida* and *Kiwa hirsuta*, courtesy of Shane Ahyong from Thurber et al. (Thurber et al. 2011) and Macpherson et al. (Macpherson et al. 2005) respectively. Photographs of *Kiwa* sp. ESR and *Kiwa* SWIR are originals.

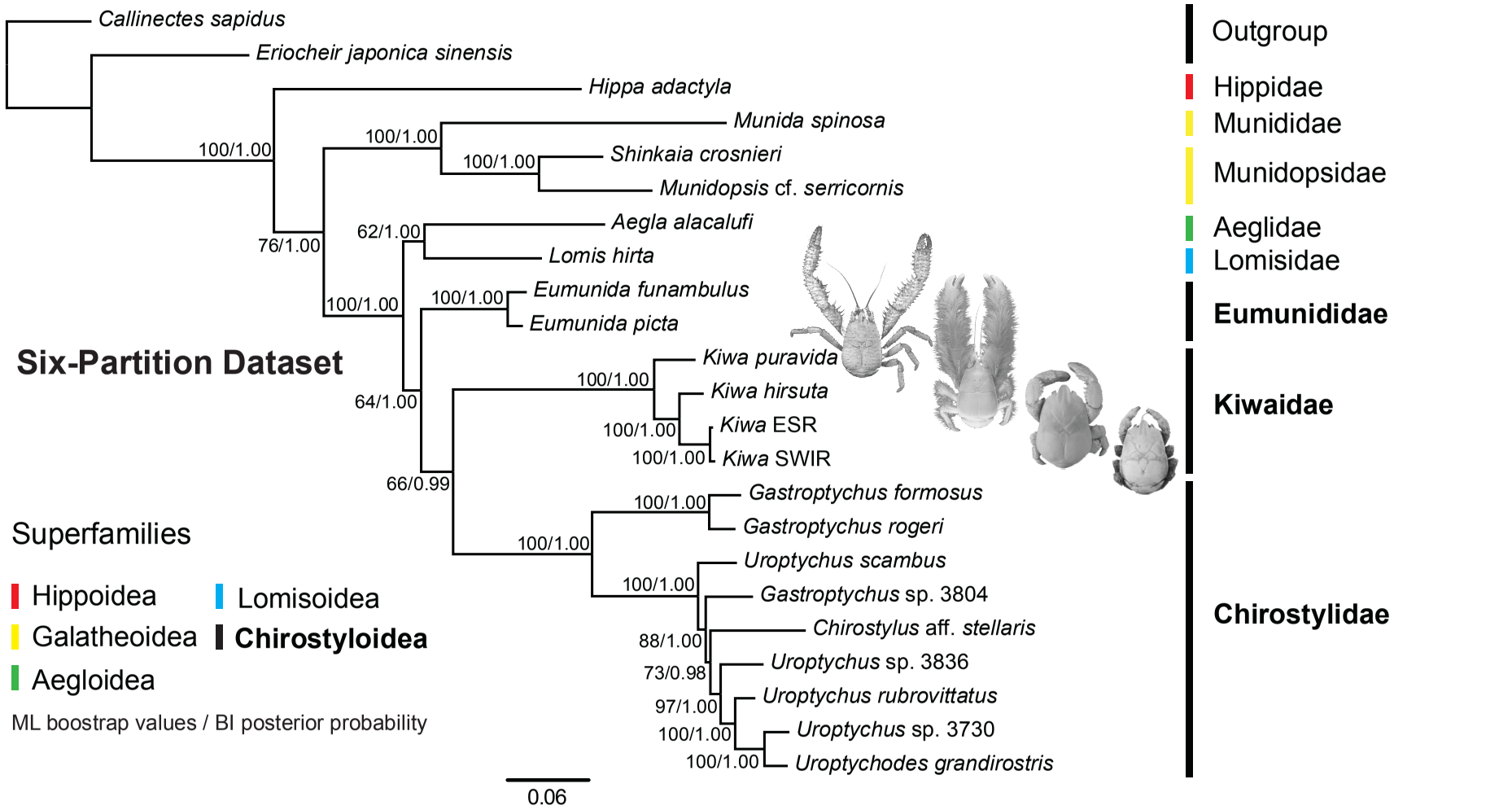

Figure 2.4. Maximum likelihood and Bayesian topology of a nine-gene concatenated dataset with six partitions. Node support numbers represent ML bootstrap percentages and Bayesian posterior probabilities. Photographs of the four known kiwaids are superimposed next to their names. Photographs of *Kiwa puravida* and *Kiwa hirsuta*, courtesy of Shane Ahyong from Thurber et al. (Thurber et al. 2011) and Macpherson et al. (Macpherson et al. 2005) respectively. Photographs of *Kiwa* sp. ESR and *Kiwa* SWIR are originals.

The Bayesian topology hypothesis tests, using the stepping-stone method, produced consistent results between the nine and six-partition datasets; mean marginal likelihoods supported the monophyly of Kiwaidae-Chirostylidae over Kiwaidae-Eumunididae (by 17.35 and 10.78 mean log likelihood units for the nine and six-partition models respectively) and over Eumunididae-Chirostylidae (23.59 and 23.74 mean log-likelihood units respectively) (Table 2.4).

Table 2.4. Stepping-stone topology tests examining interfamilial relationships within the Chirostyloidea. Mean log-likelihood values are displayed with the highest mean likelihoods in bold and the preferred model shaded. Eu = Eumunididae, Ch = Chirostylidae, Kiw = Kiwaidae.

Nine-Partition Model	((Eu-Ch)Kiw)	((Eu-Kiw)Ch)	((Kiw-Ch)Eu)
Run 1	-30836.06	-30828.15	-30809.55
Run 2	-30832.78	-30826.72	-30810.26
Mean	-30833.44	-30827.2	**-30809.85**
Six-Partition Model	**((Eu-Ch)Kiw)**	**((Eu-Kiw)Ch)**	**((Kiw-Ch)Eu)**
Run 1	-31004.43	-30990.7	-30979.78
Run 2	-31003.3	-30990.81	-30980.2
Mean	-31003.71	-30990.75	**-30979.97**

Within Chirostylidae the basal split is between *Gastroptychus* s.s., represented here by *G. formosus* and *G. rogeri* and the remaining chirostylid taxa, including the second group of *Gastroptychus*, represented by *Gastroptychus* sp. 3804. *Gastroptychus*, as currently defined is therefore not monophyletic. Likewise, the monophyly of *Uroptychus* is not supported in this study. *Uroptychus scambus*, resides outside a clade comprising the other *Uroptychus* species, *Chirostylus* aff. *stellaris, Gastroptychus* sp. 3804 and *Uroptychodes grandirostris*. The location of *U. grandirostris* in the tree also renders the larger *Uroptychus* group paraphyletic. All four species of *Kiwa* cluster together in this study supporting the monophyly of Kiwaidae. There is a basal split between the seep-endemic *Kiwa puravida* and a vent-endemic clade comprising *K. hirsuta* and the ESR and SWIR *Kiwa* species (Figs. 2.3 & 2.4).

2.4.2.2 Node Support

This discrepancy in reported support values between the ML and BI analyses, where bootstrap support appears weaker than BI posterior probabilities, has received much attention. Simulations reveal that ML non-parametric bootstraps and BI posterior probabilities should not be considered approximately equivalent to each other, rather that bootstrap values can be expected to be conservative relative to BI posterior probabilities, as is the case in this study (Erixon et al. 2003). The same simulations also show that occasionally, false topologies can be strongly supported in BI (more so than with ML analyses), especially if the models used for analyses are under-parameterised (Erixon et al. 2003). Given that in this study the topologies of the ML and BI analyses are identical and there is agreement between the nine-partition scheme and the less complex six-partition scheme, potential concerns of under-parameterisation resulting in misleading topologies are probably unwarranted.

2.4.2.3 Divergence Dates

The nine and six-partitioned datasets produced very similar divergence estimates for the key nodes of interest (Figs. 2.5 & 2.6), although the nine-partition dataset consistently produced slightly more recent divergence dates. For ease of reporting, therefore, the 95% highest posterior density (HPD) divergence date ranges from the two partition schemes will be combined, with the median ages of both partition schemes following in parentheses.

According to both partition schemes, Chirostyloidea likely split from sister taxa no more recently than 111.4-144.0 Ma (median ages of 123.4 and 127.6 Ma for the nine and six-partition schemes respectively). The divergences that resulted in the formation of the chirostyloid

families occurred soon afterwards, with the eumunidid lineage splitting off 101.3-131.7 Ma (medians of 114.8 and 115.8 Ma) and the split between Kiwaidae and Chirostylidae occurring 92.8-134.4 Ma (medians of 106.4 and 112.5 Ma).

Within Chirostylidae, the basal split between the *Gastroptychus* s.s. clade and the other clades occurred 61.2-97.2 Ma (medians of 78.4 and 73.5 Ma). The remaining clade radiated 30.7-53.4 Ma (medians of 38.4 and 42.5 Ma). Extant Kiwaidae radiated 22.7-43.7 Ma (medians of 30.6 and 32.9 Ma), with the split between the Pacific and non-Pacific lineages occurring 13.4-28.1 Ma (medians 19.1 and 20.3 Ma). The divergence between ESR and SWIR kiwaids was (0.6-2.7 Ma (medians of 1.6 Ma for both partition schemes)

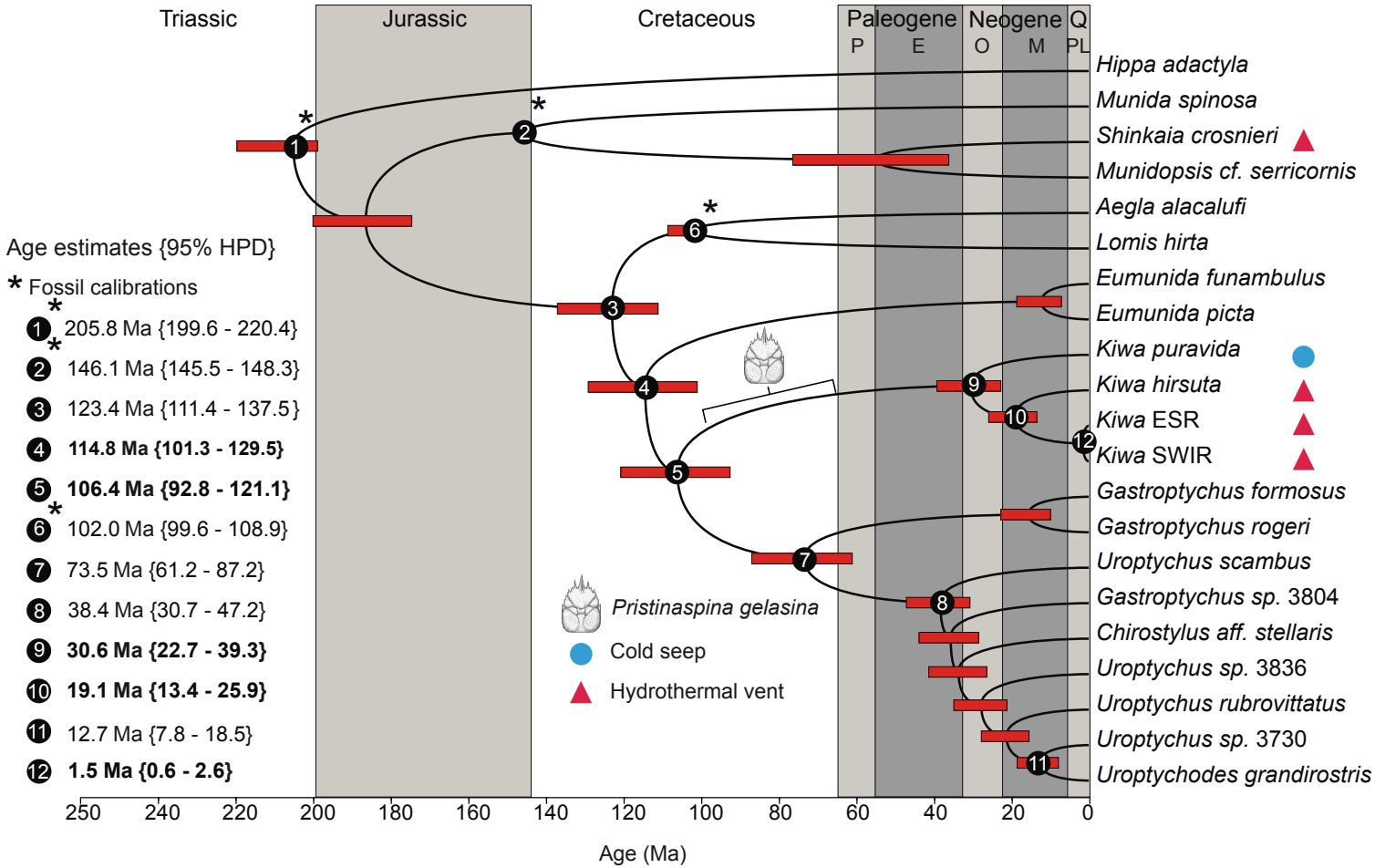

Figure 2.5. Divergence time estimates for the nine-gene concatenated dataset with nine partitions as calculated with a relaxed lognormal clock on Beast 1.7.4. Node bars represent the 95 % highest posterior density (HPD) interval for nodal age. Numbered nodes show dates of interest to this study and quoted age values show median age estimates followed by the 95 % HPD ranges in parentheses. Dates highlighted in bold are of particular interest. Nodes marked with an asterisk are fossil calibrated. Carapace illustration of the fossil *Pristinaspina gelasina* shows the date-range for the fossil. Geological periods are shown at the top, with recent epochs represented as letters: P = Paleocene, E = Eocene, O = Oligocene, M = Miocene, Pl = Plio-Pleisocene and Q = Quaternary.

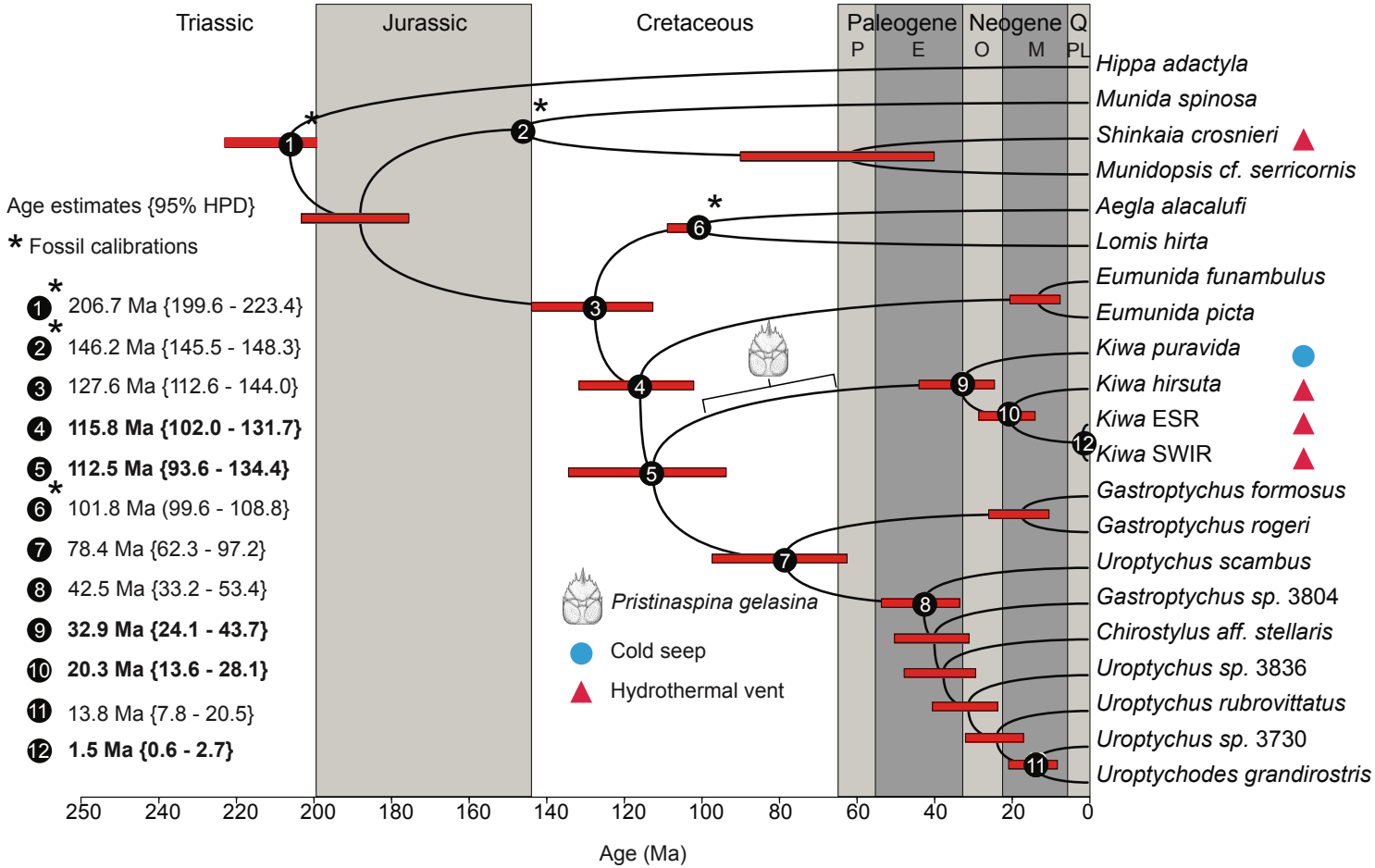

Figure 2.6. Divergence time estimates for the nine-gene concatenated dataset with six partitions as calculated with a relaxed lognormal clock on Beast 1.7.4. Node bars represent the 95 % highest posterior density (HPD) interval for nodal age. Numbered nodes show dates of interest to this study and quoted age values show median age estimates followed by the 95 % HPD ranges in parentheses. Dates highlighted in bold are of particular interest. Nodes marked with an asterisk are fossil calibrated. Carapace illustration of the fossil *Pristinaspina gelasina* shows the date-range for the fossil. Geological periods are shown at the top, with recent epochs represented as letters: P = Paleocene, E = Eocene, O = Oligocene, M = Miocene , Pl = Plio-Pleisocene and Q = Quaternary.

2.5 Discussion

2.5.1 Phylogeny of Chirostyloidea

2.5.1.1 Broad Patterns

The higher-level phylogenetic patterns presented here are consistent with previous trees (Schnabel et al. 2011a; Tsang et al. 2011). The monophyly of Aegloidea-Lomisoidea-Chirostyloidea supports the suggestion by Ahyong et al. (2011) that given the present-day locations of chirostyloids, aegloids and lomisoids, along with the fossil locations of aegloids and *Pristinaspina gelasina*, it seems likely that all three superfamilies and their constituent families share a Palaeo-Pacific origin (Ahyong et al. 2011).

2.5.1.2 Kiwaidae-Chirostylidae

The main difference between this study and previous ones is that all four trees, as well as the Bayesian topology hypothesis tests, supported the monophyly of Kiwaidae-Chirostylidae within Chirostyloidea. The Kiwaidae-Chirostylidae clade reported here contradicts the five-gene study of Tsang et al. (2011), which showed strong support for a Kiwaidae-Eumunididae clade. Kiwaidae-Chirostylidae monophyly is, however, supported by the presence of broad, flattened rostra in many chirostylids and all kiwaids, the absence of horizontal carapace striations (Fig. 2.1) and perhaps more tellingly, the production of large eggs with highly abbreviated larval development, indicative of lecithotrophy (Baba et al. 2011; Thurber et al. 2011), unlike Eumunididae, which produce small eggs, with planktotrophic larvae. In hydrothermal vent-

endemic invertebrates, as well as in squat lobsters in general, mode of larval morphology and development has been shown to be largely taxonomically constrained, rather than determined by habitat, which accounts for the myriad of dispersal strategies exhibited by vent-endemic fauna, despite being faced with the same challenges of dispersal from one 'island' to another (Van Dover and Williams 1991; Tyler and Young 1999).

2.5.1.3 Chirostylidae

The polyphyly of *Gastroptychus* and *Uroptychus* with Chirostylidae suggests that there has been convergent evolution in body form within the family; the second group of *Gastroptychus* could have evolved the elongated, gracile form independently, or alternatively, the common ancestor of all Chirostylidae may have exhibited a gracile, *Gastroptychus*-type form, which was subsequently lost by the lineage represented by *Uroptychus scambus*.

Cases of convergent evolution such as this may not be so surprising given that chirostylids produce lecithotrophic larvae with abbreviated development (Baba et al. 2011) indicative of a potentially limited dispersal capacity (McClain and Hardy 2010) and are believed to be associated with the patchy island-like cold-water soft coral (antipatharians, alcyonaceans and gorgonaceans) ecosystems of seamounts, mid-ocean ridges and continental slopes (Baba 2005). This potentially limited dispersal capability, coupled with a requirement for isolated soft coral habitats, and even specific sponge and coral species (Le Guilloux et al. 2010), may explain why chirostylids tend to show greater range restrictions compared to galatheoids (Schnabel et al. 2011b). These life history traits and habitat requirements may therefore lead to similar forms independently evolving in different localities. In the light of these results, however, there is clearly a need for a thorough, systematic review of chirostylid genera. The polyphyly of *Gastroptychus* and *Uroptychus* echoes the findings of Schnabel et al. (2011a) and this

discrepancy between morphological taxonomy and molecular phylogenetics will have to be explored in more detail in the future.

2.5.1.4 Kiwaidae

The kiwaid phylogeny produced in this study has implications for our understanding of this families' evolutionary history as well as the evolution of megafauna in chemosynthetic ecosystems in general. The Pacific location of the two basal kiwaids is consistent with a Pacific origin, as previously suggested (Ahyong et al. 2011), with a subsequent migration into the Atlantic sector of the Southern Ocean via the Drake Passage and then on to the Indian Ocean (Figs. 2.3 & 2.4). The alternative scenario, that Kiwaidae spread west from the Pacific into the Indian Ocean and finally to Atlantic Sector of the Southern Ocean, seems unlikely as prevailing currents in the Southern Hemisphere are easterly and kiwaids are apparently absent further east in the Indian Ocean at the Central Indian Ridge. However, the basal split between a Northern Hemisphere kiwaid (*K. puravida*) and the Southern Hemisphere kiwaids and the Alaskan location for the possible stem-lineage kiwaid fossil, *Pristinaspina gelasina*, suggests a North Pacific origin for the family rather than the southern one previously proposed (Ahyong et al. 2011), although the future discovery of fossils in the Southern Hemisphere could change this. The tree topology revealed in this study also suggests that the body form with elongated chelae is most likely the ancestral state for extant kiwaids, with a trend of decreasing proportional chela length from Pacific species to the Southern and Indian Ocean species. The discovery of kiwaids recovered from the East Pacific Rise (EPR) (Wang et al. 2013), is consistent with these two hypotheses, as it has a body form very similar to *K. puravida* and *K. hirsuta* (Fig. 2.2), with elongated setae-covered chelae and preliminary comparison of the rRNA ribosomal genes 16S and 28S, indicates that this new *Kiwa* is closely related to *K. puravida* with a possible basal split between these two kiwaids (Northern Hemisphere) and the others (Southern Hemisphere)

(Xinming Lui personal communication) (Fig. 2.7) The affinity of this species in relation to the others will only become clear once more genes are sequenced and a consensus tree produced.

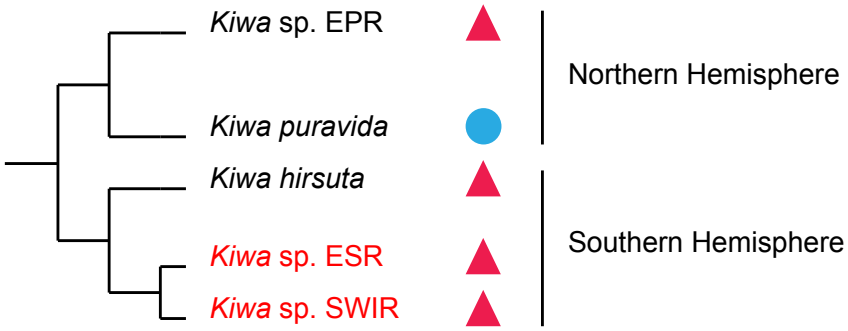

Figure 2.7. Cladogram of extant Kiwaidae, based on preliminary 16S and 28S gene trees, courtesy of Xinming Liu. Branch lengths do not reflect genetic distances. The red triangle denotes hydrothermal vent locations and the blue circle denotes cold seeps. Species names in red are those found at non-Pacific locations.

The kiwaid tree topology produced in this study revealed a basal split between the cold seep lineage and the deeper vent lineages, which would appear to be consistent with the hypothesis that some fauna endemic to deep-sea hydrothermal vents evolved from ancestors that inhabited shallower, more temporally stable and less thermally extreme cold seeps on continental slopes (Hecker 1985). Molecular phylogenetics shows some limited support for this hypothesis, at least with vestimentiferan tubeworms, vesicomyid clams and possibly mytilid mussels, where seep-endemic species generally fall out basally to the vent clades as would be expected if vent fauna evolved from seep inhabitants (Halanych 2005; Jones et al. 2006; Decker et al. 2012). The Pacific location for the seep-endemic *K. puravida* and the vent-endemic *K. hirsuta* suggests that, if a seep-to-vent progression did occur, it could have occurred along the eastern Pacific plate boundaries.

However, preliminary molecular phylogenetics of the EPR kiwaid throws some doubt on this hypothesis as it *tentatively* indicates that the EPR kiwaid and *K. puravida* are part of the same clade, with a basal split between this Northern Hemisphere group and the other Southern Hemisphere kiwaids (Fig. 2.7). This raises the possibility that the common ancestor to all extant kiwaids may have existed at vents and that the seep lifestyle of *K. puravida* is derived, or

alternatively a seep-to-vent evolution did occur, but that vent-endemism evolved twice. The word *tentatively* is used here because these are preliminary results from only a few loci (16S, 28S), although the overall morphology of the new kiwaid is certainly similar to *K. puravida* (Figs 2.1 & 2.2). It seems therefore that for the time being the question of whether kiwaids first evolved to live at seeps before vents will have to remain just that until more species are discovered. The presence of a new species of kiwaid on the EPR does perhaps increase the likelihood that kiwaids may have inhabited vents along the Southern EPR (SEPR), but have since gone extinct, given the location of *K. hirsuta* on the Pacific-Antarctic Ridge (see Fig. 2.2).

2.5.2 Chirostyloid Radiations

The mid-Cretaceous origins (no later than 101.3 Ma) for the chirostyloid families (Figs. 2.5 & 2.6) indicate that *Pristinaspina gelasina* (65.5-99.6 Ma) cannot be a stem-lineage chirostyloid. These results are therefore consistent with the suggestion by Ahyong et al. (2011) that this fossil is a stem-lineage kiwaid, based on its distinctive carapace markings (Fig. 2.1), although the possibility of it being a stem lineage chirostylid-kiwaid cannot be completely ruled out as Kiwaidae and Chirostylidae diverged 92.8-134.4 Ma. The dates for the formation of the three families are concomitant with a wider global pattern of decapod radiations that occurred during the late Jurassic and mid-to-late Cretaceous, when eustatic sea levels were higher than they are today and there was an expansion of shallow, productive seas (Klompmaker 2012). However, with the exception of the split between the *Gastroptychus* s.s. clade and the remaining Chirostylidae, the radiations within Kiwaidae and Chirostylidae occur well into the Cenozoic, long after these two families diverged from one another. This pattern is consistent with limited fossil evidence suggesting the end of the Cretaceous was marked by the extinction of many decapod genera, but not families (Feldmann and Schweitzer 2006), which survived to the Cenozoic and subsequently re-radiated. The timeframe for these radiations reported here

coincides with a general intensification of global ocean circulation and possible deep-water ventilation from the Late Eocene/Oligocene onwards following a warmer episode in the deep sea at the Palaeocene/Eocene boundary (McClain and Hardy 2010), perhaps allowing the exploitation of new niches in the deep sea.

The Cenozoic radiation of Kiwaidae augments the ever-expanding list of vent and seep-endemic fauna that are now known to have recently evolved, rather than being considered 'living fossils' from the Mesozoic or Palaeozoic (Little and Vrijenhoek 2003). A preliminary comparison of the 16S and 28S genes showing a close affinity between the new EPR kiwaid and *K. puravida* (Xinming Liu personal communication) (Fig. 2.7) indicates that the radiation date of extant kiwaids presented here is probably reasonably robust. A comprehensive appraisal of the estimated radiation dates for vent and seep taxa suggests that most of them radiated after the Paleocene/Eocene Thermal Maximum, a warm episode in the deep sea that may have resulted in widespread anoxia/dysoxia probably causing the extinction of many deep sea foraminifera genera (Vrijenhoek 2013). The dates for the radiation of Kiwaidae (22.7-43.7 Ma) are very similar to the estimated ages for the radiation of other chemosynthetic decapods, such as bythograeid crabs (~ 49 Ma) (Vrijenhoek 2013) and alvincaridid shrimps (~ 20-49 Ma) (Shank et al. 1999; Vrijenhoek 2013). It may be that all three chemosynthetic clades radiated at around the same time owing to a change in oceanic conditions, which increased the viability of a chemosynthetic lifestyle for such animals.

These results presented here may therefore reinforce the idea that chemosynthetic fauna could be inherently vulnerable to reduction in oxygen levels in the deep sea as a result of changes to climate and ocean circulation, because they must occupy narrow redox zones at the limit of their physiological tolerance (Vrijenhoek 2013). The recent radiation (or re-radiation) of Kiwaidae, is reflected by their association with ectosymbiont bacteria, which in terms of host-symbiont relationships, may be an early evolutionary step towards more intimate symbiotic associations with bacteria (Smith 1979), e.g., the housing of chemosynthetic symbionts in specialized

internal organs (Goffredi 2010). It is notable that other decapods associated with ectosymbionts, the munidopsid squat lobster genus *Shinkaia* and the shrimp family Alvinocarididae may also have Cenozoic origins based on fossil and molecular evidence respectively (Shank et al. 1999; Schweitzer and Feldmann 2008).

2.5.2.1 Possible Vicariance in Kiwaidae

In order to interpret the divergence date estimates for kiwaids, it is necessary to appreciate that unlike other Chirostyloidea, they have evolved to reside in physiologically challenging and isolated chemosynthetic habitats in the deep sea. *Kiwa puravida* has been found at continental slope cold seeps off the Pacific coast of Costa Rica, and *Kiwa hirsuta*, *Kiwa* ESR and *Kiwa* SWIR have been found at hydrothermal vents in the Pacific, Southern Ocean and Indian Ocean at depths in excess of ~ 2400 m (Macpherson et al. 2005; Thurber et al. 2011; Rogers et al. 2012) (SWIR Cruise report). Animals that are endemic to such challenging ecosystems must maintain effective metapopulations across these island ecosystems by broadcasting their larvae into the ocean currents. The geographical range of any given species is therefore determined by factors such as larval longevity, current direction and strength, distance between 'islands', shelf and ridge topography and the longevity of individual seep and vent fields (Tyler and Young 1999; Tyler et al. 2002; Vrijenhoek 2010).

Research over the last 30 years has shown that in many cases the biogeography of hydrothermal vent-endemic fauna, can be understood in terms of vicariance caused by past changes in mid-ocean ridge position, activity, topography (bottom currents are often rectified by ridge topography for example) and changes in current regime (Tunnicliffe and Fowler 1996; Tunnicliffe et al. 1998; Van Dover 2000; Tyler et al. 2002; Van Dover et al. 2002; Johnson et al. 2006; Plouviez et al. 2009; Plouviez et al. 2010; Vrijenhoek 2010). However, attempting to

reconstruct likely scenarios to explain present-day biogeographic patterns is not always clear-cut: explanations that rely on inferences regarding the past location of ridges, coastlines or current regimes are only as good as the latest reconstructions, which tend to be less 'accurate' the further into the past one peers. Regardless, there are some examples where candidate palaeo-events can be pinpointed. The subduction of the Pacific-Farallon ridge under the west coast of North America ~ 30 Ma for example, can account for the divergence of species of vent fauna that today are found on the East Pacific Rise (EPR) and on the Northeast Pacific ridges. The well-dated appearance of microplates or fracture zones, can similarly account for the genetic divergence of species (Won et al. 2003; Hurtado et al. 2004; Johnson et al. 2006). Consequently it is tempting to think that such events may also be responsible for the divergence of some Kiwaidae. Caution, however, should be the mantra when attempting to explain divergences by means of past tectonics and palaeoclimatology, as future work may radically change our understanding of past events. Nevertheless, an attempt has been made to derive a series of possible narratives.

Given the recent discovery of kiwaids on the EPR that may form a monophyletic clade with *K. puravida*, the hypothesis of a seep-to-vent trajectory for the genus is on shakier ground than appeared at the time when these results were published. It is still possible that the common ancestor of these two kiwaids (and therefore all kiwaids) is seep-endemic, but that would suggest that vent-endemism evolved more than once within Kiwaidae (once with the Southern Hemisphere vent-endemic kiwaids and once with the EPR kiwaid), rather than the more parsimonious theory that seep-endemism evolved once with *K. puravida*. Given the preliminary nature of the formal description of this new EPR species (Xinming Liu personal communication) it is impossible to confidently link geological events to the earliest divergence in Kiwaidae (the basal split in extant Kiwaidae), although the transition from living in non-chemosythetic ecosystems to chemosynthetic ones most likely occurred in the East Pacific and the age range for the radiation of Kiwaidae (22.7-43.7 Ma) is contemporary with two episodes when mid-ocean ridges, cold seeps and continental slope were in close proximity:

1. The subduction of the Pacific-Farallon ridge under the North American plate ~ 30 Ma (Schellart et al. 2010).
2. The formation of the ridges, of which the Galapagos Ridge is the descendent ~ 23 Ma, which would have connected the EPR to Central America (Meschede and Barckhausen 2001).

Regardless of the precise evolutionary pathway and location of where Kiwaidae became associated with vent and seep habitats, the location of the new kiwaid at the junction between the EPR and the Galapagos Rift, along with the location of *K. puravida* at seeps off Costa Rica (Fig. 2.2), where the now extinct Cocos Ridge meets Central America, possibly hints that the divergence of these two kiwaids (assuming the preliminary molecular results of Xinming Liu are robust) is related to the evolution of ridges in this area. As already mentioned, the ridges forming ~ 23 Ma effectively connected the EPR to Central America, with the portion closest to Central America being the Cocos Ridge (Meschede and Barckhausen 2001), but around 14.7 Ma, spreading on this ridge ceased, although the reorganisation of spreading in this area is very complex and some hotspot volcanism around the present location of Cocos Island may have existed as recently as 2 Ma (Meschede and Barckhausen 2001). 16S divergence between *Kiwa* sp. EPR and *K. puravida* is 2% (Xinming Liu personal communication), which is far smaller than the genetic distance between *Kiwa hirsuta* and *Kiwa* sp. ESR (6.45%) (Rogers et al. 2012). Given the oldest estimated divergence date between these two kiwaids is 28.1 Ma, it would suggest that the divergence between the Northern Hemisphere kiwaids would be at least a third of that, suggesting that they have diverged within the last ~ nine million years or so (or less). This date estimate may be consistent with divergence associated with tectonic changes associated with hotspot evolution in the area, although the precise mechanism remains unclear.

The absence of the *Kiwa* genus in the fossil record and the uncertainty regarding the past

configuration of ridges means that the precise mechanism and time whereby vent and seep-endemic kiwaids evolved may be sadly unfathomable. However, further exploration of SE Pacific cold seeps, as well as vents on the Galapagos Rift and neighbouring seamounts, the P-AR and the Chile Rise may provide a clearer picture.

The phylogeny presented in this study shows that *K. hirsuta* and the ESR and SWIR *Kiwa* form a monophyletic clade and the preview of a 16S gene phylogeny with the new EPR species of *Kiwa* incorporated, courtesy of Xinming Liu, doesn't appear to alter this finding. Therefore it seems likely that the ESR and SWIR *Kiwas* are descended from a Pacific vent-endemic ancestor. A key question in the biogeography of Kiwaidae, therefore, is how they managed to spread from vents in the Pacific to those on the ESR and SWIR. The known present-day locations of Kiwaidae (Fig. 2.2) in combination with the phylogeny present here, suggests they entered the Atlantic sector of the Southern Ocean from the Pacific via the Drake Passage. The estimated date range for the split between the Pacific and non-Pacific lineages (13.4-28.1 Ma) is compatible with this scenario, as the deep-water connection in the Drake Passage probably occurred ~ 30 Ma (Lawver et al. 2011).

Today, the ESR is isolated from the Pacific ridge systems and the means by which kiwaids arrived from the Pacific into the Scotia Sea are not readily apparent. However, ~ 20 Ma, there was a near continuous chain of ridge segments from the Pacific into the widening Scotia Sea via the Chile Rise, Antarctic-Phoenix Ridge and the West Scotia Ridge (WSR) (Barker 2001; Livermore 2003; Eagles et al. 2005; Vérard et al. 2012) (Fig. 2.8), which could have provided a dispersal 'highway' for vent larvae, allowing the spread of kiwaids from the Pacific into the Atlantic sector of the Southern Ocean. The ESR was forming by ~ 15 Ma (Livermore 2003) at the eastern end of the WSR and by 12 Ma the subducting Chile Rise had left a ~ 1,000 km gap between the Chile Rise and Antarctic-Phoenix Ridge (A-PR) (Breitsprecher and Thorkelson 2009; Eagles et al. 2009; Vérard et al. 2012) (Fig. 2.8 B-D). This subduction of the Chile Rise under the South American plate, starting ~ 16 Ma, coincides with the most recent divergence

date estimate for the Pacific and non-Pacific kiwaids (13.4 Ma), possibly indicating that this widening gap between the Chile Rise and the A-PR could have isolated kiwaid colonies, leading to divergence. An alternative explanation for the divergence of the non-Pacific lineage from the *K. hirsuta* lineage is that the formation and subsequent expansion of large fracture zones on the Chile Rise ~ 28-26 Ma (Fig. 2.8 F) when there was a near 90˚ realignment in the axis of spreading (Tebbens and Cande 1997) could have isolated vent fauna on the Pacific-Antarctic Ridge from Chile Rise populations, including those that the non-Pacific kiwaids may be descended from. The oldest possible inferred divergence date of 28.1 Ma (Fig. 2.6) is close enough to this event for it to be worth considering as a cause of the divergence we see today. Discovering kiwaids on the as-yet unexplored Chile Rise may resolve this question.

One last possibility, still compatible with the tree topology and divergence estimates presented herein, is that the divergence between Pacific and non-Pacific lineages owes less to vicariance along ridges and more to the onset of the Antarctic Circumpolar Current (ACC). Some estimates place this onset in the Miocene rather than the Oligocene owing to the possible lack of deep basins in the Scotia Sea until this time, which may have prevented an earlier onset (Barker 2001; Barker et al. 2013). The divergence dates of the Pacific and non-Pacific lineages are compatible with this hypothesised Miocene ACC onset. Conceivably therefore, a fast, cold ACC in the Miocene could have transported kiwaid larvae directly from the southern P-AR across abyssal plains and deposited them at vents in the Scotia Sea (see Fig. 2.2). If larval transport were insufficient to maintain genetic homogeneity, then the two populations would have immediately commenced diverging into separate species. In this scenario, Scotia Sea kiwaids are not descended from Chile Rise populations. While this idea may seem remote, given the non-ridge distances between the southern P-AR and the Scotia sea are in excess of ~ 3500 km, recent study of the larval morphology of *Kiwa* sp. ESR revealing very large yolk reserves, possibly affording larval lifespans in excess of a year (Sven Thatje et al. manuscript in preparation), necessitates serious consideration of this possibility. Exploration of vents on the

Southern P-AR and the Chile Rise may allow these hypotheses to be tested in the future.

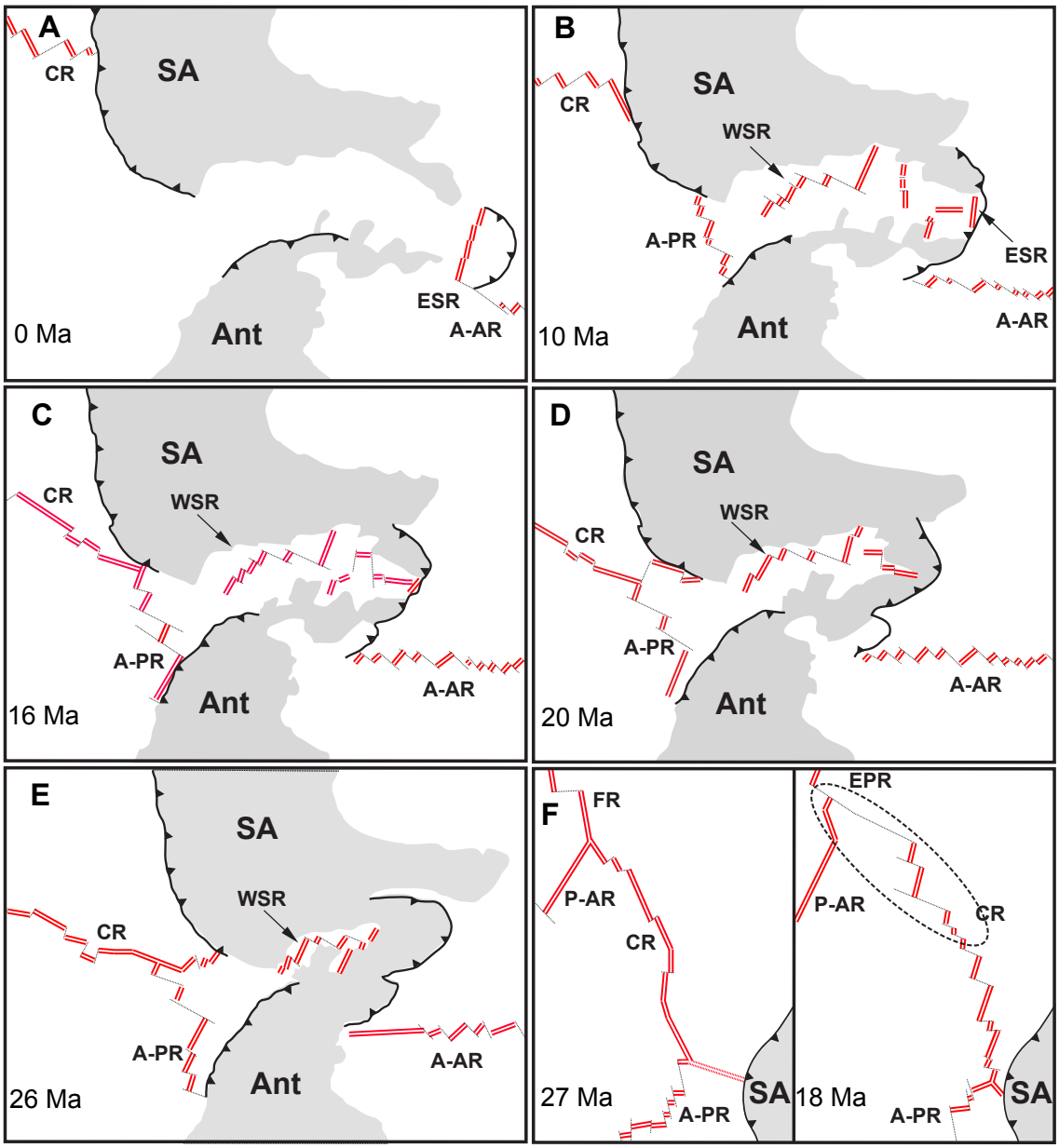

Figure 2.8. Schematic representing the evolution of ridge positions in the Drake Passage and Southeast Pacific relevant to the divergence of Pacific and non-Pacific kiwaids during the Oligocene and Miocene, modified from Verard et al. (2012) and Breitsprecher & Thorkelson (2009). Panels A-E show how kiwaids may have spread from the Pacific to the East Scotia Ridge and beyond via the Chile Rise and other spreading ridges that are now extinct, with the subsequent divergence of the Pacific and non-Pacific lineages possibly the consequence of the Chile Rise subducting under the South American plate. Panel F represents the development of large fracture zones (dashed ellipse) on the Chile Rise in the late Oligocene/early Miocene that may also account for this divergence. Grey areas represent non-oceanic plate regions. Double lines denote active spreading segments of the ridges. Fine lines represent faults and fracture zones. Solid black lines with triangles denote subduction zones. Abbreviations are: SA = South America, Ant = Antarctica, CR = Chile Rise, A-PR = Antarctic-Phoenix Ridge, WSR = West Scotia Ridge, A-AR = American-Antarctic Ridge, P-AR = Pacific-Antarctic Ridge, FR = Farallon Ridge.

In order to interpret the divergence dates (0.6-2.7 Ma) inferred in this study between the ESR and SWIR kiwaids, it is necessary to acquaint oneself with the tectonic and hydrographic setting of this region (see Fig. 2.2). The ESR very nearly connects at the southern end to a series of large fracture zones and spreading ridge segments called the American-Antarctic Ridge (A-AR), which follows an easterly path and is then called the SWIR after the Bouvet Triple Junction. The SWIR then follows a northwest path, although with some very large fracture zones offsetting these ridges, such as the Andrew Bain Fracture Zone (ABFZ), until reaching the Central Indian Ridge (CIR). Given the present-day locations of the ESR and SWIR kiwaids, it stands to reason that some hydrothermal vents along the intervening ridge segments could also host *Kiwa*, and furthermore, the absence of *Kiwa* on the CIR (Hashimoto et al. 2001; Van Dover et al. 2001; Van Dover 2002; Watanabe and Hashimoto 2002; Okutani et al. 2004) indicates that the SWIR may represent the eastern-most range limit for the family, although, their presence on unexplored areas of the CIR and the SE Indian Ridge cannot be ruled out.

The divergence between the ESR and SWIR kiwaids is very recent compared to the other kiwaids (0.6-2.7 Ma). During this time, there appear to have been no major changes in ridge configuration between the ESR and SWIR to easily account for such a divergence (Sauter and Cannat 2010) as in the case of the divergence of Pacific and non-Pacific kiwaids. One possibility is that there could have been a recent drop in the number of hydrothermal vent fields along portions of the intervening ridges, which would have reduced the dispersal capability of vent fauna by effectively increasing the distance between adjacent vent fields, leading to isolation and subsequent divergence.

Another possibility is that there is a strong isolation-by-distance (IBD) effect, as could be expected along a very large stretch of mid-ocean ridge (Vrijenhoek 2010), culminating in populations becoming sufficiently divergent over time at both ends that they may be considered

separate species – a sort of linear ring species. If this is the case, then a continuum of intermediate forms should be expected along the A-AR and the Western reaches of the SWIR. In this scenario, the divergence could have begun to slowly build up longer than the estimated divergence dates inferred here. A variant of this model is one where relatively homogenous populations are broken up by ridge discontinuities (e.g., the ABFZ) where gene flow is very low. In this scenario, kiwaids would have spread along the A-AR and parts of the SWIR before reaching these discontinuities. In very rare circumstances, larvae could have traversed these discontinuities and established populations further east, which would have been effectively isolated from populations further west leading to divergence. The time since these discontinuities were traversed would be reflected in the level of divergence. These rare circumstances could merely be the result in the inherent stochasticity of larval dispersal.

Alternatively, changes in current regime may be responsible: large portions of the intervening ridge segments between the ESR and the SWIR are bathed by the ACC, which is the dominant force in determining the dispersal direction of larvae throughout the Southern Ocean (Rogers 2007). Changes to the ACC could have affected the dispersal range of *Kiwa* larvae, and in particular, their ability to traverse large potential barriers to gene flow, such as the Andrew Bain Fracture Zone (ABFZ) (Sclater et al. 2005), which effectively splits the SWIR into a lower and an upper portion (Fig. 2.2).

Today, the Subantarctic and Polar Fronts of the ACC cut across the ABFZ (Orsi et al. 1995) which is 750 km long and up to ~ 6,000 m deep (Sclater et al. 2005), potentially isolating vent fauna on either side. Changes in the intensity and latitude of the ACC fronts during the Mid-Pleistocene Transition, which occurred between ~ 1.2 Ma and 650 Ka, could have transported *Kiwa* larvae across the ABFZ to regions that are now isolated. During this episode, orbitally-forced glacial cycles switched in periodicity from 41 to 100 kyr cycles, resulting in colder, extended glacial conditions and northerly shifts in the ACC polar front in the South Atlantic far beyond the northerly extent of recent glacial front migrations (Diekmann and Kuhn 2002).

Sediment analyses off the Antarctic Peninsula indicates there has been a decline in ACC strength since ~ 2.5 Ma (Hassold et al. 2009), which might have cut off the supply of *Kiwa* larvae across fracture zones like the ABFZ at some point. Exploration of the American-Antarctic Ridge and lower reaches of the SWIR around the Bouvet Triple Junction may elucidate present-day barriers to gene flow between the ESR and SWIR kiwaids, and help in the inference of the past changes responsible for their divergence. The investigation of vent fields east of the Dragon vent field will aid in determining the extent of this genus on the SWIR, but at a wider scale, the discovery of vent communities along the Southeast Indian Ridge, and along the Pacific Antarctic Ridge will help reveal the global extent of vent-endemic Kiwaidae.

2.6 Conclusion

The nine-gene dataset featured in this study has revealed, in accordance with previous work, that Chirostyloidea are monophyletic. However, in contrast to earlier studies, our results suggest the monophyly of Kiwaidae-Chirostylidae, which is supported morphologically by their similar larvae. Within Chirostylidae, *Uroptychus* and *Gastroptychus* are polyphyletic and need taxonomic re-examination. All three families appear to have mid-Cretaceous origins, although kiwaids and some chirostylids radiated after the late Eocene. The basal split in Kiwaidae between the seep-endemic *Kiwa puravida* and a vent-endemic clade, although superficially consistent with a seep-to-vent evolutionary trajectory, is complicated by the recent discovery of an EPR kiwaid with a close relationship to *K. puravida*, raising doubts about its validity as a theory in this case, although more evidence will be needed to determine this. The Southern Hemisphere vent clade then likely spread via mid-ocean ridges from the East Pacific, through the Drake Passage to the East Scotia and Southwest Indian ridges within the last 25.9 million years, although a Miocene onset of the ACC could also have transported southern P-AR kiwaid larvae to the Scotia Sea, bypassing the Chile Rise with subsequent divergence. Like many other chemosynthetic taxa, the Cenozoic radiation of Kiwaidae may indicate an inherent vulnerability of chemosynthetic fauna to climatic changes affecting the availability of oxygen in the deep sea, with consequences for their future conservation.

CHAPTER 3

Population Genetics of Vent Fauna in the Scotia Sea Using mtDNA

3.1 Abstract

The genetics of hydrothermal vent populations have been intensely studied as model environments in which to explore the effects of metapopulation dynamics on genetic diversity and connectivity, particularly in the East Pacific. Here, the first multispecies study of vent-endemic megafauna from the Southern Ocean is presented, using the mitochondrial gene cytochrome c oxidase subunit I (COI). Analyses of three recently discovered undescribed vent-endemic species, a kiwaid crustacean, *Kiwa* sp., a peltospirid gastropod and a limpet, *Lepetodrilus* sp., from vents in the Scotia Sea reveals no evidence of genetic differentiation between vent fields ~ 440 km apart at the northern and southern end of the East Scotia Ridge (ESR), consistent with panmixia along the length of the ridge. However, limpets sampled at the Kemp Caldera, at the southern end of the South Sandwich back-arc chain of volcanoes ~ 95 km to the east of the ESR appear genetically distinct from ESR limpets with AMOVA F_{ST} values > 0.45, possibly owing to a ~ 1,000 m depth difference between the Kemp and ESR vents and the likely hydrographic isolation of the Kemp Caldera. Of the three species, *Lepetodrilus* sp. has the lowest haplotype diversity and consequently, the lowest effective population size, with the peltospirid gastropod as intermediate and *Kiwa* sp. the most diverse (h = 0.996), despite on-site observations suggesting that the limpets are the most numerous and kiwaids the least. This pattern of diversity is the consequence of more recent genetic bottlenecks in the gastropods compared to the kiwaids, which can be accounted for either by demographic changes perhaps owing to differential connectivity over time as a result of stochastic variations in vent activity and/or current regime within a metapopulation dominated by non-equilibrium processes or by selective sweeps, or a combination of the two.

3.2 Introduction

3.2.1 Vent Ephemerality

Unlike much of the world's deep-sea floor, which is generally considered a low biomass, homogeneous and stable environment, deep-sea hydrothermal vents - springs of geothermally-heated water enriched in sulphides - host large densities of endemic animals surviving in highly changeable conditions. These megafauna are sustained by chemosynthetic bacteria, which oxidise reduced chemicals in the vent fluid as a source of energy for primary production (Gage and Tyler 1992). Vents, which form on mid-ocean ridges, back-arc spreading basins and seamounts, are generally found in discrete patches known as vent fields and in ecological terms can be thought of as islands of high biomass, separated by large stretches (tens to hundreds of kilometres) of deep-sea floor (Van Dover 2000). These vent fields are considered ephemeral with a limited lifespan (decades to centuries) because plate tectonic movements and seismic events can cut fields off from their geothermal source, whilst eruptions can suddenly resurface large areas with fresh basalt (Van Dover 2000). Nascent, senescent and dead vent patches have been observed as a consequence of these processes (Tunnicliffe et al. 1997; Von Damm 2000; Vrijenhoek 2010; Mullineaux et al. 2012).

The extreme patchiness and ephemerality of vent fields necessitates the maintenance of viable metapopulations for endemic species across many vent fields by releasing their larvae into the ocean currents (Vrijenhoek 2010). This spatial and temporal patchiness, combined with the linear arrangement of vent fields along mid-ocean ridges, has made vent communities an ideal model for examining the way realised larval dispersal, as determined by factors such as dispersal strategy, hydrography, habitat patchiness and longevity, as well as sea floor

topography, affects inter-deme connectivity (gene flow), genetic diversity and demographic history in benthic marine metapopulations (Vrijenhoek 1997; Jollivet et al. 1999; Vrijenhoek 2010).

3.2.2 Connectivity

Vent fauna share a common trait in the need to disperse between vents or risk eventual extinction. However, this evolutionary pressure must be balanced by the advantage of ensuring that larvae are retained close to the natal site where the probability of successful colonization is higher. Despite experiencing these same pressures, there is a surprising diversity of dispersal strategies amongst different vent taxa, which appear to be largely determined by taxonomic affiliation (Tyler and Young 2003). Some species produce planktotrophic larvae (e.g. the alvinellid shrimp *Rimicaris exoculata*), whilst others produce larger, lecithotrophic larvae (e.g., the tubeworm *Riftia pachyptila*) whilst others brood their young (the vent amphipod *Ventiellia sulphuris*). The fact that *Rimicaris exoculata* produces larvae that can rise up the water column and feed on algae, thus allowing for an extended larval lifespan (Dixon and Dixon 1996; Copley et al. 1998; Herring and Dixon 1998; Allen et al. 2001), may explain why along ~ 7000 km of the Mid-Atlantic Ridge (MAR), there is no evidence for population subdivision (Teixeira et al. 2012b), compared to *R. pachyptila* over a similar range of the East Pacific Rise (EPR) (Coykendall et al. 2011).

The populations of species either side of large discontinuities along mid-ocean ridges, (e.g., transform faults, fracture zones and microplates) have been shown to be divergent, indicating that these features are filters to larval dispersal (Johnson et al. 2006; Plouviez et al. 2009; Plouviez et al. 2010; Coykendall et al. 2011). However, these features often restrict gene flow for some species and not others (Hurtado et al. 2004; Plouviez et al. 2009) and larval dispersal strategy and morphology along with current regimes have been used to account for such

differences. It has been suggested, for example, that larval longevity as determined by the size of yolk sac, may affect the ability of larvae to traverse the equatorial region of the EPR, which experiences strong cross-axis currents (Plouviez et al. 2009). Recently it has been observed that larvae from as far away as ~ 300 km have colonised vents in the EPR previously defaunated by eruption (Mullineaux et al. 2010) and it has been theorised that meso-scale eddies could explain examples of rare connectivity over large distances (Adams et al. 2011). Finally, it has been suggested that ridge spreading rate, a proxy for vent field longevity and density along a ridge may also affect connectivity. Vent fields on fast-spreading ridges are believed to be more ephemeral, lasting on a scale of decades, but are more closely packed, potentially aiding dispersal, whereas vents on slow-spreading ridges are more stable, but may be more distant from each other with numerous intervening ridge discontinuities (Van Dover 2000; Vrijenhoek 2010).

3.2.3 Diversity & Demography

These same factors affecting connectivity are likely to affect the genetic diversity and demographic history of vent metapopulations. Vrijenhoek (1997) suggested that site occupancy along a ridge was key in influencing genetic diversity within a metapopulation, as the greater the number of colonies that are within a reachable distance of each other, the greater the effective size of the population. Conversely, population subdivision owing to limited dispersal capability either because of intrinsic (larval type) or extrinsic (currents, ridge topography and discontinuities) factors could lead to a depression of overall genetic diversity as genetic drift exerts greater influence on the smaller subpopulations. The ephemerality of vent fields also means that vent metapopulations may be subject to demographic fluctuations leading to the loss of diversity from population bottlenecks. This process could be accentuated if demes are small and poorly connected. A population genetics metadata analysis for species along the EPR

appears to show a positive relationship between site occupancy and genetic diversity as predicted (Vrijenhoek 2010), with also limited support for greater genetic diversity in early colonising populations perhaps owing to greater metapopulation stability and site occupancy. A correlation between ridge spreading rate (a proxy for vent ephemerality) and genetic diversity has been shown for *R. pachyptila* along the EPR, where vent fields hold less diversity in the southern stretches (SEPR) where spreading rates are much faster (Coykendall et al. 2011).

The case for the general ephemerality of vents depressing diversity in vent fauna is bolstered by the common presence of star-like haplotype networks (visual representations of haplotype relatedness and numerical dominance in populations; Posada and Crandall 2001) for mtDNA, which, along with significantly negative Tajima's *D*, Fu's *F*s and also mismatch distributions (summary statistics showing deviations from neutrality) possibly signal 'recent' population expansions for species at Pacific vents (Hurtado et al. 2004; Young et al. 2008; Plouviez et al. 2009; Plouviez et al. 2010) as well as *Rimicaris exoculata* in the Atlantic (Teixeira et al. 2010). Whilst the possibility of selective sweeps reducing genetic diversity cannot be ignored, the recent study of multiple taxa as well as multiple loci with the polychaete *Alvinella pompejana* along the EPR shows that expansion signatures were stronger for populations of all species and loci on the faster-spreading SEPR (Plouviez et al. 2009; Plouviez et al. 2010).

3.2.4 Vent Studies Globally

Since the first discovery of hydrothermal vents on the Galapagos Rift in 1976 (Corliss et al. 1979), vent communities on mid-ocean ridges in the East Pacific have been the focus of most vent population genetics studies (Grassle 1985; Bucklin 1988; France et al. 1992; Black et al. 1994; Craddock et al. 1995; Jollivet et al. 1995; Black et al. 1998; Won et al. 2003; Hurtado et al. 2004; Johnson et al. 2006; Fusaro 2008; Matabos et al. 2008; Young et al. 2008; Faure et al. 2009; Plouviez et al. 2010). This is in part a result of the wealth of background data available to

population geneticists by studying populations on the most heavily researched portion of mid-ocean ridge in the world (Van Dover 2000). Recently, vent population genetics research has extended further afield to the Atlantic (Creasey et al. 1996; Peek et al. 2000; Teixeira et al. 2010; Teixeira et al. 2012b), and the West and Southwest Pacific (Watanabe et al. 2006; Thaler et al. 2010). However, vast areas in the Indian Ocean, the Arctic, the South Pacific, the South Atlantic and the Southern Ocean remain unexamined and population genetics offers the opportunity to make inferences not only about the ecology of vent endemic species in these regions, but also to offer clues about the current and past geophysical conditions influencing these populations.

3.2.5 Southern Ocean Study Sites

3.2.5.1 Geology & Hydrography

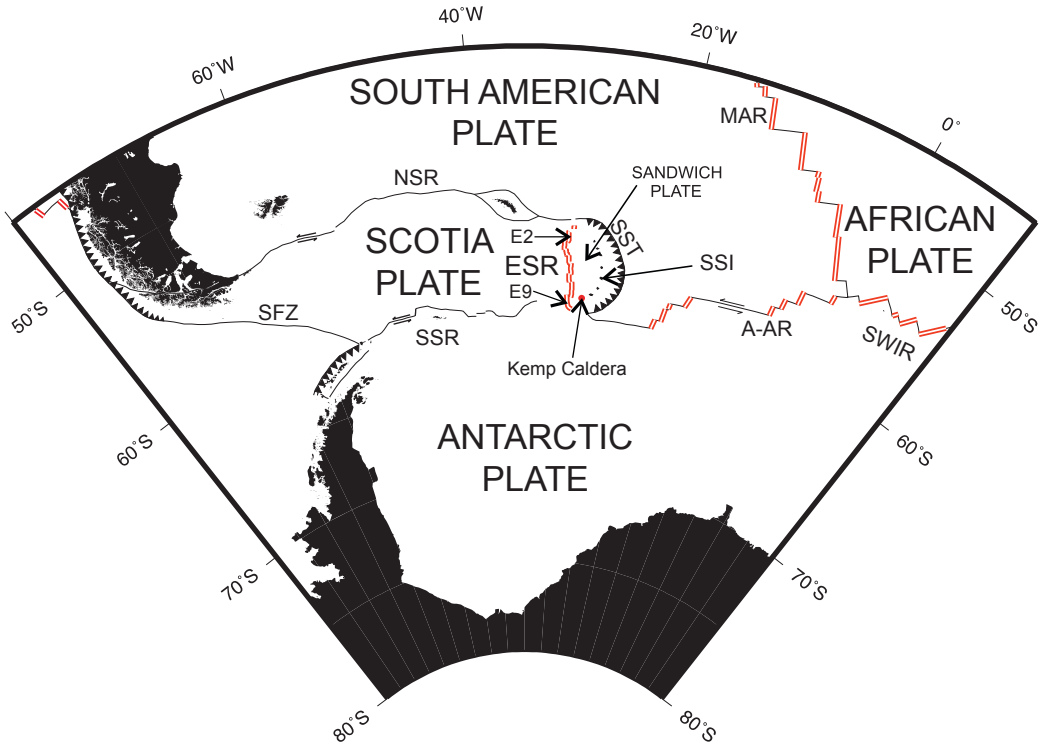

Figure 3.1. Configuration of plates and plate boundaries in the South Atlantic Ocean, modified from Livermore (2006), with the locations of the E2, E9 and Kemp Caldera hydrothermal vent fields. SFZ = Sovanco Fracture Zone, NSR = North Scotia Ridge, SSR = South Scotia Ridga, ESR = East Scotia Ridge, SSI = South Sandwich Islands, SST = South Sandwich Trench, MAR = Mid-Atlantic Ridge, A-AR = American-Antarctic Ridge, SWIR = Southwest Indian Ridge. Lines with triangles represent subduction zones, double red lines represent active spreading ridge and split bi-directional arrows represent relative plate movements along fault lines.

The South Sandwich Island (SSI) arc and the accompanying East Scotia Ridge (ESR) is the oldest known back-arc spreading system in the world, with spreading on the ESR having started > 15 Ma (and possibly since 20 Ma) (Larter et al. 2003). Subduction of the South American plate under the eastward-moving Sandwich plate (oceanic trench rollback) (Fig. 3.1) results in volcanism adjacent to the trench (SSI) and in concert with the southwest-moving Scotia plate,

accounts for the spreading, at an intermediate rate of 62-70 mm yr^{-1}, of the ESR owing to tensional forces (Livermore 2003). The ESR is divided into nine segments, E1-E9 and spans ~ 500 km, north to south. Segments E3-E9 have deep axial valleys reminiscent of the Mid-Atlantic Ridge, with depths of 3,500-4,000 m, whereas the E2 and E9 segments are characterized by shallow, axial highs (~ 2,500 m depth) suggestive of underlying buoyant magma plumes (Fig. 3.2) whose cause is related to the proximity of these segments to the trench volcanic front (Fretzdorff et al. 2002; Livermore 2003). Confirmation of hydrothermal venting on the ESR has been found at the E2 and E9 segments (Rogers et al. 2012) and a plume signature has also been found at the E5 segment as well (German et al. 2000). The only other area with confirmed venting is in a submerged caldera adjacent to the Kemp seamount (referred herein as the Kemp Caldera) at the southwest extremity of the SSI arc (Rogers 2010). Whilst the full extent of hydrothermal venting on the ESR is unknown, as only the E2 and E9 segments have been systematically surveyed (German et al. 2000), it has been suggested that the presence of venting at the topographical highs of the E2 and E9 segments and the existence of a vent plume signature above the shallowest part of the E5 segment may indicate that venting is only restricted to such shallow sites and may be rare in other segments of the ridge (Baker et al. 2005; Livermore 2006) (Fig. 3.2).

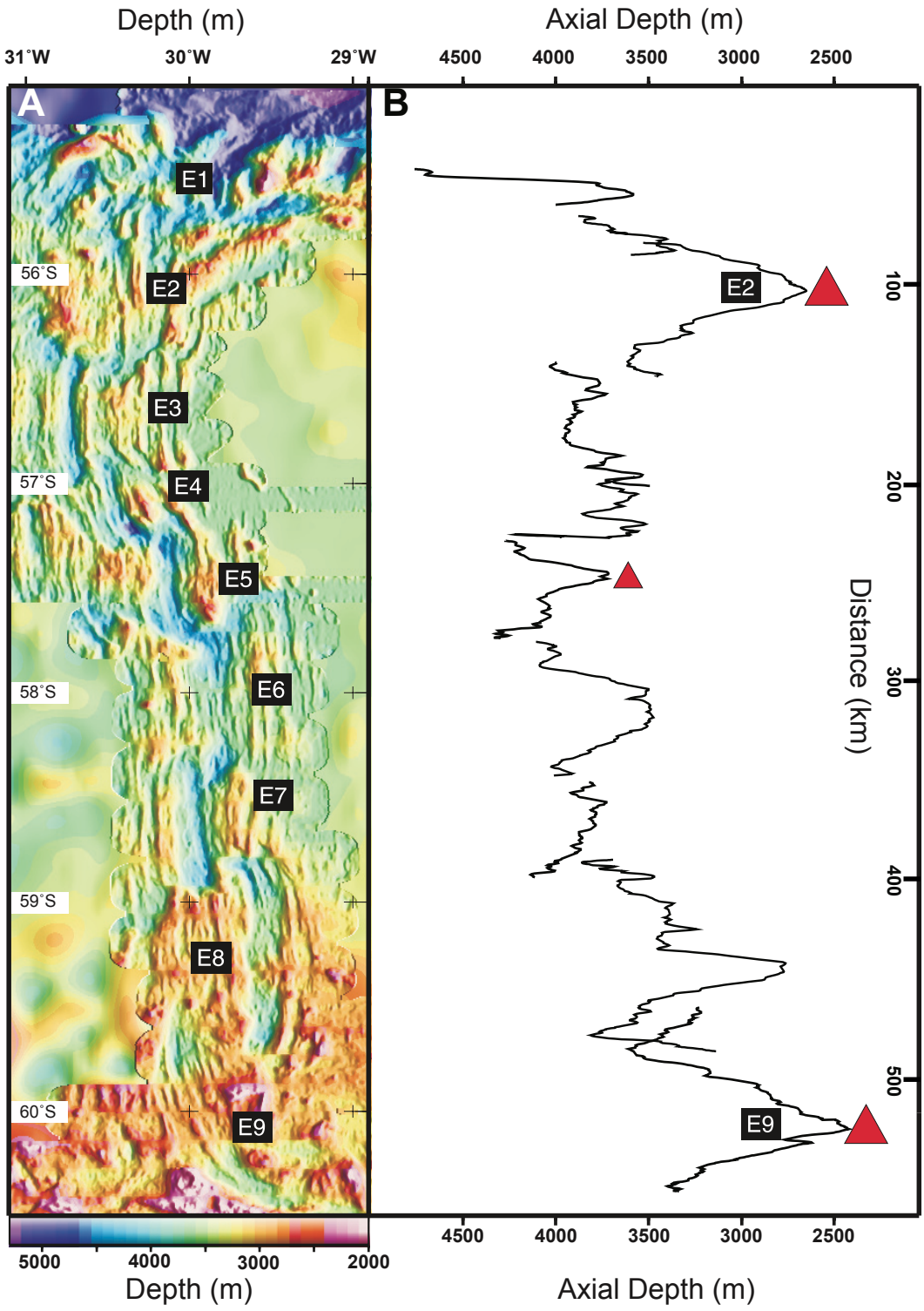

Figure 3.2. Topographical and spreading characteristics of the East Scotia Ridge, modified from Livermore (2006). (A) HAWAII-MR1 Sonar bathymetry of the East Scotia Ridge, with labeled ridge segments. (B) Depth of ridge axis from HAWAII-MR1 sonar with red triangles marking the locations of possible hydrothermal plumes (German et al. 2000). Large triangles denote confirmed venting at the E2 and E9 segments.

The current regime of the Southern Ocean is ultimately dominated by the easterly-flowing Antarctic Circumpolar Current (ACC), but within the eastern reaches of the Scotia Sea, the ACC is largely deflected north of the ESR and SSI and there is a complex mixing zone of various distinct deep and bottom waters of differing origins, the paths of which are to a certain extent constrained by the tectonically-generated sea floor topography (e.g. remnants of the West Scotia Ridge, the ESR and the SSI) of the region (Meredith et al. 2001; Naveira-Garabato et al. 2002). In general, bottom waters around the ESR and SSI are dominated by Weddell Sea Deep Water (WSDW) (flowing broadly northeasterly), variants of the Circumpolar Deep Water (CDW) and South Pacific Deep Water (SPDW) (generally flowing east and northeasterly) which flow through the Drake Passage (Fig. 3.3) (Naveira-Garabato et al. 2002; Meredith et al. 2008). No direct long-term current measurements have been made on the East Scotia Ridge or around the Kemp Caldera at depths relevant to this study, however.

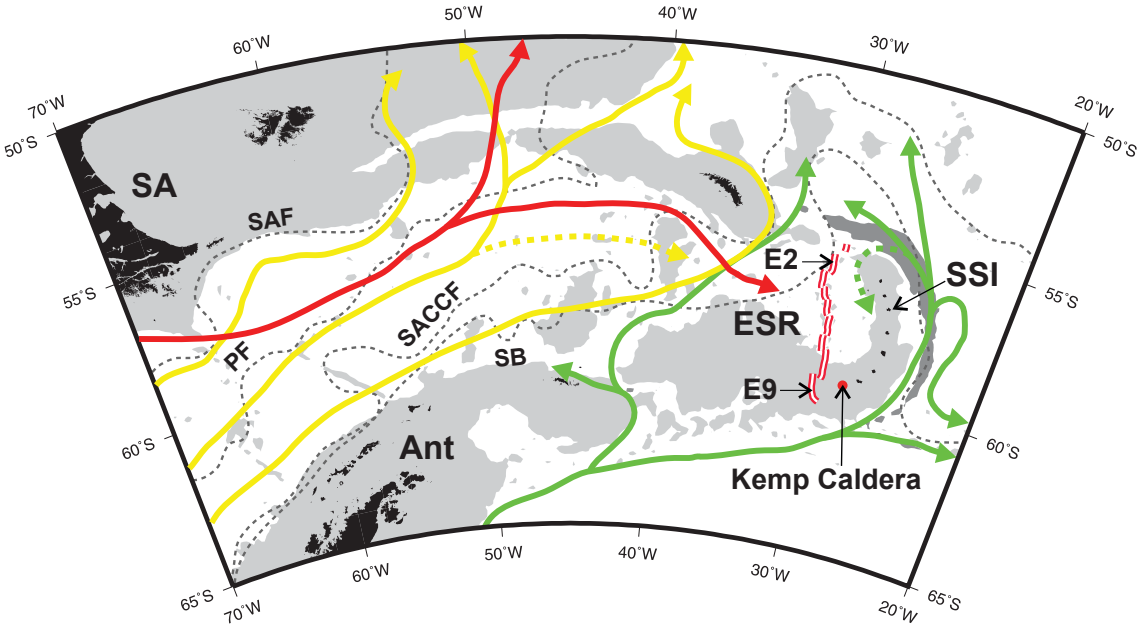

Figure 3.3. Deep-water currents in the Scotia Sea, modified from Naveira-Garabato et al. (2002), Meredith et al. (2008) and Livermore (2006). Green arrows represent the flow of Weddell Sea Deep Water (WSDW), yellow arrows denote Circumpolar and South Pacific Deep Water (CDW & SPDW) flow (dotted = hypothetical) and red arrows denote the flow of South Pacific Deep Shelf Water (SPDSW). SA = South America, Ant = Antarctica, ESR = East Scotia Ridge, SSI = South Sandwich Islands. Areas shaded in light grey are at 3,000 m depth or shallower, with areas in dark grey, 6,000 m or deeper. Grey dotted lines denote current boundaries of the Antarctic Circumpolar Current (ACC). SAF = Sub-Antarctic Front, PF = Polar Front, SACCF = Southern ACC Front, SB = Southern Boundary of the ACC.

3.2.5.2 Sampling Locations

In 2010, hydrothermal vents were sampled for the first time in the Southern Ocean (Atlantic sector), at two sites, one at the E2 segment (~ 2,600 m depth) and one at the E9 segment (~ 2,400 m depth) along the ESR (Rogers et al. 2012) and at the Kemp Caldera (~ 1,400 m depth) (Rogers 2010), a submerged part of the SSI back-arc system (Fig. 3.1).

Hydrothermal vents on the ESR host undescribed species of *Kiwa* squat lobsters, *Lepetodrilus* limpets, neolepadine barnacles, peltospirid gastropods and actinostolid anemones (Fig. 3.4). The E2 and E9 vent fields both feature black smoker venting at temperatures in excess of 350 ˚C, as well as extensive diffuse venting and are situated roughly 440 km apart at the northern and southern ends of the ridge respectively (Rogers et al. 2012).

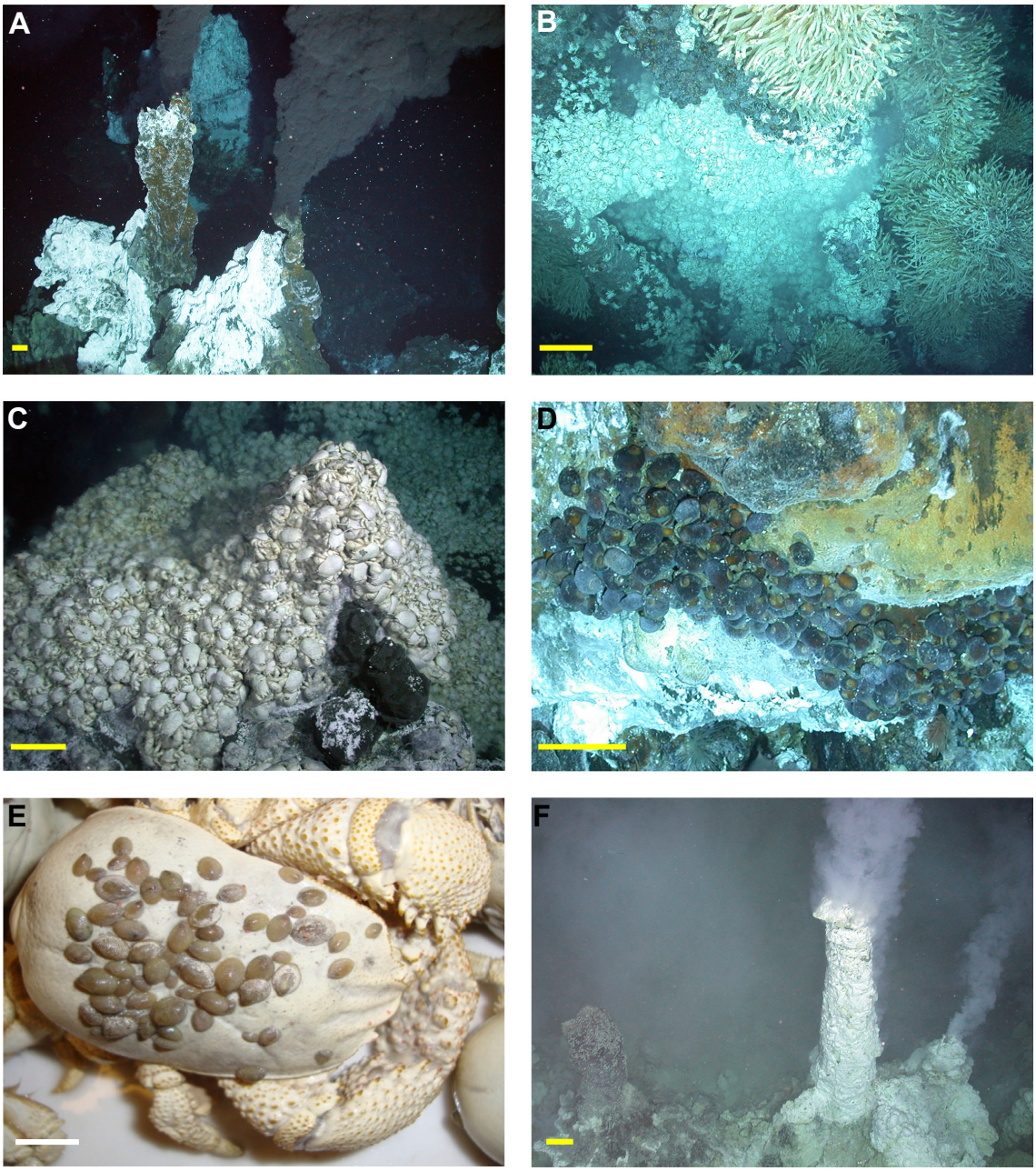

Figure 3.4. Photographs of venting and megafauna at the East Scotia Ridge (ESR) and the Kemp Caldera. (A) Active 'black smoker' venting at the E2 vent fields on the ESR. (B) Dominant vent-endemic megafauna at the ESR, with kiwaid crabs, peltospirid gastropods, lepetodrilid limpets, neolepadine barnacles and actinostolid anemones. (C) Dense stands of *Kiwa* sp. at E9 vents on the ESR. (D) Dense aggregation of peltospirid gastropods on a sulphide chimney at E2. (E) *Lepetodrilus* sp. individuals on the carapace of a *Kiwa* sp. specimen collected from E9. (F) Sulphide 'white smoker' chimneys covered in elemental sulphur. Small speckles are lepetodrillid limpets. White bars = 1 cm and yellow bars = 10 cm.

The Kemp Caldera vents are situated on a volcanic knoll within a caldera feature adjacent to the Kemp Seamount (Fig. 3.5). The knoll rises ~ 200 m above the floor of the ~ 1,600 m deep caldera, the rim of which rises to ~ 800 m depth. Venting witnessed in 2010 was either diffuse or white smoking, with end member fluid temperatures in excess of 200 ˚C emanating from chimneys coated in elemental sulphur. Chimneys were largely lacking in fauna, with 'dead zones' where squid and shrimp carcasses were commonly seen (Fig. 3.4F). Areas of hard substrata around the vents were dominated by *Lepetodrilus* and *Pyropelta* limpets, *Sericosura* pycnogonids and actinostolid anemones, whereas sedimented areas with diffuse venting hosted thiasyrid and vesicomyid clams, all of which were undescribed at the time of discovery.

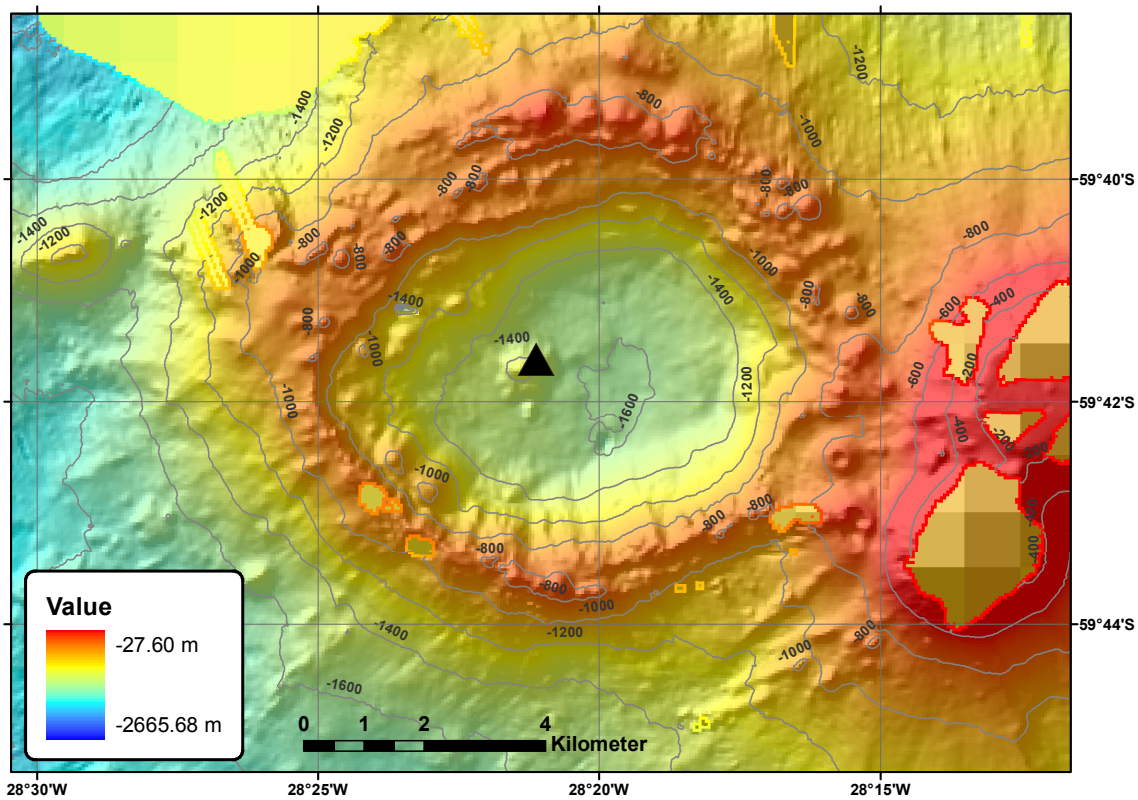

Figure 3.5. Bathymetry map of the Kemp Caldera showing the location of hydrothermal vents, courtesy of Alistair Graham and Rob Larter of the British Antarctic Survey. Triangle denotes location of hydrothermal vents from where *Lepetodrilus* sp. individuals were collected.

3.2.5.3 Study Animals

Lepetodrilus sp. limpets

These limpets have been observed at high densities (excess of 50,000 m^{-2} at the E9 site; Leigh Marsh, personal communication) and at all three sites at both diffuse and more actively venting areas. Although little is known presently of the biology of this particular species, there is a wealth of data on other members of the genus. *Lepetodrilus* spp. appear to produce non-feeding, actively swimming lecithotrophic larvae (Lutz et al. 1986), with continuous production, although oocytes are so small as to be in the size range (< 90 μm) of species producing planktotrophic larvae (Kelly and Metaxas 2007; Tyler et al. 2008). *Lepetodrilus* sp. larvae have been found in high numbers both suspended within the buoyant vent plume > 200 m above the Juan de Fuca Ridge (Mullineaux et al. 1995) and also a few meters above the seafloor on the EPR (Mullineaux et al. 2005). Although precise laboratory-based estimates of potential larval longevity (and therefore dispersal capability) is lacking, connectivity along the EPR appears high, with the exception of the equatorial region where cross-ridge axis currents may impede gene flow (Plouviez et al. 2009). Limpets have also been observed as early colonizers at vents recently defaunated owing to volcanic eruptions (Mullineaux et al. 2012). Examination across several species from both the Pacific and the Atlantic show that *Lepetodrilus* spp. are highly fecund with one individual of *L. elevatus* containing ~ 1,800 oocytes, although most individuals contained < 1,000 oocytes (Tyler et al. 2008). Examinations of soft tissue of *L. gordensis* and *L. fucensis* has revealed that despite these limpets having fully functional radulas and guts, their gills also house symbionts, indicative of a flexible feeding strategy (grazing, filter feeding and symbiosis) that may explain why limpets are found in a variety of venting conditions (Johnson et al. 2006; Bates 2007; Mullineaux et al. 2013). Examination of *L. fucensis* distribution around vents also indicates that males and juveniles were found further from active venting compared

to females and that transplant experiments showed that female survival significantly reduced if they were moved from vigorously venting chimneys to diffuse areas of venting (Bates 2006; Bates 2008).

Peltospirid gastropod

As this is an undescribed species, aside from inferences from physiology, little is presently known of the ecology of this species. Nevertheless, the inferences made from physiology are consistent with what is known from other peltospirid and neomphaloid gastropods (Chen et al., submitted). Observations of the distribution of the peltospirids at E9 indicate that they occupy intermediate distances from the most vigorous vents, generally further away from vent effluent than the kiwaid crabs, but closer in than the barnacles and at minimum densities of 1062 m^{-2} (Marsh et al. 2012). The protoconch morphology is consistent with a lecithotrophic larval stage and an enlarged oesophageal gland with a reduced gut suggests that this species derives much of its nutrition by symbiosis with chemosynthetic bacteria (Chen et al., submitted). Whilst endosymbiotic bacteria are commonly found in the gills of molluscs, enlarged esophageal glands housing endosymbionts have been found in another as-yet undescribed peltospirid found in the Indian Ocean, the scaly-foot gastropod (Goffredi et al. 2004). Study of the reproductive biology of five species of peltospirid reveals maximum oocyte size ranges to be 120-184 µm (Tyler et al. 2008; Matabos and Thiebaut 2010), with a fecundity of two species at < 600 and < 400 oocytes per female respectively (Tyler et al. 2008), which is indicative of a lecithotrophic mode of larval dispersal (Tyler et al. 2008; Matabos and Thiebaut 2010). Oocyte production appears to be continuous (Tyler et al. 2008; Matabos and Thiebaut 2010) and as with *Lepetodrilus* spp., peltospirid larvae have been found both on the buoyant hydrothermal plume and close to the seafloor around vents (Mullineaux et al. 1995; Mullineaux et al. 2005), but presently there are no within-species connectivity studies to assess dispersal potential.

Kiwa sp.

As with the other two species, little is known about the ecology of *Kiwa* sp. owing to its recent discovery. Observations from the E9 vents show they occupy the zone closest to vent effluent at densities in excess of 700 m^{-2} (Marsh et al. 2012), which is at least three orders of magnitude greater than the densities observed for *Kiwa hirsuta* on the Pacific-Antarctic Ridge (Macpherson et al. 2005). Three size-class assemblages were observed, with large males found closest to the vent fluid and the other two assemblages further out consisting of smaller juveniles and females (Marsh et al. 2012). Isotope analyses indicate that *Kiwa* sp. derives the vast majority of its nutrition from chemosynthetic bacteria (Reid et al. 2013), and observations of *Kiwa puravida* indicate that episymbiotic chemosynthetic bacteria that grow on carapace setae are ingested as this food source (Thurber et al. 2011). Very little is known of the dispersal capability of this family of squat lobster presently. One gravid female specimen of *K. puravida* contained 800 oocytes of about 1 mm diameter (Thurber et al. 2011) and examination of *Kiwa* sp. eggs indicates that they are of similar size, or larger (Leigh Marsh personal communication). Preliminary examinations of larvae freshly hatched from brooding females suggests that *Kiwa* sp. ESR larvae hatch as megalopa in an advanced stage of development, with a massive yolk sac, so large as to suggest that they may be able to survive on these reserves for at least a year, based on what is known of larval longevity in other anomura (Sven Thatje et al. manuscript in preparation), making this the only decapod known to science with such an abbreviated lecithotrophic dispersal strategy. These larvae show a great deal of similarity to the zoea of the chirostylid *Chirostylus ortmanni* which are non-feeding (lecithotrophic), non-swimming (demersal-drifting) and exhibit highly abbreviated development, indicative of a very limited dispersal potential (Clark and Ng 2008). Conservatively, therefore the expectation is that the larvae of *Kiwa* sp. ESR are negatively buoyant demersal drifters with sufficient food reserves for survival on the scale of many months or even years.

3.2.6 Study Aim

The aim of this study, is to assess genetic connectivity, diversity and demographic history for three undescribed species of vent-endemic fauna: *Kiwa* sp., a peltospirid gastropod and *Lepetodrilus* sp., found at two locations at either end of the East Scotia Ridge and in the case of *Lepetodrilus* sp., at the Kemp Caldera as well, by the analyses of sequences of the mtDNA cytochrome c oxidase subunit I (COI) gene. The purpose of this is to infer the dispersal capability of these animals and how this capability is influenced by hydrography and topography of the region. This is the first such study of chemosynthetic fauna in the Southern Ocean.

3.3 Methods

3.3.1 Setting & Sampling

Megafauna were sampled from hydrothermal vent fields found at three locations using the ROV *ISIS*. Specimens of *Kiwa* sp. ESR, the peltospirid and *Lepetodrilus* sp. were collected from hydrothermal vents on the East Scotia Ridge (ESR) from two spreading segments, E2 and E9 (Rogers et al. 2012). Specimens of *Lepetodrilus* sp. were also collected from hydrothermal vents found within the Kemp Caldera, adjacent to the Kemp Seamount, at the SW end of the South Sandwich Island arc and ~ 100 km ENE of the vents at E9 (59˚ 41.695' S, 28˚ 20.982' W, at 1,434 m depth) (Fig. 3.5).

At E2, *Kiwa* sp. individuals were collected from a site with diffuse shimmering hydrothermal activity, called 'Crab City' (56˚ 05.348' S, 30˚ 19.131' W) at a depth of 2,641 m. The peltospirid gastropod and *Lepetodrilus* sp. individuals were collected from the sides of a black smoker chimney called 'Cinderella's Castle' (59˚ 41.695' S, 28˚ 29.982' W) at 2645 m depth. At E9, *Kiwa* sp. and *Lepetodrilus* sp. individuals were collected from the black smoker chimney, 'Black and White' (60˚ 02.564' S, 29˚ 58.898' W) at 2,402 m depth and specimens of the peltospirid were collected from a diffuse and white smoking site called Marshland (60˚ 02.807' S, 29˚ 58.708' W) at 2,394 m depth.

3.3.2 Tissue & DNA Extraction

Tissue was excised from the animals immediately after the ROV came on deck and placed in

Corning® 5 ml cryotubes in 96% ethanol and then stored in freezers at -20 ˚C. In the case of the two gastropods, foot tissue was excised and in the case of the kiwaid, muscle from one or more pereopods was chosen. For all animals, total genomic DNA was extracted from the tissue using the Qiagen DNeasy® Blood and Tissue Kit (Cat. 69506) following the manufacturers' instructions.

For all three species of interest, a portion of the mitochondrial gene cytochrome c oxidase subunit 1 (COI) was chosen for comparison amongst individuals from the different sites. COI has been used extensively in marine population genetics and phylogenetics owing to its relatively high mutation rate and ease of alignment as a protein-coding gene (France and Hoover 2002; Knowles et al. 2005; Plouviez et al. 2009; Plouviez et al. 2010; Teixeira et al. 2010; da Silva et al. 2011).

A total of 90 *Kiwa* sp. individuals were sequenced; 45 from E2 and 45 from E9. A total of 84 individuals of the peltospirid were sequenced; 43 from E2 and 41 from E9. 140 *Lepetodrilus* sp. limpets were sequenced; 47 from E2, 47 from E9 and 46 from the Kemp Caldera.

3.3.3 PCR & Sequencing Protocol

Reactions were performed in 9 µl volumes, containing 0.6 µl of each primer (forward and reverse) at a concentration of 4 pmol/µl, 6 µl of Qiagen HotStarTaq Master Mix, 1.5 µl of DNA template (~ 50-100 ng/µl) and 0.3 µl of double-distilled water. All PCR reactions were performed on a Bio-Rad C1000 Thermal Cycler.

The PCR thermal cycling protocols used are as follows:

Kiwa sp.

Initial HotStarTaq denaturation at 95 ˚C for 15 minutes, followed by 40 cycles of 94 ˚C for 45 seconds, 50 ˚C for I min, 72 ˚C for 1 min, and a final extension of 5 min at 72 ˚C.

The peltospirid & *Lepetodrilus* sp.

Initial HotStarTaq denaturation at 95 ˚C for 15 minutes, followed by 40 cycles of 94 ˚C for 45 seconds, 50 ˚C for 1 min, 72 ˚C for 1 min, and a final extension of 5 min at 72 ˚C.

Universal invertebrate primers, LCO1490 and HCO2198 (Folmer et al. 1994) were used to amplify COI in *Kiwa* sp. and the peltospirid, yielding fragments ~ 500 bp in length:

LCO1490 5’-GGTCAACAAATCATAAAGATATTGG-3’

HCO2198 5’-TAAACTTCAGGGTGACCAAAAAATCA-3’

These universal primers did not work very well for *Lepetodrilus* sp.. Instead, new primers were designed for this study from a complete COI gene assembled from short fragments of genomic DNA generated by Roche 454 sequencing (Leese et al. 2012) of an individual. This primer worked exceptionally well, and could well be very effective with other members of the genus.

Forward 5’-TAACGATATGCGTTGACCATT-3’

Reverse 5’-ACCCGGGAAGAATCAGAATA-3’

3.3.4 Sequencing

All sequencing reactions were performed on a Bio-Rad C1000 Thermal Cycler. PCR product was purified using QIAquick® PCR Purification Kit (Cat.28106). Sequencing reactions were performed in 10 µl volumes, containing 2.5 µl cleaned PCR product, 2 µl H_2O, 2.5 µl of 0.8 pmol/µl primer 2.5 µl BetterBuffer and 0.5 µl BigDye™. The sequencing reaction protocol was as follows:

Initial denaturation at 96 ˚C for 1 minute, followed by 25 cycles of 96 ˚C for 10 seconds, 50 ˚C for 5 seconds, 60 ˚C for 4 min, and a final cool down to 4 ˚C.

Sequences were resolved using an Applied Biosystems 3100 DNA and consensus sequences were generated from forward and reverse strands using Geneious Pro 5.4.6. (Drummond et al. 2010).

3.3.5 Data Analyses

3.3.5.1 Descriptive Statistics & F_{ST}

For each population, basic descriptive statistics, including the number of haplotypes (*h*) and haplotype diversity (*Hd*) was determined using DnaSP v5 (Librado and Rozas 2009) based on un-weighted pairwise differences between haplotypes. AMOVA (Analysis of MOLecular VAriance) was performed (using pairwise differences) in Arlequin 3.5.1.2 (Excoffier and Lischer 2010) to provide an F_{ST} value indicating the degree of genetic differentiation between the two populations. Unlike traditional *F* statistics, which is based upon comparison of gene frequencies among populations, AMOVA is able to utilize the fact that molecular data can also

tell us something about the amount of mutational differences between different genes or haplotypes, i.e., instead of just focusing on allele frequencies, AMOVA also takes into account the degree of differentiation between the alleles (Excoffier et al. 1992). Statistical significance of the F_{ST} was evaluated by permuting haplotypes among samples (10,000 permutations).

3.3.5.2 Neutrality Tests & Demographic Analyses

To test for neutrality, Tajima's *D* and Fu's *Fs* tests were implemented in Arlequin. Tajima's *D* (Tajima 1989) test is based on the difference between θ (mutation-scaled effective female population) estimated from the number of polymorphic sites (θ_k) and θ estimated from the average sequence pairwise divergence (θ_π). Alternatively Fu's *F*s (Fu 1996) uses θ_π as an estimate of θ and generates samples from a neutral coalescent model with that parameter and compares the observed and expected number of alleles (haplotypes). Essentially, both of these measures represent the excess of low frequency allelic variants in the population (i.e., the number of low frequency allelic variants relative to the expected number in a population at Hardy-Weinberg Equilibrium with neutral loci). For both statistics, a negative value is indicative of either a recent population expansion or a selective sweep (purifying selection) at the locus. Fu's *Fs* is better at inferring population expansion or selective sweeps than Tajima's *D* (Fu 1996). If a population rapidly expands, new mutations are less and less likely to be lost as a result of drift (which is weaker in larger populations) leading to an excess of single nucleotide variants of the common haplotypes (i.e., low pairwise divergence). If population size were to remain stable, but purifying selection was occurring at the locus, the only mutations to accumulate would be low frequency mutations at silent sites, resulting in a similar pattern of diversity as would occur in a demographic expansion scenario.

Testing of Tajima's *D* and Fu's *Fs* was conducted in Arlequin by bootstrap pseudo-replication

with 10,000 replicates. Historical demography was analysed by calculating mismatch distributions (representation of the frequency distribution of pairwise differences among haplotypes in a sample) and then using Harpending's raggedness index (Hri) (Rogers and Harpending 1992) in Arlequin, which assesses the degree of unimodality in a mismatch distribution. Populations that are stable over time exhibit bimodal or multimodal mismatch distributions for loci not under selection, whereas unimodal distributions suggest recent and rapid population expansion, which would result in a non-significant Hri ($P > 0.05$) indicating that the null hypothesis of a stable population history can be rejected. Median-Joining networks, representing the most parsimonious relationships between haplotypes were calculated using Network 4.6.1.1. (Bandelt et al. 1999) and then edited on Adobe Illustrator CS3 in order to visualise the relationship between different haplotypes.

In cases where there was strong evidence of a genetic bottleneck in the past (based on Tajima's *D*, Fu's *Fs* and the mismatch distributions) Bayesian Skyline Plots (BSPs) were used to date this change. BSPs enable the estimation of historical demographic change from a genealogy based on coalescent theory within a bayesian computational framework. BSPs reconstruct demographic history by estimating effective population size from inferred genealogies going back in time to the coalescent (Ho and Shapiro 2011). In this study, Beast v.1.7.4 (Drummond and Rambaut 2007) was used to construct BSPs for populations as defined by F_{ST}.

All analyses ran for 100 million Markov Chain Monte Carlo (MCMC) generations with the first 10% discarded as 'burn-in'. Genealogies and model parameters were sampled every thousand generations. For each species, analyses were replicated twice to ensure consistent results. Both runs were then combined using LogCombiner v.1.7.4 (Drummond and Rambaut 2007) to estimate parameters. The model of evolution for each population was chosen with PartitionFinder (Lanfear et al. 2012), which uses a maximum likelihood approach to determine the best fitting model of evolution to a sequence alignment, using both the Akaike information criterion (AIC) and the more conservative Bayesian information criterion (BIC), which

penalises against over-parameterised models more than the AIC (Minin et al. 2003). PartitionFinder was set to only test models that can be used in Beast. Both criteria favoured the Tamura-Nei model with invariant sites for all three species, with the addition of gamma distributed rate variation among sites for the kiwaids.

The genealogies were calibrated with different COI substitution rates of molecular evolution under a strict molecular clock model depending on the species. For *Kiwa* sp. three substitution rates were used. The first is based on the divergence of *Bythograea* spp. across the Easter Microplate on the Southern East Pacific Rise (SEPR) (Guinot and Hurtado 2003). These are the only vent crabs for which a divergence (7.3% Kimura 2-parameter) can be linked to the formation of a dated mid-ocean ridge discontinuity, the microplate, which formed ~ 5.25-2.47 Ma (Naar and Hey 1991; Rusby and Searle 1995). In this study a mean age for the microplate (3.86 Ma) has been used to get a substitution rate of 9.45596 x 10^{-9} substitutions per locus per year. The second substitution rate was generated by using the K2P COI divergence between the *Kiwa* sp. individual from the ESR and the *Kiwa* sp. individual collected from the Southwest Indian Ridge (SWIR) (3.7%) for the phylogenetic analyses in Chapter 2. Although no ridge discontinuity can be used for calibration, the estimated median divergence date (1.5 Ma with the AIC partition scheme) between these two *Kiwas*, based on fossil calibrations were used (Chapter 2) to yield an estimated substitution rate of 1.23333 x 10^{-8} substitutions per locus per year. The third rate is based on the divergence (8.7%) of *Synalpheus* spp. shrimps across the Panama Isthmus which formed ~ 2.8 Ma (Lessios 2008), giving a faster rate of 1.55357 x 10^{-8}.

For the peltospirid, two general substitution rates were used based on vicariance of geminate species either side of the Panama Isthmus (Lessios 2008). A slow rate of 1.32143 x 10^{-8} based on a 7.4% K2P divergence of *Strombus* spp. and a faster rate of 1.64286 x 10^{-8} based on a 9.2% K2P divergence of *Conus* spp. In addition, a Neomphaline-specific substitution rate (1.45078 x 10^{-8}) was estimated based on the 7.9% divergence of *Pachydermia* spp. across the Easter

Microplate (Matabos et al. 2011).

For the limpet, a *Lepetodrilus*-specific rate was used based on the 8% divergence of *L. pustulosus* across the Easter Microplate (Johnson et al. 2008) (mean age of 3.86 Ma), giving a rate of 1.03627×10^{-8}. Slower substitution rates have been used for *Lepetodrilus* before, based on the divergence of species resulting from the subduction of the Pacific Farallon Ridge under the N. American plate (~ 28 Ma) or the formation of the Cascadia depression in the Blanco Transform Fault (~ 5 Ma) (Johnson et al. 2006; Plouviez et al. 2009). However, using such old divergence dates to estimate substitution rates when attempting to infer demographic changes on the timescale of within-species population variation is likely to drastically underestimate the true substitution rate owing to saturation (Ho et al. 2011). The fast mollusc rate based on *Conus* spp., divergence across the Panama Isthmus was also used. BSP reconstructions were conducted in TRACER v.1.5 (Rambaut and Drummond 2007) and refined using Adobe Illustrator CS3.

3.4 Results

3.4.1 Population Diversity & Structure

For a 642 bp segment of COI, a total of 79 haplotypes were recovered from 90 kiwaid individuals across the ESR. Consequently, the haplotype diversity (*h*), and therefore the female effective population size for this species was very high: 0.996 (0.998 both at E2 and E9) (Table 3.1). At E2, 36 individuals had haplotypes unique to that location (private haplotypes) as did the same number at E9. For the peltospirid, 24 haplotypes were recovered from 84 individuals, with an *h* of 0.859 (0.865 and 0.855 at E2 and E9 respectively). For *Lepetodrilus* sp., 36 haplotypes accounted for the diversity of 140 individuals across E2, E9 and the Kemp Caldera with an *h* of 0.833 across all locations (0.614, 0.743 and 0.85 for E2, E9 and Kemp respectively). Limpet haplotype diversity was noticeably higher at Kemp compared to the two localities on the ESR; indeed, there were almost as many haplotypes at Kemp as there were at the two ESR locations combined (20 and 22 haplotypes respectively).

Table 3.1. Genetic diversity indices, for *Kiwa* sp., a peltospirid gastropod and *Lepetodrilus* sp. sampled at vent sites on the East Scotia Ridge and the Kemp Caldera. Sample size (*n*), number of haplotypes (*N*h), number of private haplotypes (*Np*h), number of polymorphic sites (*k*), haplotype diversity (*h*), mean number of pairwise differences (π1), nucleotide diversity (π2) are reported. Tests for deviation from neutrality, Tajima's D (*D*) and Fu's FS (*Fs*) are also reported, with significant negative values (after 10,000 boostrap pseudoreplicates) indicative of population expansion or a selective sweep. Significant neutrality test results ($P < 0.05$) highlighted in bold.

Species	Location	*n*	*Size (bp)*	*k*	*N*h	*Np*h	*h*	π1	π2	*D*	*Fs*
Kiwa sp.	E2	45	642	52	43	36	0.998 (0.005)	7.527	0.012	-1.288	**-24.971**
	E9	45	642	46	43	36	0.998 (0.005)	6.102	0.010	-1.464	**-25.253**
	ESR	90	642	69	79	72	0.996 (0.003)	6.821	0.011	-1.376	**-25.112**
Peltospirid	E2	43	437	13	15	9	0.865 (0.030)	1.934	0.004	-1.098	**-8.150**
	E9	41	437	20	18	12	0.855 (0.044)	2.224	0.005	**-1.726**	**-11.783**
	ESR	84	437	25	27	21	0.859 (0.024)	2.069	0.005	-1.412	**-9.967**
Lepetodrilus sp.	E2	47	618	10	10	6	0.614 (0.064)	0.947	0.002	**-1.687**	**-5.926**
	E9	47	618	12	13	8	0.743 (0.047)	1.099	0.002	**-1.781**	**-9.483**
	ESR	94	618	18	19	14	0.682 (0.039)	1.025	0.002	**-2.037**	**-17.755**
	Kemp	46	618	20	19	14	0.850 (0.040)	1.661	0.003	**-2.052**	**-16.177**
	Total	140	618	36	37	28	0.833 (0.022)	1.772	0.003	**-1.840**	**-10.529**

There was no evidence for population differentiation between E2 and E9 for all three species in this study, with non-significant F_{ST} values of 0.00191, -0.00631 and 0.0054 for the kiwaid, peltospirid and lepetodrillid respectively, despite being separated by ~ 440 km of spreading ridge. Conversely, there was strong evidence for population differentiation between lepetodrillid limpets on the ESR and the Kemp Caldera (~ 95 km from nearest point on ESR), with F_{ST} > 0.45 (Table 3.2). This divergence is also visible in the median-joining network for *Lepetodrilus* sp., where very few haplotypes are shared between the ESR limpets and those at Kemp. In contrast, haplotypes shared by two or more individuals on the ESR for all three species are generally shared between E2 and E9 (Figs. 3.7-3.9).

Table 3.2. F_{ST} *Pairwise* comparisons of *Kiwa* sp., a peltospirid gastropod and *Lepetodrilus* sp., at vent sites on the East Scotia Ridge and the Kemp Caldera in the Scotia Sea. Significant F_{ST} (10,000 permutations, $P < 0.05$ in Arlequin) values highlighted in bold.

Species	Pairwise Comparison	F_{ST}	P Value
Kiwa sp.	E2 vs E9	0.00191	0.31545
Peltospirid	E2 vs E9	-0.00631	0.61287
Lepetodrilus sp.	E2 vs E9	0.00540	0.22047
***Lepetodrilus* sp.**	**E2 vs Kemp**	**0.45397**	**0.00000**
***Lepetodrilus* sp.**	**E9 vs Kemp**	**0.50051**	**0.00000**

3.4.2 Neutrality/Demography

Tajima's *D* and Fu's *Fs* both assess deviations from neutrality and significantly negative scores ($P < 0.05$) will indicate either that there has been a recent population expansion, or that there has been a recent selective sweep. For the kiwaids, Tajima's *D* values were not significant and only the E9 location was significantly negative for the peltospirids. All three locations were significantly negative for the limpets, however. Fu's *Fs* were significantly negative for all species at all locations. Mismatch distributions were largely unimodal for all three species at all

locations, with the exception of the kiwaids, which produced a bimodal distribution (Fig. 3.6), perhaps indicative of two phases of demographic expansion. Harpending's raggedness index (Hri) scores for all species were non-significant, signifying that the null hypothesis of exponential population expansion cannot be rejected. For the limpet and the peltospirid, the median-joining networks revealed a distinctive star-like pattern (Figs 3.8 & 3.9). A similar pattern was also noticeable with the kiwaid, however the number of equally parsimonious connections was too great for visualisation, and instead, one of several equally parsimonious trees was presented instead (Fig. 3.7).

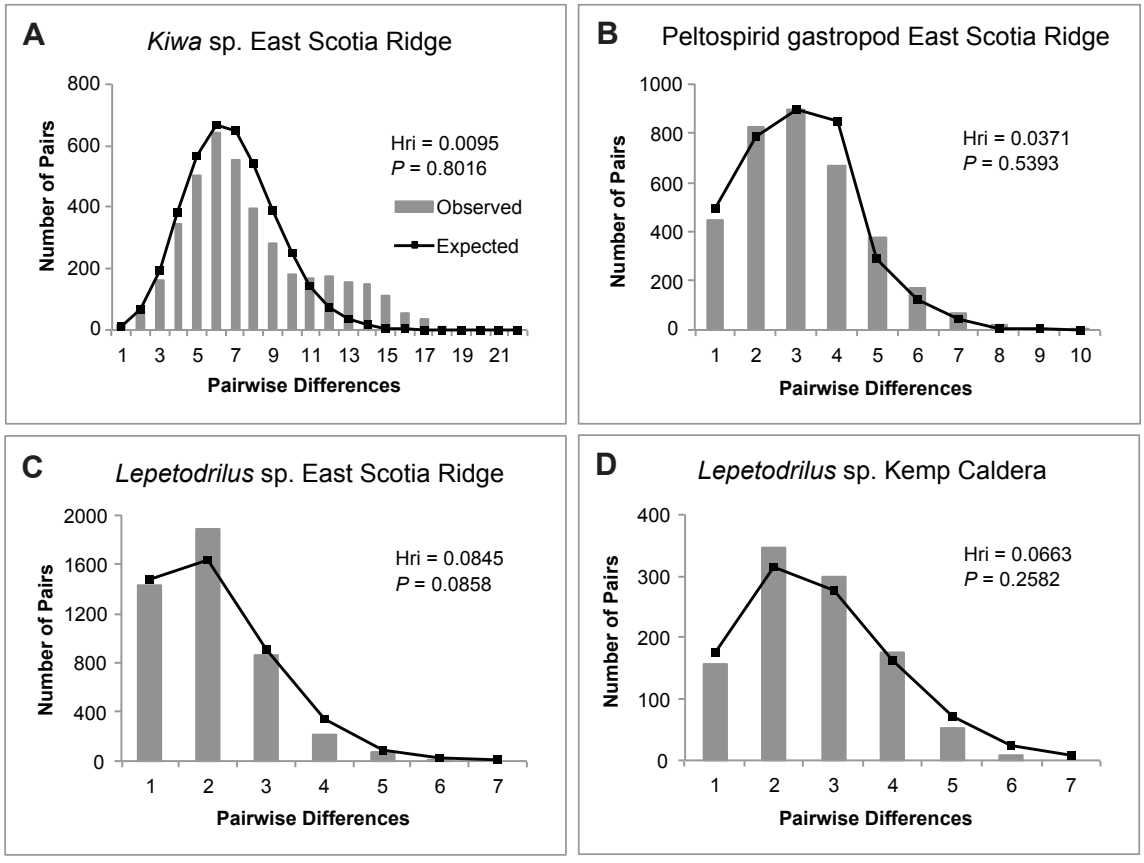

Figure 3.6. Observed and expected (demographic expansion model) mismatch distributions of COI nucleotide pairwise differences for *Kiwa* sp., a peltospirid gastropod and *Lepetodrilus* sp., at the East Scotia Ridge (A-C) and *Lepetodrilus* sp. at the Kemp Caldera in the Scotia Sea. Analyses performed in Arlequin 3.5 with 10,000 bootstrap replicates. Harpending's raggedness index (Hri) and associated *P* values displayed.

The BSP plots for all three species (Figs. 3.10 & 3.11) showed a pattern of demographic expansion within the last million years. According to the 95% confidence intervals of the different substitution rates used per species, *Kiwa* sp. underwent a demographic expansion (or recovery from a selective sweep) ~ 250-750 Ka. The peltospirid population expanded more recently at ~ 50-125 Ka with all three mutation rates suggesting that this expansion has levelled off. The two limpet populations have different expansion signatures, with the Kemp Caldera population expanding 65-200 Ka and the ESR population expanding more recently at ~ 25-75 Ka. Unlike the gastropods, which appear to exhibit a single expansion event, the kiwaid BSP shows a 'stepped' pattern i.e., two phases of population expansion, with the second one beginning ~ 100-300 Ka.

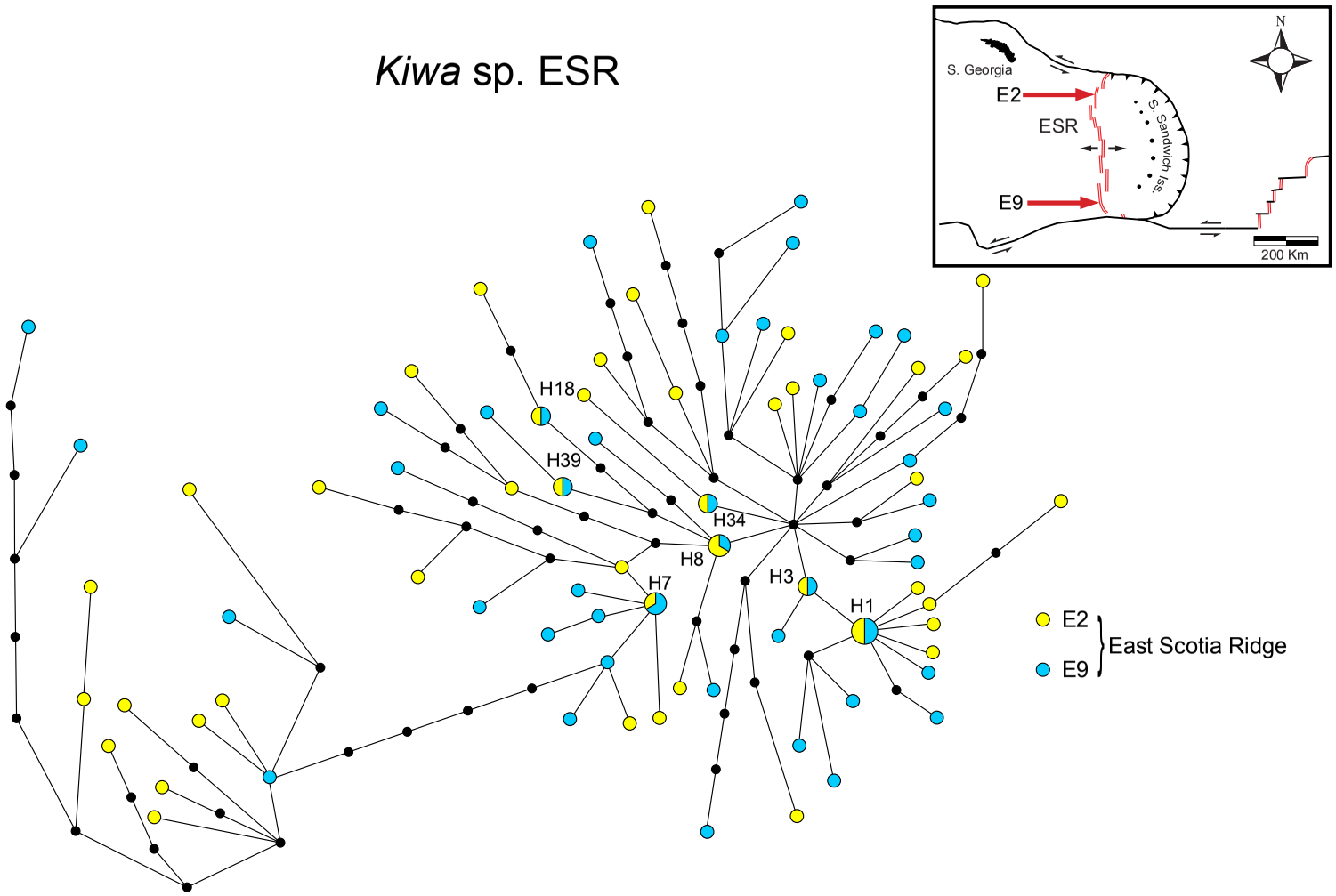

Figure 3.7. One of several equally parsimonious median-joining COI haplotype trees of *Kiwa* sp. from the East Scotia Ridge (ESR on inset map) collected at the E2 and E9 vent fields and calculated in Network 4.6.1.1. The network is omitted owing to its extreme complexity. Each circle represents a COI haplotype. Black circles denote missing hypothesized haplotypes. Coloured circles are scaled to the number of individuals. Unlabelled haplotypes represent a single individual.

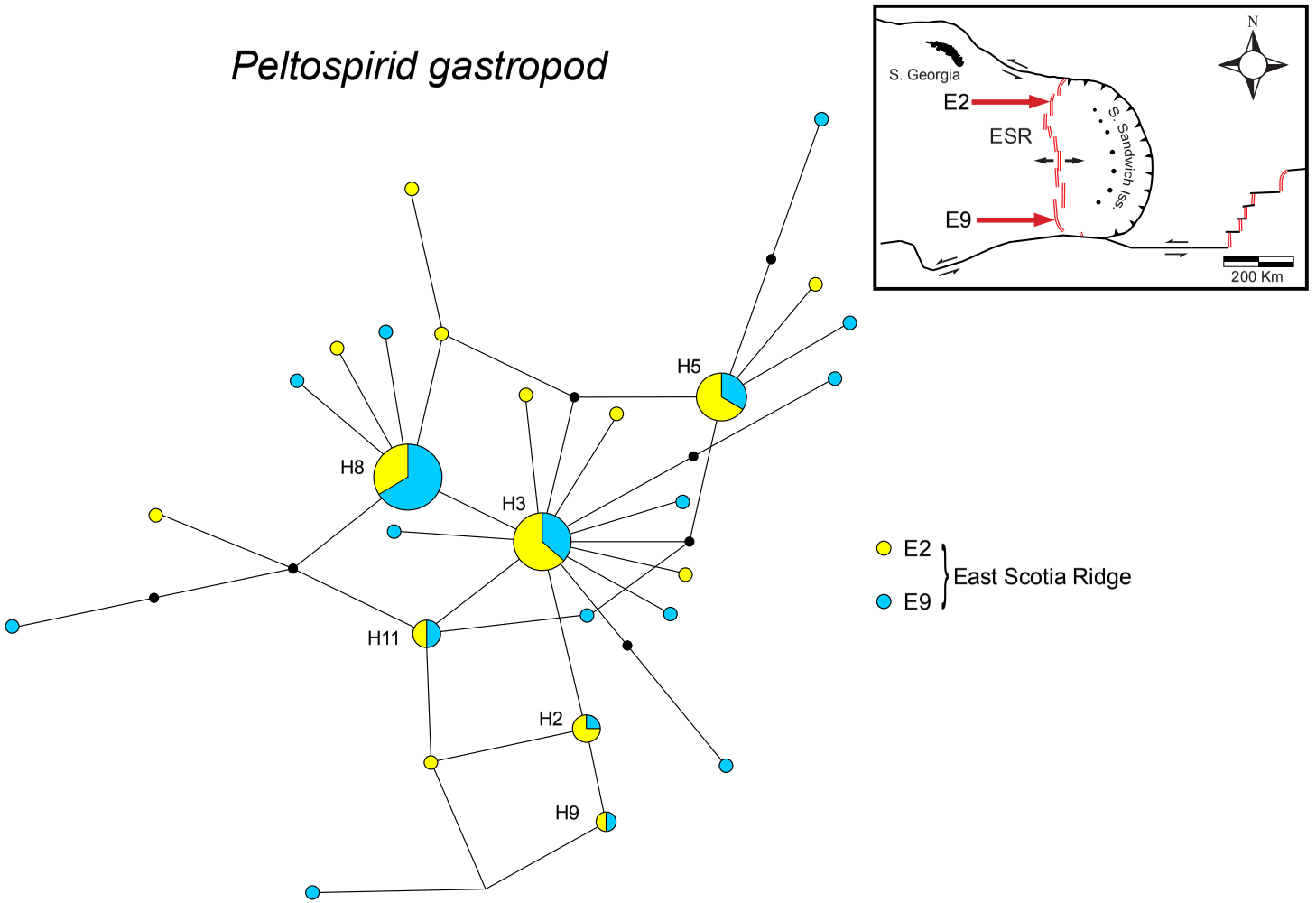

Figure 3.8. Median-joining COI haplotype network of an undescribed species of peltospirid gastropod from the East Scotia Ridge (ESR on inset map) collected at the E2 and E9 vent fields calculated using Network 4.6.1.1. Circles represent haplotypes. Black circles denote missing hypothesized haplotypes. Coloured circles are scaled to the number of individuals, with unlabelled circles representing a single individual.

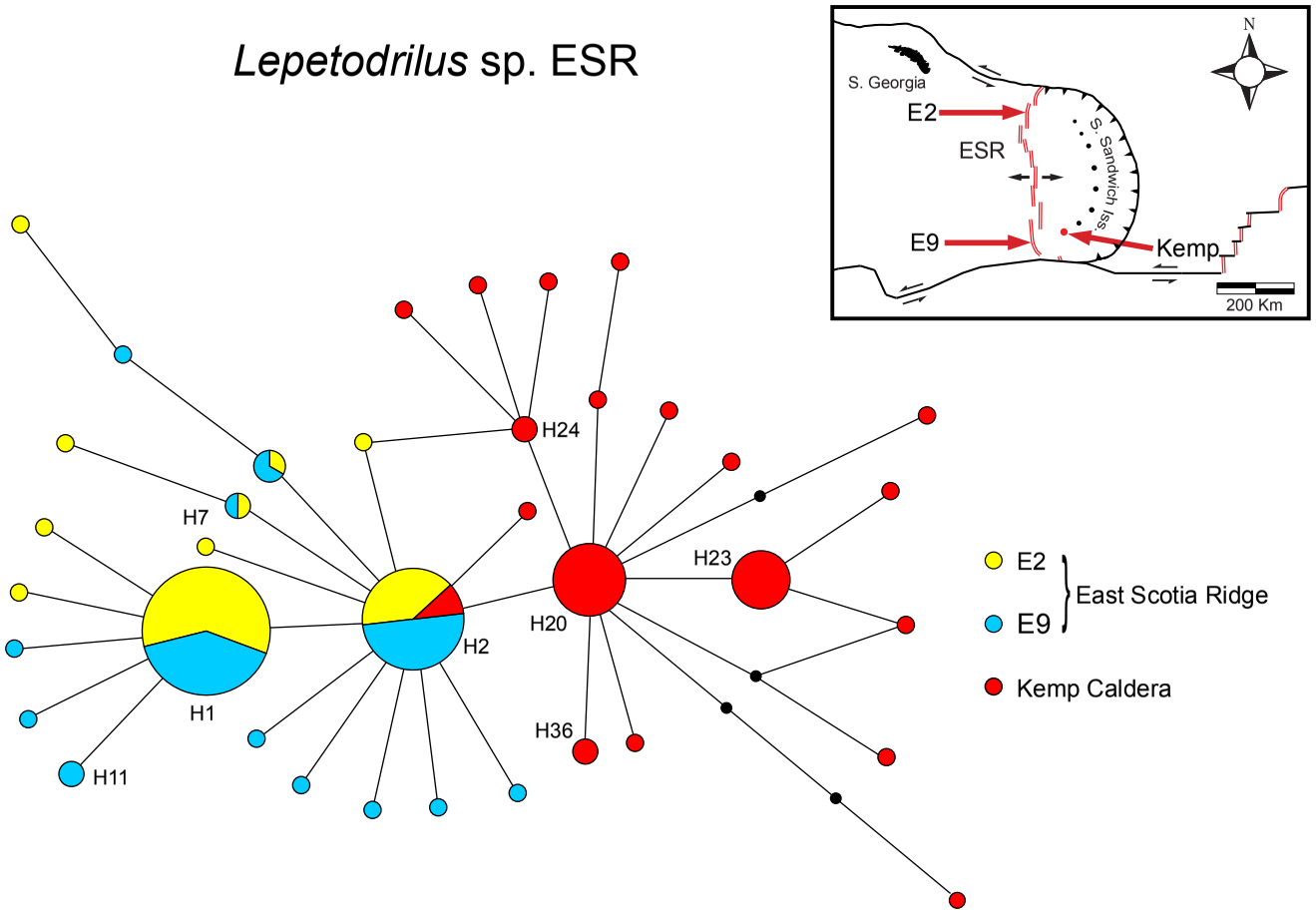

Figure 3.9. Median-joining COI haplotype network of *Lepetodrilus* sp. from the E2 and E9 vent fields on the East Scotia Ridge (ESR on inset map), as well as the Kemp Caldera. Calculated using Network 4.6.1.1. Circles represent haplotypes. Black circles denote missing hypothesized haplotypes. Coloured circles are scaled to the number of individuals, with unlabelled circles representing a single individual.

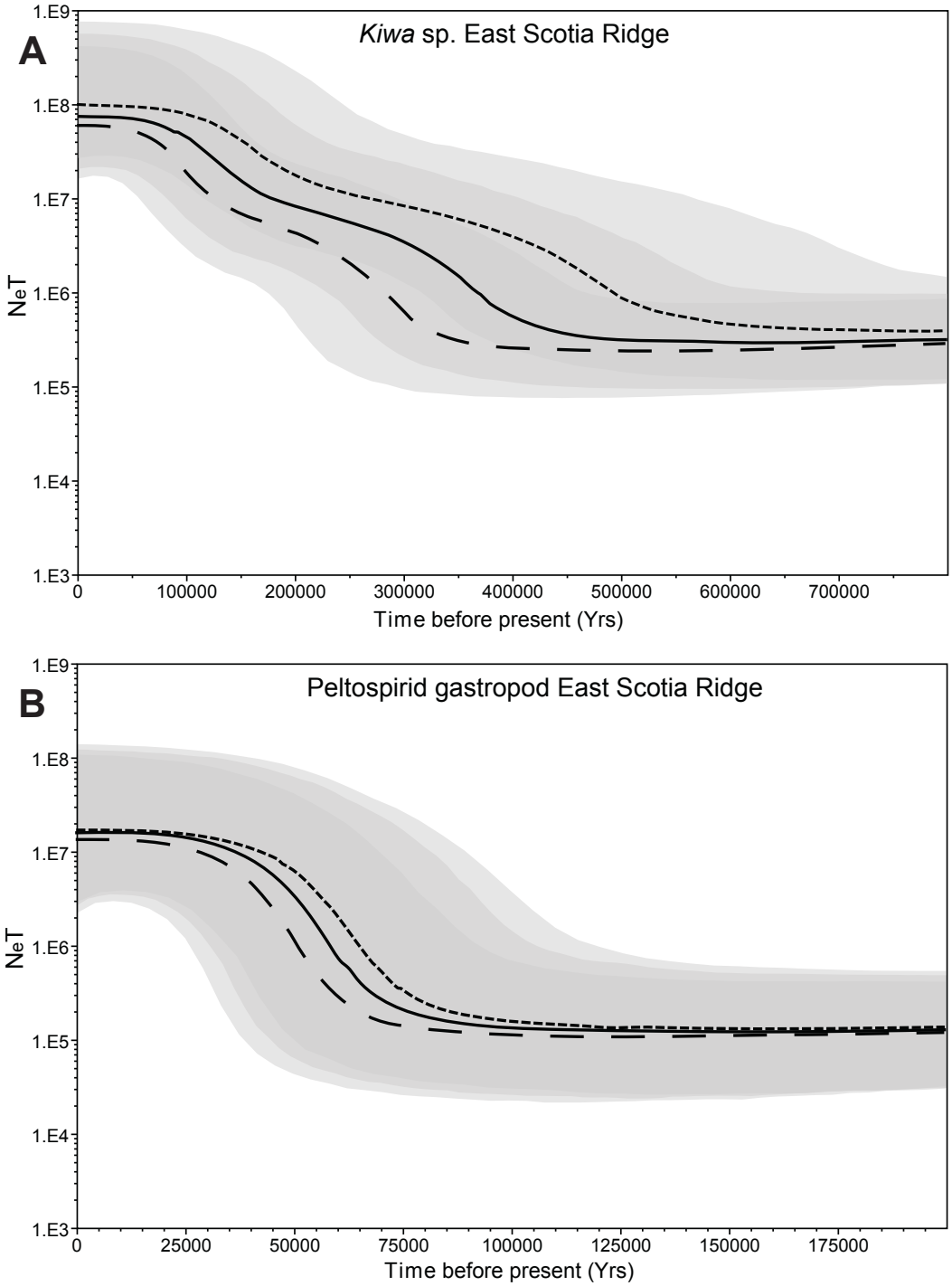

Figure 3.10. Bayesian skyline plots depicting changes in effective population size over time based on mitochondrial COI sequence data of (A) *Kiwa* sp. and (B) a peltospirid gastropod from the East Scotia Ridge under a model of population expansion (calculated in Beast 1.7.4.). Black lines (both dashed and solid) denote median estimates with shaded areas representing 95 % confidence intervals. For *Kiwa* sp., three substitution rates were used: one based on divergence of bythograeid crabs either side of the Easter Microplate (Guinot and Hurtado 2003) generating a rate of 9.45596 x 10^{-9} substitutions per locus per year (short-dash line), one based on the inferred 1.5 Ma divergence of kiwaid crabs between the East Scotia Ridge and the Southwest Indian Ridge based on divergence date estimates from Chapter 2, (rate of 1.23333 x 10^{-8}; solid line) and one based on the divergence of *Synalpheus* spp. across the Panama Isthmus (Lessios 2008) giving a rate of 1.55357 x 10^{-8} (long-dash line). For the peltospirid, three rates were used: one based on the divergence of neomphaline gastropods across the Easter Microplate (Matabos et al. 2011), (rate of 1.45078 x 10^{-8}; solid line) and two rates based on mollusc divergence due to the formation of the Panama Isthmus (Lessios 2008), a slow rate, 1.32143 x 10^{-8} (short-dash line) based on the divergence of *Strombus* spp. and a faster rate of 1.64286 x 10^{-8} (long-dash line) based on the divergence of *Conus* spp. NeT on the y-axis represents the effective population size (Ne) scaled by generation time (T).

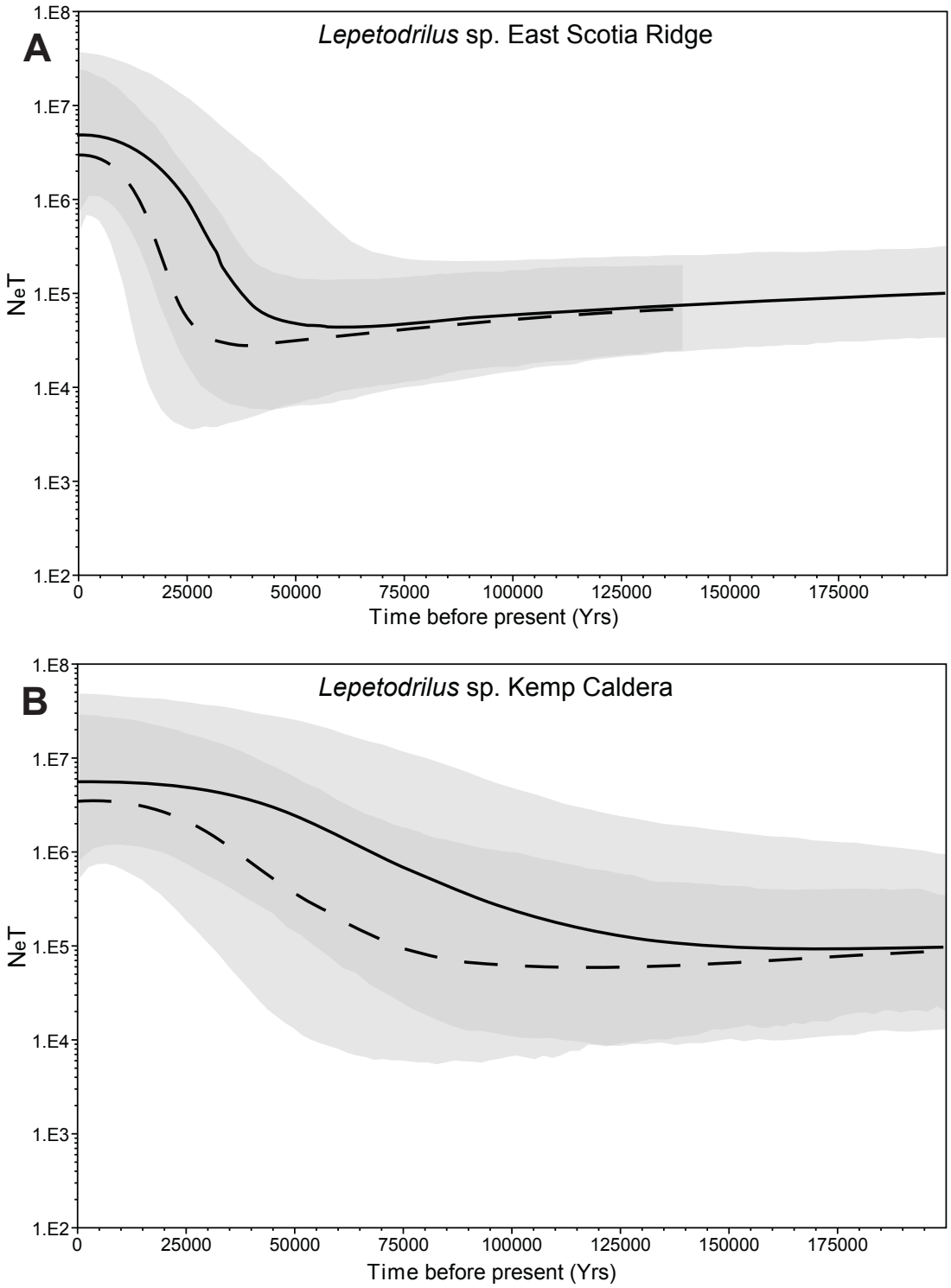

Figure 3.11. Bayesian skyline plots calculated in Beast 1.7.4 depicting changes in effective population size over time, based on mitochondrial COI sequence data of *Lepetodrilus* sp. from (A) the East Scotia Ridge and (B) the Kemp Caldera. Black lines (both dashed and solid) denote median estimates with shaded areas representing the 95 % confidence intervals. Two substitution rates were used: one based on divergence of *Lepetodrilus* spp. across the Easter Microplate (Johnson et al. 2008), generating a rate of 1.03627×10^{-8} substitutions per locus per year (solid line) and a fast rate based on *Conus* spp. divergence due to the formation of the Panama Isthmus (~ 2.8 Ma)(Lessios 2008), yielding a rate rate of 1.64286×10^{-8} (long-dash line). NeT on the y-axis represents the effective population size (Ne) scaled by generation time (T).

3.5 Discussion

3.5.1 Connectivity

3.5.1.1 ESR

The results of AMOVA F_{ST} analyses indicate that across ~ 440 km of the East Scotia Ridge there is no evidence of COI differentiation for all three species. Given these results, the possibility of panmixia along the ridge cannot be rejected, i.e., that genetic similarity between E2 and E9 is maintained by sufficient levels of gene flow to negate the differentiating effects of drift and mutation. Conversely, there is a clear signal of differentiation between ESR limpets and those at the Kemp Caldera, which is only ~ 95 km east of the ESR. The lack of differentiation along the ESR is consistent with gene sequence differentiation found previously at the EPR for the tubeworm *Riftia pachyptila*, where at scales below ~ 1,000 km, pairwise F_{ST} between vent fields are non-significant (Coykendall et al. 2011). Given the possibility that *Kiwa* sp. has a very poor potential dispersal range based on the size and buoyancy of its larvae, the lack of differentiation over such a scale is nevertheless surprising. There are however, other ways of accounting for a lack of differentiation without assuming panmixia. One possibility is that low sampling effort by using only a single locus dataset may have underestimated the true differentiation (Audzijonyte and Vrijenhoek 2010) between E2 and E9. A study using multilocus data should reduce this possibility, however.

Another explanation could be that a lack of differentiation is the product of a recent range expansion where insufficient time has passed for the attainment of migration-drift equilibrium between subpopulations, which tallies with the expansion signatures of all three species (e.g.

significant Fu's *Fs*, mismatch distribution, etc.). Following on from this idea, populations that span a series of vent fields, each with a probability of extinction and recolonization, can be thought of as metapopulations (Vrijenhoek 1997; Vrijenhoek 2010): if new colonies are repopulated by neighbouring ones and this extinction-recolonization process occurs at a rate faster than the time needed for adjacent colonies to achieve migration-drift equilibrium, then genetic differentiation between the colonies may be perpetually depressed (Slatkin 1977; Slatkin 1993) relative to the expectations of the Island Model (Wright 1943), as has been modelled for vent polychaetes (Jollivet et al. 1999). This scenario can be thought of as a near continuous state of small-scale range expansions occurring throughout the metapopulation. A different way of conceptualizing this is that if the *time-averaged mean distance* between vents on a ridge is within the dispersal capability of a given species then a metapopulation with little or no differentiation can exist, even if at any specific moment in time, some of the vents are too far apart for contemporary gene flow.

Indeed, given the fact that populations spanning multiple ephemeral vent fields or colonies so closely match the classic definition of a metapopulation (population of subpopulations that can be born, go extinct and/or be recolonized; Levins 1969), it seems reasonable, perhaps to assume that vent populations are non-equilibrium metapopulations until proven otherwise. In this context, it is unsurprising that the genetic diversity patterns of vent populations are consistent with demographic/range expansion (Vrijenhoek 2010). Vent populations, as *defined* by a region where genetic differentiation is lacking, may be far larger than should be the case based on the actual realised dispersal range of larvae because of the historic effect of non-equilibrium processes, which depress genetic differentiation within a metapopulation. In such situations, therefore, demographic/range expansion signatures in populations defined in this way should be common, as is the case.

A lack of differentiation accompanied with a clear signal of recent demographic expansion, therefore, is compatible with a metapopulation model dominated by non-equilibrium processes.

Although in the face of things, panmixia may be the simplest explanation for a lack of differentiation, it would be based on the assumption that vent colonies are at drift-migration equilibrium with each other, which is a big assumption in an environment where vent fields are born and die over decades and centuries along spreading ridges. Whether or not there is a panmictic population spanning the ESR, based on estimates of bottom water flow in the Scotia Sea that this gene flow probably occurs despite a broadly easterly or northeasterly current regime in the region (Meredith et al. 2008).

One factor that may enhance the dispersal capability of all three species is the temperature regime of the Southern Ocean. Bottom temperatures encountered at the ESR ranged from ~ -1.3-0 ˚C (Rogers et al. 2012) and such low temperatures may enhance larval longevity by slowing metabolism substantially. The development of *Alvinella pompejana* larvae appears arrested at 2 ˚C, a temperature typical of the deep Pacific, suggestive of cold-water enhanced dispersal (Pradillon et al. 2001). Low temperatures in the Southern Ocean could conceivably allow kiwaid larvae to survive well beyond the conservative estimate of a year, based on the yolk sac volume (Sven Thatje et al. manuscript in preparation). Study of echinoderm larvae in laboratory conditions, for example, (Shilling and Manahan 1994) suggests that lecithotrophic larvae with sizeable yolk sacs could survive in frigid Antarctic waters for nearly five years!

The physiology of the kiwaids may exaggerate this effect further: the apparent decline in activity of reptant decapods at temperatures approaching 0 ˚C, which has been attributed to poor low-temperature magnesium excretion (Frederich et al. 2001), might boost the dispersal capability of a species if energetically costly development is delayed until exposure to higher temperatures (e.g., a hydrothermal vent). Analyses of the effect of temperature and magnesium concentration on the larvae of the subantarctic lithodid *Paralomis granulosa* crabs (Wittmann et al. 2010) indicates they respond to temperatures in the same way and the authors go on to

suggest that the low activity demersal drifting strategy of the larvae minimises their exposure to the hypoxia that a more active larvum might experience; one of the possible reasons why lithodid crabs have been recently found in Antarctic waters warmer than 1 ˚C (Thatje et al. 2005): their lecithotrophic larvae can survive drifting in colder deep waters and as long as the destination is warm enough for larval development through to adulthood, populations may be viable. The likely dispersal strategy of kiwaids, (demersal drifting non-feeding larvae) therefore at worst minimises any negative effects of this trait in cold water and at best combines with it to enhance dispersal, if lower muscular and metabolic activity reduces the requirement for oxygen and nutrients. The fact that the depths of the Scotia Sea are exposed to highly oxygenated deep waters (Naveira-Garabato et al. 2002) can only assist in the survival of these larvae during their planktonic phase.

3.5.1.2 ESR-Kemp Differentiation

The high differentiation (F_{ST} > 0.45) between ESR and Kemp despite such a close proximity to the ESR is, perhaps, more expected given the topography of the region. The Kemp Caldera vents are ~ 1,000 m shallower than those on the ESR and are effectively cut off from the surrounding marine environment by shallow (~ 800 m depth) caldera walls, which would mean that limpet lecithotrophic larvae would have to traverse a vertical distance of ~ 1,700 m. Differentiation owing to depth variation is not uncommon in vent population genetics (as summarised by Vrijenhoek et al. 2010) and there is increasing evidence of bathymetric isolation and speciation among species of continental slope taxa (France and Kocher 1996; Etter et al. 1999; Cho and Shank 2010). Abnormal temperature profiles relative to the surrounding ocean measured within the caldera in 2009 when the site was first visited (Larter 2009), which have since been attributed to a prior volcanic event, highlights the potential hydrographic isolation of the caldera (Rob Larter, personal communication). While the absence of the other two species at vents in the caldera may be the consequence of a variety of factors, such as vent fluid chemistry

or depth adaptation, it is worth noting that the *Lepetodrilus* spp. release very small eggs (< 90 µl diameter) (Tyler et al. 2008), which may increase the chances of some traversing such a depth range, compared to the other two species. Given the presumed demersal drifting of *Kiwa* sp. larvae, their absence at the caldera is perhaps unsurprising.

The large F_{ST} value between the two limpet populations may not be solely the result of contemporary or past gene flow. Based on the observations of elemental sulphur chimneys and dead squid and shrimp in the vicinity of the vent chimneys in the Kemp Caldera (Rogers 2010), it is likely that the vent fluid chemistry, and therefore possibly the associated bacterial flora may be very different from the ESR. Against a backdrop of limited gene flow, differential selection on the mitochondrial genome between the two environments could conceivably lead to an inflated F_{ST} value. The analyses of neutral multilocus markers should be more accurate in assessing differentiation between populations, and hence contemporary and historical gene flow.

3.5.2 Diversity, Demography & Selection

3.5.2.1 Overview

The haplotype diversity for the two gastropods is consistent with previously measured diversity for hydrothermal vent molluscs (Johnson et al. 2006; Plouviez et al. 2009; Johnson et al. 2013), in contrast, the diversity of *Kiwa* sp. (h = 0.996) is the highest yet for any vent-endemic species (where > 10 individuals have been sampled), the nearest being 0.970 for *Branchipolynoe symmytilida* on the EPR (Plouviez et al. 2009) and higher, even, than the diversity of the vent crustacean *Rimicaris exoculata* on the Mid-Atlantic Ridge (excluding the poorly sampled South MAR site) (Teixeira et al. 2010). Such a high diversity for a crustacean has only been reported

for Southern Ocean krill swarms (Goodall-Copestake et al. 2010) and amphipods (Ashton et al. 2008). Under the expectations of the Neutral Theory of evolution (Kimura 1984) therefore, such a high diversity would be indicative of a very large population, which is supported by the observations of kiwaids piled on top of each other. Paradoxically, the diversity of the peltospirids is lower and the limpets lowest, despite observations on the ESR suggesting that, while kiwaid density is high, density is higher for the peltospirids and highest for the limpet (Marsh et al. 2012). Likewise, the diversity for limpets across the whole ESR is lower than the diversity for the Kemp Caldera limpets which, based on topographic and hydrographic observations, are likely part of a smaller, enclosed population.

3.5.2.2 Genetic Bottlenecks

Examination of the tests for neutrality and/or demographic change accounts for this discrepancy in diversity by showing evidence of genetic bottlenecks for all three species (Tajima's *D*, Fu's *Fs* and mismatch distributions), with indications of a more recent bottleneck for the limpets compared to the kiwaid, with the peltospirid intermediate, as evidenced by mismatch distributions revealing fewer pairwise differences between limpet haplotypes than the other species. BSPs modelling demographic expansion using a coalescent approach also show that the ESR limpets experienced the most recent genetic bottleneck followed by the peltospirids and the kiwaids. Two main arguments have been used to explain bottleneck patterns, those relating to demographic changes and those relating to selective sweeps (e.g. Vrijenhoek 2010).

With vent populations, bottleneck signatures in mtDNA loci generally appear the norm (Johnson et al. 2006; Young et al. 2008; Faure et al. 2009; Plouviez et al. 2009; Teixeira et al. 2010; Thaler et al. 2011; Teixeira et al. 2012b) perhaps owing to metapopulation demographic instability as a consequence of vent field ephemerality (Vrijenhoek 2010). This idea is strengthened by evidence showing stronger bottleneck signatures for vent fauna inhabiting the

faster spreading Southern EPR (SEPR) than the Northern EPR (NEPR) (Plouviez et al. 2009; Plouviez et al. 2010). Plouviez et al. (2009) suggested that similar bottleneck signatures across several species on the SEPR might be evidence for an eruptive event decimating colonies along the ridge within the last million years.

Given the different dates for the bottlenecks according to BSP analyses here, a single event is unlikely to account for this pattern, as for this to be the case, kiwaid substitution rates would have to be ~ 10 times faster (or limpet rates ten times slower). An alternative approach is to see if life history and dispersal can account for the discrepancy in diversity and possible demographic history against a backdrop of vent and current activity on the ESR over time. Vrijenhoek (1997) hypothesised that, diversity of vent metapopulations are likely to be affected by site occupancy (determined by vent field density or successional stage of colonisation), vent ephemerality, larval dispersal capacity and ridge characteristics (e.g. presence of larval retaining axial valleys). The only factors listed above that can account for differences between species on the same ridge are variable dispersal capability and the successional stage of colonization. Early colonisers are expected to maintain populations on vent fields for longer, enhancing the overall metapopulation size and minimising demographic fluctuations, which depress diversity (Vrijenhoek 1997). For this to be the case here, the limpets would have to be late-stage colonisers, but this does not tally with the observations of *Lepetodrilus tevnianus* as a first coloniser and individuals of *L. elevatus* arriving shortly afterwards on vents recently defaunated owing to volcanic eruptions (Mullineaux et al. 2012).

One possibility is that, although limpets were observed in both vigorous and diffusely venting areas on the ESR (Marsh et al. 2012), females are generally found closer to black smoker venting (Bates 2006; Bates 2008) on the EPR and perhaps periodic declines in vent activity leading to more diffuse venting may have disproportionately affected mtDNA diversity in limpets as the effective female population size precipitously declined. A decline in active

venting all along the ESR would probably also leave a bottleneck signature in the other species as well – especially the kiwaids, which are found closest to the active venting counting against this explanation.

3.5.2.3 Differential Connectivity

An alternative scenario therefore, is that differences in realized dispersal capability may lead to the depression in diversity of ESR limpets relative to the other two species. Mid-ocean ridges are likely to be subject to stochastic fluctuations in vent activity over time (Vrijenhoek 1997) and added to this, changes in current strength and direction may have a differential effect on the *realised* dispersal capability of these animals. The Southern Ocean is likely to have experienced a variety of current regimes during the Pleistocene on account of orbitally-forced glacial cycles resulting in large shifts in the intensity and latitude of the Antarctic Circumpolar Current (ACC), as well as changes in the production of bottom water, such as Weddell Sea Deep Water (WSDW) (Diekmann 2007). Some glacial episodes have been more prolonged and intense than others such as those during the Mid-Pleistocene Transition ~ 0.6-1.2 Ma (Diekmann and Kuhn 2002) and some of these episodes may have been associated with current changes in the Scotia Sea.

Although not an idea proposed by Plouviez et al. (2009) at the time, the fact that strong equatorial cross-axis currents appeared to act as a filter for *Lepetodrilus* limpets (which release small larvae) but not for polychaetes with much larger larvae on the EPR, could owe less to propagule longevity and more to the ease by which smaller, lighter, possibly more buoyant eggs/larvae are carried off axis by currents. It may be, therefore, that stochastic changes in vent activity (e.g. greater inter-field distances or a change in vent-field distribution) along the ESR, or during episodes of enhanced current flow across the ridge axis (or a combination of the two), some larval types are more likely than others to be transported off axis, resulting in decreased

connectivity. Such a drop in connectivity could lead to population fragmentation/contraction and consequently a reduction in diversity owing to the founder effect. Against a backdrop of stochastic fluctuations in vent and current activity along the ridge, species that may be more effective at larval *retention*, such as the kiwaid with its large, probably demersal-drifting larvae, could experience these bottlenecks less often over time than the limpet if its larvae are more likely to be retained close to the sea floor.

In combination with the low ambient sea temperatures in the deep Southern Ocean which could dramatically increase larval longevity by arresting development, a capacity for larval retention could result in high connectivity and a relatively stable population during all but the most extreme changes in vent and current activity therefore allowing genetic diversity to accumulate to the high level reported here ($h = 0.996$).

An additional possibility not explicitly mentioned previously is that differences in adult lifespan may also have an effect on diversity within metapopulations by enhancing the probability that any individual will produce successfully colonising larvae during its lifespan. On ridges where larval retention is a problem for species, those with an extended adult lifespan may have greater success in maintaining connectivity than those with short adult lifespans, thus maintaining diversity. Little can be said about this presently, as lifespans for these species are unknown, but the greater size of *Kiwa* sp. relative to the other species may signify a longer lifespan compared to the gastropods, based on an albeit rather weak relationship between body size and lifespan in invertebrates (Blueweiss et al. 1978).

Regardless of the precise mechanism at work, the general process of differential larval dispersal/retention against a backdrop of stochastic fluctuations in vent activity and current regime, over time, could result in some species experiencing genetic bottlenecks more commonly than others. The higher diversity of Kemp Caldera limpets relative to the ESR

population could therefore be explained by larval retention being higher in this semi-enclosed environment, or, if the Kemp population is part of a larger, shallower South Sandwich Island population, perhaps vent stability/longevity could be a factor. If the species featured in this study are subsequently found on the American-Antarctic Ridge (A-AR) and the southern reaches of the Southwest Indian Ridge (SWIR) the general west-to-east orientation of these ridges may reduce this realised differential dispersal, as larvae will be less likely to be transported off-axis if currents flow along the axis (the ACC), regardless of larval size or adult longevity. Consequently, the discrepancy in diversity between the species could be less. If larval size/buoyancy is a key factor, then perhaps along these stretches of ridge, limpet diversity could be greater than the other two species owing to connectivity across a greater number of vent fields. The slower spreading rates further east, especially on the SWIR (Sauter and Cannat 2010), could also boost genetic diversity if vent fields are more temporally stable.

The idea of larval retention being key in the maintenance of connectivity along the ESR has wider implications. Firstly, the absence of species with planktotrophic larvae on the ESR, as reported by Rogers et al. (2012) may have less to do with the general paucity of planktotrophy as a dispersal strategy in the Southern Ocean, perhaps owing to the intense high latitude seasonality (Pearse et al. 1991), and more to do with need for high retention on a ridge where currents may not always align with the axis. The Central Indian Ridge (CIR) (Watanabe and Hashimoto 2002) as well as the upper reaches of the SWIR (Copley 2011) both host *Rimicaris* shrimp, which are believed to have planktotrophic larvae that drift up the water column to feed (Tyler and Young 1999). Given the close genetic affinity of the CIR *R. kairei* to *R. exoculata* on the Mid-Atlantic Ridge (Watanabe and Hashimoto 2002), it may be that stretches of the SWIR that are further south, close to the Bouvet Triple Junction, where the MAR, American-Antarctic Ridge (A-AR) and SWIR meet, is populated by these shrimp. If this is shown to be the case, then it seems likely that the reason why a species with planktotrophic dispersal can survive there is because the dominant ACC current (Boehme et al. 2008) is aligned with the general axis of the ridge as otherwise, larval retention would be effectively zero. A logical progression from

this idea is that vast sections of the Pacific-Antarctic Ridge (P-AR) may also host fauna with planktotrophic dispersal strategies as the most southerly portions of the ridge are east-west aligned and bathed in the ACC. The broad unidirectionality of currents in the Southern Ocean therefore, may highlight why planktotrophy as a dispersal mechanism for vent fauna appears rare in general (Tyler and Young 1999). The probability of larvae landing at other vents would be very low unless currents and ridges align.

3.5.2.4 Selection

An entirely different explanation for the discrepancy in genetic diversity relates to the effect of selection on the mitochondrial genome. Recent analyses show that across the animal kingdom, population size does not correlate with mtDNA diversity, but does with nuclear DNA (Bazin et al. 2006). For example, invertebrate populations, whose populations are orders of magnitude larger than mammal populations do not exhibit higher mtDNA diversity. To account for this, Bazin (2006) invoked the concept of 'Genetic Draft', whereby selective sweeps are more likely to occur for loci (or linked loci) continuously or periodically under selection in larger populations than smaller ones, leading to a loss of genetic diversity. Beneficial mutations at a locus under selection are more likely to occur by chance and be fixed in a larger population where drift is weaker and therefore any neutral diversity in linked loci, such as the whole mitochondrial genome, will be lost in a selective sweep (genetic hitchhiking) (Meiklejohn et al. 2007). This phenomenon could be more pronounced in mtDNA because of the lack of recombination (Galtier et al. 2009). Traditionally, mitochondrial genes, which are generally associated with respiration/metabolism have been considered to be neutral or nearly neutral, as most mutations would be either neutral (synonymous) or selectively deleterious, rendering the possibility of selective sweeps unlikely (Kimura 1984), but in a metabolically challenging environment such as at hydrothermal vents, it may be that the mitochondrial genome is under

selection. Given the extreme and fluctuating temperatures that vent fauna are subject to (Van Dover 2000) for example, temperature could well be a selective force on the mitochondrial genome and has been implicated experimentally in the purifying selection of *Drosophila* mtDNA (Ballard et al. 2007).

Selective sweeps in mtDNA have been suggested as an alternative explanation for past bottlenecks to demographic changes in vent literature (e.g. Teixeira et al. 2010), but the presence of past bottlenecks in mtDNA across several species along a ridge has been interpreted as evidence of demographic change rather than selection (Plouviez et al. 2009), as the chances of selection occurring simultaneously across several species are perceived as remote. The broad pattern of bottleneck signatures revealed in this study, however, is what would be expected if genetic draft were in effect. The limpets, which outnumber the other species (in density terms) by at least an order of magnitude, bear the most recent bottleneck signature and lowest diversity, with the less numerous peltospirids as intermediate and the least numerous kiwaids being the most diverse. Furthermore if the population size of the limpets on the ESR is larger than the Kemp Caldera population (as is expected given observations), then the Kemp Caldera population should be more diverse, which is exactly what is observed. It is impossible at this stage to say how much of an effect Genetic Draft has on masking demographic effects on mtDNA diversity in vent fauna, but with the likely huge populations of vent limpets on mid-ocean ridges, this process cannot be ignored.

To assess the relative effects of selection versus demography, a common approach is to analyse a multilocus dataset e.g., with nuclear sequence data (Plouviez et al. 2010), or with multi-allelic genotype data such as microsatellites (Teixeira et al. 2012b). If a bottleneck signature is found at multiple loci, then this could be indicative of demographic effects on diversity rather than selective sweeps as specific loci. However, the absence of a strong demographic expansion/contraction signature in nuclear loci does not rule out demographic effects, because the much higher mutation rates of some markers compared to sequence data (e.g.

microsatellites) (Selkoe and Toonen 2006) could mean that only the most recent demographic changes are detectable. Even slower-evolving loci, such as nuclear protein-coding sequences may be poor at detecting demographic change owing to the larger effective population ($4N$) reducing the effect of drift on diversity and the possibility that slow mutation rates in genes with very limited diversity may fail to pick up only very long-term demographic changes.

Excluding the use of multiple loci, one way of narrowing down the likely cause of expansion signatures in mtDNA for these three species is to examine populations on ridges (A-AR and SWIR) in line with the prevailing easterly current (ACC), as already mentioned. Encountering more diverse populations heading eastwards along these ridges would meet expectations that past bottlenecks on the ESR are the product of metapopulation demographic changes owing to differential connectivity over time as a result of stochastic variations in vent activity and current regime.

One problem with the idea that selective sweeps can explain *all* of the mtDNA diversity in these species is that mismatch expansion signatures should be unimodal, which doesn't account for the bimodal pattern in kiwaids (Fig. 3.6), which produces the stepwise expansion pattern in the BSP (Fig. 3.10). At the very least, the second 'burst' of genetic diversification may reflect a demographic influence, therefore. For the kiwaids at least then, selection cannot explain fully the pattern of diversity shown here. Interestingly, the more recent 'burst' may be in phase with the BSP expansion of the peltospirids. It may be that events leading to a bottleneck in the peltospirid left a weaker imprint in the diversity of the kiwaids, the event associated with the limpet bottleneck having a negligible impact on their genetic diversity.

3.5.3 Study Limitations

There are two principle limitations to this study. The first is that conclusions about connectivity and demography from using a single mitochondrial locus dataset (mtDNA) are statistically weaker than those using independent multilocus datasets owing to the distorting effect of selection and the lack of recombination at such loci (Bazin et al. 2006). In addition to this, mitochondrial genes, while having been shown to be more variable than some allozymes and nuclear sequence data (e.g., Craddock et al. 1995; Won et al. 2003; Plouviez et al. 2009; Plouviez et al. 2010), may not be as good at assessing present-day or very recent gene flow as faster-evolving markers like microsatellites (Selkoe and Toonen 2006) or SNP markers where many loci (tens to hundreds) can be sampled across the entire genome (Brito and Edwards 2009).

The second major limitation of this study is the low sampling effort, (only two locations sampled for two species and three for the other) compared to other vent population genetics studies (e.g. Fusaro 2008; Faure et al. 2009; Plouviez et al. 2009; Matabos and Thiebaut 2010; Thaler et al. 2011; Teixeira et al. 2012b). At the scale of the ESR, inferences about connectivity are limited by fact that the entire ridge is no larger than a single ridge segment on the EPR or the Mid-Atlantic Ridge (Van Dover 2000) and only *Lepetodrilus* sp. was found at the Kemp Caldera vents beyond the ESR. However, given the close affinity of the ESR *Lepetodrilus* sp. limpet to *Lepetodrilus atlanticus* (Katrin Linse, manuscript in preparation) and the close affinity of the kiwaids and peltospirids in this study to those sampled at the Dragon vent field on the SWIR, it is highly probably that populations exist along the A-AR and lower reaches of the SWIR where relative connectivity can be better assessed.

3.6 Conclusion

The analyses of the mtDNA COI gene for three vent-endemic species, a kiwaid crustacean *Kiwa* sp., an undescribed peltospirid gastropod and the limpet, *Lepetodrilus* sp., sampled from vents in the Scotia Sea reveals no evidence of genetic differentiation along the bulk of the isolated ESR, although *Lepetodrilus* sp. limpets sampled at the Kemp Caldera ~ 95 km to the east of the ESR appear genetically distinct from ESR limpets, possibly owing to a ~ 1,000 m depth difference between the Kemp and ESR vents. The lack of differentiation along the ESR is compatible with previous research in the Pacific where differentiation was only detectable at scales greater ~ 1,000 km for *R. pachyptila* (Coykendall et al. 2011). The very high diversity of the kiwaids (h = 0.996) on the ESR appears compatible with observations of high density at vents and is consistent with a theory of high connectivity over time owing to potential high larval retention on the ESR in combination with a hypothesized cold-water enhanced larval longevity. The lower diversity of the two gastropods on the ESR is a result of more recent genetic bottlenecks than *Kiwa* sp., which may indicate a greater vulnerability of these species to disruptions in along-ridge connectivity owing to changes in vent activity or prevailing ocean currents. It is hypothesised that this vulnerability relates to life history traits such as adult longevity, larval longevity and larval entrainment by ridge topography. Alternatively, the lower diversity of the two gastropods and in particular the vent limpet *Lepetodrilus* sp., could be the consequence of selective sweeps, which may be more likely in species with large populations (Genetic Draft). The fact that that connectivity appears high for *Kiwa* sp., despite an inferred poor dispersal capability, highlights the importance of larval retention in ensuring connectivity along the ESR, with perhaps wider implications for the presence (or lack) of vent species with planktotrophic larvae in the Southern Ocean.

CHAPTER 4

Microsatellite Development

4.1 Abstract

Microsatellite loci have been developed for three undescribed species discovered at hydrothermal vents on the East Scotia Ridge (ESR) in the Southern Ocean: a yeti crab, *Kiwa* sp. (Kiwaidae), a peltospirid gastropod and a limpet, *Lepetodrilus* sp. (Lepetodrilidae). Nine, twelve and fourteen loci were developed for the three species respectively, with two loci deviating significantly from Hardy-Weinberg expectations. Observed heterozygosity ranged from 0.08 to 1 (means of 0.62, 0.44 and 0.63 for the three species respectively). These loci are being used to determine connectivity between vents at the northern and southern end of the ESR and between the ESR and the Kemp Caldera, a submerged part of the South Sandwich Island chain. These data will be crucial in understanding the ecology of the first hydrothermal vent systems discovered in the Southern Ocean.

4.2 Introduction

Hydrothermal vents host unique communities in the deep sea where bacterial primary producers support high densities of megafauna by the oxidation of reduced chemicals in hydrothermal fluid emanating at the sea floor, typically on mid-ocean ridges (Van Dover 2000). Vent-endemic fauna maintain populations along these ridges by broadcasting their larvae between island-like vent fields. Genetic studies over the last ~ 30 years (Bucklin 1988; Black et al. 1998; Hurtado et al. 2004; Fusaro 2008; Plouviez et al. 2010; Teixeira et al. 2012b), indicate that species' ranges are determined by factors such as larval longevity, current direction and strength, distance between vent fields, shelf and ridge topography and vent field longevity (Tyler and Young 1999; Vrijenhoek 2010).

A key part of this research is the development of population genetic markers sufficiently sensitive to determine connectivity patterns for a given species along mid-ocean ridges, as well as to estimate current and past population sizes. Microsatellites, rapidly evolving, tandemly-repeated sequences of non-coding DNA, otherwise known as short tandem repeats (STRs) or simple sequence repeats (SSRs) are one such type of marker, consisting of short sequence motifs 1-6 bp in length which are repeated several times (e.g., CACACACACA) (Guichoux et al. 2011). These co-dominant markers, which are spread throughout the genome, have been used increasingly in the last two decades for population genetics and are characterized by high heterozygosity with multiple alleles, indicative of high mutation rates compared to DNA sequence data (Ellegren 2004). With such high mutation rates (10^{-2} to 10^{-6} mutations per locus per generation), selectively neutral markers such as these should be ideal for estimating population parameters that reflect recent processes such as migration and demographic changes (Selkoe and Toonen 2006).

Given the popularity of microsatellites (10^3 citations of SSR studies per year in the scientific literature since ~ 1996; Guichoux et al. 2011) there have been surprisingly few studies using microsatellites on megafauna from hydrothermal vents, with only a few marker suites developed (Daguin and Jollivet 2005; Fusaro et al. 2008; Cabezas et al. 2009; Thaler et al. 2010; Zelnio et al. 2010; Schultz et al. 2011; Teixeira et al. 2012a; Jacobson et al. 2013). Of these suites that were developed, only two have resulted in published population genetics studies (Thaler et al. 2011; Teixeira et al. 2012b). This lack of SSR usage in vent population genetics can be partly explained by the fact that sampling deep-sea hydrothermal vents on distant mid-ocean ridges or on seamounts is exceptionally expensive compared to sampling in other marine and terrestrial environments. However, added to these costs is the considerable expense associated with the development of species-specific microsatellite markers – both in time and money (Guichoux et al. 2011). Until only four years ago, microsatellite development generally required the construction of a genomic library, enriched for repeat motifs with the isolation and sequencing of bacterial clones containing microsatellites, followed by primer design, PCR optimisation and polymorphism testing on several individuals, which is a time-consuming and costly procedure with few guarantees that effective markers will result (Guichoux et al. 2011). Recently, however, a new approach has been introduced which takes advantage of so-called "next generation" sequencing (NGS) methods (Abdelkrim et al. 2009). Abdelkrim et al. (2009) used Roche 454 sequencing technology to generate thousands of short (200-300 bp) fragments of DNA from across the genome and then used software to detect sequence fragments containing microsatellites with flanking regions long enough for primers to be designed, which reduced the time and overall cost of marker development. This advance has made it possible to develop microsatellites for multiple undescribed species within the time frame of a D.Phil research project.

In this study, microsatellite markers have been developed for three species recently discovered at hydrothermal vents on the East Scotia Ridge (ESR) (Rogers et al. 2012): a yeti crab

(Kiwaidae) *Kiwa* sp., a peltospirid gastropod (Chen et al. submitted) and a vent limpet, *Lepetodrilus* sp., which was also found on the Kemp Caldera, adjacent to a submerged seamount in the South Sandwich Island chain. The aim in the development of these markers is to assess the connectivity of these species between hydrothermal vents in the Scotia Sea, and in the future to determine if they maintain populations on as yet undiscovered portions of adjacent mid-ocean ridge in the South Atlantic and Southern Ocean.

4.3 Materials & Methods

4.3.1 DNA Extraction & Next-Generation Sequencing

Total genomic DNA was extracted from pereopods in the case of *Kiwa* sp. and from foot tissue in the case of peltospirids and the *Lepetodrilus* sp. limpets using the Qiagen DNeasy® Blood and Tissue Kit following the manufacturer's instructions.

For all three species, 454 sequencing libraries were generated and microsatellites detected broadly in the manner described by Abdelkrim et al. (2009). In the case of *Lepetodrilus* sp. 5 µg of template DNA from a single individual was sent to Macrogen Inc. (Seoul, South Korea). Un-enriched libraries were generated and analysed on Roche 454 sequencers using the GS FLX titanium chemistry (Roche Life Sciences, Branford, CT, USA). In the case of *Kiwa* sp. and the peltospirids 5 µg of template DNA from a single individual was sent to Ecogenics GmbH (Switzerland) for sequence generation, where size-selected fragments from genomic DNA were enriched for SSR content using Dynabeads M-280 Streptavidin from Invitrogen and biotin-labelled CT and GT repeat oligonucleotides (Microsynth AG, Switzerland). The enriched library was then analysed on a Roche 454 sequencer with GS FLX titanium chemistry.

4.3.2 Microsatellite Detection & Primer Design

Microsatellites with sufficiently large flanking regions for primer development were detected using MSATCOMMANDER (Faircloth 2008), a simple program designed to locate di, tri, tetra, penta and hexa microsatellite repeats within standard fasta files generated from the 454

sequencing. While this program can also design primers, it was found that in some cases potential microsatellite loci were missed. In the interests of maximising the number of potential loci found, each 454 fragment containing microsatellites was manually checked to see if a microsatellite had sufficiently large flanking regions (> 20 bp on each end of the microsatellite).

Primers were then designed on Geneious Pro 5.4.6 (Drummond et al. 2010) using the Primer3 package (Rozen and Skaletsky 2000). Primers were designed to be a minimum of 18 bp long, with a CG content of 25-0% and an optimal melting temperature (Tm) of 58 ˚C (± 8 ˚C) (and no more than 2 ˚C apart between primer pairs). Primers with more than three mononucleotide repeats were automatically rejected and were also checked by eye to ensure that there were no more than two dinucleotide repeats present. Where possible, a spread of microsatellite fragment sizes were designed so as to maximise options when designing multiplexes later on. At this point, all microsatellite loci were manually cross-checked to ensure that there were no duplicate loci, e.g. two loci that turned out to be reverse duplicates of one another, or two that were nearly identical but for a couple base pair differences, probably owing to sequencing errors. These newly designed primers were then generated by Eurofins MWG Operon (Ebersberg, Germany).

4.3.3 Testing

Initially all loci were tested on four individuals. PCR Reactions were performed in 9 µl volumes, containing 0.6 µl of each primer (forward and reverse) at a concentration of 4 pmol/µl, 6.3 µl of Qiagen Taq MasterMix, 1.5 µl of DNA template (~10-50 ng/µl). All PCR reactions were performed on a Bio-Rad C1000 Thermal Cycler. Not all loci from the three species performed equally well with the same PCR protocol. For *Kiwa* sp., one of two protocols was used: 95 ˚C for 5 minutes, followed by 25 cycles of 94 ˚C for 35 seconds, 50 ˚C for 35 seconds, 72 ˚C for 1 minute, and a final extension of 72 ˚C for 1 hour, or the same protocol, but with 50, 50 and 75 seconds for the three cycle steps respectively. For *Lepetodrilus* sp. a similar protocol

was used, but with cycle steps either of 25, 25 and 45 seconds or 35, 35 and 60 seconds. For the peltospirids, cycle steps used were either 20, 20 and 40 seconds or 35, 35 and 60 seconds. PCR product was visualised on 1% agarose gel using ethidium bromide.

Loci that produced smears, multiple bands or completely failed to amplify were discarded unless another primer could be designed. A second failure resulted in discarding of the locus. The remaining loci were then tested for polymorphism on eight individuals by reordering the forward primers with a 6-FAM (6-carboxy-flourescine) fluorescent label and repeating the PCR protocols. Size-fragment analysis of the PCR product was conducted on an ABI 3730xl DNA analyser. Chromatograms were scored using Peak Scanner^{TM} software v1.0.

Loci that appeared non-polymorphic were tested on a further eight individuals before being discarded. At this point, primers were redesigned for some loci that were polymorphic, but hard to score because of stuttering, or inconsistent amplification. Stuttering is where replication slippage during the PCR amplification of microsatellites results in the appearance of minor peaks, known as stutter bands, that differ from each main product by multiples of the repeat unit length (Ellegren 2004), which can be a real problem when attempting to accurately score microsatellites. In some cases, redesigning primers reduced stuttering, but in many cases, loci were discarded owing to this tendency. Another approach was to 'tighten' the PCR protocol by reducing the length of PCR cycling steps – in particular the annealing step – to 10-20 seconds or by reducing the number of cycles, with varying levels of success. Polymorphic loci that were easy and reliable to score were then tested on 24 individuals from the E2 vent field at the north end of the East Scotia Ridge in order to assess their applicability to population genetics.

4.3.4 Analysis

Genetic diversity statistics as well as tests for deviation from Hardy-Weinberg Equilibrium (HWE) and linkage disequilibrium were generated with Arlequin 3.5 (Excoffier and Lischer 2010) and corrected for multiple comparisons using the sequential Bonferroni approach (Rice 1989). The linkage disequilibrium test assesses the degree to which alleles of different loci co-vary, i.e. the non-random association of alleles between different loci. Loci that are linked cannot be considered as separate in population genetics analyses. In Arlequin, the test is performed with a likelihood ratio test whose empirical distribution is achieved with permutation (10,000 in this study). The exact test of Hardy-Weinberg Equilibrium (HWE) assesses the non-random association of alleles within diploid individuals, or rather the degree to which the genotype frequencies of a locus deviate from Hardy-Weinberg expectations based on the allele frequencies. In Arlequin, this is achieved using a Markov Chain Monte Carlo method (Excoffier and Lischer 2010). In this study, the test was performed with 10^6 Markov chain steps (and 10^5 dememorisation steps).

Presence of null alleles, excessive stutter and large allele dropout were assessed using MicroChecker with 1,000 randomizations (van Oosterhout et al. 2004). MicroChecker looks at patterns of homozygote excess (greater homozygosity than expected from a population at HWE) using a Monte Carlo simulation method to generate expected homozygote and heterozygote allele size difference frequencies. The pattern of homozygote excess can be revealing. If there is an excess of homozygotes over most allele sizes, for example, then it is likely that some heterozygotes are being scored as homozygotes (null alleles) because there are base pair differences at primer-binding sites. A deficiency of heterozygotes with alleles one or two repeats apart indicates that excessive stuttering is hiding one of the alleles. A general pattern of homozygote excess may indicate that the population sample came from more than one discrete deme (Wahlund effect) or that there is large allele drop-out, where large alleles fail to amplify in PCR.

4.4 Results

For the three species in this study, 454 Roche sequencing yielded 12,453 sequence contigs (assembled overlapping DNA fragments) for *Kiwa* sp., 14,743 contigs for the peltospirid and 8,707 contigs for *Lepetodrilus* sp.. For the kiwaid, 818 sequences contained microsatellites of five or more repeats (excluding mononucleotide repeats), of which 63 loci (7.7% of sequences with > five-repeat microsatellites) contained suitable flanking regions for primer design and were initially tested for amplification. Of these 63 loci, 33 were tested for polymorphism with eight individuals, resulting in nine loci that were polymorphic, reproducible and free from excessive stutter (27.27% of loci tested for polymorphism). For the peltospirid, 1,032 sequences contained microsatellites and of these, 74 (7.17%) contained loci with flanking regions suitable for primer design. Thirty loci were then tested for polymorphism resulting in 12 loci that were polymorphic (40% of loci tested for polymorphism). 1,148 lepetodrilid sequences contained microsatellites, of which, 87 contained loci with flanking regions suitable for primer design (7.58%). Forty-nine loci were then tested for polymorphism across eight individuals producing 14 loci that were polymorphic, reproducible and not prone to stuttering (28.57% of loci tested for polymorphism).

For all three species there was no evidence for linkage disequilibrium, however, two loci deviated from HWE after sequential Bonferroni corrections (PeltESR_08 & PeltESR_12). Null alleles were detected for the loci KiwESR_04, PeltESR_12 and LepESR_05.

Table 4.1. Polymorphic loci from 24 individuals for *Kiwa* sp.. Annealing temperature (T_A), size range of alleles (base pairs), number of alleles (N_A), observed heterozygocity (H_O), expected heterozygosity (H_E), and probability (P) of deviation from Hardy-Weinberg Equilibrium (exact test) are reported. Significant P values (after a sequential Bonferroni correction) are highlighted in bold.

Species	Locus name	Repeat Motif	Allele Size	Primer Sequence	Size Range	N_A	H_O	H_E	P
Kiwa sp.	KiwESR_01	$(GTT)_8$	166	F: CAAGTAGCTCTGACCAGACAAA	148-193	9	0.83	0.76	0.98123
				R: GTTTGTGTGTTGGTTCACGA					
	KiwESR_02	$(TGT)_6$	272	F: CAAGTAAATAACCAGAAACAATAAAAA	269-275	3	0.75	0.57	0.16174
				R: CCTGATTTTATTAAGCTCATTCAG					
	KiwESR_03	$(TG)_8$	155	F: TACTCAGATGACACCCGGTAA	157-169	5	0.50	0.58	0.7721
				R: GAGAATCATCGATCTACCTACAAC					
	KiwESR_04	$(TGT)_7$	209	F: TAAGGAGGAAGATGGGAGAAA	200-212	4	0.29	0.49	0.03512
				R: ACATCCCTTCCTCGTTCAC					
	KiwESR_05	$(AT)_6$	206	F: TGTTTACTGGATTCCGGAGTTA	204-208	3	0.21	0.26	0.3982
				R: GATGGACCGTAGGTATCTGACT					
	KiwESR_06	$(TG)_7$	145	F: ACGTCGTATTAGTAGCCACCAC	143-149	4	0.46	0.55	0.1362
				R: CAAATTTAAGGAAATGCATGATAA					
	KiwESR_07	$(AT)_5$ $(AC)_{12}$	135	F: GAAGCAAGAAGTTATACACCCAAT	119-177	21	0.92	0.95	0.70659
				R: GGGAACGAGAGGATCAGCTA					
	KiwESR_08	$(AC)_{15}$	100	F: CCAAGAGCACGGTCATCAGTA	80-146	23	1.00	0.97	1
				R: ACACGTCTGCCTCGTGTG					
	KiwESR_09	$(CAA)_8$	127	F: AATGAGTCCCAGCAAGTGTC	106-121	6	0.63	0.77	0.06516
				R: TAGTGTTCGGGAGGAGAT					

Table 4.2. Polymorphic loci from 24 individuals for the peltospirid gastropod. Annealing temperature (T_A), size range of alleles (base pairs), number of alleles (N_A), observed heterozygocity (H_O), expected heterozygosity (H_E), and probability (P) of deviation from Hardy-Weinberg Equilibrium (exact test) are reported. Significant P values (after a sequential Bonferroni correction) are highlighted in bold.

Species	Locus name	Repeat Motif	Allele Size	Primer Sequence	Size Range	N_A	H_O	H_E	P
Peltospirid	PeltESR_01	$(CA)_7$	126	F: TGGGAGAGACAAACAGACAGA	118-124	4	0.29	0.33	0.60035
				R: CGAACTCCTTGTTGGAGATG					
	PeltESR_02	$(AC)_9$	137	F: ACATTGGATTAATGTGCGTGT	127-135	4	0.29	0.27	1
				R: TGTCAATTAGCCAGATTTATCCA					
	PeltESR_03	$(AC)_{11}$	375	F: AACCGCCGCTAGTGTGAC	367-371	2	0.54	0.44	0.35644
				R: AGCGAAGAGGTTTACCGAAT					
	PeltESR_04	$(CTAT)_9$	344	F: TGGGATTATAACCCGCATC	312-336	5	0.25	0.34	0.1684
				R: TTGAGTTGCGTACACCTTTG					
	PeltESR_05	$(CATT)_{13}$	235	F: ACTCAATAACCGATGTATGTTTCG	207-255	11	0.83	0.90	0.66916
				R: ATCGCTCGCTAGAGTGGTAA					
	PeltESR_06	$(TC)_5$	167	F: AGGGTCCTCTCTAAAGGAAAG	163-165	2	0.33	0.42	0.34444
				R: TTGTTTAACACCACCTCAGC					
	PeltESR_07	$(GT)_6$	198	F: CTAAGGTTCAGGCACGTCTC	198-200	2	0.08	0.08	1
				R: GGGTTTCCTCCCTCAATATC					
	PeltESR_08	$(GT)_8$ $(GT)_4$ $(GT)_{11}$	303	F: AGTCGTTACACTCGCTCTGG	271-335	11	0.42	0.55	**0.00191**
				R: TCGTCCGCCATATACACAC					
	PeltESR_09	$(GT)_6$	158	F: TGGTCGGTGCATGTATATTG	158-160	2	0.58	0.51	0.67977
				R: ACCATACCTCAGTGACAGCAC					
	PeltESR_10	$(GTT)_5$ $(GTT)_9$	357	F: GACGTAGCCCAGTGGTAAAG	351-363	6	0.50	0.49	0.26071
				R: CCCAGGATAGTGCTTAAACCAT					
	PeltESR_11	$(TA)_5$	146	F: GTCCGACTAATGGCAGTGAG	138-146	4	0.50	0.59	0.1415
				R: CTCCTGCATTTAGAGCCTGTG					
	PeltESR_12	$(GT)_{13}$	151	F: CTTACAATTTTGAATCAGTTGC	137-165	13	0.67	0.87	**0.00015**
				R: TTCTAAATAAGGCATTTACCG					

Table 4.3. Polymorphic loci from 24 individuals for *Lepetodrilus* sp. Annealing temperature (T_A), size range of alleles (base pairs), number of alleles (N_A), observed heterozygocity (H_O), expected heterozygosity (H_E), and probability (P) of deviation from Hardy-Weinberg Equilibrium (exact test) are reported. Significant P values (after a sequential Bonferroni correction) are highlighted in bold.

Species	Locus name	Repeat Motif	Allele Size	Primer Sequence	Size Range	N_A	H_O	H_E	P
Lepetodrilus sp.	LepESR_01	$(AAT)_{14}$	286	F: GTAGCATAATTCCCATGGCG	268-292	8	0.79	0.78	0.58051
				R: CAATCGTCTCTCAAACAGGC					
	LepESR_02	$(GT)_{14}$	195	F: CTGACGCCAACTACCTCTTC	183-209	13	0.96	0.90	0.34676
				R: CATTCAACCCGACACTAACAC					
	LepESR_03	$(TAA)_7$	179	F: AAATCGATATATTTAGTGCTTTCCA	176-227	18	0.83	0.91	0.01775
				R: GAGTTGAGAAGGAATTGAGTGC					
	LepESR_04	$(CATT)_7$	195	F: CTCATGGAAGCTGACATCATTA	195-199	2	0.08	0.08	1
				R: ACGAGCCATGCCCATAAA					
	LepESR_05	$(ATT)_{14}$	125	F: GCATGGAGTCCAGCGTATTAT	116-161	13	0.67	0.85	0.00865
				R: GGTAAATCTGACCAGTATAGGTTTG					
	LepESR_06	$(ATT)_{13}$	107	F: TGGCGCGCTCTACAAATG	86-110	8	0.67	0.81	0.10431
				R: GTTCCATGGTACTTATTGCTGA					
	LepESR_07	$(TTA)_{14}$	129	F: GATTCCAGCGCCTTATACAC	114-210	21	0.88	0.96	0.09741
				R: CAGATATCACAGCACATG					
	LepESR_08	$(ACC)_{10}$	357	F: AAGTCGACCTCCTTTGTAGC	348-360	5	0.33	0.43	0.05771
				R: CATCTGACTGGATATTGCTGTG					
	LepESR_09	$(AC)_{12}$	117	F: AGTGTCGAGAGTTGTTGGTG	101-161	16	0.88	0.92	0.19682
				R: GAGTGACTCCATTGATGCAG					
	LepESR_10	$(TA)_8$	106	F: GGTCATTGTCATGAATATTCTCAAT	92-108	8	0.29	0.37	0.11123
				R: CTGGCCCGTAATTACTGTTG					
	LepESR_11	$(ACT)_{20}$	211	F: GTTATGTAAACTACCAACAGTCG	187-259	20	1.00	0.95	1
				R: GGTCACTAGCATGCAGAAAG					
	LepESR_12	$(TA)_7$	218	F: GTGACCAAGATAATATGCCAGA	198-226	7	0.58	0.67	0.18678
				R: AGATGTGCTGAATGCAGTTTC					
	LepESR_13	$(TAA)_7$	158	F: GATTACAATGGGCCAGTCG	149-176	7	0.54	0.69	0.21993
				R: ATTGAGCAGATCCTGTGTCC					
	LepESR_14	$(CT)_7$	115	F: GCTGAGGTATTCTGTTCCATTC	107-109	2	0.33	0.28	1
				R: GATGGTCTAGGACATCTTGG					

4.5 Discussion

Historically, the development of microsatellites with crustaceans and molluscs has been problematic owing to a hypothesised paucity of microsatellite loci within the genomes of some taxa and also the existence of repeat elements in microsatellite flanking regions (Brooker et al. 2000; Weetman et al. 2007; Bailie et al. 2010; McInerney et al. 2010). Whilst there was no evidence of this paucity when searching for microsatellites amongst the 454 fragments, occasionally in this study, some loci were rejected at the test amplification stage (prior to polymorphism testing) because PCR product gel runs produced 'smears' spread across a wide size range, rather than clearly defined bands. On closer inspection, these smears were multiple bands tightly packed, suggesting that the flanking regions in which the primer sites are located could be sequence elements repeated throughout the genome, as has been found in other crustaceans and molluscs (Bailie et al. 2010; McInerney et al. 2010). Despite this problem, the method of using NGS to find and develop microsatellites as used by Abdelkrim et al (2009), resulted in the development of a respectable haul of markers, similar in quantity to other hydrothermal vent crustaceans (Zelnio et al. 2010; Teixeira et al. 2012a) and gastropods (Thaler et al. 2010) developed using clonal libraries. The key advantage of the method used here is the reduction in the time required to get to the primer-testing phase, making the simultaneous development of markers for three marine invertebrate species feasible over the timescale of a D.Phil.

Whilst the range of these three species is currently unclear, owing to the lack of vent exploration on Southern Hemisphere mid-ocean ridges and seamounts, a kiwaid very similar to *Kiwa* sp. has been found on the Southwest Indian Ridge (see Chapter 2) along with a peltospirid gastropod

closely related to the one from the ESR (Chen et al. submitted) and it may be likely that the loci developed here could cross amplify with these closely related species, as has been shown for species of hydrothermal vent shrimp (Jacobson et al. 2013). The same could also be true for *Lepetodrilus atlanticus*, a vent limpet found on the Mid-Atlantic Ridge, which has a very close affinity to *Lepetodrilus* sp. from the ESR (Katrin Linse, manuscript in preparation).

4.6 Conclusion

This is the first development of a suite of microsatellite markers for a kiwaid crab, a lepetodrilid limpet or a peltospirid gastropod. The method of using NGS to find microsatellites has proved effective in the simultaneous development of markers for three species of invertebrate, a group of animals for which microsatellite development has in the past been considered problematic. This toolkit will determine the nature of connectivity between individuals collected at the Northern and Southern end of the ESR as well as between individuals on the ESR, on other vents nearby, and possibly along the American-Antarctic and Southwest Indian Ridges.

CHAPTER 5

Population Genetics of Vent Fauna in the Scotia Sea Using Microsatellites

5.1 Abstract

The first multispecies study of vent-endemic megafauna from the Southern Ocean using recently designed microsatellite loci is presented herein. No evidence of genetic differentiation was found for three undescribed species, a kiwaid crab, *Kiwa* sp., a peltospirid gastropod and a lepetodrillid limpet, *Lepetodrilus* sp., between the E2 and E9 vent fields on the East Scotia Ridge (ESR), which are ~ 440 km apart. A lack of differentiation is consistent with panmixia, despite the potentially limited dispersal capability of kiwaid larvae, although dispersal of Southern Ocean vent fauna may be enhanced as a consequence of hypothesised cold-water induced arrested development. Alternatively, no indication of differentiation may be the consequence of metapopulation non-equilibrium processes dominating between vent fields. Evidence of recent demographic change for all three species is consistent with a model of demographic instability within a metapopulation framework, supporting the evidence from the COI dataset. Despite the high apparent connectivity of the limpets along the ESR, strong differentiation exists between limpets on the ESR and those found in the Kemp Caldera, ~ 95 km to the East, perhaps owing to the topographical isolation of the vents within the Caldera, unfavourable currents or a lack of venting along the intervening sea floor. Under the Isolation with Migration model, IMa2 analyses revealed an historic ESR to Kemp gene flow since the divergence of these two populations, compatible with a hypothesised broadly easterly or northeasterly current regime in the region.

5.2 Introduction

Hydrothermal vent-endemic species, which inhabit patchy, ephemeral sites along spreading ridges and on seamounts must maintain their populations by broadcasting larvae into ocean currents (Vrijenhoek 2010). Unlike much of the deep-sea floor, which is comparatively homogeneous (Gage and Tyler 1992), this patchiness affords population geneticists the opportunity to examine how factors such as larval dispersal strategy, hydrography, vent field ephemerality, and sea floor topography affects connectivity, genetic diversity and demographic history in these populations. The inferences made from these examinations have applications beyond the realm of hydrothermal vent ecosystems because the dispersal strategy of vent fauna is largely constrained by taxonomic affiliation (Tyler and Young 2003) potentially allowing inferences about realised dispersal capability to be applied more widely in deep-sea ecology.

Since the earliest hydrothermal vent population genetics study (Grassle 1985) nearly thirty years ago, there has been a shift in the use of genetic markers from allozymes (e.g., Bucklin 1988; Black et al. 1994; Craddock et al. 1995; Jollivet et al. 1995; Creasey et al. 1996; Karl et al. 1996; Southward et al. 1996; Black et al. 1998), through mitochondrial and nuclear DNA sequence data, (e.g., Black et al. 1998; Hurtado et al. 2004; Plouviez et al. 2009; Teixeira et al. 2010; Coykendall et al. 2011) to microsatellites most recently (Fusaro 2008; Thaler et al. 2011; Teixeira et al. 2012b).

Microsatellites are short tandem repeats of simple sequence motifs, (e.g. mono, di, tri, tetra etc. repeats) which are co-dominant and theoretically neutral (Ellegren 2004). The markers have been used increasingly in the field of population genetics owing to a faster mutation rate than other markers (10^{-6}-10^{-2} mutations per locus per generation; Schlötterer 2000) affording a higher resolution in the study of population processes, a presumed lower likelihood of being under the

influence of selection by being generally found in non-coding regions of the genome and relatively cheap genotyping allowing the use of multiple loci to better sample the genome (Selkoe and Toonen 2006). The disadvantages of microsatellites, on the other hand, are well documented. Most notably, mutational mechanisms are still unclear, with the most commonly used model of evolution, the stepwise mutational model (SMM; where mutations are in the form of single repeat variations owing to strand slippage during DNA replication), considered unrealistic in some cases (Ellegren 2004). Furthermore, as microsatellites are scored as fragment lengths, their high rate of mutation makes them prone to homoplasy, either because alleles may have the same number of repeats but do not share descent (undetectable homoplasy) or because point mutations leave the overall size of the allele unchanged or insertions and deletions in flanking regions mimic the size of another allele (detectable homoplasy) (Adams et al. 2004) although models such as the SMM can take into account undetectable homoplasy (Slatkin 1995) and detectable homoplasy is considered rare (Adams et al. 2004).

In recent years, the presumed selective neutrality of these markers, owing to their presence in non-coding regions has come into question. It has been suggested that microsatellites in non-coding regions may be linked to several functions that could be under the influence of selection, such as in chromatin organisation, gene expression, recombination, (Li et al. 2002) and loci that are close to regions under selection may be prone to genetic hitchhiking (Selkoe and Toonen 2006) although software exists to detect loci under selection (e.g. Antao et al. 2008) so that they can be weeded out during analyses. The high specificity of microsatellites to a given species is both an advantage and a disadvantage: as they are generally species specific, cross-contamination with other species is less likely than approaches that use universal primers, but this high specificity ensures that marker suites must be developed *de novo* for any new species encountered, which can be costly both in time and money (Selkoe and Toonen 2006). Recently, the costs of microsatellite development have decreased with the development of sequence libraries by next-generation sequencing methods, where microsatellite loci can be detected

(Abdelkrim et al. 2009).

Despite these problems, the fast mutation rates of microsatellites afford population geneticists the opportunity to examine much more recent processes compared to most other genetic markers (Selkoe and Toonen 2006) and can be used in concert with more slowly evolving markers to examine connectivity and genetic diversity at a variety of timescales, such as with the vent-endemic shrimp, *Rimicaris exoculata* (Teixeira et al. 2012b) and the vent gastropod *Ifremeria nautilae* (Thaler et al. 2011) where concordance between mtDNA datasets and microsatellites has improved confidence in the study conclusions.

5.2.1 Study Aims

The purpose of this study is to implement recently developed microsatellite markers (see Chapter 4) to investigate the population genetics of three hydrothermal vent species recently discovered in the Scotia Sea, a species of kiwaid crab, *Kiwa* sp., a peltospirid gastropod and a lepetodrillid limpet, *Lepetodrilus* sp.. In particular the results generated here are designed to complement the findings of the study in Chapter 3 based on the single-locus cytochrome c oxidase subunit I (COI) mtDNA dataset by providing evidence of connectivity and genetic diversity on a more recent timescale to that of the mtDNA dataset.

Specifically, the presumed faster mutation rates of microsatellites should reveal any fine-scale population structure that the mtDNA dataset has failed to detect and the theoretically selective neutrality of these microsatellite loci may help resolve uncertainties about the influence of selection on the mtDNA genetic diversity of these animals. In addition, the use of a multilocus dataset will allow the estimation of effective population sizes and the direction and magnitude of immigration rates between adjacent populations. More broadly, the insights gained from this study are designed to build a more complete picture of how environmental and biological forces

affect populations of vent fauna in the Scotia Sea and at a wider scale, in the Southern Ocean and beyond.

5.3 Methods

5.3.1 Sampling, Tissue & DNA Extraction

The same individuals, tissue and DNA extract used in Chapter 3 for COI analyses were used for microsatellite analyses (see section 3.3). A total of 90 *Kiwa* sp. individuals were genotyped: 45 from E2 and 45 from E9. A total of 84 peltospirid individuals were genotyped: 43 from E2 and 41 from E9. 140 *Lepetodrilus* sp. limpets were genotyped: 47 from E2, 47 from E9 and 46 from the Kemp Caldera.

5.3.2 Microsatellite PCR Amplification & Genotyping

All microsatellite markers developed in Chapter 4 (see Tables 4.1-4.3) were used in this study: nine loci for *Kiwa* sp., 12 loci for the peltospirid and 14 loci for *Lepetodrilus* sp.. Initially, attempts were made to create multiplex reactions - PCR reactions that simultaneously amplify multiple loci, with forward primers tagged with different colour florescent dyes. Multiplex reactions were designed using the software MultiplexManager 1.0 (Holleley and Geerts 2009). The aim was to create a multiplex toolkit in order to save future time and cost in the amplification of these loci. Unfortunately, a series of test runs failed to produce reliable results for all loci in each multiplex reaction, owing to a degree of primer interference. Although some progress was made in reducing this, further multiplex development was abandoned owing to short-term time constraints, and the desire for attaining the highest level of accuracy in genotyping. Consequently, all loci were amplified in singleplex reactions with 6-Fam tagged forward primers as per the PCR protocols detailed in Chapter 4 (section 4.3.3). All individuals

were genotyped, including those previously used in the quality control analyses in Chapter 4 (section 4.3.3).

As in Chapter 4, size-fragment analyses of the PCR products were conducted on an ABI 3730xl DNA analyser. Chromatograms were scored using Peak Scanner™ software 1.0. A total of 90 *Kiwa* sp. individuals were genotyped: 45 from E2 and 45 from E9. A total of 84 individuals of the peltospirids were genotyped: 43 from E2 and 41 from E9. 140 *Lepetodrilus* sp. limpets were genotyped: 47 from E2, 47 from E9 and 46 from the Kemp Caldera.

5.3.3 Quality Control & Analyses

Genotyping error rates were calculated by comparing the re-genotyped 24 individuals from E2 with those same individuals genotyped in Chapter 4. Genetic diversity statistics as well as tests for deviation from Hardy-Weinberg Equilibrium (HWE) and linkage disequilibrium were generated with Arlequin 3.5 (Excoffier and Lischer 2010) and corrected for multiple comparisons using the sequential Bonferroni approach (Rice 1989). Allelic richness was calculated with Fstat 2.9.3.2 (Goudet 1995). Linkage Disequilibrium (LD) was tested in Arlequin, with a likelihood ratio test (10,000 permutations). The exact test of Hardy-Weinberg Equilibrium (HWE) was performed with 10^6 Markov chain steps (and 10^6 dememorisation steps). Presence of null alleles, excessive stutter and large allele dropout were assessed using MicroChecker with 1,000 randomizations (van Oosterhout et al. 2004). Loci were screened using LOSITAN (Antao et al. 2008) to test for the potential influence of selection by an F_{ST} outlier method (Beaumont and Nichols 1996), which plots F_{ST} against heterozygosity and compares this distribution against the expectations of Wright's Island Model (Wright 1950) 1,000,000 simulations were performed, with the Infinite Alleles mutational Model (IAM) for all three species, as well as the Stepwise Mutational Model (SMM) in the case of the limpets,

which lack any compound loci. The IAM (Kimura and Crow 1964) assumes that every new mutation gives rise to a new unique allele (i.e., no homoplasy). This model is simple but unrealistic with microsatellites, which have broadly been shown to evolve by gain or loss of single repeats (Weber and Wong 1993). Consequently, where the repeat number is known, the SMM (Ohta and Kimura 1973) is preferable, although spurious results can result when loci do not adhere to the SMM (Balloux et al. 2000). Lositan was set to compute the initial mean F_{ST} after removing potentially selected loci in an initial run, and then to force the average simulated F_{ST} to approximate the average value found in the real data set. Significance was set at the 95% confidence level with a False Discovery Rate of 0.1 to mitigate false positives. Microsatellite markers that showed deviations from HWE expectations were immediately discarded, and loci deemed under selection were excluded from gene flow and demographic analyses. F_{ST} and STRUCTURE analyses were conducted both with and without loci under selection.

5.3.4 F_{ST}, R_{ST} & Structure Analyses

Pairwise AMOVA F_{ST} analyses (Analysis of MOlecular VAriance) were performed in Arlequin 3.5.1.2 (Excoffier and Lischer 2010) with 10,000 permutations. With the same software, R_{ST} analyses (the microsatellite equivalent of F_{ST} incorporating the stepwise mutational model) were also performed with any compound loci excluded, as the number of motif repeats cannot be estimated. In order to test the number of distinct populations represented in this study for all three species, the Bayesian clustering program STRUCTURE version 2.3.4 (Pritchard et al. 2000) was used, which assigns individuals to groups (assuming that loci are at Hardy-Weinberg Equilibrium) within each population and estimates the population of origin (K) for each individual from the observed genotypes. An admixture ancestry model with correlated allele frequencies and sample locations as priors was used in all runs. Analyses were based on a 100,000 step 'burn-in' with 1,000,000 Markov Chain Monte Carlo steps (MCMC) with three

iterations for each *K* from 1 to n+1, with n being the number of sample locations. The most likely number of populations was determined from the average Ln P(D) of the three iterations.

5.3.5 Demographic Analyses

To test for recent demographic change with microsatellites, the Wilcoxon sign-rank test was used in BOTTLENECK 1.2.02 (Cornuet and Luikart 1996). This test assesses the significance of the mismatch between expected heterozygosities estimated from the allele frequencies (H_e) and heterozygosities estimated from the number and spread of alleles (H_{eq}) based on the assumption of mutation-drift equilibrium and a specific mutational model. During a bottleneck, alleles are lost because of drift and heterozygosity at polymorphic loci also decreases. However, allele number decreases faster than the heterozygosity, resulting in H_{eq} being smaller than H_e for populations that have recently experienced a bottleneck. The reverse would be the case if the population has recently expanded ($H_{eq} > H_e$) (Cornuet and Luikart 1996). Two models have been used in these analyses, the Stepwise Mutation Model (SMM) and the Two Phase Model (TPM), which has been shown to be more realistic to real world observations of microsatellite evolution, by allowing a certain percentage of mutations involving the gain or loss of more than one repeat unit (Di Rienzo et al. 1994). This is achieved by 'mixing' the SMM with a certain percentage of the IAM. Here, two TPM models have been explored: one that is 95% SMM as per the software authors' instructions (Piry et al. 1999) and one that is a conservative 70% SMM. 10,000 iterations were performed.

5.3.6 Long-term Gene Flow Estimation

A key aim of this study is to estimate gene flow between demes. Coalescent tools are capable, within a Bayesian inference computational framework, of inferring the mutation rate–scaled

effective size of a population (θ) as well as the mutation rate-scaled per generation immigration rate (M). IMa2, the latest version of the Isolation with Migration series of programs (Hey 2010) considers cases in which two populations have recently diverged from a common ancestor and estimates θ for each population and for the ancestor population, as well as the divergence time and subsequent bidirectional migration rates (M) among the daughter populations. IMa2 has an advantage over the stable population approaches (e.g. Migrate-n and LAMARC), in that it does not assume that populations have been stable for ~ $4N$ generations, (Kuhner 2009), an assumption that is unlikely to be realistic for many marine populations (Hellberg 2009). Different models of gene flow within the population-splitting framework can be compared in IMa2 L-mode with likelihood ratio tests (Hey 2010).

IMa2 was only used if there was clear evidence for differentiation between locations, using F_{ST}, R_{ST} and STRUCTURE analyses. The COI dataset used in Chapter 3 was added to the microsatellite dataset and any compound microsatellite loci were discarded as not conforming to the SMM, which IMa2 uses to model microsatellite evolution. Initial short IMa2 runs were performed to optimize model parameters and find reasonable priors to optimise MCMC search efficiency. The following uniform prior limits were used in final runs: θ (mutation-scaled effective population) = 150, M (mutation-scaled immigration rate per generation) = 5, and τ (mutation rate-scaled splitting time) = 10. Nine independent analyses (using random number seeds), each with 100 geometrically heated chains, were run for 2,000,000 steps (genealogy sampling every 100 steps, yielding 20,000 trees) with the length of 'burn-in' determined by the scrutiny of trend plots printed every six hours. Final burn-in lengths for the runs were ~1,500,000 steps per independent run.

Microsatellite data typically results in very low effective sample size (ESS) values in IMa2, even with many heated chains designed to maximise MCMC efficiency and avoid local optima, which is why many independent runs were used and trend plots assessed to ensure that results were consistent between runs. Sample genealogies were then combined in L-mode (180,000

trees) and the significance of inferred immigration rates tested using likelihood-ratio tests (LLR) (Nielsen and Wakeley 2001). Nested models were compared and ranked with LLR tests. As nothing is presently known of microsatellite mutation rates in the study species, mutation rates were pegged to a COI mutation rate in order to estimate the time since splitting. The rate used was based on the divergence of *Lepetodrilus pustulosus* across the Easter Microplate, which formed ~ 5.25-2.47 Ma (Naar and Hey 1991; Rusby and Searle 1995). In this study a mean age for the microplate (3.86 Ma) has been used to get a mean substitution rate of 6.404145 x 10^{-6} substitutions per *gene* per year, with a range of 4.7085714 x 10^{-6} to 1.0008097 x 10^{-5} based on the 5.25-2.47 Ma date range.

5.3.7 Current Gene Flow

Recent gene flow (within the last several generations) was estimated with BayesAss 3.03 (Wilson and Rannala 2003), which uses an assignment method without incorporating genealogies within a Bayesian MCMC framework. First or second generation immigrants, for example, will present different multilocus genotypes than expected for native individuals without recent immigrant ancestors. The advantage of this method is that it requires fewer assumptions than the long-term approaches and does not require populations to be at drift-migration equilibrium or in HWE either, although this approach can be more vulnerable to homoplasy as there is no model of evolution incorporated that can accommodate it. The output is in the form the fraction of individuals from, e.g., population 0 that are migrants from population 1. Individuals can also be designated as first or second-generation migrants, with accompanying probabilities. The approach assumes that the source populations have been sampled. Three runs, each with 20,000,000 iterations and a 'burn-in' of 2,000,000 were performed with different random number seeds, and then the average was taken. DeltaA, DeltaF and DeltaM (mixing parameters for allele frequencies, inbreeding coefficients and migration

rates respectively) were set to 0.2, 0.35 and 0.15 respectively. The authors of this software stress that this approach does not allow one to estimate directly the total proportion of individuals that *emigrate* from a population. For example, if a small population provides a large proportion of its individuals as migrants per generation to a much larger population, these immigrants will only make up a small proportion of the total number of individuals in the destination population, which would be reflected in a low immigration rate estimate (Wilson and Rannala 2003).

5.4 Results

5.4.1 Error Rates

Genotyping of the same 24 individuals used in Chapter 4 revealed a high level of consistency in the scoring of alleles. No more than two errors were ever detected across 24 individuals per locus. Mean error rates across loci per species were 2.3%, 3.1% and 2.9% for *Kiwa* sp., the peltospirids and *Lepetodrilus* sp. respectively.

5.4.2 Genetic Variability

In total, 35 microsatellite loci were amplified across all three species and all locations: nine loci for *Kiwa* sp., 12 for the peltospirid and 14 for *Lepetodrilus* sp.. Within *Kiwa* sp., locus allelic richness ranged from four to 27 at E2 and two to 28 at E9 (Table 5.1). Total mean allelic richness across all loci was 10.778 and 10.111 for individuals collected at E2 and E9 respectively (mean expected heterozygosity, H_{exp}, of 0.647 and 0.630 respectively) (Table 5.4). With the peltospirids, allelic richness ranged from two to 25 at E2 and two to 13 at E9 (Table 5.2). Total mean allelic richness across all loci was 6.719 and 5.583 at E2 and E9 respectively (H_{exp}, of 0.496 and 0.507 respectively) (Table 5.4). Within *Lepetodrilus* sp., locus allelic richness ranged from two to 26 at E2, two to 28 at E9 and three to 14 at the Kemp Caldera (Table 5.3). Total mean allelic richness across all loci was 12.857, 13.308 and 8.5 at E2, E9 and Kemp respectively (H_{exp}, of 0.689, 0.684 and 0.634 respectively) (Table 5.4).

Table 5.1. Microsatellite summary statistics per locus for *Kiwa* sp. at vent sites on the East Scotia Ridge. Repeat motif, locus size range, number of individuals (N), number of alleles (N_A), allelic richness (A_R), observed heterozygosity (H_{obs}), expected heterozygosity (H_{exp}), and probability (P) of deviation from Hardy-Weinberg Equilibrium (exact test, 1,000,000 permutations, 1,000,000 dememorisation steps) are reported. Significant P values (after a sequential Bonferroni correction) are highlighted in bold, with the relevant location and locus shaded.

Location		Locus KiwESR_01	KiwESR_02	KiwESR_03	KiwESR_04	KiwESR_05	KiwESR_06	KiwESR_07	KiwESR_08	KiwESR_09
E2	Repeat Motif	$(GTT)_n$	$(TGT)_n$	$(TG)_n$	$(TGT)_n$	$(AT)_n$	$(TG)_n$	$(AT)_n (AC)_n$	$(AC)_n$	$(CAA)_n$
	Size Range	142-190	266-278	151-169	200-213	204-212	143-151	119-177	80-146	106-133
	N	45	45	45	45	45	45	45	45	45
	N_A	12	5	8	5	4	5	24	27	7
	A_R	12	5	8	5	4	5	24	27	7
	H_{obs}	0.8	0.64444	0.46667	0.48889	0.24444	0.37778	0.93333	1	0.62222
	H_{exp}	0.77104	0.59875	0.55406	0.51735	0.27665	0.48489	0.94707	0.9598	0.71436
	P	0.55558	0.02837	0.20519	0.53847	0.29582	0.01728	0.41026	0.10856	0.07335
E9	Repeat Motif	$(GTT)_n$	$(TGT)_n$	$(TG)_n$	$(TGT)_n$	$(AT)_n$	$(TG)_n$	$(AT)_n (AC)_n$	$(AC)_n$	$(CAA)_n$
	Size Range	148-202	266-275	141-163	200-213	204-206	143-151	121-187	80-146	109-124
	N	45	45	45	45	45	45	45	45	45
	N_A	11	4	8	6	2	4	22	28	6
	A_R	11	4	8	6	2	4	22	28	6
	H_{obs}	0.66667	0.53333	0.44444	0.4	0.37778	0.51111	0.91111	0.95556	0.75556
	H_{exp}	0.73308	0.5171	0.5191	0.43895	0.3618	0.5186	0.95356	0.96404	0.66292
	P	0.19433	0.25195	0.48833	0.84352	1	0.94726	0.61755	0.8212	0.05369

Table 5.2. Microsatellite summary statistics per locus for a peltospirid gastropod at vent sites on the East Scotia Ridge. Repeat motif, locus size range, number of individuals (N), number of alleles (N_A), allelic richness (A_R), observed heterozygosity (H_{obs}), expected heterozygosity (H_{exp}), and probability (P) of deviation from Hardy-Weinberg Equilibrium (exact test 1,000,000 permutations, 1,000,000 dememorisation steps) are reported. Significant P values (after a sequential Bonferroni correction) are highlighted in bold, with the relevant location and locus shaded.

Location		Locus PeltESR_01	PeltESR_02	PeltESR_03	PeltESR_04	PeltESR_05	PeltESR_06	PeltESR_07	PeltESR_08	PeltESR_09	PeltESR_10	PeltESR_11	PeltESR_12
E2	Repeat Motif	$(CA)_n$	$(AC)_n$	$(AC)_n$	$(CTAT)_n$	$(CATT)_n$	$(TC)_n$	$(GT)_n$	$(GT)_n$ $(GT)_n$ $(GT)_n$	$(GT)_n$	$(GTT)_n$ $(GTT)_n$	$(TA)_n$	$(GT)_n$
	Size Range	118-124	127-135	367-373	312-336	203-267	163-165	198-202	271-337	158-160	345-363	138-148	129-165
	N	43	43	43	43	43	43	43	43	43	43	43	43
	N_A	4	5	4	5	15	2	3	15	2	6	6	15
	A_R	3.998	4.907	3.907	4.952	14.809	2	2.953	14.625	2	5.95	5.86	14.671
	H_{obs}	0.32558	0.32558	0.4186	0.2093	0.83721	0.51163	0.13953	0.5814	0.5814	0.44186	0.67442	0.74419
	H_{exp}	0.34446	0.2922	0.46731	0.25636	0.90451	0.45964	0.15294	0.67825	0.50479	0.4643	0.61176	0.81505
	P	0.64734	1	0.39166	0.15852	0.81062	0.51647	0.07684	0.1194	0.36802	0.00828	0.19724	0.00469
E9	Repeat Motif	$(CA)_n$	$(AC)_n$	$(AC)_n$	$(CTAT)_n$	$(CATT)_n$	$(TC)_n$	$(GT)_n$	$(GT)_n$ $(GT)_n$ $(GT)_n$	$(GT)_n$	$(GTT)_n$ $(GTT)_n$	$(TA)_n$	$(GT)_n$
	Size Range	118-124	129-135	367-373	324-336	203-259	163-165	198-202	271-337	158-160	348-363	142-148	135-165
	N	41	41	41	41	41	41	41	41	41	41	41	41
	N_A	4	3	3	4	13	2	3	12	2	6	4	11
	A_R	4	3	3	4	13	2	3	12	2	6	4	11
	H_{obs}	0.36585	0.19512	0.39024	0.31707	0.90244	0.43902	0.26829	0.78049	0.43902	0.68293	0.46341	0.7561
	H_{exp}	0.41102	0.25896	0.42668	0.28335	0.90575	0.43842	0.2966	0.74466	0.46974	0.57663	0.50015	0.77537
	P	0.5183	0.1126	0.62037	1	0.53163	1	0.3222	0.8105	0.74133	0.37447	0.60041	0.43408

Table 5.3. Microsatellite summary statistics per locus for *Lepetodrilus* sp. at vent sites on the East Scotia Ridge and Kemp Caldera. Repeat motif, locus size range, number of individuals (N), number of alleles (N_A), allelic richness (A_R), observed heterozygosity (H_{obs}), expected heterozygosity (H_{exp}), and probability (P) of deviation from Hardy-Weinberg Equilibrium (exact test 1,000,000 permutations, 1,000,000 dememorisation steps) are reported. Significant P values (after a sequential Bonferroni correction) are highlighted in bold, with the relevant location and locus shaded.

Location		Locus LepESR_01	LepESR_02	LepESR_03	LepESR_04	LepESR_05	LepESR_06	LepESR_07	LepESR_08	LepESR_09	LepESR_10	LepESR_11	LepESR_12	LepESR_13	LepESR_14
E2	Repeat Motif	$(AAT)_n$	$(GT)_n$	$(TAA)_n$	$(CATT)_n$	$(AT)_n$	$(ATT)_n$	$(TTA)_n$	$(ACC)_n$	$(AC)_n$	$(TA)_n$	$(ACT)_n$	$(TA)_n$	$(TAA)_n$	$(CT)_n$
	Size Range	268-292	179-225	170-230	195-199	107-161	86-116	117-210	348-360	99-163	92-110	181-361	198-248	149-176	105-111
	N	47	47	47	47	47	47	47	47	47	47	47	47	47	47
	N_A	9	18	20	2	16	10	21	5	22	8	26	9	10	4
	A_R	8.957	17.893	19.914	2	15.914	9.978	20.894	5	21.829	7.915	25.85	8.978	9.957	3.957
	H_{obs}	0.7234	0.97872	0.85106	0.04255	0.78723	0.7234	0.87234	0.42553	0.87234	0.34043	0.91489	0.59574	0.61702	0.38298
	H_{exp}	0.78037	0.90391	0.91993	0.0421	0.84763	0.81148	0.94761	0.46099	0.91741	0.39876	0.95287	0.64997	0.67605	0.32052
	P	0.64303	0.62122	0.03293	1	0.39829	0.16625	0.39172	0.11999	0.53525	0.16999	0.34999	0.35962	0.59156	0.53911
E9	Repeat Motif	$(AAT)_n$	$(GT)_n$	$(TAA)_n$	$(CATT)_n$	$(AT)_n$	$(ATT)_n$	$(TTA)_n$	$(ACC)_n$	$(AC)_n$	$(TA)_n$	$(ACT)_n$	$(TA)_n$	$(TAA)_n$	$(CT)_n$
	Size Range	253-292	179-209	176-233	195-199	98-155	86-110	111-240	342-368	99-157	92-106	181-430	198-220	152-179	105-119
	N	47	47	47	47	47	47	47	47	47	47	47	47	47	47
	N_A	11	14	18	2	18	9	22	8	24	5	28	8	10	5
	A_R	10.915	13.957	17.935	2	17.893	8.979	21.893	7.936	23.786	4.978	27.807	7.978	9.978	4.957
	H_{obs}	0.7234	0.87234	0.97872	0.04255	0.80851	0.6383	0.95745	0.6383	0.80851	0.38298	0.87234	0.59574	0.59574	0.38298
	H_{exp}	0.73027	0.85198	0.92244	0.0421	0.87943	0.84512	0.94395	0.52917	0.90734	0.41478	0.95562	0.64287	0.5795	0.32693
	P	0.49977	0.47906	0.15254	1	0.11192	**0.00155**	0.90364	0.92581	0.23484	0.12024	0.04686	0.1898	0.32505	0.80367
Kemp	Repeat Motif	$(AAT)_n$	$(GT)_n$	$(TAA)_n$	$(CATT)_n$	$(AT)_n$	$(ATT)_n$	$(TTA)_n$	$(ACC)_n$	$(AC)_n$	$(TA)_n$	$(ACT)_n$	$(TA)_n$	$(TAA)_n$	$(CT)_n$
	Size Range	268-283	179-225	179-224	191-211	89-158	89-116	126-177	348-357	97-147	98-110	184-274	198-220	158-173	107-165
	N	46	46	46	46	46	46	46	46	46	46	46	46	46	46
	N_A	6	14	14	4	11	9	14	4	10	6	11	5	3	8
	A_R	6	14	14	4	11	9	14	4	10	6	11	5	3	8
	H_{obs}	0.78261	0.76087	0.54348	0.56522	0.69565	0.73913	0.78261	0.78261	0.76087	0.3913	0.69565	0.63043	0.1087	0.36957
	H_{exp}	0.69374	0.8667	0.57788	0.54682	0.81199	0.79575	0.86288	0.7322	0.715	0.46369	0.75155	0.58624	0.14453	0.33086
	P	0.22138	0.03605	0.15953	0.16909	0.0915	0.25435	0.0221	0.19027	0.48548	0.46644	0.21212	0.31834	0.02228	1

Table 5.4. Microsatellite summary statistics for *Kiwa* sp., a peltospirid gastropod and *Lepetodrilus* sp. at vent sites on the East Scotia Ridge and the Kemp Caldera. Statistics included for *Lepetodrilus* sp., with 13 loci and seven loci after removal of loci not in Hardy-Weinberg Equilibrium as well as those under selection respectively. Number of individuals (*N*), number of loci (*nLoci*), mean number of loci (*A*), mean allelic richness (A_R), observed heterozygosity (H_{obs}) and expected heterozygosity (H_{exp}) are reported.

Species	Location	*N*	*nLoci*	*A*	A_R	H_{exp}	H_{obs}
Kiwa sp.	E2	45	9	10.778 (8.715)	10.778	0.647	0.620
	E9	45	9	10.111 (8.95)	10.111	0.630	0.617
Peltospirid	E2	43	12	6.833 (5.096)	6.719	0.496	0.483
	E9	41	12	5.583 (4.033)	5.583	0.507	0.500
Lepetodrilus sp.	E2	47	14	12.857 (7.533)	12.788	0.689	0.652
	E9	47	14	13.071 (7.985)	12.928	0.684	0.664
	Kemp	46	14	8.5 (3.937)	8.500	0.634	0.615
Lepetodrilus sp.	E2	47	13	13.077 (7.794)	13.004	0.678	0.646
	E9	47	13	13.308 (8.107)	13.232	0.671	0.666
	Kemp	46	13	8.462 (4.095)	8.462	0.622	0.605
Lepetodrilus sp.	E2	47	7	11 (7.394)	10.948	0.635	0.590
	E9	47	7	11.571 (7.254)	11.504	0.622	0.626
	Kemp	46	7	6.571 (3.994)	6.571	0.596	0.571

5.4.3 Quality Control

No loci were linked according to LD pairwise tests and only one locus, LepESR_06, significantly deviated from HWE (heterozygote deficiency) (Table 5.3) after correction for multiple tests, where the presence of null alleles was also detected. With *Kiwa* sp. and the peltospirids, no loci were under the influence of directional or balancing selection, however, four *Lepetodrilus* sp. loci were found to be under balancing selection (LepESR_02, LepESR_05, LepESR_07 and LepESR_14) and one under directional selection (LepESR_10). Additionally, under the SMM, another locus was found to be under directional selection (LepESR_11) (Table 5.5). With these loci excluded from the diversity statistics (including

LepESR_06), total mean allelic richness across all loci was 10.948, 11.504 and 6.571 at E2, E9 and Kemp respectively.

Table 5.5. Microsatellite loci of *Lepetodrilus* sp. detected under balancing or direction selection (shaded), according to the F_{ST} outlier method using Lositan software (1,000,000 simulations) with the Infinite Alleles and Stepwise Mutational Models (IAM & SMM). Significance set at 95 % with a false discovery rate of 0.1. *He* denotes expected heterozygosity.

SMM					IAM				
Locus	*He*	*F*st	*P*	Selection	Locus	*He*	*F*st	*P*	Selection
LepESR_01	0.843744	0.129128	0.713295		LepESR_01	0.843744	0.129128	0.607713	
LepESR_02	0.877595	0.003872	0.003482	Balancing	LepESR_02	0.877595	0.003872	0	Balancing
LepESR_03	0.899157	0.102771	0.712186		LepESR_03	0.899157	0.102771	0.489199	
LepESR_04	0.320235	0.343176	0.961476		LepESR_04	0.320235	0.343176	0.952896	
LepESR_05	0.863452	0.019804	0.038852		LepESR_05	0.863452	0.019804	0.000207	Balancing
LepESR_06	0.859032	0.048406	0.2138		LepESR_06	0.859032	0.048406	0.068892	
LepESR_07	0.944503	0.027907	0.250754		LepESR_07	0.944503	0.027907	0.002757	Balancing
LepESR_08	0.706611	0.1875	0.784885		LepESR_08	0.706611	0.1875	0.775534	
LepESR_09	0.929627	0.089328	0.793141		LepESR_09	0.929627	0.089328	0.415995	
LepESR_10	0.723712	0.411722	0.990177	Directional	LepESR_10	0.723712	0.411722	0.995117	Directional
LepESR_11	0.972511	0.088257	0.985948	Directional	LepESR_11	0.972511	0.088257	0.613273	
LepESR_12	0.725391	0.136522	0.623462		LepESR_12	0.725391	0.136522	0.599214	
LepESR_13	0.507316	0.080076	0.516505		LepESR_13	0.507316	0.080076	0.516705	
LepESR_14	0.327194	0.00333	0.01632	Balancing	LepESR_14	0.327194	0.00333	0.01449	Balancing

5.4.1 Population Structure

AMOVA F_{ST} analyses revealed no pattern of differentiation on the ESR for all three species. R_{ST} analyses, with compound loci excluded, showed the same pattern (Table 5.6). However, significant F_{ST} and R_{ST} differentiation was detected between lepetodrillid limpets collected at Kemp and those on the ESR for datasets with and without loci under selection: the 13 loci dataset (HWE deviant LepESR_06 removed) yielded significant F_{ST} and R_{ST} values in excess of 0.1598 and 0.15283 respectively and the seven locus dataset produced F_{ST} and R_{ST} values in excess of 0.18775 and 0.29294 respectively (Table 5.6). STRUCTURE analyses produced similar results (Table 5.7), with assignment tests indicating that individuals across all three species collected from the ESR came from one population, with limpets from Kemp assigned to another population: for both *Kiwa* sp., and the peltospirid, $K = 1$ was favoured and $K = 2$ was favoured for *Lepetodrilus* sp..

Table 5.6. Pairwise F_{ST} and R_{ST} microsatellite analyses for *Kiwa* sp., a peltospirid gastropod and *Lepetodrilus* sp. from vent sites on the East Scotia Ridge and the Kemp Caldera, using Arlequin (10,000 permutations). Significant differentiation ($P < 0.05$) indicated in bold. *nLoci* denotes number of loci.

Species	*nLoci*	Pairwise Comparison	F_{ST}	*P*	R_{ST}	*P*
Kiwa sp.	*9*	E2 vs E9	-0.00037	0.55084	-0.00606	0.57885
Peltospirid	*12*	E2 vs E9	0.00593	0.06663	0.01122	0.15147
Lepetodrilus sp.	*13*	E2 vs E9	0.00268	0.10256	-0.00485	0.75715
		E2 vs Kemp	**0.16506**	**0.00000**	**0.16057**	**0.00000**
		E9 vs Kemp	**0.1598**	**0.00000**	**0.15283**	**0.00000**
Lepetodrilus sp.	*7*	E2 vs E9	0.00459	0.07415	-0.00585	0.70518
		E2 vs Kemp	**0.19349**	**0.00000**	**0.29294**	**0.00000**
		E9 vs Kemp	**0.18775**	**0.00000**	**0.32297**	**0.00000**

Table 5.7. STRUCTURE results comparing different population assignment models, from one population to the number of sample locations + 1 for *Kiwa* sp. (*K*1 – *K*3), a peltospirid gastropod (*K*1 – *K*3) and *Lepetodrilus* sp. (*K*1 – *K*4). Mean negative log likelihoods from three iterations are reported, with the most likely model highlighted in bold. 1,000,000 Markov chain Monte Carlo steps performed with a burn-in of 100,000. *Nloci* denotes number of loci.

Species	*nLoci*	K1 Mean	K2 Mean	K3 Mean	K4 Mean
Kiwa sp.	*9*	**-2562.57**	-2570.77	-2564.87	NA
Peltospirid	*12*	**-2177.47**	-2180.00	-2186.67	NA
Lepetodrilus sp.	*13*	-6914.47	**-6315.77**	-6390.97	-6426.63
Lepetodrilus sp.	*7*	-3262.47	**-2937.17**	-2976.53	-2987.33

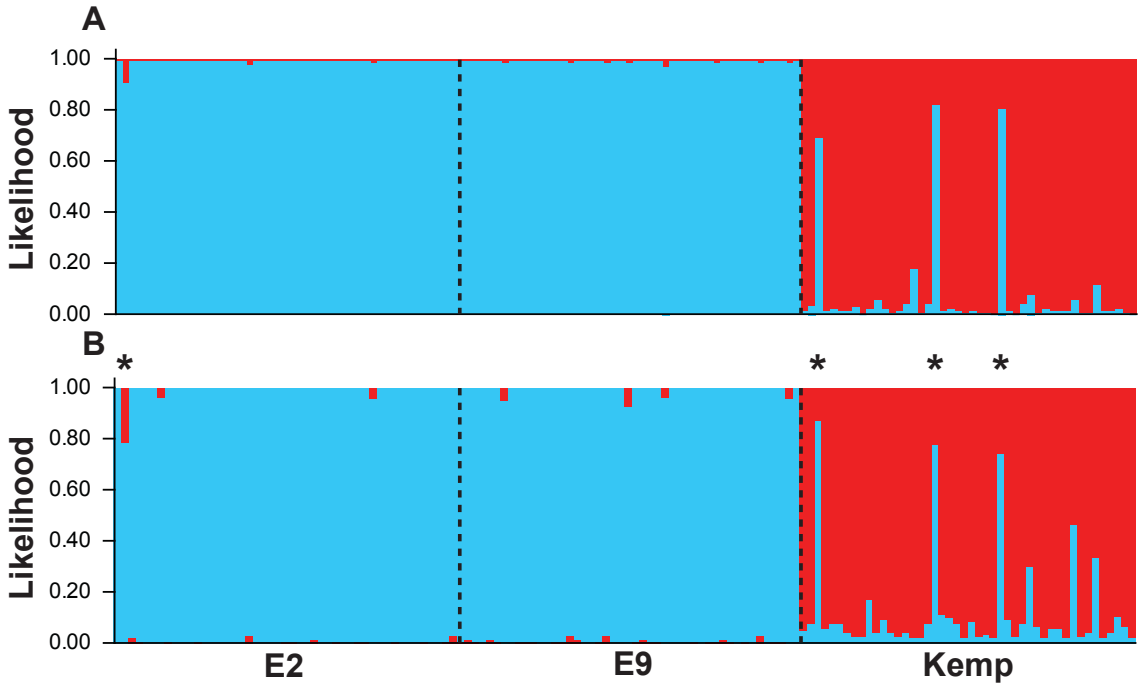

Figure 5.1. Bar plots produced in STRUCTURE showing the assignment likelihood of *Lepetodrilus* sp. individuals collected at hydrothermal vents on the East Scotia Ridge (E2 and E9) and the Kemp Caldera in the Scotia Sea based on the most likely two population model (K = 2) using 13 microsatellite loci (A) and 7 loci after removal of loci possibly under selection according to Lositan (B). Individuals identified as possible migrants according to BayesAss 2.0 are marked with asterisks. Sample locations, E2, E9 and Kemp are delineated with dashed lines.

5.4.2 Long-term Gene Flow

Based on the F_{ST}, R_{ST} and STRUCTURE results, which only revealed differentiation between ESR and Kemp limpets, estimates of θ and M (and therefore the population per generation immigration rates, 2NM) for the ESR and Kemp populations, as well as time since these populations split from an ancestral population (as per the Isolation with Migration model) were estimated using IMa2. In IMa2, the *Lepetodrilus* sp. substitution rate (substitutions per *gene* per year) used for calibrating the analyses was based on the divergence (8%) of *L. pustulosus* across the Easter Microplate, which formed ~ 3.86 Ma (2.47-5.25 Ma) (Naar and Hey 1991; Rusby and Searle 1995) giving a mean rate of 6.40415 x 10^{-6} (4.70857 x 10^{-6}-1.00081 x 10^{-5}).

Trace outputs did not reveal any trends and estimated parameters were smooth and unimodal, with the exception of estimates of splitting time (Fig. 5.2D). Consequently the estimated splitting date range should be treated with some caution. θ for the ancestral population did not reach zero at the upper prior boundary and therefore the mean and the highest posterior density interval may be unrepresentative (Fig. 5.2C).

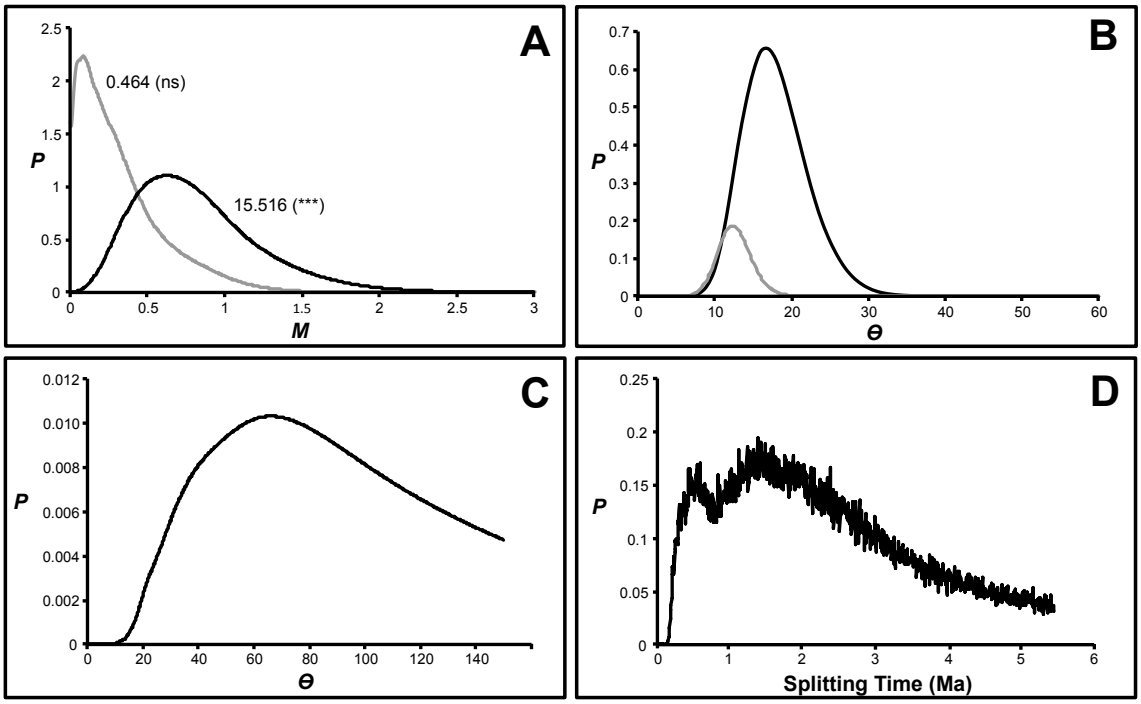

Figure 5.2. Marginal posterior densities (*P*) of model parameters generated in L-mode of IMa2 (180,000 genealogies) for two populations of *Lepetodrilus* sp. limpets collected from hydrothermal vents on the East Scotia Ridge (ESR) and the Kemp Caldera in the Scotia Sea. A = immigration rates (*M*), with likelihood-ratio test results (ns = non significant, *** = highly significant ($P < 0.001$)), with the grey line denoting immigration rates into the ESR from Kemp, and the black line, vice versa. B = estimates of θ, the mutation rate-scaled effective population size (4Nu), with the grey line denoting the θ of Kemp and the black line, that of the ESR. C = estimates of θ for the ancestral population. D = estimate of the splitting time (in millions of years) of the ancestral population into the two populations examined here.

Table 5.8. Summary results of IMa2 analyses (180,000 genealogies) on two populations of hydrothermal vent limpets, *Lepetodrilus* sp., from the East Scotia Ridge (ESR) and the Kemp Caldera, a submerged part of the South Sandwich Island arc, both in the Scotia Sea. Parameter values are taken from estimated marginal posteriors with 'High Point' values denoting peak values, and HDP95% values are taken from the estimated 95% highest posterior density interval. Displayed estimated parameters are the mutation rate–scaled effective size of the populations (θ), the mutation rate-scaled per generation immigration rate (M) into Kemp from the ESR, τ (mutation rate-scaled splitting time) and the splitting time in years calculated by dividing τ by the COI mutation rate, adjusted by its mutation-rate scalar.

	High Point	Mean	HPD95% Low	HPD95% High
θ ESR	12.22	12.61	8.175	17.18
θ Kemp	2.475	2.61	1.125	4.425
θ Ancestral	66.08	81.87	27.98	146.9
M ESR > KEMP	0.6225	0.8246	0.1525	1.643
τ	2.525	4.109	0.365	9.035
Splitting Time (yrs)	1375623	2238815	198852	4922280

IMa2 results, based on the Isolation with Migration model of an ancestral population splitting into two populations with subsequent gene flow between them (Nielsen and Wakeley 2001; Hey and Nielsen 2004) revealed that the ESR population is larger than the Kemp Caldera population, though both populations are far smaller than the ancestral population (Table 5.8). According to LLR tests, immigration rates into the ESR from Kemp were non-significant, but rates into Kemp from the ESR were highly significant ($P < 0.001$) (Fig. 5.2A), meaning that the favoured model in L-mode was the full model, but with zero migration from the Kemp Caldera to the ESR.

5.4.3 Contemporary Immigration

As with IMa2, analyses were only conducted between ESR limpets and those of the Kemp Caldera owing to a lack of differentiation for all three species between E2 and E9 on the ESR. BayesAss reports results in terms of the proportion of individuals in population 0 that are

migrants from population 1. This approach could be interpreted as equivalent to a recent immigration rate as a ratio, but not as a measure of per individual migration rates, unless populations are equal in size, which is unlikely, given the mismatch in expected heterozygocity and allelic richness between the two populations and the output of IMa2 analyses. The per generation immigration rate to the ESR from Kemp, was 0.124, whereas the immigration rate into Kemp from the ESR was 0.401. The individual assignments produced in BayesAss (Table 5.8) suggest that one individual on the ESR, F128_3 from the E2 field, may be a second generation migrant from Kemp (mean posterior probability of 0.663) and individuals F622_3, F622_19 and F622_28 may be first generation migrants from the ESR (mean posterior probabilities of 0.988, 0.699 and 0.822 respectively) (Table 5.9).

Table 5.9. Contemporary gene flow estimates according to BayesAss software for *Lepetodrilus* sp., between the East Scotia Ridge and the Kemp Caldera in the Scotia Sea. Per generation mean rates from three replicate runs (20,000,000 iterations, burnin-in of 2,000,000) are reported as ratios of individuals sampled from a population that are assigned to a source population. Popn denotes population.

Popn	Source Popn	Mean Rate
ESR	ESR	0.9876
ESR	Kemp	0.0124
Kemp	ESR	0.0401
Kemp	Kemp	0.9599

Table 5.10. Mean probability (three iterations) of migrant assignment of *Lepetodrilus* sp. individuals from vent populations in the Scotia Sea (either 1st or 2nd generation migrants), as determined by BayesAss. Popn denotes population, Gen Mig denotes the inferred migrant generation. Highlighted individuals are those with a H2 COI haplotype, which is the second most common haplotype on the East Scotia Ridge, but rare at the Kemp Caldera. Each replicate was run for 20,000,000 iterations, with a 'burn-in' of 2,000,000.

Individual	Popn	Source Popn	Gen Mig	Mean Prob
F128_3	ESR	Kemp	2nd	0.663
F622_3	Kemp	ESR	1st	0.988
F622_19	Kemp	ESR	1st	0.699
F622_28	Kemp	ESR	1st	0.820

5.4.4 Recent Demographic Change

BOTTLENECK analyses revealed a significant ($P < 0.05$) pattern of heterozygote deficiency relative to the heterozygosity estimated from the number and spread of alleles (H_{eq}) under SMM for all three species (Table 5.10). However $H_{eq} > H_e$ was not significant for the peltospirids under a TPM that was 95% SMM and 5% IAM and was not significant for the peltospirids and the Kemp limpets under a more relaxed TPM (70% SMM, 30% AIM), although still significant for *Kiwa* sp. and the ESR limpets.

Table 5.11. *P* values for Wilcoxon-Rank tests examining the deficiency of microsatellite heterozygosity as determined from allele frequencies (H_e) compared to heterozygosity, determined by the number and spread of alleles (H_{eq}), given a specific mutational model and the assumption of mutation-drift equilibrium. Bottleneck was run (10,000 iterations) with three models, the Stepwise Mutational Model (SMM), the Two Phase Model with either 95% SMM and 5 % Infinite Alleles Model (IAM) or 70% SMM and 30% IAM. Significant results ($P < 0.05$) highlighted in bold.

Species	Location	SSM	TPM 95 %	TPM 70 %	IAM
Kiwa sp.	ESR	**0.00391**	**0.00586**	**0.01953**	0.67969
Peltospirid	ESR	**0.01611**	0.05273	0.1875	0.75391
Lepetodrilus sp.	ESR	**0.00391**	**0.00391**	**0.00781**	0.28906
Lepetodrilus sp.	Kemp	**0.02734**	**0.02734**	0.28906	0.59371

5.5 Discussion

5.5.1 ESR Connectivity

The complete lack of apparent genetic differentiation along the ESR for all three species using AMOVA F_{ST}, R_{ST} and STRUCTURE analyses echoes the same pattern with mtDNA in Chapter 3 and consequently, the null hypothesis of panmixia along the ESR cannot be rejected. Owing to the presumed faster mutation rates of microsatellite repeat DNA compared with sequence DNA (Ellegren 2004), a lack of differentiation with microsatellites likely reflects the more recent history of connectivity compared with mtDNA data. As with mtDNA, this lack of differentiation is similar to that of *Riftia pachyptila* on the East Pacific Rise (EPR), where there is no evidence of microsatellite differentiation within ridge segments that are equivalent in length to the entire ESR (Fusaro 2008).

As discussed at length in Chapter 3, low differentiation on such scales (10s to 100s of kilometres along ridge segments) may well reflect the dominance of non-equilibrium processes within metapopulations of vent colonies. For vent species with lecithotrophic dispersal strategies, genetic homogeneity could well be largely restricted to ridge segments as has been observed for a variety of species along the EPR (Vrijenhoek 2010). For vent species with a high potential larval dispersal capability, as is theorized for *R. exoculata* with planktotrophic larvae, low differentiation may be expected along a series of ridge segments, as has been observed by Teixeira et al. (2012).

Presently, it is very difficult to assess the relative influence of metapopulation non-equilibrium dynamics versus the possibility of long-distance *realised* larval dispersal (Island Model) in

producing the lack of differentiation generally observed along ridges and ridge segments worldwide, owing to limited information regarding the realised dispersal capabilities of vent larvae. With respect to the Southern Ocean, even less is known. Exploration of other ridges inhabited by kiwaids, for example, may help reveal the relative importance of temperature, current direction/intensity and ridge topography on larval dispersal. However, despite the promising work on larval longevity thus far (e.g., Shilling and Manahan 1994; Pradillon et al. 2001), more needs to be done to assess larval longevity in experimental conditions equivalent to those of the Southern Ocean.

5.5.1.1 Optimal Dispersal Strategies in Cold Water

As discussed in Chapter 3, given the possibility of cold-water enhanced larval longevity, the production of large, potentially demersal-drifting larvae like those of the kiwaids may be advantageous, if a higher percentage of larvae are entrained along the ridge axis. Observations of gravid females of *Kiwa* sp., with few (tens, rather than hundreds) of very large eggs (> 1 mm diameter) (Leigh Marsh personal communication) suggests that this species is geared towards high investment in relatively few offspring with large yolk food reserves indicative of long-term survival (at least a year) (Sven Thatje et al. manuscript in preparation). Thus, although the progress of individual larvae along a ridge may be slow or intermittent, large food reserves with a cold-induced low metabolism and a high probability of retention within the ridge could make kiwaids optimal dispersers in the Southern Ocean.

Another way of looking at this is in terms of the dispersal kernel, i.e., the probability distribution of larvae in relation to their starting location (as summarized by Levin 2006). The vast majority of lecithotrophic larvae adapted for retention within a patch (e.g. a vent field) will settle close to the natal site, however owing to temporal variations in current strength and direction, for example, a few larvae may travel much, much further, thus maintaining

connectivity between neighbouring patches and even further afield. A dispersal strategy optimised for retention, therefore, can be thought of as a hedge-betting evolutionary strategy 'weighted' towards retention. The 'right tail' on the dispersal kernel distribution thus maintains inter-patch connectivity, i.e., that small fraction of larvae that drift beyond the natal patch.

Kiwaids in tropical regions, such as *Kiwa puravida* that have similarly large eggs (Thurber et al. 2011) (and therefore likely similar larvae) may have a smaller dispersal potential where warmer ambient water temperatures may reduce their longevity owing to higher metabolic rates i.e., reducing the right-tailed skew in the dispersal kernel distribution. The same goes for the two gastropods in this study, but perhaps to a lesser extent and future population genetics studies of these species in the Southern Ocean, as well as kiwaid studies in warmer waters may reveal if this is the case.

If non-equilibrium dynamics within vent metapopulations are a significant means by which effective genetic connectivity is maintained, then dispersal strategies optimised for retention could be advantageous over those of long-distance dispersal, explaining why species with planktotrophic larvae presumed to have a high potential dispersal, appear comparatively rare in vent taxa (Tyler and Young 1999): the cost of such a dispersal capability, is the risk that few larvae will ever land on a vent, having been carried far away from mid-ocean ridges by unfavourable ocean currents (see Chapter 3). Larvae that remain close to the seafloor are far more likely to be entrained along the ridge axis. In short, the birth and death of vents along a ridge does a certain proportion of the 'work' in the long-term maintenance of populations in such environments.

5.5.2 ESR- Kemp Differentiation

5.5.2.1 F_{ST}, R_{ST} & STRUCTURE

The clear signal of differentiation (based on F_{ST}, R_{ST} and STRUCTURE results) between *Lepetodrilus* sp. limpets on the ESR and those in the Kemp Caldera was expected, given similar results of mtDNA analyses in Chapter 3 and the faster mutations rates of microsatellite repeats compared to sequence data. A natural expectation of these faster mutation rates is that there should be greater differentiation than the COI dataset, however in this study, the reverse is the case, with COI F_{ST} greater than 0.45, whereas microsatellite F_{ST} and R_{ST} values are greater than 0.19 and 0.29 respectively (using the seven locus dataset, the 13 locus dataset has even lower values). This discrepancy, where microsatellites appear to understate F_{ST} values between highly diverged populations, is not uncommon owing to the elevated probability of homoplasy in fast-evolving markers such as these (Balloux et al. 2000). R_{ST} is designed to compensate for this (Slatkin 1995), which is why R_{ST} values are higher than F_{ST} values with the seven-locus dataset where suspect loci (under both the IAM and SMM in Lositan) have been removed. However, these values are still far lower than the COI F_{ST} values, perhaps owing to some of the remaining loci still deviating from the SMM to a certain degree (Balloux et al. 2000).

Alternatively, given the possibility that the mtDNA locus may be under selection (Meiklejohn et al. 2007; Galtier et al. 2009), it could be that the COI F_{ST} values are inflated owing to differing selective pressures at the ESR and Kemp. Nevertheless the pattern of differentiation with neutral microsatellite loci bolsters the results from Chapter 3 indicating that despite the short distance between the ESR and Kemp (~ 95 km), gene flow between the two sites is impeded. Given the lack of differentiation along the ESR, such clear differentiation between the ESR and

Kemp limpets is likely the consequence of unfavourable currents, seafloor topography, or the hypothesised absence of intervening vent sites between the two locations. As mentioned in Chapter 3, the depth difference between the two ESR vent fields and the Kemp Caldera (when the caldera sides are taken into account) are in excess of 1,500 m leaving Kemp limpets potentially isolated.

5.5.2.2 ESR-Kemp Long-Term Gene Flow

The results of IMa2 analyses revealed a pattern of unidirectional gene flow from the ESR to the Kemp Caldera since the splitting of a hypothesised ancestral population. While the Isolation with Migration model is constrained within the framework of a population splitting with subsequence gene flow, it has the advantage over other approaches of not requiring the populations to be in drift-migration equilibrium with each other, which is unlikely in a metapopulation context (Marko and Hart 2012). Such a pattern of unidirectional gene flow is consistent with the very limited information regarding the flow of bottom and deep waters in the Scotia Sea (See Chapter 3, Fig. 3.3) indicative of broadly northeasterly or easterly current flow although current measurements over the ESR are presently lacking. Nevertheless, the pattern of unidirectional gene flow could be indicative of a long-term current regime in the region that is largely cross axis in relation to the ESR, with implications for the interpretation of COI diversity and expansion signatures (see Chapter 3 discussion), as different larval dispersal strategies may allow for better retention on the ridge and therefore metapopulations less prone to genetic bottlenecks (e.g., possibly *Kiwa* sp. ESR).

The output of the IMa2 analyses suggesting that the ESR and Kemp populations descended from a much larger population which split sometime in the Plio-Pleistocene is hard to interpret, other than the fact the this splitting precedes the more recent demographic expansion signatures

according to the COI Bayesian Skyline Plots (Chapter 3, Fig. 3.11). If these populations did form part of a larger ancestral population, it could be that major changes in geological activity affecting the number, density and vigour of vents are responsible. Alternatively, the timeframe for this splitting event is contemporary with possible oceanographic changes associated with orbitally forced glacial cycles during the Pleistocene (Diekmann 2007). The estimates for this splitting must be treated with caution owing to the lack of unimodality in the output (Fig. 5.2D). It is likely, therefore, that although trace plots were closely examined during the 'burn-in' phase to ensure no obvious trends before commencing the MCMC runs, the 'burn-in' was still insufficiently long enough with respect to this parameter, although other parameter marginal posterior density plots were smooth and unimodal (Fig. 5.2A-C).

5.5.2.3 ESR-Kemp Contemporary Gene Flow

The results of BayesAss analyses, which examines very recent immigration rates (e.g. in the last couple generations) revealed that immigration rates (as a fraction of the destination population per generation) are more than twice as high from ESR to Kemp than vice versa, which is superficially consistent with the long-term gene-flow estimates. However, as the output of this program suggests gene flow in both directions, it is incompatible with a scenario of purely unidirectional current flow in the short term. The bias in the easterly direction of immigration rates cannot be interpreted as an indicator of an easterly bias in the general current direction, because even if a large proportion of a small population (Kemp) became immigrants in a much larger population (ESR) owing to favourable currents, they would make up a much smaller proportion of that destination population. In the study reported here therefore, even if the currents were predominantly east-west in the short term, inferred immigration rates could still appear to have an easterly bias owing to the inferred size discrepancy of the two limpet populations reported in IMa2.

The presence of three first-generation migrants from the ESR at Kemp, (which account for the 0.401 per generation immigration rate into Kemp from the ESR) is unsurprising given the proximity of the Kemp Caldera to the ESR (~ 95 km) and the size of the ESR in relation to Kemp (both geographically and in population terms) (Table 5.9). Two of these individuals with the highest posterior probability of assignment to ESR, F622_3 and F622_28 also have the COI haplotype H2, which is the second most common haplotype on the ESR, bolstering the possibility that they may indeed be immigrants (see Fig. 3.9, Chapter 3).

However, what is more remarkable is the presence of a possible second-generation migrant (posterior probability of 0.663) at northern E2 vent field from Kemp. This should be treated with caution, however, as by examining the STRUCTURE results without the removal of loci possibly under selection, (Fig. 5.1) this individual appears to have a much smaller probability of being assigned to Kemp, raising the possibility that homoplasy may be confounding the results. The issue of homoplasy, particularly with low numbers of microsatellite loci should not be discounted when using an individual assignment approach such as BayesAss, where individuals could be falsely designated as immigrants. Coalescent-based genealogy sampling approaches such as IMa2 should be comparatively more robust to the confounding effect of homoplasy as it incorporates the stepping-stone mutational model to simulate the coalescing of genealogies backwards in time.

Nevertheless, if this result is taken at face value then it suggests, at least in the recent past, that currents in the region are more complex than the long-term gene flow estimates might suggest. It should be noted, however, that inferences of past and present current regimes based on long and short-term gene flow estimates must be treated with caution, given that the association between the two is often unclear (Hellberg 2009).

5.5.3 Diversity & Demography

Given the uncertainty in microsatellite mutational mechanisms (Ellegren 2004), the wide variance in marker numbers and characteristics between different taxa (Tóth et al. 2000) and the recent evidence of transposable elements in the microsatellite flanking regions of some groups of animals, which probably affects their evolution (Bailie et al. 2010; McInerney et al. 2010), interspecies comparison of microsatellite diversity is not possible. Comparisons of microsatellite diversity are, however, appropriate within species using the same loci. Given that E2 and E9 are statistically indistinguishable for all three species, the only appropriate comparison, therefore, is between the ESR vent limpets and those from the Kemp Caldera.

5.5.3.1 Mismatch with COI

In contrast to the results of the COI analyses in Chapter 3, the majority of the ESR microsatellite loci are more diverse (greater mean allelic richness and expected heterozygosity) than those of the Kemp limpets, resulting in IMa2 estimates for θ being several times larger than that of the Kemp population (Table 5.8). These results more closely meet the expectations of the on-site observations of limited venting and likely hydrographic isolation at the Kemp Caldera and that a lack of differentiation along the ESR is consistent with panmixia within a population spanning > 400 km of ridge. The fact that allelic richness at Kemp was only higher than either E2 or E9 limpets in one out of the seven loci after quality control (five out of 14 before quality control) reveals the importance of using multilocus datasets when inferring population traits.

This mismatch between the COI and microsatellite datasets on the ESR may be the consequence of different mutation rates and effective population sizes. The mtDNA genome may have had insufficient time to recover its diversity since a demographic bottleneck, in contrast with microsatellites, whose faster mutation rates (Schlötterer 2000) ensure a shorter time lag on the

recovery of diversity with demographic expansion. In addition, as the mtDNA genome represents an effective population size one fourth that of the nuclear genome, a demographic bottleneck would have a greater effect on the former, further depressing diversity in the long term. Alternatively, the ESR COI diversity may be depressed because the genetic bottleneck was the product of a selective sweep, in which case, only the microsatellite dataset truly reflects population size. Although the supposed neutrality of microsatellite markers is questioned (Li et al. 2002; Ellegren 2004), the reduced dataset after the removal of loci deemed under possible selection engenders greater confidence that the diversity patterns presented here reflect present-day and recent demography.

5.5.3.2 Bottleneck Analyses

The results of BOTTLENECK analyses, showing a significant pattern of $H_{eq} > H_e$ across all three species and at all locations using the SMM, are consistent with recent demographic expansion (Cornuet and Luikart 1996), which as with many other results in this chapter, echo the results of the COI dataset in Chapter 3. This pattern is not quite as strong, however, when more nuanced models such as the 95% and 70% TPM are used, particularly with the peltospirids and the Kemp Caldera limpets. Nevertheless, if these results are taken at face value, then they are consistent with the pattern of COI diversity revealed in Chapter 3 being the consequence of demographic change and not selective sweeps, although these results cannot reject that possibility outright.

These results indicating demographic change in both COI (excluding the possibility of selection) and microsatellites are similar to those of Teixeira et al. (2012) on *Rimicaris exoculata* and may ultimately reflect the short (microsatellites) and longer-term (mtDNA) demographic instability expected of metapopulations in changeable environments where non-

equilibrium dynamics prevail.

5.5.4 Study Limitations

Aside from the limitations associated with low sampling effort (number of sample sites) detailed in Chapter 3, which cannot be addressed without the further discovery and sampling of hydrothermal vents in the region, this microsatellite study has, to a certain extent, addressed some of the limitations of the COI study in Chapter 3, notably the use of single-locus data to make inferences about connectivity and demographic history and the use of protein-coding sequences that may be influenced by selection. The development and implementation of multiple un-linked microsatellite loci has allowed the combination of multiple independent data sources to verify the patterns of differentiation revealed in Chapter 3 and the ability to screen loci for possible selection has improved confidence in the presumed neutrality of these markers for the inference of recent demography. However, the different timescales that these markers are likely to address owing to the presumed faster rate of evolution means that microsatellites cannot be used to confirm without doubt whether the patterns of diversity in the COI dataset reflect the influence of selection or demographic history, the way that using multiple nuclear sequence data can (e.g. Plouviez et al. 2010).

One advantage with using DNA sequence data over microsatellites is that compared to the former, the mutational mechanisms involved with microsatellite evolution are still relatively unclear (Ellegren 2004) and deviations from the SMM, may produce spurious results in some cases, such as in underestimating genetic differentiation when using F_{ST} and R_{ST} (Balloux et al. 2000), which is in part addressed by using assignment-based methods such as STRUCTURE, for example. The removal of loci deemed under selection using the SMM in Lositan has the added advantage of weeding out loci that deviate from the SMM more than other loci. One possible issue associated with the weeding out of many loci in the case of the limpets is the

potential loss of statistical power in detecting population structure. Little can be done about this without the discovery of new loci, or the less 'stringent' use of Lositan, however the larger 13 locus dataset results in STRUCTURE indicates that this would not make any difference. Perhaps the discovery and implementation of many single nucleotide polymorphisms (SNPs) may add resolution in the future.

The sample sizes of < 50 individuals per site for all three species are on the small side compared to those recommended to optimise the statistical power of microsatellite loci in large populations (e.g., ~ 50-100 or more) (Ruzzante 1998; Kalinowski 2004), although they are more than twice the size of the smallest sample sizes reported in recent vent population genetics studies (< 20) (Fusaro 2008; Thaler et al. 2011; Teixeira et al. 2012b). More recent analyses however suggest that in most cases, sample sizes of 25-35 individuals are generally enough to reflect 'true' allele frequencies and pairwise F_{ST} values across a range of heterozygosities and numbers of loci (Hale et al. 2012). Given the results present here and in Chapter 3, any significant AMOVA F_{ST} or R_{ST} values that may result from a doubling of the sampling size are still likely to be very low (near zero), with the main talking points of the discussion section in both chapters remaining unchanged.

5.6 Conclusions

This is the first ever implementation of microsatellites to investigate the population genetics of hydrothermal vent-endemic fauna in the Southern Ocean. No evidence of genetic differentiation was found for a kiwaid crab, *Kiwa* sp., a peltospirid gastropod, and a lepetodrillid limpet, *Lepetodrilus* sp., between the E2 and E9 vent fields on the ESR, which are ~ 440 km apart, consistent with panmixia. This lack of apparent genetic structure matches levels of differentiation found for species of vent fauna at similar scales on the EPR, although the potentially highly limited dispersal capability of kiwaid larvae makes these results surprising. Dispersal may be assisted by cold-water arrested development of larvae in combination with high retention along the ridge axis or alternatively, high apparent connectivity may be the consequence of non-equilibrium dynamics between vent fields within a larger metapopulation, depressing genetic differentiation on the ridge, or a combination of the two. Evidence of recent demographic change for all three species is consistent with a model of demographic instability within a metapopulation framework. Despite the high apparent connectivity of the limpets along ~ 440 km of the ESR, strong differentiation exists between limpets on the ESR and those found in the Kemp Caldera, ~ 95 km to the east, perhaps owing to the topographical isolation of the vents within the caldera, unfavourable currents or a lack of venting along the intervening sea floor. Long-term gene flow estimates based on IMa2 analyses of unidirectional gene flow from the ESR to Kemp are consistent with a hypothesised easterly or northeasterly current regime in the region, although BayesAss estimates of recent bidirectional gene flow suggest that this model may be too simplistic and that the current regime in the region is more complex.

CHAPTER 6

Concluding Remarks

6.1 Key Findings

6.1.1 Kiwaid Phylogenetics & Biogeography

The research portion of this thesis commenced with the creation of the first phylogeny of the exclusively vent and seep-endemic anomuran squat lobster family Kiwaidae (yeti crabs), with the aim of tracing the evolutionary history of this clade within the superfamily Chirostyloidea and in doing so, to investigate the provenance of yeti crabs collected from the East Scotia Ridge (ESR) on the expedition JC042, part of the Chemosynthetic Ecosystems of the Southern Ocean (ChEsSO) research program. To achieve this, nine different gene regions were sequenced across 23 taxa – the largest number of gene sequence segments used in an anomuran phylogenetic study thus far.

6.1.1.1 Kiwaid Origins

Phylogenetic trees produced herein confirm the monophyly of the superfamily Chirostyloidea, but unlike previous studies (Ahyong et al. 2011; Schnabel et al. 2011a; Tsang et al. 2011), these results suggest the monophyly of Kiwaidae-Chirostylidae, which is supported by their similar larval morphology.

Dating with the aid of fossils indicates that the chirostyloid families originated in the early-mid Cretaceous, although Kiwaidae and Chirostylidae appear to have only radiated later in the Cenozoic. Within Kiwaidae, the basal split between the cold seep-dwelling *Kiwa puravida* lineage and a vent-endemic clade 22-7-43.7 Ma could indicate a seep-to-vent evolutionary trajectory for the genus, however the recent discovery of a kiwaid at vents on the EPR may cast

doubt on this hypothesis (Xinming Liu, personal communication). The East Pacific location of the two basal species, *K. puravida* and *K. hirsuta*, along with the Alaskan location of the proto-kiwaid fossil *Pristinaspina gelasina*, suggests that this clade originated in the Northeast Pacific. Within the Southern Hemisphere vent-endemic clade, the basal split is between *Kiwa hirsuta*, found on the Pacific-Antarctic Ridge, and kiwaids found on the East Scotia Ridge (ESR) in the Atlantic sector of the Southern Ocean and the Southwest Indian Ridge (SWIR) in the Indian Ocean.

A divergence date estimate of 13.4-25.9 Ma between the Pacific and non-Pacific lineages is consistent with Kiwaidae spreading into the Atlantic sector of the Southern Ocean via a newly-opened Drake Passage, possibly along a near-continuous ridge connection between the Pacific Ocean and the Scotia Sea, which subsequently broke up leading to divergence (vicariance). Alternatively, this date estimate is consistent with a hypothesised Miocene onset of the Antarctic Circumpolar Current (ACC), with kiwaids on the unexplored Pacific-Antarctic Ridge (P-AR) delivering larvae to the Scotia Sea. Further exploration of this region and the Chile Rise will be needed to determine this. A recent divergence between the non-Pacific kiwaids (~ 1.5 Ma) rules out vicariance, however, with oceanographic changes in the region affecting gene flow suggested instead.

The Cenozoic radiation of Kiwaidae adds to the growing list of chemosynthetic-associated megafauna that appear to have radiated during the Eocene or more recently (Vrijenhoek 2013). It seems therefore, that such taxa are not 'living fossils' but may be prone to extinction events in the deep sea, such as the Palaeocene-Eocene Thermal Maximum (PETM) that caused widespread anoxia in the deep sea (Vrijenhoek 2013).

6.1.1.2 Speculations

The recent discovery of kiwaids on the EPR (Wang et al. 2013) is surprising given it is the most intensively explored mid-ocean ridge in the world (Van Dover 2000) indicating that these particular kiwaids may have a very limited range. Although the precise evolutionary relationship between this species and the other kiwaids is unclear, the possibility that kiwaids may once have been more widespread along the EPR must be considered owing to their hypothesised Northern Hemisphere origins.

If kiwaids were indeed once more widespread at East Pacific vents, the reason why they may have gone extinct along large stretches of ridge is unclear. One possibility is that the larval morphology of kiwaids, with their abbreviated lecithotrophic development and large yolk reserves (Sven Thatje et al. manuscript in preparation), although indicative of longevity, may also result in a poor dispersal capability (large, heavy demersal drifters) in the absence of strong, favourable currents: geological or hydrographic changes along the EPR could have led to the isolation of kiwaids and their extinction along vast sections of the ridge. Although the lack of differentiation amongst ESR kiwaids would seem to indicate a 'good' dispersal capability, this capability may be cold-water enhanced (see discussions in Chapters 3 and 5). Metapopulation simulations by Jollivet et al. (1999) investigating the dispersal of *Alvinella pompejana* along the EPR suggests that metapopulations may be easily prone to extinction if connectivity is only slightly reduced. A small decline in connectivity along the EPR could have resulted in a precipitous decline in population stability for the kiwaids, leading to their widespread extinction and subsequent isolation. The assessment of kiwaid dispersal potential relative to other species should be testable as more sites supporting kiwaids are discovered globally.

6.1.2 Population Genetics

The second portion of this thesis (Chapters 3-5) is concerned with the population genetics of three undescribed species found at vents in the Scotia Sea: a kiwaid crab *Kiwa* sp., a peltospirid gastropod and a lepetodrillid limpet *Lepetodrilus* sp.. Two types of genetic marker were used: the mtDNA cytochrome c oxidase subunit 1 (COI) gene, which provides sequence information relating to the recent female population history and the faster-evolving co-dominant and theoretically neutral microsatellite markers, representative of the whole population (Ellegren 2004).

6.1.2.1 Differentiation

Despite the differences between the two types of marker, the results from Chapters 3 and 5 were very similar. Both COI and microsatellite datasets reveal no differentiation for all three species between the E2 and E9 vent fields across ~ 440 km the East Scotia Ridge (ESR), as has been observed for many species at similar scales along the EPR (Vrijenhoek 2010) where differentiation along whole ridge segments is generally low. In contrast, both COI and microsatellites reveal strong differentiation between *Lepetodrilus* sp. limpets on the ESR and those retrieved from the Kemp Caldera only ~ 95 km further east, a site lacking in kiwaids and peltospirids entirely. This differentiation between limpet populations may be because of the difference in depth between the ridge (~ 2500 m depth) and the caldera (~ 1500 m depth, with the caldera rim at ~ 800 m depth).

Given the low differentiation of populations at scales of ~ 1000 km or less on the EPR (Coykendall et al. 2011) this lack of differentiation of the ESR is perhaps unsurprising, although the appropriateness of comparing an extensively surveyed fast-spreading ridge (Van Dover

2000) with a medium-spreading ridge (Livermore 2006) where the full extent of venting (not to mention current regime) is unknown, is questionable at this stage. Nevertheless, the lack of kiwaid differentiation along the ESR is noteworthy, because initial morphological examinations of the larvae (Sven Thatje et al. manuscript in preparation) suggest that this animal should have a very limited range of dispersal owing to the immense size of its larvae, which presumably results in negative buoyancy.

Taken at face value then, the lack of differentiation along the ESR is indicative of panmixia where larval connectivity between vent fields is so high as to render the entire ridge a single population. With the kiwaids especially, this genetic picture is hard to marry with its larval morphology and consequently two possibilities arise:

1. If kiwaids along the ESR are part of a panmictic population, then perhaps larval transport is enhanced by the low ambient temperatures (< 0 ˚C), which could retard development. Any disadvantages in dispersal for larvae optimized for retention along a ridge (heavy, demersal drifting), may be significantly reduced in such an environment, with large yolk reserves greatly enhancing longevity, although discontinuities could present a greater problem and may explain why kiwaids (and the peltospirids) are absent from the Kemp Caldera, whereas the limpets that produce smaller larvae are not.
2. The lack of differentiation for all three species reflects the dominance of non-equilibrium processes within a metapopulation of vent colonies.

The two possibilities are not mutually exclusive of course and both may be operating. In the future it may be possible to examine isolation by distance (IBD) of species found above and below the polar front on the SWIR or the P-AR along with more laboratory experiments on larval development to examine to role of temperature in dispersal. The importance of non-equilibrium metapopulation processes in depressing differentiation is harder to examine in the field, although improving the understanding of how larval longevity, hydrography and sea floor

topography combine to result in the actual dispersal capability of a given species is key and will require the integration of various methods, e.g., ocean current modelling, trapping and collecting larvae and ideally, genetically identifying larval cohorts as well as the modelling of metapopulation dynamics on genetic diversity.

6.1.2.2 Demography

A strong reason for suspecting that non-equilibrium processes may dominate in vent populations is the evidence of recent demographic expansion commonly found in mtDNA sequence data (Vrijenhoek 2010). Metapopulations are liable to fluctuate in size over time as a consequence of the stochastic birth and death of colonies and a similar pattern was found with the COI data presented in this thesis. Previous work on EPR fauna suggests that eruptive events resulting in the simultaneous extinction of many vent fields on the southern portion of the ridge (SEPR) may be responsible for a COI bottleneck signature across several species (Plouviez et al. 2009).

All three species in this study had COI diversity patterns consistent with recent genetic bottlenecks, although not occurring at the same time, ruling out a mass eruptive event causing a simultaneous population decline across all three species. The differences in bottleneck ages are reflected in diversity: the ESR limpets have the most recent bottleneck signature and are the least diverse, despite being numerically dominant on the vent fields, whilst the less numerous kiwaids are the most diverse with the most ancient bottleneck. To account for this, differences in connectivity over time between the species owing to disparities in dispersal strategy have been proposed. Lepetodrillid limpets produce small larvae (Tyler et al. 2008) compared to the other two study species and may be sensitive to a lack of larval retention on the ESR (owing to greater buoyancy compared to the other species), against a backdrop of stochastic fluctuations

in vent activity and current regime over time. This could also explain why COI diversity was higher for the limpets in the Kemp Caldera, as the high walls of the Caldera may help retain larvae.

Alternatively, selective sweeps may be responsible for the bottleneck signatures in the mtDNA datasets (Bazin et al. 2006). While this possibility cannot be rejected outright, it seems unlikely that the patterns of COI diversity presented here do not to some extent reflect demography, because a selective sweep should not result in a bimodal mismatch distribution, as is the case with the ESR kiwaids. In addition, evidence of recent demographic expansion in the theoretically neutral microsatellite datasets in Chapter 5 bolsters the notion that these populations experienced demographic fluctuations inline with the expectations of vent metapopulation instability.

6.1.2.3 ESR-Kemp Limpet Gene Flow Estimates

The results of IMa2 analyses, which estimated long-term immigration rates for limpets between the ESR and the Kemp Caldera, suggests an historical gene flow from ESR to Kemp, but not vice versa, consistent with a hypothesised broadly easterly or northeasterly current flow in the Scotia Sea. However, BayesAss, which examines recent migration (last couple generations) indicates that there may have be some recent gene flow in both directions, although this may be the consequence of homoplasy exaggerating the influence of the Kemp Caldera population on the diversity of ESR limpets.

The possibility that currents have been broadly unidirectional, flowing from west to east across the axis of spreading on the ESR could explain both why limpets, but not the other two study species, are found in the Kemp Caldera and also why limpets on the ESR have low COI diversity compared to the other two species. The limpet production of small, buoyant larvae

could result in periodic reductions in connectivity (and hence diversity) along the ESR owing to stochastic changes in ridge activity against a setting of unfavourable cross axis currents leading to relatively poor retention on the ridge compared to the kiwaids and peltospirids. The other species with less buoyant larvae (and greater food stores) may be less prone to poor retention and connectivity is retained. Although such theorised demographic declines should also reduce microsatellite diversity, their faster mutation rates may allow the microsatellite diversity to keep better pace with the demographic recovery, with a longer time lag for slower evolving markers like COI. This very same larval buoyancy that may limit connectivity over time for the limpets on the ESR may also allow them to inhabit hydrographically isolated sites like the Kemp Caldera that are shallower than the ESR, but down current of the ridge.

6.1.3 Synthesis and Broad Conclusions

6.1.3.1 Genetic Markers

The overarching theme of this project, as the title suggests, is both the evolution and population genetics of deep-sea chemosynthetic fauna in the Scotia Sea, which is to say, that this project is concerned with the integration of phylogenetics and population genetics to generate a coherent picture of the long and short-term processes shaping the vent communities discovered in the Scotia Sea. This has been achieved by utilizing a variety of genetic markers, from the slowly-evolving nuclear genes used to reveal and date the early divergences within Chirostyloidea, to faster-evolving mitochondrial genes, used to reveal and date the divergences within the kiwaid Southern Hemisphere vent-endemic clade, and finally to fast-evolving markers such as the mtDNA COI and microsatellites, used to determine the extent and nature of kiwaid populations in the Scotia Sea.

6.1.3.2 Scientific Contribution

With respect to *Kiwa* sp. ESR, perhaps the major contribution of this study in terms of biogeography is evidence for the Pacific ancestry of Kiwaidae, their subsequent spread to the Scotia Sea and their divergence from their Pacific counterparts over a time period consistent with the evolution of spreading ridges through the Drake Passage in keeping with the predictions of Tunnicliffe and Fowler (1996), although an ACC mediated long-distance transport of larvae to the Scotia Sea from the southern P-AR cannot be discounted. Phylogenetic analysis of the peltospirid gastropod suggests that it too has a Pacific affinity (Chen et al., submitted) and preliminary phylogenetics support the same for the neolepadine barnacles as well (Rogers et al. 2012). However, the results of Chapter 2 also reveal the limits of vicariance, as kiwaids collected from the Southwest Indian Ridge (SWIR) are divergent from those at the ESR without there being any evidence for changes to the intervening ridges.

At the shorter timescale, the population genetics results are consistent with the overall patterns found elsewhere, e.g., low differentiation at equivalent scales and evidence of recent demographic change, compatible with the expectations of metapopulations under non-equilibrium conditions. However, the differential bottleneck ages in the COI dataset of the three species, if not fully the consequence of selective sweeps, may reflect life history and dispersal strategy against the backdrop of changing vent activity and current regime over time. Previous explanations of why many species have bottleneck signatures along a ridge have centred on the idea of large-scale events, such as large eruptive episodes (Plouviez et al. 2009) resulting in simultaneous population declines and subsequent recoveries. Instead, such bottleneck events may occur with different periodicities for different species along the same ridge owing to the interaction between their ecology and the nature of the change.

6.1.3.3 Wider Context

In the wider biogeographical context then, the very survival of a species between a series of vent fields could depend to a certain degree on how effective their dispersal is when conditions change (e.g., vent ephemerality, topography, currents or temperature) and the mix of species within a biogeographical province - and ecological niche roles they appear to inhabit – are only a brief snapshot of dynamic processes over different timescales, where species disappear, reappear or become more or less numerically dominant relative to others. Kiwaids may be good at retaining larvae on a ridge axis for example, even if most larvae do not travel very far, which might allow them to be dominant in some regions, but not others relative to different species, depending on the number, longevity and density vent fields, regional hydrography (currents, temperature), ridge topography (presence or absence of axial valleys) and the number and nature of ridge discontinuities. Kiwaids may once have been present along much of the EPR, for example, but evidently no longer and had this region been sampled during that period, the delineation of biogeographic provinces might have been very different.

Ultimately, the presence of a species, genus or family at vents in a particular region, therefore, is dependent on where and when the taxon in question originated (evolutionary history) and the effects of long-term processes, such as plate tectonics leading to vicariance. But the continued survival of a species in a given region may be more reliant on the resilience of its metapopulation(s) to environmental changes on a range of timescales: from the on-going stochastic birth and extinction of vent fields on a decadal/centennial scale, to oceanographic changes reflecting climate change over thousands or millions of years and changes in ridge activity over similar timescales.

6.2 Limitations

Given real world constraints (money and time), it has not been possible to conduct a full comparative analysis (phylogenetics and population genetics) between all of the species featured within this study. Work is currently underway to elucidate the evolutionary history of the peltospirid gastropod and *Lepetodrilus* sp. ESR, and perhaps in the near future it will be possible to perform a comparative phylogeographic analysis of all the dominant vent megafauna in the Scotia Sea.

Although the microsatellite dataset revealed evidence of demographic change, lack of information concerning mutation rates and uncertainty about mutational mechanisms precludes any dating of genetic bottlenecks and so microsatellites cannot be used to ascertain if the COI dataset bottlenecks likely reflect demographic history or the influence of selection. Ideally, a variety of nuclear genes for which reasonable estimates of substitution rates exist could be sequenced in the future. Similar patterns of diversity to the mtDNA dataset would improve confidence in using COI to infer recent demographic history.

A specific limitation with the use of microsatellites is the issue of subjectivity in genotyping, such that consistency with the genotyping machine as well as with the scoring individual is paramount. Combining data from multiple studies is not possible, as with sequence data, meaning these specimens would have to be re-genotyped if they were to be incorporated in any future study. This is a major disadvantage compared with the use of nuclear coding genes or single nucleotide polymorphisms (SNPs), where the data produced in one study can be integrated into another.

Perhaps the principle limitation with this study, compared to other vent population genetics studies is the sampling effort. For two of the three species, only two sites were sampled.

Ultimately, this is because the business of finding and sampling vents is exceptionally challenging in the prevailing conditions of the Southern Ocean (Rogers et al. 2012). Indeed, until recently, some had considered sampling at such high latitudes as improbable (Macpherson et al. 2005) and the fact that any data was collected at all is a testament to the skill and experience of the maritime and technical crews of the ship RRS *James Cook* and the ROV *ISIS* respectively, as well as the principle scientists involved (Rogers et al. 2012).

6.3 Future Directions

6.3.1 Biogeography

Given the principle limitation of sampling effort, a major improvement over this study would be to explore more sites within the Scotia Sea and beyond. Exploration of the southern reaches of the Mid-Atlantic Ridge (MAR) and the Pacific-Antarctic Ridge, as well the Southwest, Central and Southeast Indian Ridges will fill in knowledge gaps of the biogeography and evolution of Kiwaidae by determining the range extent of the family and its constituent species.

In particular with respect to the non-Pacific kiwaid lineage, as well as the peltospirid gastropods, the exploration of South Sandwich Islands (SSI), the American-Antarctic Ridge and the SWIR will help determine what factors have led to the divergence of the ESR and SWIR variants. Given the close genetic affinity between *Lepetodrilus* sp. and *L. atlanticus* (Katrin Linse in preparation), exploration of the southern MAR and the Bouvet Triple Junction may give clues as to how they diverged.

6.3.2 Population Genetics

As already mentioned the present three sites included in this study almost certainly do not represent the full range of the study species and more exploration of the SSI and ridges extending eastwards will be essential in determining their full extent. With the addition of more sites both in the Southern Ocean and beyond in concert with the microsatellite loci designed herein, it may be possible to investigate further the effect of the ACC and cold temperatures in enhancing dispersal in the Southern Ocean. The level of differentiation across ridge

discontinuities will add insight to the comparative dispersal capabilities of the study species as well.

In the future, with the discovery of more vent sites as well as the falling cost in genome-wide sequencing, such as RADSequencing (Davey and Blaxter 2010), the development of SNP libraries will bring vent population genetics into the population genomics era (Luikart et al. 2003). The advantages over microsatellites are that the mutation model is understood more fully (Brito and Edwards 2009), there is no need for calibration and as SNPs mutate more slowly than microsatellites, the probability of encountering homoplasy is lowered (Brito and Edwards 2009). Furthermore, as hundreds or thousands of SNP loci can be detected across the genome, the dataset will more likely reflect the influence of demographic processes, such as gene flow, inbreeding, population growth, or bottlenecks on the entire genome (Luikart et al. 2003).

References

Abdelkrim, J, BC Robertson, JAL Stanton and NJ Gemmell (2009). Fast, cost-effective development of species-specific microsatellite markers by genomic sequencing. BioTechniques **46**(3): 185-192.

Adams, DK, DJ McGillicuddy, L Zamudio, AM Thurnherr, X Liang, O Rouxel, CR German and LS Mullineaux (2011). Surface-generated mesoscale eddies transport deep-sea products from hydrothermal vents. Science **332**(6029): 580.

Adams, RI, KM Brown and MB Hamilton (2004). The impact of microsatellite electromorph size homoplasy on multilocus population structure estimates in a tropical tree (*Corythophora alta*) and an anadromous fish (*Morone saxatilis*). Molecular Ecology **13**(9): 2579-2588.

Ahyong, ST (2009). New species and new records of hydrothermal vent shrimps from New Zealand (Caridea: Alvinocarididae, Hippolytidae). Crustaceana **82**: 775-794.

Ahyong, ST, K Baba, E MacPherson and G Poore (2010). A new classification of the Galatheoidea (Crustacea: Decapoda: Anomura). Zootaxa **2676**: 57-68.

Ahyong, ST and D O'Meally (2004). Phylogeny of the Decapoda reptantia: resolution using three molecular loci and morphology. Raffles Bulletin of Zoology **52**(2): 673-693.

Ahyong, ST, K Schnabel and E Maas (2009). Anomuran phylogeny: new insights from molecular data. Crustacean Issues **18**.

Ahyong, ST, KE Schnabel and E Macpherson (2011). Phylogeny and fossil record of marine squat lobsters, CSIRO Publishing.

Allen, C, J Copley and P Tyler (2001). Lipid partitioning in the hydrothermal vent shrimp *Rimicaris exoculata*. Marine Ecology **22**(3): 241-253.

Amon, DJ, AG Glover, H Wiklund, L Marsh, K Linse, AD Rogers and JT Copley (2013). The discovery of a natural whale fall in the Antarctic deep sea. Deep Sea Research Part II: Topical Studies in Oceanography **92**: 87-96.

Antao, T, A Lopes, R Lopes, A Beja-Pereira and G Luikart (2008). LOSITAN: a workbench to detect molecular adaptation based on a Fst-outlier method. BMC bioinformatics **9**(1): 323.

Arellano, S and C Young (2009). Spawning, development, and the duration of larval life in a deep-sea cold-seep mussel. The Biological Bulletin **216**(2): 149.

Ashton, GV, MI Stevens, MC Hart, DH Green, MT Burrows, EJ Cook and KJ Willis (2008). Mitochondrial DNA reveals multiple Northern Hemisphere introductions of *Caprella mutica* (Crustacea, Amphipoda). Molecular Ecology **17**(5): 1293-1303.

Audzijonyte, A and RC Vrijenhoek (2010). When gaps really are gaps: statistical phylogeography of hydrothermal vent invertebrates. Evolution **64**(8): 2369-2384.

Baba, K (2004). *Uroptychodes*, new genus of Chirostylidae (Crustacea : Decapoda : Anomura), with description of three new species. Scientia Marina **68**(1): 97-116.

Baba, K (2005). Deep-sea chirostylid and galatheid crustaceans (Decapoda: Anomura) from the Indo-Pacific, with a list of species. Galathea Report **20**: 5-317.

Baba, K, Y Fujita, IS Wehrtmann and G Scholtz (2011). Developmental biology of squat lobsters, CSIRO Publishing.

Bachraty, C, P Legendre and D Desbruyeres (2009). Biogeographic relationships among deep-sea hydrothermal vent faunas at global scale. Deep-Sea Research Part I: Oceanographic Research Papers **56**(8): 1371-1378.

Baco, AR, AA Rowden, LA Levin, CR Smith and DA Bowden (2010). Initial characterization of cold seep faunal communities on the New Zealand Hikurangi margin. Marine Geology **272**(1-4): 251-259.

Baco, AR, CR Smith, AS Peek, GK Roderick and RC Vrijenhoek (1999). The phylogenetic relationships of whale-fall vesicomyid clams based on mitochondrial COI DNA sequences. Marine Ecology Progress Series **182**: 137-147.

Bailie, DA, H Fletcher and PA Prodohl (2010). High incidence of cryptic repeated elements in microsatellite flanking regions of galatheid genomes and its practical implications for molecular marker development. Journal of Crustacean Biology **30**(4): 664-672.

Baker, ET, GJ Massoth, K-i Nakamura, RW Embley, CE de Ronde and RJ Arculus (2005). Hydrothermal activity on near-arc sections of back-arc ridges: results from the Mariana Trough and Lau Basin. Geochemistry, Geophysics, Geosystems **6**(9).

Ballard, JWO, RG Melvin, SD Katewa and K Maas (2007). Mitochondrial DNA variation is associated with measurable differences in life-history traits and mitochondrial metabolism in *Drosophila simulans*. Evolution **61**(7): 1735-1747.

Balloux, F, H Brunner, N Lugon-Moulin, J Hausser and J Goudet (2000). Microsatellites can be misleading: an empirical and simulation study. Evolution **54**(4): 1414-1422.

Bandelt, H-J, P Forster and A Röhl (1999). Median-joining networks for inferring intraspecific phylogenies. Molecular Biology and Evolution **16**(1): 37-48.

Barker, PF (2001). Scotia Sea regional tectonic evolution: implications for mantle flow and palaeocirculation. Earth-Science Reviews **55**(1-2): 1-39.

Barker, PF, LA Lawver and RD Larter (2013). Heat-flow determinations of basement age in small oceanic basins of the southern central Scotia Sea. Geological Society, London, Special Publications **381**.

Bates, AE (2006). Population and feeding characteristics of hydrothermal vent gastropods along environmental gradients with a focus on bacterial symbiosis hosted by *Lepetodrilus fucensis* (Vetigastropoda), University of Victoria. **Doctor of Philosophy**.

Bates, AE (2007). Feeding strategy, morphological specialisation and presence of bacterial

episymbionts in lepetodrilid gastropods from hydrothermal vents. Marine Ecology-Progress Series **347**(2007): 87-99.

Bates, AE (2008). Size-and sex-based habitat partitioning by *Lepetodrilus fucensis* near hydrothermal vents on the Juan de Fuca Ridge, Northeast Pacific. Canadian Journal of Fisheries and Aquatic Sciences **65**(11): 2332-2341.

Bazin, E, S Glemin and N Galtier (2006). Population size does not influence mitochondrial genetic diversity in animals. Science **312**(5773): 570.

Beaumont, MA and RA Nichols (1996). Evaluating loci for use in the genetic analysis of population structure. Proceedings of the Royal Society of London. Series B: Biological Sciences **263**(1377): 1619-1626.

Beerli, P (2004). Effect of unsampled populations on the estimation of population sizes and migration rates between sampled populations. Molecular Ecology **13**(4): 827-836.

Beerli, P (2006). Comparison of Bayesian and maximum-likelihood inference of population genetic parameters. Bioinformatics **22**(3): 341.

Beerli, P. (2010). "Violation of assumptions, or are your migration estimates wrong when the populations split in the recent past?", from the website blog: http://popgen.sc.fsu.edu/Migrate/Blog/Blog.html.

Black, M, R Lutz and R Vrijenhoek (1994). Gene flow among vestimentiferan tube worm (*Riftia pachyptila*) populations from hydrothermal vents of the eastern Pacific. Marine Biology **120**(1): 33-39.

Black, MB, A Trivedi, PAY Maas, RA Lutz and RC Vrijenhoek (1998). Population genetics and biogeography of vestimentiferan tube worms. Deep-Sea Research Part II: Topical Studies in Oceanography **45**(1-3): 365-382.

Blair, C and RW Murphy (2011). Recent trends in molecular phylogenetic analysis: where to next? Journal of Heredity **102**(1): 130-138.

Blueweiss, L, H Fox, V Kudzma, D Nakashima, R Peters and S Sams (1978). Relationships between body size and some life history parameters. Oecologia **37**(2): 257-272.

Boehme, L, MP Meredith, SE Thorpe, M Biuw and M Fedak (2008). Antarctic Circumpolar Current frontal system in the South Atlantic: monitoring using merged Argo and animal-borne sensor data. Journal of Geophysical Research **113**(C9): C09012.

Bracken, HD, A Toon, DL Felder, JW Martin, M Finley, J Rasmussen, F Palero and KA Crandall (2009). The decapod tree of life: compiling the data and moving toward a consensus of decapod evolution. Arthropod Systematics & Phylogeny **67**(1): 99-116.

Breitsprecher, K and DJ Thorkelson (2009). Neogene kinematic history of Nazca-Antarctic-Phoenix slab windows beneath Patagonia and the Antarctic Peninsula. Tectonophysics **464**(1-4): 10-20.

Brito, PH and SV Edwards (2009). Multilocus phylogeography and phylogenetics using sequence-based markers. Genetica **135**(3): 439-455.

Brooker, AL, JAH Benzie, D Blair and JJ Versini (2000). Population structure of the giant tiger prawn *Penaeus monodon* in Australian waters, determined using microsatellite markers. Marine Biology **136**(1): 149-157.

Brooks, JM, MC Kennicutt, RR Fay, TJ McDonald and R Sassen (1984). Thermogenic gas hydrates in the Gulf of Mexico. Science **225**(4660): 409-411.

Buckeridge, JS (2000). *Neolepas osheai* sp. nov., a new deep-sea vent barnacle (Cirripedia : Pedunculata) from the Brothers Caldera, south-west Pacific Ocean. New Zealand Journal of Marine and Freshwater Research **34**(3): 409-418.

Bucklin, A (1988). Allozymic variability of *Riftia pachyptila* populations from the Galapagos Rift and 21˚ N hydrothermal vents. Deep Sea Research Part A: Oceanographic Research Papers **35**(10-11): 1759-1768.

Cabezas, P, P Bloor, I Acevedo, C Toledo, M Calvo, E Macpherson and A Machordom (2009). Development and characterization of microsatellite markers for the endangered anchialine squat lobster *Munidopsis polymorpha*. Conservation Genetics **10**(3): 673-676.

Campbell, KA (2006). Hydrocarbon seep and hydrothermal vent paleoenvironments and paleontology: past developments and future research directions. Palaeogeography Palaeoclimatology Palaeoecology **232**(2-4): 362-407.

Castresana, J (2000). Selection of conserved blocks from multiple alignments for their use in phylogenetic analysis. Molecular Biology and Evolution **17**(4): 540-552.

Cavanaugh, CM (1983). Symbiotic chemoautotrophic bacteria in marine invertebrates from sulphide-rich habitats. Nature **302**(5903): 58-61.

Chablais, J, R Feldmann and C Schweitzer (2011). A new Triassic decapod, *Platykotta akaina*, from the Arabian shelf of the northern United Arab Emirates: earliest occurrence of the Anomura. Paläontologische Zeitschrift **85**(1): 93-102.

Chanton, J, C Martens and C Paull (1991). Control of pore-water chemistry at the base of the Florida escarpment by processes within the platform. Nature **349**(6306): 229-231.

Chen, C, K Linse, CN Roterman, JT Copley and A Rogers (2013). A new genus of large hydrothermal vent-endemic gastropod (Neomphalina: Peltospiridae) with two new species showing evidence of recent demographic expansion. Zoological Journal of the Linnean Society **(Submitted)**.

Chevaldonne, P, D Jollivet, D Desbruyeres, RA Lutz and RC Vrijenhoek (2002). Sister-species of eastern Pacific hydrothermal vent worms (Ampharetidae, Alvinellidae, Vestimentifera) provide new mitochondrial COI clock calibration. Cahiers De Biologie Marine **43**(3-4): 367-370.

Cho, W and TM Shank (2010). Incongruent patterns of genetic connectivity among four ophiuroid species with differing coral host specificity on North Atlantic seamounts. Marine Ecology **31**: 121-143.

Clark, PF and PKL Ng (2008). The lecithotrophic zoea of *Chirostylus ortmanni* Miyake & Baba, 1968 (Crustacea: Anomura: Galatheoidea: Chirostylidae) described from laboratory hatched material. Raffles Bulletin of Zoology **56**(1): 85-94.

Connelly, DP, JT Copley, BJ Murton, K Stansfield, PA Tyler, CR German, CL Van Dover, D Amon, M Furlong and N Grindlay (2012). Hydrothermal vent fields and chemosynthetic biota on the world's deepest seafloor spreading centre. Nature Communications **3**: 620.

Copley, A, P Tyler and M Varney (1998). Lipid profiles of hydrothermal vent shrimps. Cahiers De Biologie Marine **39**(3-4): 229-231.

Copley, JT (2011). RRS *James Cook* research cruise JC067 Dragon vent field, SW Indian Ocean 27-30 November 2011. BODC Cruise Report.

Cordes, EE, SL Carney, S Hourdez, RS Carney, JM Brooks and CR Fisher (2007). Cold seeps of the deep Gulf of Mexico: community structure and biogeographic comparisons to Atlantic equatorial belt seep communities. Deep Sea Research Part I: Oceanographic Research Papers **54**(4): 637-653.

Corliss, JB, J Dymond, LI Gordon, JM Edmond, RPV Herzen, RD Ballard, K Green, D Williams, A Bainbridge, K Crane and TH Vanandel (1979). Submarine thermal springs on the Galapagos Rift. Science **203**(4385): 1073-1083.

Cornuet, JM and G Luikart (1996). Description and power analysis of two tests for detecting recent population bottlenecks from allele frequency data. Genetics **144**(4): 2001-2014.

Coykendall, DK, SB Johnson, SA Karl, RA Lutz and RC Vrijenhoek (2011). Genetic diversity and demographic instability in *Riftia pachyptila* tubeworms from eastern Pacific hydrothermal vents. BMC Evolutionary Biology **11**(1): 96.

Craddock, C, W Hoeh, R Lutz and R Vrijenhoek (1995). Extensive gene flow among mytilid (*Bathymodiolus thermophilus*) populations from hydrothermal vents of the eastern Pacific. Marine Biology **124**(1): 137-146.

Creasey, SS and AD Rogers (1999). Population genetics of bathyal and abyssal organisms. Advances in Marine Biology **35**: 1-151.

Creasey, SS, AD Rogers and PA Tyler (1996). Genetic comparison of two populations of the deep-sea vent shrimp *Rimicaris exoculata* (Decapoda: Bresiliidae) from the Mid-Atlantic Ridge. Marine Biology **125**(3): 473-482.

da Silva, JM, S Creer, A dos Santos, AC Costa, MR Cunha, FO Costa and GR Carvalho (2011). Systematic and evolutionary insights derived from mtDNA COI barcode diversity in the Decapoda (Crustacea: Malacostraca). Plos One **6**(5): e19449.

Daguin, C and D Jollivet (2005). Development and cross-amplification of nine polymorphic microsatellite markers in the deep-sea hydrothermal vent polychaete *Branchipolynoe seepensis*. Molecular Ecology Notes **5**(4): 780-783.

Davey, JW and ML Blaxter (2010). RADSeq: next-generation population genetics. Briefings in Functional Genomics **9**(5-6): 416-423.

Decker, C, K Olu, RL Cunha and S Arnaud-Haond (2012). Phylogeny and diversification patterns among vesicomyid bivalves. Plos One **7**(4): e33359.

Desbruyeres, D, AM Alaysedanet, S Ohta, E Antoine, G Barbier, P Briand, A Godfroy, P Crassous, D Jollivet, J Kerdoncuff, A Khripounoff, L Laubier, M Marchand, R Perron,

E Derelle, A Dinet, A Fialamedioni, J Hashimoto, Y Nojiri, D Prieur, E Ruellan and S Soakai (1994). Deep-sea hydrothermal communities in southwestern Pacific back-arc basins (the North Fiji and Lau Basins) - composition, microdistribution and food-web. Marine Geology **116**(1-2): 227-242.

Desbruyeres, D and M Segonzac (1997). Handbook of deep-sea hydrothermal vent fauna, Editions Quae.

Desbruyeres, D, J Hashimoto, and M Fabri (2006). Composition and biogeography of hydrothermal vent communities in western pacific back-arc basins. Geophysical monograph **166**: 215-234.

Di Rienzo, A, A Peterson, J Garza, A Valdes, M Slatkin and N Freimer (1994). Mutational processes of simple-sequence repeat loci in human populations. Proceedings of the National Academy of Sciences **91**(8): 3166-3170.

Diekmann, B (2007). Sedimentary patterns in the late Quaternary Southern Ocean. Deep Sea Research Part II: Topical Studies in Oceanography **54**(21-22): 2350-2366.

Diekmann, B and G Kuhn (2002). Sedimentary record of the mid-Pleistocene climate transition in the southeastern South Atlantic (ODP Site 1090). Palaeogeography, Palaeoclimatology, Palaeoecology **182**(3): 241-258.

Distel, DL, AR Baco, E Chuang, W Morrill, C Cavanaugh and CR Smith (2000). Marine ecology - Do mussels take wooden steps to deep-sea vents? Nature **403**(6771): 725-726.

Dixon, D and L Dixon (1996). Results of DNA analyses conducted on vent shrimp postlarvae collected above the Broken Spur vent field during the CD95 cruise, August 1995. Bridge Newsletter **11**: 9-15.

Doyle, JJ and EE Dickson (1987). Preservation of plant samples for DNA restriction endonuclease analysis. Taxon **36**(4): 715-722.

Drummond, A, B Ashton, M Cheung, J Heled, M Kearse and R Moir (2010). Geneious Pro, Geneious. Biomatters Ltd.

Drummond, A and A Rambaut (2007). BEAST: Bayesian evolutionary analysis by sampling trees. BMC Evolutionary Biology **7**(1): 214.

Eagles, G, K Gohl and RD Larter (2009). Animated tectonic reconstruction of the Southern Pacific and alkaline volcanism at its convergent margins since Eocene times. Tectonophysics **464**(1-4): 21-29.

Eagles, G, RA Livermore, JD Fairhead and P Morris (2005). Tectonic evolution of the West Scotia Sea. Journal of Geophysical Research **110**(B2): B02401.

Ellegren, H (2004). Microsatellites: simple sequences with complex evolution. Nature reviews genetics **5**(6): 435-445.

Erixon, P, B Svennblad, T Britton and B Oxelman (2003). Reliability of Bayesian posterior probabilities and bootstrap frequencies in phylogenetics. Systematic Biology **52**(5): 665-673.

Etter, RJ, MA Rex, MC Chase and JM Quattro (1999). A genetic dimension to deep-sea

biodiversity. Deep Sea Research Part I: Oceanographic Research Papers **46**(6): 1095-1099.

Evanno, G, S Regnaut and J Goudet (2005). Detecting the number of clusters of individuals using the software structure: a simulation study. Molecular Ecology **14**(8): 2611-2620.

Excoffier, L and HEL Lischer (2010). Arlequin suite ver 3.5: a new series of programs to perform population genetics analyses under Linux and Windows. Molecular Ecology Resources **10**(3): 564-567.

Excoffier, L, PE Smouse and JM Quattro (1992). Analysis of molecular variance inferred from metric distances among DNA haplotypes: application to human mitochondrial DNA restriction data. Genetics **131**(2): 479-491.

Faircloth, BC (2008). MSATCOMMANDER: detection of microsatellite repeat arrays and automated, locus-specific primer design. Molecular Ecology Resources **8**(1): 92-94.

Faure, B, D Jollivet, A Tanguy, F Bonhomme and N Bierne (2009). Speciation in the deep sea: multi-locus analysis of divergence and gene flow between two hybridizing species of hydrothermal vent mussels. Plos One **4**(8): e6485.

Felbeck, H (1981). Chemoautotrophic potential of the hydrothermal vent tube worm, *Riftia pachyptila* Jones (Vestimentifera). Science **213**(4505): 336-338.

Feldmann, RM and CE Schweitzer (2006). Paleobiogeography of Southern Hemisphere decapod crustacea. Journal of Paleontology **80**(1): 83-103.

Feldmann, RM, FJ Vega, SP Applegate and GA Bishop (1998). Early Cretaceous arthropods from the Tlayúa Formation at Tepexi de Rodriguez, Puebla, Mexico. Journal of Paleontology **72**(1): 79-90.

Folmer, O, M Black, W Hoeh, R Lutz and R Vrijenhoek (1994). DNA primers for amplification of mitochondrial cytochrome c oxidase subunit 1 from diverse metazoan invertebrates. Molecular Marine Biology and Biotechnology **3**(5): 294-299.

Fowler, CMR and V Tunnicliffe (1997). Hydrothermal vent communities and plate tectonics. Endeavour **21**(4): 164-168.

France, SC, RR Hessler and RC Vrijenhoek (1992). Genetic differentiation between spatially-disjunct populations of the deep-sea, hydrothermal vent-endemic amphipod *Ventiella sulfuris*. Marine Biology **114**(4): 551-559.

France, SC and LL Hoover (2002). DNA sequences of the mitochondrial COI gene have low levels of divergence among deep-sea octocorals (Cnidaria: Anthozoa). Hydrobiologia **471**: 149-155.

France, SC and T Kocher (1996). Geographic and bathymetric patterns of mitochondrial 16S rRNA sequence divergence among deep-sea amphipods, *Eurythenes gryllus*. Marine Biology **126**(4): 633-643.

Frederich, M, FJ Sartoris and HO Portner (2001). Distribution patterns of decapod crustaceans in polar areas: a result of magnesium regulation? Polar Biology **24**(10): 719-723.

Fretzdorff, S, R Livermore, CW Devey, P Leat and P Stoffers (2002). Petrogenesis of the back-arc east scotia ridge, south Atlantic ocean. Journal of Petrology **43**(8): 1435.

Fu, YX (1996). New statistical tests of neutrality for DNA samples from a population. Genetics **143**(1): 557.

Fu, YX and WH Li (1993). Statistical tests of neutrality of mutations. Genetics **133**(3): 693.

Fusaro, AJ (2008). Spatial and temporal population genetics at deep-sea hydrothermal vents along the East Pacific Rise and Galapagos Rift, Massachusetts Institute of Technology. **Doctor of Philosophy**.

Fusaro, AJ, AR Baco, G Gerlach and TM Shank (2008). Development and characterization of 12 microsatellite markers from the deep-sea hydrothermal vent siboglinid *Riftia pachyptila*. Molecular Ecology Resources **8**(1): 132-134.

Gage, JD and P Tyler (1992). Deep-sea biology: a natural history of organisms at the deep-sea floor, Cambridge University Press.

Galkin, SV (1992). The benthic fauna of hydrothermal vents in the Manus Basin. Oceanology **32**(6): 768-774.

Galtier, N, B Nabholz, S Gièmin and GDD Hurst (2009). Mitochondrial DNA as a marker of molecular diversity: a reappraisal. Molecular Ecology **18**(22): 4541-4550.

Gebruk, AV, P Chevaldonne, T Shank, RA Lutz and RC Vrijenhoek (2000). Deep-sea hydrothermal vent communities of the Logatchev area (14˚45'N, Mid-Atlantic Ridge): diverse biotopes and high biomass. Journal of the Marine Biological Association of the United Kingdom **80**(3): 383-393.

Gebruk, AV, SV Galkin, AL Vereshchaka, LI Moskalev and AJ Southward (1997). Ecology and biogeography of the hydrothermal vent fauna of the Mid-Atlantic Ridge. Advances in Marine Biology. AJSAVGECS J.H.S. Blaxter and PA Tyler, Academic Press. **32:** 93-144.

German, C, R Livermore, E Baker, N Bruguier, D Connelly, A Cunningham, P Morris, I Rouse, P Statham and P Tyler (2000). Hydrothermal plumes above the East Scotia Ridge: an isolated high-latitude back-arc spreading centre. Earth and Planetary Science Letters **184**(1): 241-250.

Glover, AG, B Kallstrom, CR Smith and TG Dahlgren (2005). World-wide whale worms? A new species of *Osedax* from the shallow North Atlantic. Proceedings of the Royal Society B - Biological Sciences **272**(1581): 2587-2592.

Goffredi, SK (2010). Indigenous ectosymbiotic bacteria associated with diverse hydrothermal vent invertebrates. Environmental Microbiology Reports **2**(4): 479-488.

Goffredi, SK, WJ Jones, H Erhlich, A Springer and RC Vrijenhoek (2008). Epibiotic bacteria associated with the recently discovered yeti crab, *Kiwa hirsuta*. Environmental Microbiology **10**(10): 2623-2634.

Goffredi, SK, VJ Orphan, GW Rouse, L Jahnke, T Embaye, K Turk, R Lee and RC Vrijenhoek (2005). Evolutionary innovation: a bone-eating marine symbiosis. Environmental Microbiology **7**(9): 1369-1378.

Goffredi, SK, A Warèn, VJ Orphan, CL Van Dover and RC Vrijenhoek (2004). Novel forms of

structural integration between microbes and a hydrothermal vent gastropod from the Indian Ocean. Applied and Environmental Microbiology **70**(5): 3082-3090.

Goodall-Copestake, W, S Perez-Espona, M Clark, E Murphy, P Seear and G Tarling (2010). Swarms of diversity at the gene cox1 in Antarctic krill. Heredity **104**(5): 513-518.

Goudet, J (1995). FSTAT (version 1.2): a computer program to calculate F-statistics. Journal of Heredity **86**(6): 485-486.

Gradstein, FM, JG Ogg, AG Smith, W Bleeker and LJ Lourens (2004). A new geologic time scale, with special reference to Precambrian and Neogene. Episodes **27**(2): 83-100.

Grassle, JP (1985). Genetic differentiation in populations of hydrothermal vent mussels (*Bathymodiolus thermophilus*) from the Galapagos Rift and 13˚ N on the East Pacific Rise. Bulletin of the Biological Society of Washington(6): 429-442.

Guichoux, E, L Lagache, S Wagner, P Chaumeil, P Léger, O Lepais, C Lepoittevin, T Malausa, E Revardel, F Salin and RJ Petit (2011). Current trends in microsatellite genotyping. Molecular Ecology Resources **11**(4): 591-611.

Guinot, D and LA Hurtado (2003). Two new species of hydrothermal vent crabs of the genus *Bythograea* from the southern East Pacific Rise and from the Galapagos Rift (Crustacea Decapoda Brachyura Bythograeidae). Comptes Rendus Biologies **326**(4): 423-439.

Halanych, KM (2005). Molecular phylogeny of siboglinid annelids (a.k.a. pogonophorans): a review. Hydrobiologia **535**: 297-307.

Halanych, KM, RA Lutz and RC Vrijenhoek (1998). Evolutionary origins and age of vestimentiferan tube-worms. Cahiers De Biologie Marine **39**(3-4): 355-358.

Hale, ML, TM Burg and TE Steeves (2012). Sampling for microsatellite-based population genetic studies: 25 to 30 individuals per population is enough to accurately estimate allele frequencies. Plos One **7**(9): e45170.

Hall, BG (2004). Phylogenetic trees made easy: a how-to manual, Sinauer Associates Sunderland.

Harpending, H (1994). Signature of ancient population growth in a low-resolution mitochondrial DNA mismatch distribution. Human biology; an international record of research **66**(4): 591.

Hashimoto, J, S Ohta, K Fujikura and T Miura (1995). Microdistribution pattern and biogeography of the hydrothermal vent communities of the Minami-Ensei Knoll in the Mid-Okinawa Trough, Western Pacific. Deep Sea Research Part I: Oceanographic Research Papers **42**(4): 577-598.

Hashimoto, J, S Ohta, T Gamo, H Chiba, T Yamaguchi, S Tsuchida, T Okudaira, H Watabe, T Yamanaka and M Kitazawa (2001). First hydrothermal vent communities from the Indian Ocean discovered. Zoological Science **18**(5): 717-721.

Hassold, NJC, DK Rea, BA van der Pluijm and JM Parés (2009). A physical record of the Antarctic Circumpolar Current: late Miocene to recent slowing of abyssal circulation. Palaeogeography, Palaeoclimatology, Palaeoecology **275**(1-4): 28-36.

Haymon, RM, DJ Fornari, KL Von Damm, MD Lilley, MR Perfit, JM Edmond, WC Shanks Iii, RA Lutz, JM Grebmeier, S Carbotte, D Wright, E McLaughlin, M Smith, N Beedle and E Olson (1993). Volcanic eruption of the mid-ocean ridge along the East Pacific Rise crest at 9˚45-52'N: Direct submersible observations of seafloor phenomena associated with an eruption event in April, 1991. Earth and Planetary Science Letters **119**(1-2): 85-101.

Hecker, B (1985). Fauna from a cold sulfur-seep in the Gulf of Mexico: Comparison with hydrothermal vent communities and evolutionary implications. Bulletin of the Biological Society of Washington(6): 465-473.

Hekinian, R, M Fevrier, F Avedik, P Cambon, JL Charlou, HD Needham, J Raillard, J Boulegue, L Merlivat, A Moinet, S Manganini and J Lange (1983). East Pacific Rise near 13˚ N: Geology of New Hydrothermal Fields. Science **219**(4590): 1321-1324.

Hellberg, ME (2009). Gene flow and isolation among populations of marine animals. Annual Review of Ecology, Evolution and Systematics **40**: 291-310.

Herring, PJ and DR Dixon (1998). Extensive deep-sea dispersal of postlarval shrimp from a hydrothermal vent. Deep-Sea Research Part I: Oceanographic Research Papers **45**(12): 2105-2118.

Hessler, RR and PF Lonsdale (1991). Biogeography of Mariana Trough hydrothermal vent communities. Deep-Sea Research Part A: Oceanographic Research Papers **38**(2): 185-199.

Hey, J (2010). Isolation with migration models for more than two populations. Molecular Biology and Evolution **27**(4): 905-920.

Hey, J and R Nielsen (2004). Multilocus methods for estimating population sizes, migration rates and divergence time, with applications to the divergence of *Drosophila pseudoobscura* and *D. persimilis*. Genetics **167**(2): 747-760.

Hickman, C (1984). A new archaeogastropod (Rhipidoglossa, Trochacea) from hydrothermal vents on the East Pacific Rise. Zoologica Scripta **13**(1): 19-25.

Ho, SYW, R Lanfear, L Bromham, MJ Phillips, J Soubrier, AG Rodrigo and A Cooper (2011). Time-dependent rates of molecular evolution. Molecular Ecology **20**(15): 3087-3101.

Ho, SYW and MJ Phillips (2009). Accounting for calibration uncertainty in phylogenetic estimation of evolutionary divergence times. Systematic Biology **58**(3): 367-380.

Ho, SYW and B Shapiro (2011). Skyline-plot methods for estimating demographic history from nucleotide sequences. Molecular Ecology Resources **11**(3): 423-434.

Holder, M and P Lewis (2003). Phylogeny estimation: traditional and Bayesian approaches. Nature Reviews Genetics **4**(4): 275-284.

Holleley, CE and PG Geerts (2009). Multiplex Manager 1.0: a cross-platform computer program that plans and optimizes multiplex PCR. BioTechniques **46**(7): 511.

Hurtado, LA (2002). Evolution and biogeography of hydrothermal vent organisms in the Eastern Pacific Ocean, Rutgers University, New Brunswick, NJ. **Doctor of Philosophy**.

Hurtado, LA, RA Lutz and RC Vrijenhoek (2004). Distinct patterns of genetic differentiation among annelids of eastern Pacific hydrothermal vents. Molecular Ecology **13**(9): 2603-2615.

Jacobson, A, S Plouviez, A Thaler and C Dover (2013). Characterization of 13 polymorphic microsatellite loci in *Rimicaris hybisae*, a shrimp from deep-sea hydrothermal vents. Conservation Genetics Resources **5**(2): 449-451.

Jannasch, HW and CO Wirsen (1979). Chemosynthetic primary production at East Pacific sea floor spreading centers. BioScience **29**(10): 592-598.

Johnson, S, A Warén, R Lee, Y Kano, A Kaim, A Davis, E Strong and R Vrijenhoek (2010). *Rubyspira*, new genus and two new species of bone-eating deep-sea snails with ancient habits. The Biological Bulletin **219**(2): 166-177.

Johnson, SB, A Waren and RC Vrijenhoek (2008). DNA barcoding of *Lepetodrilus* limpets reveals cryptic species. Journal of Shellfish Research **27**(1): 43-51.

Johnson, SB, Y-J Won, JB Harvey and RC Vrijenhoek (2013). A hybrid zone between *Bathymodiolus* mussel lineages from eastern Pacific hydrothermal vents. BMC Evolutionary Biology **13**(1): 21.

Johnson, SB, CR Young, WJ Jones, A Waren and RC Vrijenhoek (2006). Migration, isolation, and speciation of hydrothermal vent limpets (Gastropoda; Lepetodrilidae) across the Blanco Transform Fault. Biological Bulletin **210**(2): 140-157.

Jollivet, D, P Chevaldonné and B Planque (1999). Hydrothermal-vent alvinellid polychaete dispersal in the eastern Pacific. 2. A metapopulation model based on habitat shifts. Evolution **53**(4): 1128-1142.

Jollivet, D, D Desbruyeres, F Bonhomme and D Moraga (1995). Genetic differentiation of deep-sea hydrothermal vent alvinellid populations (Annelida: Polychaeta) along the East Pacific Rise. Heredity **74**(4): 376-391.

Jones, ML (1980). *Riftia pachyptila*, new genus, new species, the vestimentiferan worm from the Galapagos Rift geothermal vents (Pogonophora). Proceedings of the Biological Society of Washington **93**(4): 1295-1313.

Jones, WJ, Y Won, P Maas, P Smith, R Lutz and R Vrijenhoek (2006). Evolution of habitat use by deep-sea mussels. Marine Biology **148**(4): 841-851.

Juniper, SK and V Tunnicliffe (1997). Crustal accretion and the hot vent ecosystem. Philosophical Transactions of the Royal Society of London. Series A: Mathematical, Physical and Engineering Sciences **355**(1723): 459-474.

Kaim, A and SR Kelly (2009). Mass occurrence of hokkaidoconchid gastropods in the Upper Jurassic methane seep carbonate from Alexander Island, Antarctica. Antarctic Science **21**(3): 279-284.

Kalinowski, ST (2004). Do polymorphic loci require large sample sizes to estimate genetic distances? Heredity **94**(1): 33-36.

Karl, DM, CO Wirsen and HW Jannasch (1980). Deep-sea primary production at the Galapagos hydrothermal vents. Science **207**: 1345-1347.

Karl, S, S Schutz, D Desbruyeres, R Lutz and R Vrijenhoek (1996). Molecular analysis of gene flow in the hydrothermal vent clam (*Calyptogena magnifica*). Molecular Marine Biology and Biotechnology **5**(3): 193-202.

Katoh, K, G Asimenos and H Toh (2009). Multiple alignment of DNA sequences with MAFFT. Bioinformatics for DNA Sequence Analysis, Springer**:** 39-64.

Kelly, NE and A Metaxas (2007). Influence of habitat on the reproductive biology of the deep-sea hydrothermal vent limpet *Lepetodrilus fucensis* (Vetigastropoda: Mollusca) from the Northeast Pacific. Marine Biology **151**(2): 649-662.

Kiel, S and PR Dando (2009). Chaetopterid tubes from vent and seep sites: Implications for fossil record and evolutionary history of vent and seep annelids. Acta Palaeontologica Polonica **54**(3): 443-448.

Kiel, S and CTS Little (2006). Cold-seep mollusks are older than the general marine mollusk fauna. Science **313**(5792): 1429-1431.

Kimura, M (1984). The neutral theory of molecular evolution, Cambridge University Press.

Kimura, M and JF Crow (1964). The number of alleles that can be maintained in a finite population. Genetics **49**(4): 725.

Kimura, M and G Weiss (1964). The stepping stone model of population structure and the decrease of genetic correlation with distance. Genetics **49**(4): 561.

Kingman, JF (2000). Origins of the coalescent: 1974-1982. Genetics **156**(4): 1461-1463.

Klompmaker, AA (2012). Mesozoic decapod diversity with an emphasis on the early Cretaceous (Albian) of Spain, Kent State University. **Doctor of Philosophy**.

Knowles, JD, E Wenink, N Schult, V Tunnicliffe and D McHugh (2005). Molecular analysis indicates gene flow among populations of *Paralvinella pandorae* Desbruyeres and Laubier 1986 (Alvinellidae, Terebellida), a polychaete annelid endemic to hydrothermal vents of the northeast Pacific. Marine Ecology **26**(3-4): 216-222.

Kongsrud, J and H Rapp (2012). Nicomache (Loxochona) lokii sp. nov. (Annelida: Polychaeta: Maldanidae) from the Loki's Castle vent field: an important structure builder in an Arctic vent system. Polar Biology **35**(2): 161-170.

Kritzer, JP and PF Sale (2004). Metapopulation ecology in the sea: from Levins' model to marine ecology and fisheries science. Fish and Fisheries **5**(2): 131-140.

Kuhner, MK (2009). Coalescent genealogy samplers: windows into population history. Trends in Ecology & Evolution **24**(2): 86-93.

Lalou, C, J-L Reyss, E Brichet, M Arnold, G Thompson, Y Fouquet and PA Rona (1993). New age data for Mid-Atlantic Ridge hydrothermal sites: TAG and Snakepit chronology revisited. Journal of Geophysical Research: Solid Earth **98**(B6): 9705-9713.

Lanfear, R, B Calcott, SYW Ho and S Guindon (2012). PartitionFinder: combined selection of partitioning schemes and substitution models for phylogenetic analyses. Molecular Biology and Evolution **29**(6): 1695-1701.

Larter, R (2009). Cruise Report JR224. Chemosynthetically-driven ecosystems south of the polar front consortium programme. RRS James Clark Ross. BODC Cruise Report.

Larter, RD, LE Vanneste, P Morris and DK Smythe (2003). Structure and tectonic evolution of the South Sandwich arc. Geological Society, London, Special Publications **219**(1): 255.

Lawver, LA, LM Gahagan and IWD Dalziel (2011). A different look at gateways: Drake Passage and Australia/Antarctica. Tectonic, Climatic, and Cryospheric Evolution of the Antarctic Peninsula. Washington, DC, AGU. **63:** 5-33.

Le Guilloux, E, JM Hall-Spencer, MK Söffker and K Olu (2010). Association between the squat lobster *Gastroptychus formosus* and cold-water corals in the North Atlantic. Journal of the Marine Biological Association of the United Kingdom **90**(7): 1363-1369.

Leese, F, S Agrawal and C Held (2010). Long-distance island hopping without dispersal stages: transportation across major zoogeographic barriers in a Southern Ocean isopod. Naturwissenschaften **97**(6): 583-594.

Leese, F, P Brand, A Rozenberg, C Mayer, S Agrawal, J Dambach, L Dietz, JS Doemel, WP Goodall-Copstake, C Held, JA Jackson, KP Lampert, K Linse, JN Macher, J Nolzen, MJ Raupach, NT Rivera, CD Schubart, S Striewski, R Tollrian and CJ Sands (2012). Exploring pandora's box: potential and pitfalls of low coverage genome surveys for evolutionary biology. Plos One **7**(11): e49202.

Lemaitre, R and PA McLaughlin (2009). Recent advances and conflicts in concepts of anomuran phylogeny (Crustacea: Malacostraca). Arthropod Systematics & Phylogeny **67**(2): 119-135.

Lemey, P, M Salemi and A-M Vandamme (2009). The phylogenetic handbook: a practical approach to phylogenetic analysis and hypothesis testing, Cambridge University Press.

Lessios, HA (2008). The Great American Schism: divergence of marine organisms after the rise of the Central American Isthmus. Annual Review of Ecology Evolution and Systematics **39**: 63-91.

Levin, LA, GF Mendoza, T Konotchick and R Lee (2009). Macrobenthos community structure and trophic relationships within active and inactive Pacific hydrothermal sediments. Deep-Sea Research Part II: Topical Studies in Oceanography **56**(19-20): 1632-1648.

Levin, LA, VJ Orphan, GW Rouse, AE Rathburn, W Ussler, GS Cook, SK Goffredi, EM Perez, A Waren, BM Grupe, G Chadwick and B Strickrott (2012). A hydrothermal seep on the Costa Rica margin: middle ground in a continuum of reducing ecosystems. Proceedings of the Royal Society B: Biological Sciences **279**(1738): 2580-2588.

Levins, R (1969). Some demographic and genetic consequences of environmental heterogeneity for biological control. Bulletin of the ESA **15**(3): 237-240.

Li, Y-C, AB Korol, T Fahima, A Beiles and E Nevo (2002). Microsatellites: genomic distribution, putative functions and mutational mechanisms: a review. Molecular Ecology **11**(12): 2453-2465.

Librado, P and J Rozas (2009). DnaSP v5: a software for comprehensive analysis of DNA polymorphism data. Bioinformatics **25**(11): 1451.

Little, CTS, RJ Herrington, VV Maslennikov and VV Zaykov (1998). The fossil record of hydrothermal vent communities. Geological Society, London, Special Publications **148**(1): 259-270.

Little, CTS and RC Vrijenhoek (2003). Are hydrothermal vent animals living fossils? Trends in Ecology & Evolution **18**(11): 582-588.

Livermore, R (2003). Back-arc spreading and mantle flow in the East Scotia Sea. Geological Society, London, Special Publications **219**(1): 315.

Livermore, R (2006). The East Scotia Sea: mantle to microbe. Geophysical monograph **166**: 243-261.

Lonsdale, P and K Becker (1985). Hydrothermal plumes, hot springs, and conductive heat flow in the Southern Trough of Guaymas Basin. Earth and Planetary Science Letters **73**(2-4): 211-225.

Lorion, J, B Buge, C Cruaud and S Samadi (2010). New insights into diversity and evolution of deep-sea Mytilidae (Mollusca: Bivalvia). Molecular Phylogenetics and Evolution **57**(1): 71-83.

Lowman, P, P Masuoka, B Montgomery, J OLeary, D Salisbury and J Yates (1999). A digital tectonic activity map of the Earth. NASA(19990041078).

Luikart, G, PR England, D Tallmon, S Jordan and P Taberlet (2003). The power and promise of population genomics: from genotyping to genome typing. Nature Reviews Genetics **4**(12): 981-994.

Lutz, RA, P Bouchet, D Jablonski, R Turner and A WarÈn (1986). Larval ecology of mollusks at deep-sea hydrothermal vents. American Malacological Bulletin **4**(1): 49-54.

Macpherson, E, W Jones and M Segonzac (2005). A new squat lobster family of Galatheoidea (Crustacea, Decapoda, Anomura) from the hydrothermal vents of the Pacific-Antarctic Ridge. Zoosystema **27**(4): 709-723.

Marko, PB and MW Hart (2012). Retrospective coalescent methods and the reconstruction of metapopulation histories in the sea. Evolutionary Ecology **26**(2): 291-315.

Marsh, AG, LS Mullineaux, CM Young and DT Manahan (2001). Larval dispersal potential of the tubeworm *Riftia pachyptila* at deep-sea hydrothermal vents. Nature **411**(6833): 77-80.

Marsh, L, JT Copley, VAI Huvenne, K Linse, WDK Reid, AD Rogers, CJ Sweeting and PA Tyler (2012). Microdistribution of faunal assemblages at deep-sea hydrothermal vents in the Southern Ocean. Plos One **7**(10): e48348.

Martens, C, J Chanton and C Paull (1991). Biogenic methane from abyssal brine seeps at the base of the Florida escarpment. Geology **19**(8): 851.

Matabos, M, S Plouviez, S Hourdez, D Desbruyères, P Legendre, A Warén, D Jollivet and E Thiébaut (2011). Faunal changes and geographic crypticism indicate the occurrence of a biogeographic transition zone along the southern East Pacific Rise. Journal of Biogeography **38**(3): 575-594.

Matabos, M and E Thiebaut (2010). Reproductive biology of three hydrothermal vent peltospirid gastropods (*Nodopelta heminoda*, *N. subnoda* and *Peltospira operculata*) associated with Pompeii worms on the East Pacific Rise. Journal of Molluscan Studies **76**(3): 257-266.

Matabos, M, E Thiebaut, D Le Guen, F Sadosky, D Jollivet and F Bonhomme (2008). Geographic clines and stepping-stone patterns detected along the East Pacific Rise in the vetigastropod *Lepetodrilus elevatus* reflect species crypticism. Marine Biology **153**(4): 545-563.

McClain, CR and SM Hardy (2010). The dynamics of biogeographic ranges in the deep sea. Proceedings of the Royal Society B: Biological Sciences **277**(1700): 3533-3546.

McInerney, C, A Allcock, M Johnson, D Bailie and P Prodöhl (2010). Comparative genomic analysis reveals species-dependent complexities that explain difficulties with microsatellite marker development in molluscs. Heredity **106**(1): 78-87.

McLaughlin, PA, R Lemaitre and U Sorhannus (2007). Hermit crab phylogeny: a reappraisal and its "fall-out". Journal of Crustacean Biology **27**(1): 97-115.

Meiklejohn, CD, KL Montooth and DM Rand (2007). Positive and negative selection on the mitochondrial genome. Trends in Genetics **23**(6): 259-263.

Meredith, MP, ACN Garabato, AL Gordon and GC Johnson (2008). Evolution of the deep and bottom waters of the Scotia Sea, Southern Ocean, during 1995-2005*. Journal of Climate **21**(13): 3327-3343.

Meredith, MP, AC Naveira-Garabato, DP Stevens, KJ Heywood and RJ Sanders (2001). Deep and bottom waters in the eastern Scotia Sea: rapid changes in properties and circulation. Journal of physical oceanography **31**(8): 2157-2168.

Meschede, M and U Barckhausen (2001). The relationship of the Cocos and Carnegie ridges: age constraints from paleogeographic reconstructions. International Journal of Earth Sciences **90**(2): 386-392.

Minin, V, Z Abdo, P Joyce and J Sullivan (2003). Performance-based selection of likelihood models for phylogeny estimation. Systematic Biology **52**(5): 674-683.

Morrison, C, A Harvey, S Lavery, K Tieu, Y Huang and C Cunningham (2002). Mitochondrial gene rearrangements confirm the parallel evolution of the crab-like form. Proceedings of the Royal Society B: Biological Sciences **269**(1489): 345.

Mullineaux, LS, DK Adams, SW Mills and SE Beaulieu (2010). Larvae from afar colonize deep-sea hydrothermal vents after a catastrophic eruption. Proceedings of the National Academy of Sciences of the United States of America **107**(17): 7829-7834.

Mullineaux, LS, N Le Bris, SW Mills, P Henri, SR Bayer, RG Secrist and N Siu (2012). Detecting the influence of initial pioneers on succession at deep-sea vents. Plos One **7**(12): e50015.

Mullineaux, LS, DJ McGillicuddy Jr, SW Mills, VK Kosnyrev, AM Thurnherr, JR Ledwell and JW Lavelle (2013). Active positioning of vent larvae at a mid-ocean ridge. Deep Sea Research Part II: Topical Studies in Oceanography **92**(0): 46-57.

Mullineaux, LS, SW Mills, AK Sweetman, AH Beaudreau, A Metaxas and HL Hunt (2005). Vertical, lateral and temporal structure in larval distributions at hydrothermal vents. Marine Ecology-Progress Series **293**: 1-16.

Mullineaux, LS, P Wiebe and E Baker (1995). Larvae of benthic invertebrates in hydrothermal vent plumes over Juan de Fuca Ridge. Marine Biology **122**(4): 585-596.

Naar, DF and R Hey (1991). Tectonic evolution of the Easter Microplate. Journal of Geophysical Research **96**(B5): 7961-7993.

Naganuma, T, H Wada and K Fujioka (1996). Biological community and sediment fatty acids associated with the deep-sea whale skeleton at the Torishima Seamount. Journal of Oceanography **52**(1): 1-15.

Nakamura, K, H Watanabe, J Miyazaki, K Takai, S Kawagucci, T Noguchi, S Nemoto, T-o Watsuji, T Matsuzaki, T Shibuya, K Okamura, M Mochizuki, Y Orihashi, T Ura, A Asada, D Marie, M Koonjul, M Singh, G Beedessee, M Bhikajee and K Tamaki (2012). Discovery of new hydrothermal activity and chemosynthetic fauna on the Central Indian Ridge at 18˚-20˚ S. Plos One **7**(3): e32965.

Naveira-Garabato, AC, KJ Heywood and DP Stevens (2002). Modification and pathways of Southern Ocean deep waters in the Scotia Sea. Deep Sea Research Part I: Oceanographic Research Papers **49**(4): 681-705.

Newman, WA (1979). A new scalpellid (Cirripedia); a Mesozoic relic living near an abyssal hydrothermal spring. Transactions of the San Diego Society of Natural History **19**(11): 153-167.

Newman, WA (1985). The abyssal hydrothermal vent invertebrate fauna: a glimpse of antiquity? Bulletin of the Biological Society of Washington(6): 231-242.

Nielsen, R and J Wakeley (2001). Distinguishing migration from isolation: a Markov chain Monte Carlo approach. Genetics **158**(2): 885.

Normark, WR, JL Morton, RA Koski, DA Clague and JR Delaney (1983). Active hydrothermal vents and sulfide deposits on the southern Juan de Fuca Ridge. Geology **11**(3): 158-163.

Normark, WR, JW Murray, JE Lupton, JR Delaney, HP Johnson, RA Koski, DA Clague and JL Morton (1982). Polymetallic sulphide deposits and water-column of active hydrothermal vents on the Southern Juan De Fuca Ridge. Marine Technology Society Journal **16**(3): 46-53.

Nye, V, J Copley and S Plouviez (2012). A new species of *Rimicaris* (Crustacea: Decapoda: Caridea: Alvinocarididae) from hydrothermal vent fields on the Mid-Cayman Spreading Centre, Caribbean. Journal of the Marine Biological Association of the United Kingdom **92**(5): 1057-1072.

Ohta, T and M Kimura (1973). A model of mutation appropriate to estimate the number of electrophoretically detectable alleles in a finite population. Genetical research **22**(2): 201-204.

Okutani, T, J Hashimoto and T Sasaki (2004). New gastropod taxa from a hydrothermal vent (Kairei Field) in the Central Indian Ocean. Venus **63**(1-2): 1-11.

Olu, K, EE Cordes, CR Fisher, JM Brooks, M Sibuet and D Desbruyeres (2010). Biogeography and potential exchanges among the atlantic equatorial belt cold-seep faunas. Plos One **5**(8).

Orsi, AH, T Whitworth and WD Nowlin (1995). On the meridional extent and fronts of the Antarctic Circumpolar Current. Deep Sea Research Part I: Oceanographic Research Papers **42**(5): 641-673.

Page, R and E Holmes (1998). Molecular evolution: a phylogenetic approach, Wiley-Blackwell.

Parker, PG, AA Snow, MD Schug, GC Booton and PA Fuerst (1998). What molecules can tell us about populations: Choosing and using a molecular marker. Ecology: 361-382.

Paull, CK, A Jull, L Toolin and T Linick (1985). Stable isotope evidence for chemosynthesis in an abyssal seep community. Nature **317**: 709.

Paull, CK, W Ussler, W Borowski and F Spiess (1995). Methane-rich plumes on the Carolina continental rise: associations with gas hydrates. Geology **23**(1): 89.

Pearse, JS, JB McClintock and I Bosch (1991). Reproduction of Antarctic benthic marine invertebrates: tempos, modes, and timing. American Zoologist **31**(1): 65-80.

Pedersen, R, H Rapp, I Thorseth, M Lilley, F Barriga, T Baumberger, K Flesland, R Fonseca, G Früh-Green and S Jorgensen (2010). Discovery of a black smoker vent field and vent fauna at the Arctic mid-ocean ridge. Nature Communications **1**(8): 126.

Peek, AS, BS Gaut, RA Feldman, JP Barry, RE Kochevar, RA Lutz and RC Vrijenhoek (2000). Neutral and nonneutral mitochondrial genetic variation in deep-sea clams from the family Vesicomyidae. Journal of Molecular Evolution **50**(2): 141-153.

Peek, AS, RG Gustafson, RA Lutz and RC Vrijenhoek (1997). Evolutionary relationships of deep-sea hydrothermal vent and cold-water seep clams (Bivalvia: Vesicomyidae): results from mitochondrial cytochrome oxidase subunit I. Marine Biology **130**(2): 151-161.

Perez-Losada, M, G Bond-Buckup, C Jara and K Crandall (2004). Molecular systematics and biogeography of the southern South American freshwater "crabs" *Aegla* (Decapoda: Anomura: Aeglidae) using multiple heuristic tree search approaches. Systematic Biology **53**(5): 767-780.

Perez-Losada, M, M Harp, JT Hoeg, Y Achituv, D Jones, H Watanabe and KA Crandall (2008). The tempo and mode of barnacle evolution. Molecular Phylogenetics and Evolution **46**(1): 328-346.

Piry, S, G Luikart and J Cornuet (1999). Computer note. BOTTLENECK: a computer program for detecting recent reductions in the effective size using allele frequency data. Journal of Heredity **90**(4): 502-503.

Plouviez, S, D Le Guen, O Lecompte, FH Lallier and D Jollivet (2010). Determining gene flow and the influence of selection across the equatorial barrier of the East Pacific Rise in the tube-dwelling polychaete *Alvinella pompejana*. BMC Evolutionary Biology **10**: 220.

Plouviez, S, TM Shank, B Faure, C Daguin-Thiebaut, F Viard, FH Lallier and D Jollivet (2009). Comparative phylogeography among hydrothermal vent species along the East Pacific

Rise reveals vicariant processes and population expansion in the South. Molecular Ecology **18**(18): 3903-3917.

Poore, GCB and N Andreakis (2011). Morphological, molecular and biogeographic evidence support two new species in the *Uroptychus naso* complex (Crustacea: Decapoda: Chirostylidae). Molecular Phylogenetics and Evolution **60**(1): 152-169.

Posada, D and K Crandall (2001). Intraspecific gene genealogies: trees grafting into networks. Trends in Ecology & Evolution **16**(1): 37-45.

Powell, EN, WR Callender and RJ Stanton Jr (1998). Can shallow and deep-water chemoautotrophic and heterotrophic communities be discriminated in the fossil record? Palaeogeography, Palaeoclimatology, Palaeoecology **144**(1-2): 85-114.

Pradillon, F, B Shillito, C Young and F Gaill (2001). Deep-sea ecology: developmental arrest in vent worm embryos. Nature **413**(6857): 698-699.

Pritchard, JK, M Stephens and P Donnelly (2000). Inference of population structure using multilocus genotype data. Genetics **155**(2): 945.

Rambaut, A and A Drummond (2007). Tracer v1. 4 [computer program]. Available at website http://beast.bio.ed.ac.uk.

Ramirez-Llodra, E, TM Shank and CR German (2007). Biodiversity and biogeography of hydrothermal vent species: thirty years of discovery and investigations. Oceanography **20**(1): 30-41.

Rau, GH (1981). Hydrothermal vent clam and tube worm 13C/12C: further evidence of nonphotosynthetic food sources. Science **213**(4505): 338-340.

Reid, WDK, CJ Sweeting, BD Wigham, K Zwirglmaier, JA Hawkes, RAR McGill, K Linse and NVC Polunin (2013). Spatial differences in East Scotia Ridge hydrothermal vent food webs: influences of chemistry, microbiology and predation on trophodynamics. Plos One **8**(6): e65553.

Renard, V, R Hekinian, J Francheteau, RD Ballard and H Backer (1985). Submersible observations at the axis of the ultra-fast-spreading East Pacific Rise (17˚30' to 21˚30'S). Earth and Planetary Science Letters **75**(4): 339-353.

Rice, WR (1989). Analyzing tables of statistical tests. Evolution **43**(1): 223-225.

Robins, CM, RM Feldmann and CE Schweitzer (2012). The oldest Munididae (Decapoda: Anomura: Galatheoidea) from Ernstbrunn, Austria (Tithonian). Annalen des Naturhistorischen Museums in Wien A **114A**: 289-300.

Rogers, AD (2000). The role of the oceanic oxygen minima in generating biodiversity in the deep sea. Deep Sea Research-Part II-Topical Studies in Oceanography **47**(1-2): 119-148.

Rogers, AD (2007). Evolution and biodiversity of Antarctic organisms: a molecular perspective. Philosophical Transactions of the Royal Society B: Biological Sciences **362**(1488): 2191.

Rogers, AD (2010). Chemosynthetic Ecosystems of the Southern Ocean (CHESSO)

RRS *James Cook* Cruise 42. BODC Cruise Report.

Rogers, AD, PA Tyler, DP Connelly, JT Copley, R James, RD Larter, K Linse, RA Mills, AN Garabato, RD Pancost, DA Pearce, NVC Polunin, CR German, T Shank, PH Boersch-Supan, BJ Alker, A Aquilina, SA Bennett, A Clarke, RJJ Dinley, AGC Graham, DRH Green, JA Hawkes, L Hepburn, A Hilario, VAI Huvenne, L Marsh, E Ramirez-Llodra, WDK Reid, CN Roterman, CJ Sweeting, S Thatje and K Zwirglmaier (2012). The discovery of new deep-sea hydrothermal vent communities in the Southern Ocean and implications for biogeography. Plos Biology **10**(1): e1001234.

Rogers, AR and H Harpending (1992). Population growth makes waves in the distribution of pairwise genetic differences. Molecular Biology and Evolution **9**(3): 552.

Rona, PA, RP Denlinger, MR Fisk, KJ Howard, GL Taghon, KD Klitgord, JS McClain, GR McMurray and JC Wiltshire (1990). Major off-axis hydrothermal activity on the northern Gorda Ridge. Geology **18**(6): 493-496.

Rona, PA, G Klinkhammer, TA Nelsen, JH Trefry and H Elderfield (1986). Black smokers, massive sulphides and vent biota at the Mid-Atlantic Ridge. Nature **321**(6065): 33-37.

Ronquist, F, M Teslenko, P van der Mark, DL Ayres, A Darling, S Höhna, B Larget, L Liu, MA Suchard and JP Huelsenbeck (2012). MrBayes 3.2: efficient Bayesian phylogenetic inference and model choice across a large model space. Systematic Biology **61**(3): 539-542.

Rosenberg, NA and M Nordborg (2002). Genealogical trees, coalescent theory and the analysis of genetic polymorphisms. Nature Reviews Genetics **3**(5): 380-390.

Rouse, GW, SK Goffredi and RC Vrijenhoek (2004). Osedax: bone-eating marine worms with dwarf males. Science **305**(5684): 668-671.

Rozen, S and H Skaletsky (2000). Primer3 on the WWW for general users and for biologist programmers. Methods in Molecular Biology **132**(3): 365-386.

Rusby, RI and RC Searle (1995). A history of the Easter microplate, 5.25 Ma to present. Journal of Geophysical Research **100**(B7): 12617-12640.

Ruzzante, DE (1998). A comparison of several measures of genetic distance and population structure with microsatellite data: bias and sampling variance. Canadian Journal of Fisheries and Aquatic Sciences **55**(1): 1-14.

Samadi, S, E Quemere, J Lorion, A Tillier, R Von Cosel, P Lopez, C Cruaud, A Couloux and M Boisselier-Dubayle (2007). Molecular phylogeny in mytilids supports the wooden steps to deep-sea vents hypothesis. Comptes Rendus Biologies **330**(5): 446-456.

Sauter, D and M Cannat (2010). The ultraslow-spreading Southwest Indian Ridge. Diversity of hydrothermal systems on slow-spreading ocean ridges: American Geophysical Union Geophysical Monograph **188**: 153-173.

Schander, C, HT Rapp, JA Kongsrud, T Bakken, J Berge, S Cochrane, E Oug, I Byrkjedal, C Todt, T Cedhagen, A Fosshagen, A Gebruk, K Larsen, L Levin, M Obst, F Pleijel, S Stohr, A Waren, NT Mikkelsen, S Hadler-Jacobsen, R Keuning, KH Petersen, IH Thorseth and RB Pedersen (2010). The fauna of hydrothermal vents on the Mohn Ridge (North Atlantic). Marine Biology Research **6**(2): 155-171.

Schellart, WP, DR Stegman, RJ Farrington, J Freeman and L Moresi (2010). Cenozoic tectonics of western North America controlled by evolving width of Farallon slab. Science **329**(5989): 316-319.

Schlötterer, C (2000). Evolutionary dynamics of microsatellite DNA. Chromosoma **109**(6): 365-371.

Schnabel, KE and S Ahyong (2011). A new classification of the Chirostyloidea (Crustacea: Decapoda: Anomura). Zootaxa **2687**: 56-64.

Schnabel, KE, S Ahyong and E Maas (2011a). Galatheoidea is not monophyletic-molecular and morphological phylogeny of the squat lobsters (Decapoda: Anomura) with recognition of a new superfamily. Molecular Phylogenetics and Evolution **58**(2): 157-168.

Schnabel, KE, P Cabezas, A McCallum, E Macpherson, ST Ahyong and K Baba (2011b). Worldwide distribution patterns of squat lobsters. Biology of Squat Lobsters. GCB Poore, ST Ahyong and J Taylor, CSIRO Publishing**:** 149-182.

Schultz, T, P-Y Hsing, A Eng, K Zelnio, A Thaler, J Carlsson and C Van Dover (2011). Characterization of 18 polymorphic microsatellite loci from *Bathymodiolus manusensis*; (Bivalvia, Mytilidae) from deep-sea hydrothermal vents. Conservation Genetics Resources **3**(1): 25-27.

Schweitzer, CE and RM Feldmann (2000). First notice of the Chirostylidae (Decapoda) in the fossil record and new Tertiary Galatheidae (Decapoda) from the Americas. Bulletin of the Mizunami Fossil Museum **27**: 147-165.

Schweitzer, CE and RM Feldmann (2008). New Eocene hydrocarbon seep decapod crustacean (Anomura: Galatheidae: Shinkaiinae) and its paleobiology. Journal of Paleontology **82**(5): 1021-1029.

Sclater, JG, NR Grindlay, JA Madsen and C Rommevaux-Jestin (2005). Tectonic interpretation of the Andrew Bain transform fault: Southwest Indian Ocean. Geochemistry Geophysics Geosystems **6**(9): Q09K10.

Selkoe, KA and RJ Toonen (2006). Microsatellites for ecologists: a practical guide to using and evaluating microsatellite markers. Ecology Letters **9**(5): 615-629.

Sellanes, J, E Quiroga and C Neira (2008). Megafauna community structure and trophic relationships at the recently discovered Concepción Methane Seep Area, Chile, ,at 36˚ S. ICES Journal of Marine Science: Journal du Conseil **65**(7): 1102-1111.

Shank, TM, MB Black, KM Halanych, RA Lutz and RC Vrijenhoek (1999). Miocene radiation of deep-sea hydrothermal vent shrimp (Caridea: Bresiliidae): evidence from mitochondrial cytochrome oxidase subunit I. Molecular Phylogenetics and Evolution **13**(2): 244-254.

Shank, TM and KM Halanych (2007). Toward a mechanistic understanding of larval dispersal: insights from genomic fingerprinting of the deep-sea hydrothermal vent tubeworm *Riftia pachyptila*. Marine Ecology **28**(1): 25-35.

Shank, TM, R Lutz and R Vrijenhoek (1998). Molecular systematics of shrimp (Decapoda: Bresiliidae) from deep-sea hydrothermal vents, I: Enigmatic "small orange" shrimp from the Mid-Atlantic Ridge are juvenile *Rimicaris exoculata*. Molecular Marine

Biology and Biotechnology **7**(2): 88-96.

Shilling, FM and DT Manahan (1994). Energy metabolism and amino acid transport during early development of Antarctic and temperate echinoderms. The Biological Bulletin **187**(3): 398-407.

Sibuet, M and K Olu (1998). Biogeography, biodiversity and fluid dependence of deep-sea cold-seep communities at active and passive margins. Deep-Sea Research Part II: Topical Studies in Oceanography **45**(1-3): 517-567.

Simmons, MP and H Ochoterena (2000). Gaps as characters in sequence-based phylogenetic analyses. Systematic Biology **49**(2): 369-381.

Slatkin, M (1977). Gene flow and genetic drift in a species subject to frequent local extinctions. Theoretical Population Biology **12**(3): 253-262.

Slatkin, M (1993). Isolation by distance in equilibrium and non-equilibrium populations. Evolution **47**(1): 264-279.

Slatkin, M (1995). A measure of population subdivision based on microsatellite allele frequencies. Genetics **139**(1): 457-462.

Smedbol, RK, A McPherson, MM Hansen and E Kenchington (2002). Myths and moderation in marine 'metapopulations'? Fish and Fisheries (Oxford) **3**(1): 20-35.

Smith, CR and A Baco (2003). Ecology of whale falls at the deep-sea floor. Oceanography and Marine Biology, an Annual Review, Volume 41: An Annual Review **41**: 311-354.

Smith, CR and AR Baco (1998). Phylogenetic and functional affinities between whale-fall, seep and vent chemoautotrophic communities. Cahiers De Biologie Marine **39**(3-4): 345-346.

Smith, CR, AR Baco and AG Glover (2002). Faunal succession on replicate deep-sea whale falls: time scales and vent-seep affinities. Cahiers De Biologie Marine **43**(3-4): 293-297.

Smith, CR and H Kukert (1989). Vent fauna on whale remains. Nature **341**: 27-28.

Smith, DC (1979). From extracellular to intracellular: the establishment of a symbiosis. Proceedings of the Royal Society of London. Series B. Biological Sciences **204**(1155): 115-130.

Southward, AJ (2005). Systematics and ecology of a new species of stalked barnacle (Cirripedia: Thoracica: Scalpellomorpha: Eolepadidae: Neolepadini) from the Pacific-Antarctic Ridge at 38˚ S. Senckenbergiana Maritima **35**(2): 147-156.

Southward, EC, V Tunnicliffe, M Black, D Dixon and L Dixon (1996). Ocean-ridge segmentation and vent tubeworms (Vestimentifera) in the NE Pacific. Geological Society London Special Publications **118**(1): 211.

Spiess, FN, KC Macdonald, T Atwater, R Ballard, A Carranza, D Cordoba, C Cox, VMD Garcia, J Francheteau, J Guerrero, J Hawkins, R Haymon, R Hessler, T Juteau, M Kastner, R Larson, B Luyendyk, JD Macdougall, S Miller, W Normark, J Orcutt and C Rangin (1980). East Pacific Rise: hot springs and geophysical experiments. Science **207**(4438): 1421-1433.

Stahl, DA, DJ Lane, GJ Olsen and NR Pace (1984). Analysis of hydrothermal vent-associated symbionts by ribosomal RNA sequences. Science **224**(4647): 409-411.

Suess, E, B Carson, S Ritger, J Moore, M Jones, L Kulm and G Cochrane (1985). Biological communities at vent sites along the subduction zone off Oregon. Bulletin of the Biological Society of Washington(6): 475-484.

Tajima, F (1989). Statistical method for testing the neutral mutation hypothesis by DNA polymorphism. Genetics **123**(3): 585.

Tebbens, S and S Cande (1997). Southeast Pacific tectonic evolution from early Oligocene. Journal of Geophysical Research **102**(B6): 12,061-012,084.

Teixeira, S, MA Cambon Bonavita, EA Serrão, D Desbruyères and S Arnaud Haond (2010). Recent population expansion and connectivity in the hydrothermal shrimp *Rimicaris exoculata* along the Mid-Atlantic Ridge. Journal of Biogeography **38**(3): 564-574.

Teixeira, S, EA Serrão and S Arnaud-Haond (2012a). Characterization of 15 polymorphic microsatellite loci in *Rimicaris exoculata*, and cross-amplification in other hydrothermal-vent shrimp. Conservation Genetics Resources **4**(1): 81-84.

Teixeira, S, EA Serrão and S Arnaud-Haond (2012b). Panmixia in a fragmented and unstable environment: the hydrothermal shrimp *Rimicaris exoculata* disperses extensively along the Mid-Atlantic Ridge. Plos One **7**(6): e38521.

Terwilliger, RC, NB Terwilliger and A Arp (1983). Thermal vent clam (*Calyptogena magnifica*) hemoglobin. Science **219**(4587): 981-983.

Thaler, AD, K Zelnio, R Jones, J Carlsson, CL Van Dover and TF Schultz (2010). Characterization of 12 polymorphic microsatellite loci in *Ifremeria nautilei*, a chemoautotrophic gastropod from deep-sea hydrothermal vents. Conservation Genetics Resources **2**(1): 101-103.

Thaler, AD, K Zelnio, W Saleu, TF Schultz, J Carlsson, C Cunningham, RC Vrijenhoek and CL Van Dover (2011). The spatial scale of genetic subdivision in populations of *Ifremeria nautilei*, a hydrothermal-vent gastropod from the southwest Pacific. BMC Evolutionary Biology **11**(1): 372.

Thatje, S, K Anger, JA Calcagno, GA Lovrich, HO Portner and WE Arntz (2005). Challenging the cold: Crabs reconquer the Antarctic. Ecology **86**(3): 619-625.

Thurber, AR, WJ Jones and K Schnabel (2011). Dancing for food in the deep sea: bacterial farming by a new species of yeti crab. Plos One **6**(11): e26243.

Toon, A, M Finley, J Staples and KA Crandall (2009). Decapod phylogenetics and molecular evolution. Crustacean Issues **18**: 613-622.

Tóth, G, Z Gáspári and J Jurka (2000). Microsatellites in different eukaryotic genomes: survey and analysis. Genome Research **10**(7): 967-981.

Tsang, LM, T-Y Chan, ST Ahyong and KH Chu (2011). Hermit to king, or hermit to all: multiple transitions to crab-like forms from hermit crab ancestors. Systematic Biology **60**(5): 616-629.

Tunnicliffe, V (1991). The biology of hydrothermal vents: ecology and evolution. Oceanography and Marine Biology **29**: 319-407.

Tunnicliffe, V (1992). Hydrothermal-vent communities of the deep sea. American Scientist **80**: 336-349.

Tunnicliffe, V, M Botros, ME Deburgh, A Dinet, HP Johnson, SK Juniper and RE McDuff (1986). Hydrothermal vents of Explorer Ridge, northeast Pacific. Deep-Sea Research Part A: Oceanographic Research Papers **33**(3): 401-412.

Tunnicliffe, V, RW Embley, JF Holden, DA Butterfield, GJ Massoth and SK Juniper (1997). Biological colonization of new hydrothermal vents following an eruption on Juan de Fuca Ridge. Deep-Sea Research Part I: Oceanographic Research Papers **44**(9-10): 1627-1644.

Tunnicliffe, V and CMR Fowler (1996). Influence of sea-floor spreading on the global hydrothermal vent fauna. Nature **379**(6565): 531-533.

Tunnicliffe, V, A McArthur and D McHugh (1998). A biogeographical perspective of the deep-sea hydrothermal vent fauna. Advances in Marine Biology **34**: 353-442.

Tyler, PA, CR German, E Ramirez-Llodra and CL Van Dover (2002). Understanding the biogeography of chemosynthetic ecosystems. Oceanologica Acta **25**(5): 227-241.

Tyler, PA, S Pendlebury, SW Mills, L Mullineaux, KJ Eckelbarger, M Baker and CM Young (2008). Reproduction of gastropods from vents on the East Pacific Rise and the Mid-Atlantic Ridge. Journal of Shellfish Research **27**(1): 107-118.

Tyler, PA and C Young (1999). Reproduction and dispersal at vents and cold seeps. Journal of the Marine Biological Association of the UK **79**(02): 193-208.

Tyler, PA and CM Young (2003). Dispersal at hydrothermal vents: a summary of recent progress. Hydrobiologia **503**(1-3): 9-19.

Van Dover, CL (2000). The ecology of deep-sea hydrothermal vents, Princeton University Press.

Van Dover, CL (2002). Trophic relationships among invertebrates at the Kairei hydrothermal vent field (Central Indian Ridge). Marine Biology **141**(4): 761-772.

Van Dover, CL, CR German, KG Speer, LM Parson and RC Vrijenhoek (2002). Evolution and biogeography of deep-sea vent and seep invertebrates. Science **295**(5558): 1253-1257.

Van Dover, CL, SE Humphris, D Fornari, CM Cavanaugh, R Collier, SK Goffredi, J Hashimoto, MD Lilley, AL Reysenbach, TM Shank, KL Von Damm, A Banta, RM Gallant, D Gotz, D Green, J Hall, TL Harmer, LA Hurtado, P Johnson, ZP McKiness, C Meredith, E Olson, IL Pan, M Turnipseed, Y Won, CR Young and RC Vrijenhoek (2001). Biogeography and ecological setting of Indian Ocean hydrothermal vents. Science **294**(5543): 818-823.

Van Dover, CL and AB Williams (1991). Egg size in squat lobsters (Galatheoidea): constraints and freedom. Crustacean(7): 143-156.

van Oosterhout, C, WF Hutchinson, DP Wills and P Shipley (2004). Microchecker: software for identifying and correcting genotyping errors in microsatellite data. Molecular Ecology Notes **4**(3): 535-538.

Vérard, C, K Flores and G Stampfli (2012). Geodynamic reconstructions of the South America-Antarctica plate system. Journal of Geodynamics **53**(0): 43-60.

Von Cosel, R and B Marshall (2003). Two new species of large mussels (Bivalvia: Mytilidae) from active submarine volcanoes and a cold seep off the eastern North Island of New Zealand, with description of a new genus. The Nautilus **117**(2): 31-46.

Von Damm, K (2000). Chemistry of hydrothermal vent fluids from 9-10˚ N, East Pacific Rise: "Time zero" the immediate posteruptive period. Journal of Geophysical Research: Solid Earth (1978-2012) **105**(B5): 11203-11222.

Vrijenhoek, RC (1997). Gene flow and genetic diversity in naturally fragmented metapopulations of deep-sea hydrothermal vent animals. Journal of Heredity **88**(4): 285-293.

Vrijenhoek, RC (2010). Genetic diversity and connectivity of deep-sea hydrothermal vent metapopulations. Molecular Ecology **19**(20): 4391-4411.

Vrijenhoek, RC (2013). On the instability and evolutionary age of deep-sea chemosynthetic communities. Deep Sea Research Part II: Topical Studies in Oceanography **92**: 189-200.

Vrijenhoek, RC, SB Johnson and GW Rouse (2009). A remarkable diversity of bone-eating worms (*Osedax*; Siboglinidae; Annelida). BMC Biology **7**.

Wang, J, R Lin, RN Bamber and D Huang (2013). Two new species of Sericosura Fry & Hedgpeth, 1969 (Arthropoda: Pycnogonida: Ammotheidae) from a hydrothermal vent on the East Pacific Rise. Zootaxa **3669**(2): 165-171.

Watanabe, H and J Hashimoto (2002). A new species of the genus Rimicaris (Alvinocarididae : Caridea : Decapoda) from the active hydrothermal vent field, "Kairei field," on the Central Indian Ridge, the Indian Ocean. Zoological Science **19**(10): 1167-1174.

Watanabe, H, R Kado, M Kaida, S Tsuchida and S Kojima (2006). Dispersal of vent-barnacle (genus *Neoverruca*) in the Western Pacific. Cahiers De Biologie Marine **47**(4): 353-357.

Webber, W (2004). A new species of *Alvinocaris* (Crustacea: Decapoda: Alvinocarididae) and new records of alvinocaridids from hydrothermal vents north of New Zealand. Zootaxa **444**: 1-26.

Weber, JL and C Wong (1993). Mutation of human short tandem repeats. Human Molecular Genetics **2**(8): 1123-1128.

Weetman, D, A Ruggiero, S Mariani, PW Shaw, AR Lawler and L Hauser (2007). Hierarchical population genetic structure in the commercially exploited shrimp *Crangon crangon* identified by AFLP analysis. Marine Biology **151**(2): 565-575.

Wiens, J and D Moen (2008). Missing data and the accuracy of Bayesian phylogenetics. Journal of Systematics and Evolution **46**: 307-314.

Wiens, JJ (2006). Missing data and the design of phylogenetic analyses. Journal of Biomedical Informatics **39**(1): 34-42.

Williams, AB and PA Rona (1986). Two new caridean shrimps (Bresiliidae) from a hydrothermal field on the Mid-Atlantic Ridge. Journal of Crustacean Biology **6**(3): 446-462.

Williams, N, D Dixon, E Southward and P Holland (1993). Molecular evolution and diversification of the vestimentiferan tube worms. Journal of the Marine Biological Association of the UK **73**(02): 437-452.

Wilson, GA and B Rannala (2003). Bayesian inference of recent migration rates using multilocus genotypes. Genetics **163**(3): 1177-1191.

Wittmann, AC, D Storch, K Anger, HO Portner and FJ Sartoris (2010). Temperature-dependent activity in early life stages of the stone crab *Paralomis granulosa* (Decapoda, Anomura, Lithodidae): a role for ionic and magnesium regulation? Journal of Experimental Marine Biology and Ecology **397**(1): 27-37.

Won, Y, CR Young, RA Lutz and RC Vrijenhoek (2003). Dispersal barriers and isolation among deep-sea mussel populations (Mytilidae : *Bathymodiolus*) from eastern Pacific hydrothermal vents. Molecular Ecology **12**(1): 169-184.

Wright, S (1932). Evolution in Mendelian populations. Genetics **16**: 97-159.

Wright, S (1943). Isolation by distance. Genetics **28**(2): 114.

Wright, S (1950). Genetical structure of populations. Nature **166**: 247-249.

Xie, W, PO Lewis, Y Fan, L Kuo and M-H Chen (2011). Improving marginal likelihood estimation for Bayesian phylogenetic model selection. Systematic Biology **60**(2): 150-160.

Yang, Z and B Rannala (2012). Molecular phylogenetics: principles and practice. Nature Reviews Genetics **13**(5): 303-314.

Yao, HM, M Dao, T Imholt, JM Huang, K Wheeler, A Bonilla, S Suresh and C Ortiz (2010). Protection mechanisms of the iron-plated armor of a deep-sea hydrothermal vent gastropod. Proceedings of the National Academy of Sciences of the United States of America **107**(3): 987-992.

Young, CM, E Vazquez, A Metaxas and P Tyler (1996). Embryology of vestimentiferan tube worms from deep-sea methane/sulphide seeps. Nature **381**: 514-516.

Young, CR, S Fujio and RC Vrijenhoek (2008). Directional dispersal between mid-ocean ridges: deep-ocean circulation and gene flow in *Ridgeia piscesae*. Molecular Ecology **17**(7): 1718-1731.

Zelnio, K, A Thaler, R Jones, W Saleu, T Schultz, C Van Dover and J Carlsson (2010). Characterization of nine polymorphic microsatellite loci in *Chorocaris* sp. (Crustacea, Caridea, Alvinocarididae) from deep-sea hydrothermal vents. Conservation Genetics Resources **2**(1): 223-226.

Zwickl, DJ (2006). Genetic algorithm approaches for the phylogenetic analysis of large biological sequence datasets under the maximum likelihood criterion, University of Texas at Austin. **Doctor of Philosophy**.

Appendix

First and Co-Authored Research Papers

Published in the Course of this D.Phil

In Chronological Order

OPEN ACCESS Freely available online

PLoS BIOLOGY

The Discovery of New Deep-Sea Hydrothermal Vent Communities in the Southern Ocean and Implications for Biogeography

Alex D. Rogers[1]*, Paul A. Tyler[2], Douglas P. Connelly[3], Jon T. Copley[2], Rachael James[3], Robert D. Larter[4], Katrin Linse[4], Rachel A. Mills[2], Alfredo Naveira Garabato[2], Richard D. Pancost[5], David A. Pearce[4], Nicholas V. C. Polunin[6], Christopher R. German[7], Timothy Shank[7], Philipp H. Boersch-Supan[1,8], Belinda J. Alker[3], Alfred Aquilina[2], Sarah A. Bennett[3¤a], Andrew Clarke[4], Robert J. J. Dinley[2], Alastair G. C. Graham[4], Darryl R. H. Green[3], Jeffrey A. Hawkes[2,3], Laura Hepburn[2], Ana Hilario[9], Veerle A. I. Huvenne[3], Leigh Marsh[2], Eva Ramirez-Llodra[10], William D. K. Reid[6], Christopher N. Roterman[1,2], Christopher J. Sweeting[6], Sven Thatje[2], Katrin Zwirglmaier[4]

1 Department of Zoology, University of Oxford, Oxford, United Kingdom, **2** Ocean and Earth Science, National Oceanography Centre, Southampton, University of Southampton, Southampton, United Kingdom, **3** Natural Environment Research Council, National Oceanography Centre, Southampton, Southampton, United Kingdom, **4** British Antarctic Survey, Cambridge, United Kingdom, **5** School of Chemistry, University of Bristol, Bristol, United Kingdom, **6** School of Marine Science and Technology, Newcastle University, Newcastle upon Tyne, United Kingdom, **7** Woods Hole Oceanographic Institution, Woods Hole, Massachusetts, United States of America, **8** Scottish Oceans Institute, University of St Andrews, St Andrews, United Kingdom, **9** Centro de Estudos do Ambiente e do Mar, Departmento Biologia, Universidade de Aveiro, Aveiro, Portugal, **10** Institut de Ciències del Mar, Consejo Superior de Investigaciones Científicas, Barcelona, Spain

Abstract

Since the first discovery of deep-sea hydrothermal vents along the Galápagos Rift in 1977, numerous vent sites and endemic faunal assemblages have been found along mid-ocean ridges and back-arc basins at low to mid latitudes. These discoveries have suggested the existence of separate biogeographic provinces in the Atlantic and the North West Pacific, the existence of a province including the South West Pacific and Indian Ocean, and a separation of the North East Pacific, North East Pacific Rise, and South East Pacific Rise. The Southern Ocean is known to be a region of high deep-sea species diversity and centre of origin for the global deep-sea fauna. It has also been proposed as a gateway connecting hydrothermal vents in different oceans but is little explored because of extreme conditions. Since 2009 we have explored two segments of the East Scotia Ridge (ESR) in the Southern Ocean using a remotely operated vehicle. In each segment we located deep-sea hydrothermal vents hosting high-temperature black smokers up to 382.8°C and diffuse venting. The chemosynthetic ecosystems hosted by these vents are dominated by a new yeti crab (*Kiwa* n. sp.), stalked barnacles, limpets, peltospiroid gastropods, anemones, and a predatory sea star. Taxa abundant in vent ecosystems in other oceans, including polychaete worms (Siboglinidae), bathymodiolid mussels, and alvinocaridid shrimps, are absent from the ESR vents. These groups, except the Siboglinidae, possess planktotrophic larvae, rare in Antarctic marine invertebrates, suggesting that the environmental conditions of the Southern Ocean may act as a dispersal filter for vent taxa. Evidence from the distinctive fauna, the unique community structure, and multivariate analyses suggest that the Antarctic vent ecosystems represent a new vent biogeographic province. However, multivariate analyses of species present at the ESR and at other deep-sea hydrothermal vents globally indicate that vent biogeography is more complex than previously recognised.

Citation: Rogers AD, Tyler PA, Connelly DP, Copley JT, James R, et al. (2012) The Discovery of New Deep-Sea Hydrothermal Vent Communities in the Southern Ocean and Implications for Biogeography. PLoS Biol 10(1): e1001234. doi:10.1371/journal.pbio.1001234

Academic Editor: Jonathan A. Eisen, University of California Davis, United States of America

Received June 6, 2011; **Accepted** November 22, 2011; **Published** January 3, 2012

Funding: The ChEsSo research programme was funded by a NERC Consortium Grant (NE/DO1249X/1) and supported by the Census of Marine Life and the Sloan Foundation, and the Total Foundation for Biodiversity (Abyss 2100)(SVTH) all of which are gratefully acknowledged. We also acknowledge NSF grant ANT-0739675 (CG and TS), NERC PhD studentships NE/D01429X/1(LH, LM, CNR), NE/H524922/1(JH) and NE/F010664/1 (WDKR), a Cusanuswerk doctoral fellowship, and a Lesley & Charles Hilton-Brown Scholarship, University of St. Andrews (PHBS). The funders had no role in study design, data collection and analysis, decision to publish, or preparation of the manuscript.

Competing Interests: The authors have declared that no competing interests exist.

Abbreviations: AIC, Akaike Information Criterion; CTD, conductivity–temperature–depth; ESR, East Scotia Ridge; ICL, inductively coupled link; MRT, multivariate regression tree; Mya, million years ago; NOC, National Oceanography Centre, Southampton; ROV, remotely operated vehicle; SHRIMP, Seabed High Resolution Imaging Platform

* E-mail: alex.rogers@zoo.ox.ac.uk

¤a Current address: NASA Jet Propulsion Laboratory, California Institute of Technology, Pasadena, California, United States of America

Author Summary

Deep-sea hydrothermal vents are mainly associated with seafloor spreading at mid-ocean ridges and in basins near volcanic island arcs. They host animals found nowhere else that derive their energy not from the sun but from bacterial oxidation of chemicals in the vent fluids, particularly hydrogen sulphide. Hydrothermal vents and their communities of organisms have become important models for understanding the origins and limits of life as well as evolution of island-like communities in the deep ocean. We describe the fauna associated with high-temperature hydrothermal vents on the East Scotia Ridge, Southern Ocean, to our knowledge the first to be discovered in Antarctic waters. These communities are dominated by a new species of yeti crab, stalked barnacles, limpets and snails, sea anemones, and a predatory seven-armed starfish. Animals commonly found in hydrothermal vents of the Pacific, Atlantic, and Indian Oceans, including giant *Riftia* tubeworms, annelid worms, vent mussels, vent crabs, and vent shrimps, were not present at the Southern Ocean vents. These discoveries suggest that the environmental conditions of the Southern Ocean may act as a barrier to some vent animals and that the East Scotia Ridge communities form a new biogeographic province with a unique species composition and structure.

Introduction

The discovery of hydrothermal vents along the Galápagos Ridge in 1977 [1] led to the identification of chemoautotrophic symbiosis [2] and forced marine biologists to reassess the contribution chemosynthesis makes to marine primary production, particularly in the deep sea, where it supports a high biomass in an otherwise food-limited ecosystem. The existence of life in the extremely harsh conditions of hydrothermal vents has stimulated an increasing research effort on the diversity, ecology, and physiology of vent organisms, as well as new avenues of research into the origins of life on Earth [3] and even into the occurrence of life elsewhere within and outside the solar system. Because of the characteristics of hydrothermal vent communities—in particular the high levels of species endemism, their constraint to discrete habitats separated at different spatial scales and by geological/environmental barriers, their global distribution, and their historical coupling to plate tectonics—they are regarded as unique ecosystems. In particular, ecologists recognise that the unusual characteristics of deep-sea vents compared to other deep-sea habitats, coupled with the ephemeral nature of hydrothermal circulation, have probably had important implications for the composition, diversity, and biogeography of their communities and the dispersal and genetic population structure of vent species [4–6].

Several decades of exploration have resulted in the detection of numerous vent sites and faunal assemblages at many mid-ocean ridges and back-arc basins. These discoveries have resulted in an apparent global biogeography of vent organisms with separate provinces in the East Pacific, the North East Pacific, West Pacific back-arc basins, the shallow and deep Atlantic, and the Indian Ocean [7], although a more recent analysis has proposed a single province for the Atlantic, a single province for the North West Pacific, a single province for the South West Pacific and Indian Ocean, and a biogeographic separation of the North East Pacific, North East Pacific Rise, and South East Pacific Rise [8]. These biogeographic provinces are based on sampling undertaken by human-occupied vehicles and remotely operated vehicles (ROVs), and for the most part lie within the tropics and sub-tropics, where deep submergence operations are less limited by prevailing sea conditions than at high latitudes [6,9]. Weather conditions have constrained the discovery of hydrothermal vents at high latitudes, although there is evidence from water column plumes that vents occur in the Arctic along the Gakkel Ridge [10], the Mohn Ridge, [11] and the Arctic Mid-Ocean Ridge [12], and in the Southern Ocean, in Antarctica, along the East Scotia Ridge (ESR), in the Scotia Sea [13], in the Bransfield Strait, west of the northern Antarctic Peninsula [14,15], and along the Pacific-Antarctic Ridge [16]. In the Arctic, animal communities have been described at deep-sea hydrothermal vents on the Mohn and Arctic Mid-Ocean Ridges, although only the latter appears to host a high biomass of vent-endemic fauna [11,12]. Here we show, to our knowledge for the first time, the presence of black smokers, diffuse venting, and associated chemosynthetically driven ecosystems along the ESR, a geographically isolated back-arc spreading centre in the Atlantic sector of the Southern Ocean, Antarctica (Figure 1A). Based on biological observations we also present a re-analysis of the global biogeography of the deep-sea hydrothermal vent fauna, including that of the Antarctic hydrothermal vents.

The Scotia Sea is defined by a loop of shallow banks and islands, known as the Scotia Arc, that extends eastwards from Cape Horn, south of the Falkland Islands (Burdwood Bank, Shag Rocks, and South Georgia), then southwards along the South Sandwich Arc, and westwards along the South Scotia Ridge, including the South Orkney Islands, to the tip of the Antarctic Peninsula near Elephant Island. The western boundary is formed by the Shackleton Fracture Zone. With the exception of these peripheral ridges, the ESR (Figure 1A) and various shallow banks (e.g., Pirie Bank, Bruce Bank), much of the Scotia Sea extends to depths in excess of 3,000 m. West of the ESR, the floor of the Scotia Sea forms part of the Scotia Plate. To the east of the ESR lies the small South Sandwich Plate, beneath which the South American Plate is being subducted at the South Sandwich Trench. To the north, the Scotia Plate abuts the South American Plate at the North Scotia Ridge, while to the south is the Antarctic Plate boundary at the South Scotia Ridge. Both of these are strike-slip plate boundaries [17]. The ESR is ~500 km long, and spreading was initiated more than 15 million years ago (Mya) [18] and is presently proceeding at an average full spreading rate of ~70 mm y^{-1}. The ESR consists of nine second-order ridge segments (E1 to E9), separated by non-transform discontinuities [19]. E3 to E8 have well-developed deep rift valleys, but E2 and E9 are characterised by smooth volcanic highs, typical of faster-spreading mid-ocean ridges. An axial magma chamber is known to underlie segment E2 [20], and another is suspected to underlie segment E9 [21]. The southern end of segment E9 is curved to the east because of changes in the stress field as the strike-slip faults separating the South Sandwich and Scotia plates from the Antarctic plate are approached.

The first evidence of hydrothermal activity along the ESR was from data obtained by a light-scattering sensor attached to the Towed Ocean Bottom Instrument (TOBI), a deep-towed sonar system, during a geophysical mapping survey along the ESR in 1999 [13]. Additional evidence was obtained from conductivity–temperature–depth (CTD) profiles and manganese anomalies in water samples collected at depth during that survey. In the austral summer of 2009 we conducted a survey of segments E2 and E9 using a CTD sensor that was continuously raised and lowered in the water column (“tow-yo”), with attached light-scattering sensor and redox potential (Eh) sensors to track hydrothermal plumes and locate potential vent sites to within 100 to 500 m. We then used a lowered camera system, Seabed High Resolution Imaging

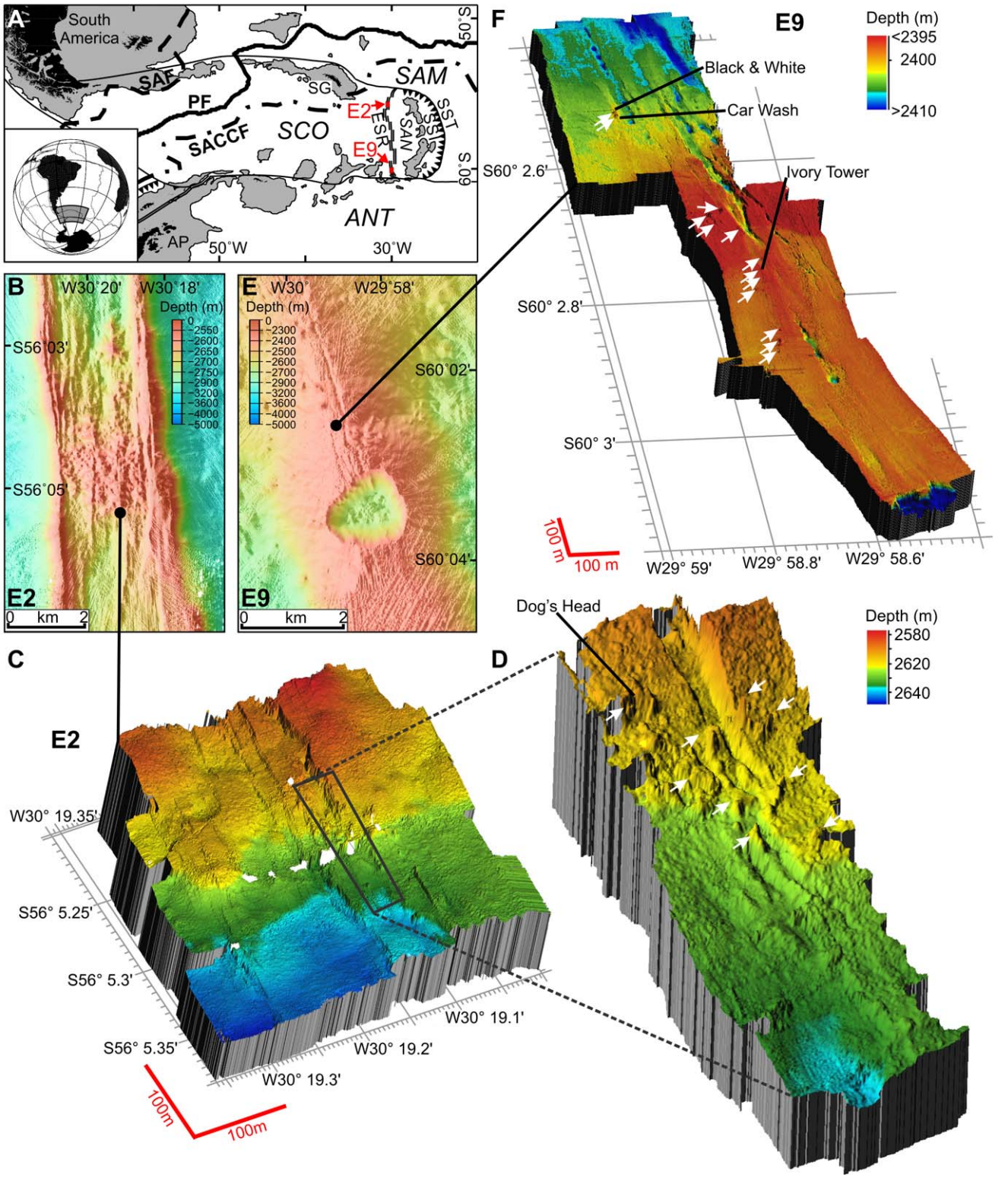

Figure 1. Maps of the position and geophysical setting of the ESR vents. (A) The Scotia Sea showing the ESR in relation to the Scotia Plate (SCO), South Sandwich Plate (SAN), South American Plate (SAM), the Antarctic Plate (ANT), the Antarctic Peninsula (AP), and the South Sandwich Trench (SST). Oceanographic features shown include the Polar Front (PF), the Sub-Antarctic Front (SAF), and the southern Antarctic Circumpolar Current Front (SACCF). The sites E2 and E9 are indicated by red arrows. (B) Ship-based swath bathymetry of the vent sites at E2 showing the axial summit graben. The black circle indicates the sites of main venting. (C and D) ROV-based 3-D swath bathymetry of E2 (C) and high-resolution swath bathymetry of the major steep-sided fissure that runs north–south through the centre of the site, between longitude 30° 19.10′W and 30° 19.15′W (D). Dog's Head vent site is indicated. White arrows indicate vent sites not mentioned in text. (E) Ship-based swath bathymetry of the vent sites at E9 showing the axial fissures and the collapsed crater called the Devil's Punchbowl. The black spot indicates the sites of main venting. (F) ROV-based 3-D

swath bathymetry of the vent sites at E9. The vent sites Ivory Tower, Car Wash, and Black and White are indicated. Other vent sites are indicated by white arrows.
doi:10.1371/journal.pbio.1001234.g001

Platform (SHRIMP), with down-looking and oblique video cameras to survey the seafloor in as systematic a fashion as possible. At E2 we located black smoker chimneys, as well as observing associated fauna, and at E9 we found considerable evidence of diffuse hydrothermal venting, with anemones and stalked barnacles being the dominant megafauna. Because SHRIMP is controllable only in the vertical plane, we withdrew it from the vent sites to prevent unnecessary damage, in accordance with InterRidge guidelines [22]. In the austral summer of 2010 we returned with the ROV *Isis* and conducted a full and systematic survey of the previously located vent sites at E2 and E9. This was supplemented by additional video analysis using SHRIMP in the austral summer of 2011.

Results

Hydrothermal Setting of Vents at E2 and E9

The vent sites at E2 lie just south of the segment axial high (called the Mermaid's Purse [20]), between 56° 5.2′ and 56° 5.4′ S and between 30° 19′ and 30° 19.35′W at ~2,600 m depth (Figure 1B). Prominent north–south structural fabric to the seafloor defines a series of staircased, terraced features that are divided by west-facing scarps (Figure 1C and 1D). A major steep-sided fissure runs north–south through the centre of the site, between longitude 30° 19.10′W and 30° 19.15′W (Figure 1D). The fissure is filled in places by lobes of pillow basalts, and the main hydrothermal vents are located at the intersection between this main fissure and a west–east striking fault or scarp, consistent with the expected location of active venting on back-arc spreading ridges. Relict (extinct) and actively venting chimneys are resolvable in the high-resolution multibeam bathymetry obtained by the ROV *Isis*, clustered in a band running approximately northwest–southeast. Numerous volcanic cones and small volcanic craters are also apparent around the vent field. Chimneys of variable morphology were up to 15 m tall and venting clear fluid with a maximum measured temperature of 352.6°C, which formed focused black smokers on contact with cold seawater (Figure 2A). Some of the chimneys have expanded tops with hot vent fluid (>300°C) emanating from the underside (Figure 2B), similar to the flanges found at North East Pacific vents [23]. Diffuse vent flow was observed at a variety of locations, with temperatures varying from 3.5 to 19.9°C, compared with a background temperature of ~0.0°C. Around the periphery of the active high-temperature vents and diffuse flow sites are microbial mats that form a halo around the venting area at E2 (Figure 2C).

The vent sites at E9 are situated between 60° 02.5′ and 60° 03.00′S and between 29° 59′ and 29° 58.6′W, at ~2,400 m depth, amongst relatively flat sheet lavas to the north of a major collapse crater (named the Devil's Punchbowl; Figure 1E). The ridge axis is heavily crevassed and fissured, with numerous collapse features, lava drain-back features, and broken pillow lava ridges. Major fissures run north-northwest–south-southeast through the site, breaking up an otherwise flat and unvaried terrain (Figure 1F). Topographic highs in the centre of the study site are possibly dead magma domes, with no hydrothermal activity around these sites. Most active venting appears to lie along one of the smaller fissures, west of a main north–south trending feature. Diffuse flow and black smokers line the feature intermittently, but activity becomes reduced and dies away farther south, towards the "punchbowl" itself. The chimneys were either emitting high-temperature fluids with a maximum temperature of 382.8°C (Ivory Tower; Figure 1F) or had lower temperature diffuse flow between 5 and 19.9°C (Car Wash vent; Figure 1F). Low-temperature diffuse flow was associated with fissures and fine cracks in the sheet lava; the background temperature at E9 varied from −0.11°C to −1.3°C.

Chemical and Physical Characteristics of E2 and E9

A summary of the preliminary chemical and physical data from the vents on both E2 and E9 north and south is given in Table 1. This table also includes data for the closest known vent sites to the ESR in the Atlantic, Indian, and Pacific Oceans, as well as from other hydrothermal vents associated with back-arc basins [24–28]. The chemical composition of fluids from E2 is distinct from that at E9, and within E9 there are notable differences in the vent fluid chemistry between vents in the northern part of the site and those in the southern part (Table 1). The chloride (Cl) concentration of fluids from E2 is similar to that of seawater, whereas fluids from E9 have very low levels of Cl and, as a consequence, they have lower concentrations of the major cations such as sodium, and higher concentrations of volatiles including hydrogen sulphide (H_2S). This has the potential to impact the energy available for microbial populations at the vent sites, with volatile-dominated systems having higher hydrogen sulphide and hence higher microbial populations [29].

Initial analysis of the data from the seafloor-mounted acoustic doppler current profiler, deployed at E2 and E9 for 7 d each, suggests a semidiurnal north–south tidal flow with velocities between 50 and 100 mm s^{-1} in the bottom 50 m at E2. The flow in the bottom 50 m at E9 is more complicated, with an underlying semidiurnal tidal flow up to 100 mm s^{-1} plus an asymmetric west–east–west flow of ~50 mm s^{-1}.

Microbial and Faunal Composition and Distribution at E2 and E9

Examination of 16S rDNA clone libraries from water samples taken within the buoyant vent plumes over E2 and E9 show a highly similar composition of the microbial communities at both sites. Proteobacteria make up 70% of the bacterial community at E2 (66% at E9). Within the proteobacteria, gammaproteobacteria are the dominant group (58% and 55% at E2 and E9, respectively). More than half of the gammaproteobacterial sequences (59% at E2 and 58% at E9) show high similarity (>99%) to bacterial endo- and epi-symbionts of hydrothermal vent fauna from elsewhere. Within the alphaproteobacteria, more than 90% of the sequences fall within the SAR11 clade, a group of ubiquitous heterotrophic bacteria found throughout the oceans. Other numerically abundant sequences in the clone libraries are closely related to Bacteroidetes (12% at E2 and 13% at E9) and Deferribacterales (11% at E2 and 12% at E9). Sequences for the bacterial clone libraries have been deposited in GenBank (http://www.ncbi.nlm.nih.gov/genbank/; accession numbers JN562472–JN562714).

At E2 and E9, the fauna is visually dominated by extensive dense aggregations of a new species of yeti crab, *Kiwa* n. sp. (Figure 2D and 2E). This species shows sequence divergences for mitochondrial 16S rDNA and nuclear 18S and 28S rDNA of

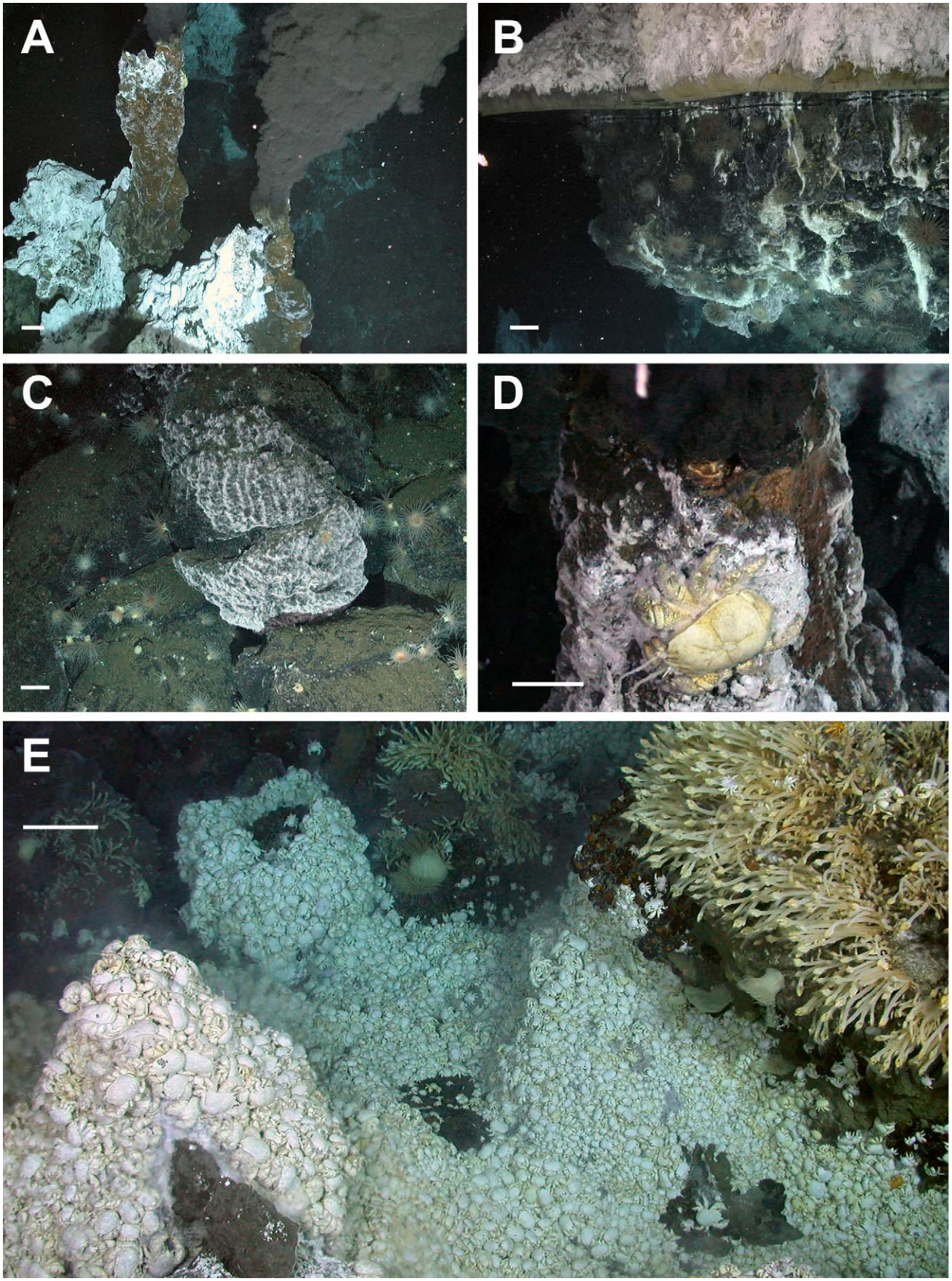
A
B
C
D
E

Figure 2. Photographs of vents and associated biological communities. (A) Active black smoker chimneys at E2 (Dive 128, 2,602 m depth). (B) Vent flange at E2 with trapped high-temperature reflective hydrothermal fluid (Dive 129, 2,621 m depth). (C) Microbial mat covering rock surfaces on vent periphery at E2 (Dive 134, 2,604 m depth). (D) Active vent chimney at E9 supporting the new species of the anomuran crab *Kiwa*. (Dive 144, 2,396 m depth). (E) Dense mass of the anomuran crab *Kiwa* n. sp. at E9 with the stalked barnacle cf. *Vulcanolepas* attached to nearby chimney (Dive 138, 2,397 m depth). Scale bars: 10 cm for foreground.
doi:10.1371/journal.pbio.1001234.g002

6.45%, 0.49%, and 1.8%, respectively, when compared with *K. hirsuta* from the Pacific-Antarctic Ridge (GenBank accession numbers JN628249, JN628250, JN628251). This variation is within the range of congeneric species comparisons for the Anomura [30], and a phylogenetic analysis, using Bayesian inference, of anomuran taxa, indicates that *Kiwa* n. sp. is the sister taxon of *K. hirsuta* (Figure S1). Using known substitution rates from geminate species pairs of anomuran crustaceans from either side of the Isthmus of Panama, the 16S data suggest a putative divergence between *K. hirsuta* and *Kiwa* n. sp. from the ESR at ~12.2 Mya (0.53% per million years [31]), although such a preliminary date of divergence is subject to a high level of error. The new species of *Kiwa* from the ESR has dense mats of two distinct types of setae covering the ventral surface of the body, in contrast to *K. hirsuta*, which has sparse long setae on the ventral surface and a dense covering of long setae on the pereopods and particularly the chelipeds [9]. Filamentous bacteria were observed attached to the setae, as also seen in *K. hirsuta* [31]. Macpherson et al. [9] suggested that *K. hirsuta* is omnivorous, following observations of individuals consuming damaged mussels. However, the presence of sulphur-oxidising bacteria on the setae of this species [32] suggests that *K. hirsuta* may harvest bacteria as a nutritional source [9], and if this is the case, *Kiwa* n. sp. from E2 and E9 may also utilise epibiotic bacteria in the same way. At E2 dense aggregations of crabs may be found adjacent to and on chimneys, with large individuals closely associated with the vent orifice. At E9 *Kiwa* n. sp. was more abundant than at E2, completely covering the seabed in some areas and reaching densities of 600 m^{-2} (Figure 2E). At some sites this species formed multiple layer aggregations. The distribution of sexes appears to be influenced by distance from vent sources, possibly determined by temperature or vent fluid composition. Males were found closest to vent orifices (Figure 2D), and non-berried females adjacent to the vent but in cooler waters. Berried females and juveniles were associated with low-temperature flow, ~5°C (as on Car Wash), and at the periphery of vent influence. They had considerably fewer filamentous bacteria on their setae than crabs near or on the chimneys, suggesting that the bacteria rely on the higher temperatures and chemistry in the immediate vicinity of the vent orifice for optimal growth.

Additional common fauna at the sites (Table 2) includes at least five morphospecies of sea anemone, three of which are found in diffuse flow associated with chimneys or sheet and pillow lavas in densities of up to ~70 m^{-2} (Figure 3A–3D). These include four putative species of Actinostolidae, a family that includes the anemones *Pacmanactis* and *Marianactis* found on deep-sea hydrothermal vents elsewhere. There is also a red anemone that is similar in appearance to *Chondrophellia* sp. or *Hormathia spinosa* (personal communication, E. Rodriguez, Division of Invertebrate Zoology, American Museum of Natural History). The most obvious gastropod is an undescribed peltospiroid species (Figures 3B, 3D, and 4), generally found in dense aggregations up to ~1,000 m^{-2}. A second common gastropod is a limpet of the genus *Lepetodrilus* (Figure 3D). Phylogenetic analysis of the mitochondrial cytochrome oxidase I gene of this limpet (GenBank accession number JN628254) and a range of other *Lepetodrilus* species, using Bayesian inference, places the ESR limpet as a sister taxon to *L. atlanticus* (Figure S2), with a sequence divergence from this species of 5.48%. This level of genetic divergence is consistent with that found between *Lepetodrilus* species within complexes of sister taxa where interspecific distances of between 3% and 15% have been observed [33]. This new species is ubiquitous in low-temperature diffuse flow, being found on bare rock, sulphides, *Kiwa* n. sp., peltospiroid gastropods, and stalked barnacles. On the carapace of *Kiwa* n. sp., a halo of pale colouration surrounding the limpets indicates where *Lepetodrilus* n. sp. is grazing epizoic microbes. *Lepetodrilus* species have also been found previously on the carapaces of bythograeid crabs [33], as well as on the shells of

Table 1. Chemical composition of the vent fluid end-member at E2 and E9 vent fields.

Region	Site	Maximum Temperature (°C)	[Cl−] (mM)	pH	H_2S (mM)	Na (mmol kg^{-1})	Si (mmol kg^{-1})
ESR	E2 (this study)	353	531	2.9	7.0	420	19
	E9N (this study)	383	98	3.4	9.5	96	8
	E9S (this study)	351	179	3.2	13.6	169	163
Mid-Ocean Ridges							
Atlantic Ocean	Nibelungen [26]	372	567	2.9	1.1	449	13.7
Indian Ocean	Kairei [25]	360	587	5.23		531	
Pacific Ocean	South East Pacific Rise [24]	340	190	3	8.6	125	10.6
Back-Arc Basins	Lau Basin [27]	334	650–800	2		520–615	14
	Pacmanus [28]	341	625	2.6	6.3	495	17.8
Seawater			541	7.9		464	0.18

Data from the Nibelungen vent field on the Mid-Atlantic Ridge [26], Kairei on the Central Indian Ridge [25], the 17.5°S site on the South East Pacific Rise [24], and sites in the Lau and Pacmanus back-arc basins [27,28] are provided for comparison. These represent the closest known mid-ocean ridge vent sites to E2 and E9 and geologically comparable back-arc basin sites.
doi:10.1371/journal.pbio.1001234.t001

Table 2. Dominant fauna at East Scotia Ridge vents E2 and E9.

Higher Taxon Levels			Species (or Lowest Taxonomic Identification)	
Phylum	**Subphylum or Class**	**Taxon Level 3**	**E2**	**E9**
Porifera	Demospongiae	Cladorhizidae	*Cladorhiza* n. sp. 1	*Cladorhiza* n. sp. 1
				Abyssocladia n. sp. 1
Cnidaria	Anthozoa	Hormathiidae		*Chondrophellia* sp. or *Hormathia spinosa*
		Actinostolidae		Actinostolidae n. sp. 1
			Actinostolidae n. sp. 2	Actinostolidae n. sp. 2
			Actinostolidae n. sp. 3	Actinostolidae n. sp. 3
			Actinostolidae n. sp. 4	
Annelida	Polychaeta		Polynoidae sp. 1	
				Polynoidae sp. 2
				Polynoidae sp. 3
				Polynoidae sp. 4
Mollusca	Gastropoda		Peltospiroidea n. sp.	Peltospiroidea n. sp.
			cf. *Protolira* sp.	cf. *Protolira* sp.
			Lepetodrilus n. sp.1	*Lepetodrilus* n. sp.1
			Provannid sp. 1	Provannid sp. 1
				Provannid sp. 2
	Cephalopoda			Octopodidae
Arthropoda	Crustacea	Cirripedia	*Vulcanolepas* n. sp.	*Vulcanolepas* n. sp.
		Anomura	*Kiwa* n. sp.	*Kiwa* n. sp.
	Pycnogonida		*Sericosura* sp. 1	*Sericosura* sp. 1
			Sericosura sp. 2	*Sericosura* sp. 2
				Sericosura sp. 3
			Colossendeis cf. *concedis* (vent periphery)	*Colossendeis* cf. *concedis* (vent periphery)
			Colossendeis cf. *elephantis* (vent periphery)	*Colossendeis* cf. *elephantis* (vent periphery)
Echinodermata	Asteroidea	Stichasteridae	Stichasteridae n. sp.	Stichasteridae n. sp.
		Freyellidae	*Freyella* cf. *fragilissima*	*Freyella* cf. *fragilissima*
Chordata	Vertebrata			Zoarcid fish

All identifications are putative and await detailed taxonomic and molecular analysis.

doi:10.1371/journal.pbio.1001234.t002

vent molluscs and the tubes of siboglinid worms [34]. Not as visually apparent, but abundant in sediment residue in the ROV sample bioboxes from vent and diffuse flow areas at E2 and E9, is a small species of provannid gastropod. Several unidentified octopi were also observed within hydrothermal vent fields at E9 (Figure 3F). The vent fauna also includes dense aggregations of a stalked barnacle morphologically consistent with the genus *Vulcanolepas* (Figures 2E, 3A, 3B, and 3E). Phylogenetic analyses using Bayesian inference of the histone H3 and 28S rDNA [35] of the ESR *Vulcanolepas* (GenBank accession numbers JN628252, JN628523) and stalked barnacles from other hydrothermal vents (Figure S3) confirmed that the ESR barnacles were most closely related to, but a distinct species from, *V. osheai* (divergence of 0.34% and 0.22%, respectively). The latter species was described from the Brothers Caldera, Kermadec Ridge, South West Pacific [36]. The ESR *Vulcanolepas* occurs at densities of up to $\sim$750 m^{-2}, particularly at E9 along the broken edge of sheet lava bathed in diffuse vent flow, as well as forming erect, dense colonies on chimneys emitting diffuse flow. Also scattered throughout the vent systems at E2 and E9 are at least three species of the vent pycnogonid *Sericosura* (Figure 3D), with the larger species *Colossendeis* cf. *concedis* and *C.* cf. *elephantis* occurring on the peripheral areas of the vents (personal communication, C. Arango, Queensland Museum South Bank). As at other vent sites in the Pacific and Atlantic Oceans [37–39], swarms of an unidentified amphipod were observed at E9. Although a variety of echinoderms were found during our observations, only one species, a seven-armed sea star from the family Stichasteridae (personal communication, C. Mah, Smithsonian National Museum of Natural History), appeared to be vent endemic (Figure 3E). This undescribed species was indicative of the proximity of vents in our 2009 observations, and during the 2010 campaign was found both peripherally and in areas of low-temperature diffuse venting. We observed it feeding on vent fauna, especially *Kiwa* n. sp. and barnacles. Fish were generally uncommon at the vent sites, and the only species that were observed were several species of macrourids on the vent periphery and a zoarcid, several specimens of which were recovered in baited traps at E9.

In order to examine how the fauna at E2 and E9 fit into the current understanding of the biogeography of deep-sea hydrothermal vents, we undertook an analysis of the global dataset on species presence/absence of most of the known hydrothermal vent

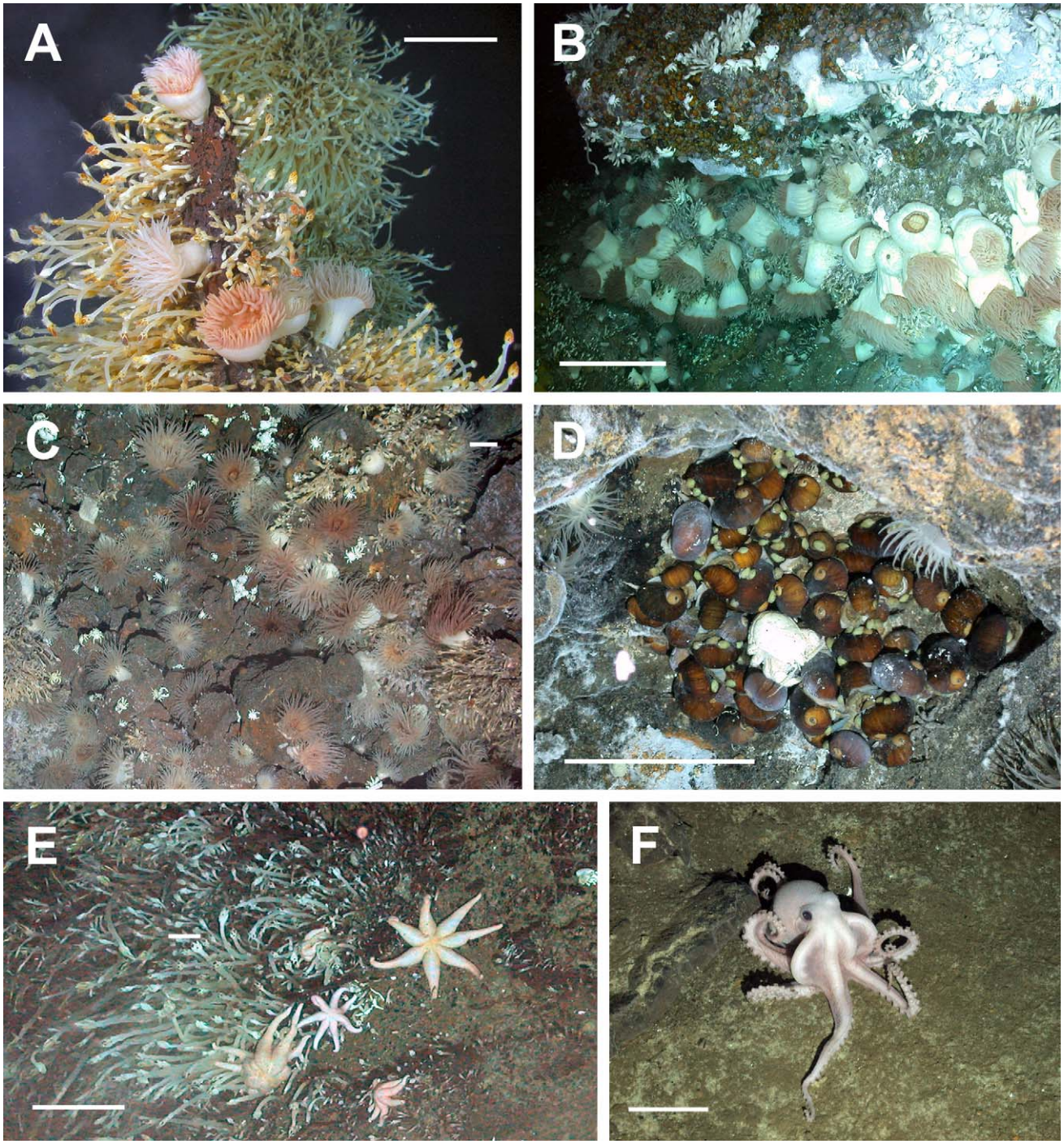

Figure 3. Photographs of the ESR vent fauna. (A) Actinostolid sea anemones surrounded by cf. *Vulcanolepas* on a chimney with diffuse hydrothermal venting at E9 (Dive 138, 2,396 m depth). (B) Dense field of actinostolid sea anemones along with peltospiroid gastropods (Dive 140, 2,394 m depth). (C) Anemone field at E9 with juvenile *Kiwa* n. sp. interspersed (Dive 139, 2,398 m depth). (D) Undescribed peltospiroid gastropod at E2 surrounding single *Kiwa* n. sp. and partially covered by *Lepetodrilus* n. sp. The pycnogonid cf. *Sericosura* is at the bottom right of the image (Dive 132, 2,608 m depth). (E) An undescribed seven-arm sea star predatory on the stalked barnacles cf. *Vulcanolepas* at E9 (Dive 139, 2,402 m depth). (F) Unidentified octopus at E9 (Dive 144, 2,394 m depth). Scale bars: 10 cm for foreground.
doi:10.1371/journal.pbio.1001234.g003

communities using multivariate regression trees (MRT) after Bachraty et al. [8], but with modifications (see Materials and Methods). The MRT analyses, with cross-validation, produced a series of trees, many of which were only marginally worse than the best predictive tree (Figure 5). The optimal tree size, based on cross-validation error, varied between three and ten provinces for the Bachraty et al. [8] dataset and three and 11 provinces for the Bachraty et al. [8] dataset plus E2 and E9 (combined dataset). The most common optimal trees were the five- and seven-province models for the Bachraty et al. [8] dataset (Text S1; Figure S4A)

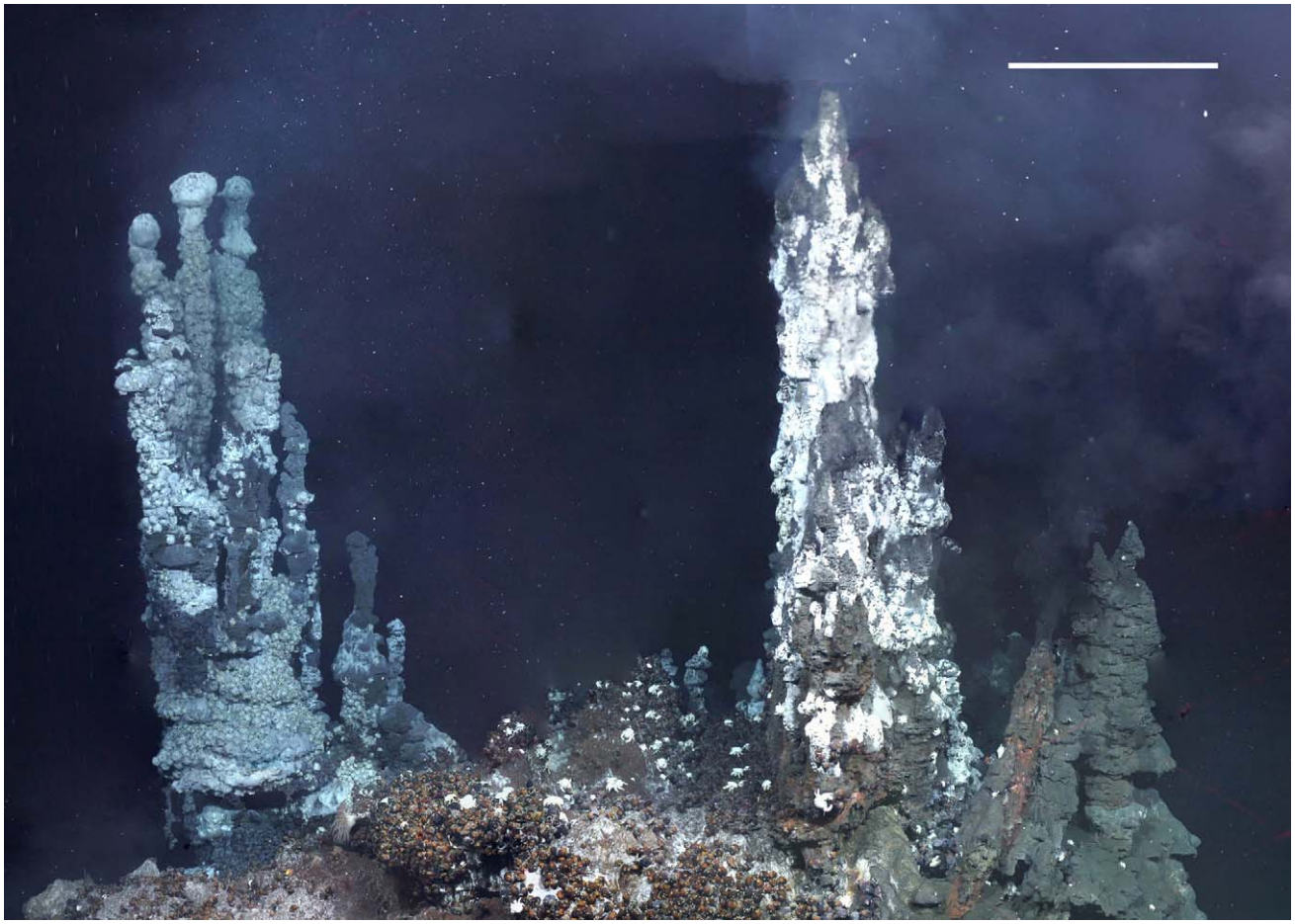

Figure 4. Collage of frame grabs of high-definition video to show fauna dispersion on the E9 vent site Ivory Tower. The vertical chimneys are covered with the anomuran *Kiwa* n. sp., and the area between the chimneys is occupied primarily by an undescribed peltospiroid gastropod (Dive 142, 2,398 m depth, ROV heading 090°). Scale bar: 1 m for foreground. Collage created by L. M.
doi:10.1371/journal.pbio.1001234.g004

and an 11-province model for the combined dataset (Figure 6). The six-province model proposed by Bachraty et al. [8] was not found to be the most frequently selected optimal tree. The 11-province model retained the Atlantic and East Pacific clusters but split up the Indo-Pacific province into five smaller clusters (Figure 6). In all iterations of the model (Figures 6 and S4) the sites south of the Easter Microplate in the South Pacific formed a separate cluster from all other East Pacific sites. E2 and E9 form a separate cluster for the optimal 11-province model (and seven-province model; see Figure S4) for the combined dataset, also suggesting that these sites form a new biogeographic province (but see discussion on the MRT method).

Discussion

Implications for Antarctic Biodiversity

Recent investigations of the deep-sea ecosystems of the Southern Ocean have revealed a high proportion of previously undescribed species, many of which are unknown from elsewhere [40]. Particularly notable in this respect are groups of the Isopoda, Ostracoda, Gastropoda, and Nematoda. It has been suggested that Southern Ocean species of these groups are not found outside of the Southern Ocean because they have life histories that are characterised by a low potential for dispersal [40]. Likewise, analyses of the fauna of the shelf and slopes of the islands of the Scotia Arc, as far north as Shag Rocks, suggest that the fauna is largely composed of Antarctic endemics [41]. The finding of a unique vent-endemic fauna within the Southern Ocean is consistent with this pattern of species distribution and is further evidence of the high regional endemism of the Antarctic marine biota. This study also provides the first identification and description, to our knowledge, of high-biomass hydrothermal-vent-endemic chemosynthetic communities in the Southern Ocean. Exploration of deep-sea hydrothermal vents in other sectors of the Southern Ocean, such as the Pacific-Antarctic Ridge [16], are likely to reveal further chemosynthetic communities.

Implications for Hydrothermal Vent Biogeography

The fauna observed at the vents along the ESR contains none of the dominant vent species normally found at vents along the main mid-ocean ridge systems. The ESR sites are notable for the absence of siboglinid tubeworms, alvinellid polychaetes, vesicomyid clams, bathymodiolid mussels, and alvinocaridid shrimp. In addition, there is an absence of typical predators such as bythograeid crabs. Species found at the ESR vents include anemones, lepetodrilid limpets, provannid gastropods, stalked barnacles, and at least three species of pycnogonids, thus these vents share some faunal elements with communities found at vents associated with back-arc basins in the West and South West Pacific, the mid-ocean ridge in the South East Pacific, and the

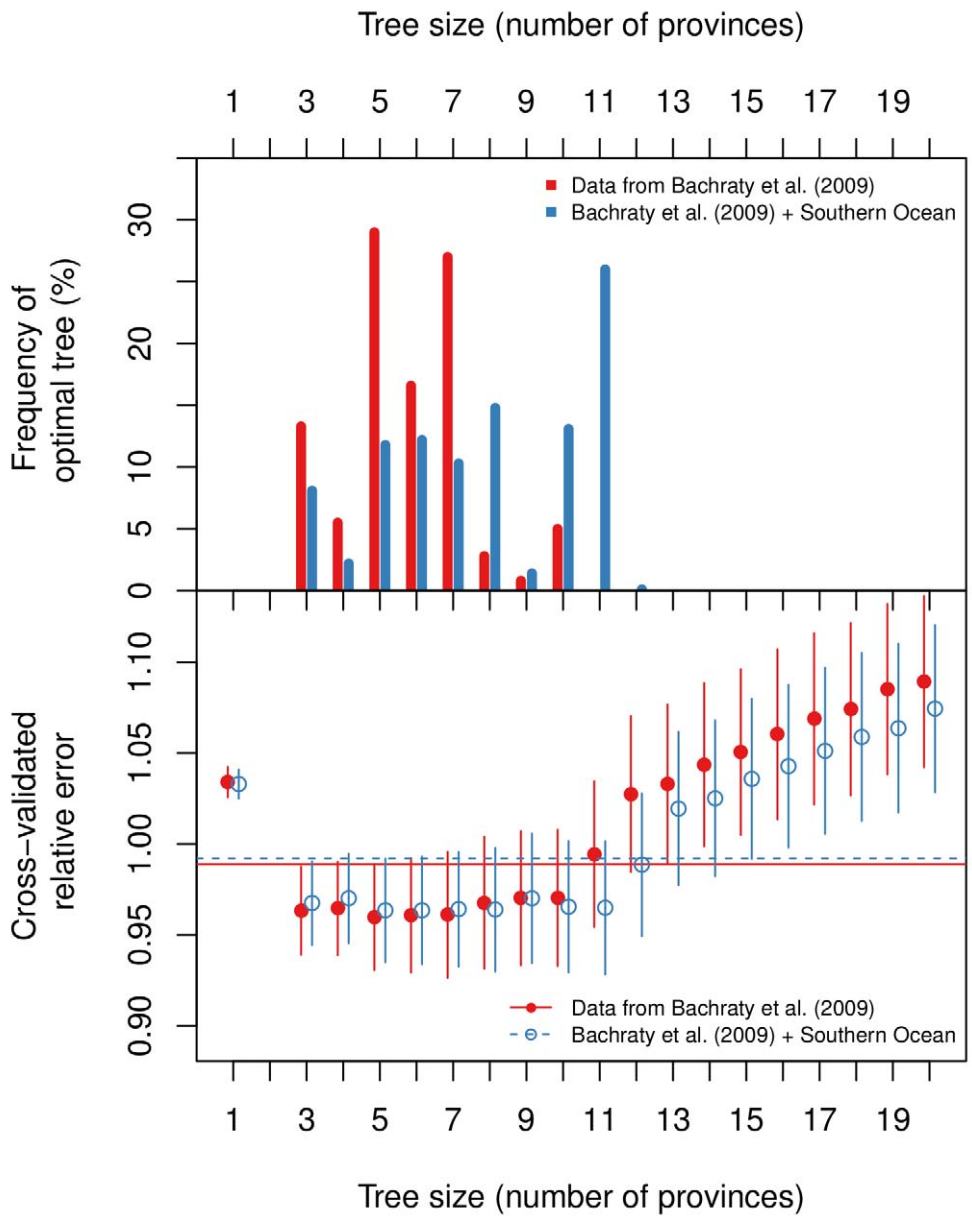

Figure 5. Selection of the multivariate regression tree for the global datasets of vent species. The datasets are species data from Bachraty et al. [8] (red/filled circles/solid line) and the same dataset with Southern Ocean vent sites added (blue/open circles/dashed line). Top panel: Frequency plot of the optimal tree size for 1,000 multiple cross-validations. The most common optimal tree size was five or seven provinces for the Bachraty et al. [8] dataset and 11 provinces for the combined dataset. Bottom panel: The cross-validated relative error indicates that predictive power is similar for a wide range of tree sizes. Vertical bars indicate ± one standard error, and the horizontal lines indicate one standard error above the minimum cross-validated relative error.
doi:10.1371/journal.pbio.1001234.g005

Mid-Atlantic Ridge. The dominant species at the ESR vents is an anomuran crab of the genus *Kiwa*, which has congeneric species along the Pacific-Antarctic Ridge and at cold seeps off Costa Rica [9,42].

Connections among the biogeographic provinces identified over the last ten years are consistent with dispersal of taxa along mid-ocean ridge systems, with vicariance events being related to severance of ridges through subduction or other processes [43]. This connectivity is also consistent with gene-flow studies that have demonstrated significant relationships between measures of genetic differentiation (F_{ST}) and whether populations are present on the same ridge segment, are separated by transform faults, or are present on different ridges [6,44]. However, the biogeographic patterns exhibited by hydrothermal vent communities may also be influenced by larval dispersal on deep-ocean currents that do not follow the line of ridge axes, with or without the aid of evolutionary stepping stones provided by other chemosynthetic ecosystems such as cold seeps and whale falls [6–8]. Examples of where such dispersal routes may have been important include the dispersal routes between the eastern Pacific and Mid-Atlantic Ridge, and the eastern Pacific, South Atlantic, and Indian Ocean [7,8].

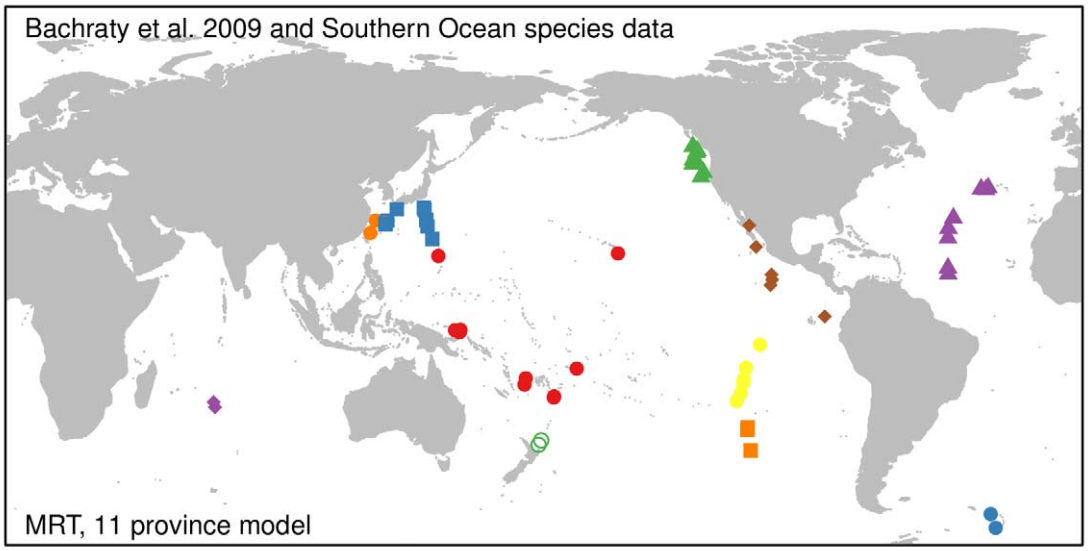

Figure 6. Results of geographically constrained clustering using multivariate regression trees. An 11-province model based on the combined dataset was the most frequent optimal model when using multiple cross-validations. Vent provinces are resolved comprising the Mid-Atlantic Ridge, the ESR, the northern, central, and southern East Pacific Rise, a further province located south of the Easter Microplate, four provinces in the western Pacific, and a further Indian Ocean province.
doi:10.1371/journal.pbio.1001234.g006

Our data from vents at E2 and E9 along the ESR provide three lines of evidence that the fauna at these sites represents a separate and new biogeographic province from those previously described for the global ocean [7,8]. First, the taxa of the vent fields at E2 and E9 are distinct from those of other provinces at least at the species level (e.g., *Kiwa* n. sp., *Vulcanolepas* n. sp., and *Lepetodrilus* n. sp.). Second, the structure of the assemblages differs from that of other provinces where fauna are shared at higher taxonomic levels. For example, at the nearest vent site where another species of *Kiwa* has been reported (*K. hirsuta*; 38°S, Pacific-Antarctic Ridge), that species occurs in the periphery with a reported population density of 0.1–0.2 m^{-2}, and in diffuse venting areas along with other widespread vent fauna, such as *Bathymodiolus* sp. and bythograeid crabs [9]. In contrast, at the ESR vents, *Kiwa* n. sp. occurs at high population densities (~600 m^{-2}) proximal to fluid exits, in the niches usually taken by taxa such as alvinellid polychaetes [45] or aggregations of alvinocaridid shrimp [46]. Also distinct in the assemblages of the ESR vents is the variety of vent-endemic anemones, and the presence of an undescribed seven-arm stichasterid sea star as a predator, and a conspicuous rarity of polychaetes, other than polynoid scale worms. Finally, the MRT analyses of the combined dataset indicate that using the most common optimal tree, E2 and E9 form a separate cluster from other vent provinces. These analyses also indicated that several other areas, especially the eastern Pacific vent sites south of the Easter Microplate, consistently form a separate biogeographic province in a range of optimal trees. This region has been recognised as a biogeographic boundary, known as the Easter Microplate boundary, in several other studies [6].

With regards to the third line of evidence, the MRT results should be interpreted with care. First, the Indian Ocean, South East Pacific Rise, and Antarctic sites are significantly under-sampled compared to sites in the northern and central East Pacific Rise, the Mid-Atlantic Ridge, and western Pacific back-arc basins. Second, the species lists presented in Bachraty et al. [8] do not account for many of the cryptic species that have been identified amongst some groups of vent taxa (e.g., *Lepetodrilus* [33]). Both of these factors introduce significant potential errors into the resolution of biogeographic patterns of the vent fauna using multivariate methods. Notwithstanding these problems, our analysis failed to reproduce the six-province model proposed by Bachraty et al. [8], and we see two major problems with their analysis. The first concerns the stability of the statistical method they used; the second concerns the choice of constraining variables for the cluster analysis. Regarding stability, the MRT method does not give a clear preference to a certain number of provinces, but rather a series of similarly "good" trees. The reason for the choice of the six-province model, given the data of Bachraty et al. [8], is unclear. Breiman et al. [47] recommend picking the smallest tree within one standard error of the minimum tree when there is no clear optimum, which would lead to a model with three provinces for both the Bachraty et al. [8] dataset and the combined dataset used in this study. We chose instead to present models with more than three provinces in this study, based on the results of multiple cross-validation. However, we suspect that the lack of stability of tree size is based on a combination of two things. First, vent biogeographic provinces appear to be hard to resolve based on the current presence/absence data alone. This idea is supported by the marginal differences between a range of preferential trees in the MRT (Figure 5) and by variation in the results across a number of unconstrained agglomerative cluster analyses we undertook whilst exploring the Bachraty et al. [8] and combined datasets for this study (see Text S1 and Figure S5). It is also notable that studies of other deep-sea ecosystems have demonstrated that analyses of species presence/absence can miss significant differences in the structure of marine communities that can be resolved using species abundance or ranked abundance data (e.g., seamounts [48]). Secondly, we think that latitude and longitude are not a sensible choice of constraining variables both from a mathematical and a biological perspective. In the MRT analysis, latitude and longitude are effectively treated as Cartesian coordinates, which is not an appropriate representation of geographic distances on the Earth's surface. This introduces a bias where sites at high latitude appear to be more distant along a

latitude circle than sites at low latitude. Furthermore, by encoding the longitude into 0–360° east of Greenwich, Bachraty et al. [8] introduce the implicit assumption that the Atlantic and Indo-Pacific are two extremes of the spatial spectrum, whereas in reality the two are joined around the Cape of Good Hope. Not surprisingly, different representations of longitude yield different MRT results, both in terms of optimal tree size and in the assignment of sites to "provinces" (see Text S1 and Figure S6). Apart from this geographical issue, present-day locations may not be good predictors for vent biogeography as they neither reflect geographic proximity on evolutionary time scales nor take into account other features and processes that are thought to influence deep-sea biogeography. These include factors such as depth, topography, currents, and oceanic fronts, many of which can act as variable dispersal filters [6,49–51].

Overall, our evidence for a separate biogeographic province for the ESR is consistent with the history and present physical environment of the Southern Ocean. The Southern Ocean is separated from the remaining global ocean by the surface-to-seabed Polar Front [52], which is a major barrier to dispersal of fauna to and from Antarctic waters [53]. This region represents a sharp boundary in physical conditions that was established after the initiation of the Antarctic Circumpolar Current and became more extreme at the middle Miocene climate transition (~13.8 Mya [54]), a time that is close to the initiation of spreading at the ESR. Taxa commonly found in the rest of the world's oceans, such as brachyuran crabs and decapod lobsters, are absent from the Antarctic, and the non-vent marine fauna of the Southern Ocean is highly endemic [40,55,56]. Explanations for this have included physiological barriers, an example being the decapod crustaceans, which have an inability to down-regulate blood magnesium levels sufficiently below that of seawater, leading to a loss of activity and eventual death at polar water temperatures [57]. It is also notable that a high proportion of Antarctic marine invertebrates have life histories that include direct or lecithotrophic larval development, although some common species, associated with unstable habitats, exhibit planktotrophy [58]. The reason for this is uncertain, although it is likely to be an adaptation to the extreme seasonality of the Antarctic and poor food supply for large parts of the year [58]. With the exception of the Siboglinidae, the taxa that are absent from the vents of the ESR have planktotrophic larval development (including the alvinocaridid shrimp and vent mussels). It is notable that the deep-sea vent ecosystems recently described from the Arctic also show an absence of vent shrimp and vent mussels [12]. In the Arctic, the niche usually occupied by shrimp in Atlantic vent fields is occupied by an amphipod with chemoautotrophic gill symbionts [12]. The biological filter represented by the Polar Front may thus explain the absence of bythograeid crabs, shrimps of the Alvinocarididae, and other taxa commonly associated with vents.

Current flow south of the Polar Frontal Zone is dominated by the eastward-flowing ACC, and maps of potential vorticity and evidence from ocean tracers of the high southern latitudes give rise to the possibility of larva-mediated dispersal and faunal similarities among the disjunct South East Pacific Rise, Chile Rise, ESR, and southernmost Mid-Atlantic Ridge [7,59]. Our observations are consistent with this hypothesis in the identification of a new species of *Kiwa*, other species of which has been found on the Pacific-Antarctic Ridge and on the continental slope of Costa Rica. Other faunal elements may also be shared between the vents on the ESR and those of the South East and South West Pacific. Early investigation of the life history of *Kiwa* n. sp. from the ESR also suggests that the larvae are brooded and hatch from eggs at a morphologically advanced stage, which is probably not conducive to long-distance dispersal in deep water. However, inferring dispersal capability from life history characteristics should be undertaken with caution, given that life history only partially explains the observed patterns of gene flow for other marine species [60,61]. A test of the importance of current-mediated dispersal in the evolution of communities at the ESR would be faunal and phylogenetic comparisons of this community with the biota present at the South East Pacific Rise and Chile Rise, along with that at vents along the Antarctic Peninsula in the Bransfield Strait [14].

The discovery of vent biota on the ESR with faunal connections to other southern hemisphere vent systems, including those in both the Pacific and the Atlantic, suggests a more complex picture of vent biogeography than previously considered. A full understanding of the relationships of the fauna of the ESR vents with those elsewhere will only be realised with complete analyses of the fauna collected at 56°S and 60°S at the ESR, and the location and documentation of further hydrothermal vent communities at high latitudes in the Southern Ocean and southern Pacific, Atlantic, and Indian Oceans. Further exploration of high-latitude ridges is critical for a full understanding of the global biogeography of vent ecosystems, given the potential role of the Southern Ocean as a gateway or a barrier between the major ocean ridges and back-arc basins.

Finally, our direct observations of hydrothermal vent fields south of 40°S latitude in the southern hemisphere represent the culmination of a 30-y poleward trend in hydrothermal exploration, which began at low latitudes. However, a seafloor image taken as long ago as 1966 at 2,377 m depth on ESR segment E9 shows a faunal assemblage similar to that which we now identify as associated with hydrothermal vents on this segment [62]. Thus, it appears that a vent community may have been observed but not recognised at high latitudes a decade prior to the original discovery of vent communities in the Galápagos Rift [1]. It is interesting to reflect that if this seafloor assemblage had been investigated in greater detail at that time, the entire history of global-scale hydrothermal exploration could have followed a quite different path.

Materials and Methods

Bathymetric and Geophysical Surveys

Two modes of geophysics data acquisition were carried out during the cruises: (1) ship-based geophysical survey and (2) ROV geophysical survey. On both RRS *James Clark Ross* 224 and RRS *James Cook* 042, ship-based geophysical data collection consisted of seafloor mapping using hull-mounted Kongsberg-Simrad EM120 multibeam echo sounders, and sub-bottom profiling using a hull-mounted parametric echo sounder. ROV geophysics data collection consisted of high-resolution seafloor mapping using the ROV *Isis* Simrad SM2000 multibeam echo sounder. Few ship-based surveys were carried out during the RRS *James Cook* 042 cruise.

Water Column Sampling

The majority of the water samples were collected using a Seabird +911 CTD on a titanium frame with up to 24 externally sprung Niskin bottles. This is a clean system, specifically designed for the sampling of waters with low levels of trace metals and nutrients. The bottles are Teflon lined, with Teflon taps and non-metallic parts; any metallic components are titanium or high-quality stainless steel.

The CTD Carousel Niskin and ROV Mini-Niskin bottles were sampled for (in order): (1) methane (125 ml, poisoned with HgCl

for analysis at the National Oceanography Centre, Southampton [NOC]); (2) dissolved inorganic carbon (250 ml, poisoned with HgCl for analysis at NOC); (3) total dissolved organic carbon (20 ml, filtered through a 0.2-μm filter and acidified with HCl for analysis at NOC); (4) trace metals (filtered through a 0.2-μm filter into an 500-ml acid-cleaned LDPE bottle for analysis at NOC); (5) metal speciation (filtered through a 0.2-μm filter into duplicate 250-ml bottles and frozen for analysis at NOC); and (6) siderophores—remaining volume for Mini-Niskin bottles, usually 10 l for large Niskin bottles—filtered and sucked through an Isolute ENV+ column (frozen) for characterisation at NOC. Finally, the filters were all washed for salts with Milli-Q water (pH 8) and stored frozen for analysis at NOC.

Hydrothermal Fluid Sampling

Collection of these samples was achieved using titanium (Ti) samplers, equipped with an inductively coupled link (ICL) high-temperature sensor to ensure the collection of high-quality samples. In the case of diffuse flow, or for sampling of friable chimney structures, the Ti samplers were used in conjunction with a specially constructed Ti diffuse sampler, which was used to prevent entrainment of surrounding seawater into the path of the fluid during sampling.

The Ti samplers were cleaned thoroughly before deployment using a solvent flux remover and rinsed with Milli-Q water. All Ti–Ti surfaces were lubricated with Fluorolube. Sample bottles were deployed in pairs, although each bottle had its own nozzle for insertion into the vent orifice (or diffuse flow sampler). Each pair of Ti samplers was coupled to an ICL high-temperature sensor that was located at the tip of the sample nozzles. Pins for firing the bottles were set at a distance of 22–31 mm above the top of the Ti sampler; however, when the pins were set high (31 mm), it proved difficult to couple the ICL temperature probe (for this reason, no temperature was recorded for some samples). The optimal setting for the pins was found to be ~27 mm.

Diffuse Flow Sampling

For optimal sampling of diffuse flow, the diffuse flow sampler was placed over the area to be sampled, and allowed to equilibrate until fluid was observed to be flowing out of the sampler. The nozzles of the Ti samplers were then inserted into the diffuse flow sampler, and the ram was slowly lowered until a reading was obtained on the ICL sensor. Once the temperature reading was considered to be steady, sampling proceeded in the same way as for a focussed fluid.

As soon as the samplers returned to the surface, they were rinsed in Milli-Q water, and the fluid was withdrawn. Separate sub-samples were collected for (1) refractive index, (2) alkalinity, (3) dissolved inorganic carbon and carbon isotopes, (4) pH, (5) gases (including CH_4, CO_2, and H_2), (6) anions and silica, (7) nutrients, (8) dissolved organic carbon, (9) O and H isotopes, and (10) bacteria, in that order. The remainder of the sample was emptied into an acid-cleaned 1-l HDPE bottle for analysis of all other constituents, including cations and the transition metals. Any residue remaining in the bottle was washed in to an acid-clean 30-ml HDPE bottle with Milli-Q water.

Analysis of "time-critical" parameters (e.g., pH) and key indicators of sample quality (e.g., Cl) was carried out onboard. Other constituents were transported back to NOC for analysis over the following 18 mo.

Microbiology

Samples were taken on the RRS *James Clark Ross* 224 cruise (January–February 2009). Water from within the buoyant vent plume was sampled with a CTD. Two litres of water was filtered through a 0.2-μm pore-size nitrocellulose filter. The filters were frozen at −80°C until further analysis. DNA was extracted from the filters using a phenol/chloroform protocol [63]. The 16S rDNA gene was amplified by PCR using the universal primers 27F and 1492R. PCR conditions were 3 min at 94°C, followed by 30 cycles of 60 s at 94°C, 45 s 50°C, 90 s at 72°C, and a final elongation of 5 min at 72°C. PCR products were cloned into the pCR2.1 vector by TOPO TA cloning (Invitrogen), following the manufacturer's recommendations and plated on LB-ampicillin plates containing X-gal for blue-white screening. White clones were checked for correct insert size by PCR using the plasmid primers M13F and M13R. In total, 285 clones (166 from E2 and 119 from E9) were sequenced from the 3′ end by Sanger sequencing at LGC Genomics. The average sequence length was 885 bp. The sequences were trimmed and quality-control checked with the software package Geneious [64] and subsequently aligned to a reference database (SILVA, version 102 [65]) and identified phylogenetically within ARB [66].

Faunal Imaging

Two equipment arrangements were used to conduct video-graphic surveys during ROV *Isis* dives. "Horizontal" surveys (surveys of horizontal substratum) were undertaken using a downward-looking Atlas three-chip charge coupled device video camera. The camera housing was mounted to view the seafloor through an aperture cut in the port forward corner of the ROV tool tray. A downward-facing HMI light was similarly mounted through the starboard forward corner of the tool tray. Two parallel lasers, 0.1 m apart, were mounted parallel to the focal axis of the camera to provide scale in images. Footage from the downward-looking Atlas camera was recorded to DVCAM tapes and DVD in the ROV control van. Controls for the Atlas camera (iris, zoom, focus, and colour balance) were adjusted from the ROV control van to obtain the clearest possible images for faunal identification.

"Vertical" video-graphic surveys (surveys of vertical substrata such as vent chimneys) were undertaken using the high-definition pilot pan-and-tilt camera of the ROV *Isis*. For these surveys, this camera was configured to view horizontally forwards from the vehicle, so that its focal axis was perpendicular to vertical substratum surfaces. Two parallel lasers, 0.1 m apart, were mounted parallel to the focal axis of the camera to provide scale in images.

Vertical surveys were undertaken using closed control of the ROV to maintain constant vehicle heading, and Doppler lock to enable movements of the vehicle over precise distances relative to the seafloor. These features enabled the ROV to undertake vertical lines up and down chimneys, offset by fixed horizontal distances, to obtain overlapping video images of the structure from a particular heading. Distance from the vehicle to the structure was kept constant, so that survey lines lay on a flat vertical plane a fixed distance from the structure being surveyed. Camera zoom was set in vertical surveys to achieve image frames approximately 1 m wide, with no adjustments during lines, and images were subsequently mosaicked together from overlapping lines for analysis.

Faunal samples were collected either by suction sampler or by scoop and brought to the surface in ambient seawater. Once on board, samples were immediately transferred to cold water in the controlled temperature laboratory (~4°C), where individuals were dissected and either frozen or stored in molecular grade ethanol for molecular analysis, frozen for isotope analysis, or fixed in 10% seawater formalin for morphological analysis.

Molecular Studies

DNA isolation, amplification, and sequencing. Genomic DNA was isolated from tissue samples of selected specimens, using different tissues depending on the taxon (*Kiwa* n. sp./pycnogonid: muscle tissue in merus/femur; gastropod/anemone: foot). DNA was extracted with the DNeasy Tissue Extraction Kit (Qiagen) as directed by the manufacturer.

Targeted gene regions were amplified via PCR using one or more sets of primers. Reactions were performed in 25-µl volumes, containing 2 µl of each primer (forward and reverse) at a concentration of 10 pmol/µl, 16 µl of Qiagen HotStarTaq Master Mix, 4 µl of DNA template (~50 ng), and 1 µl of double-distilled water. Cytochrome oxidase I reactions were performed in 10-µl volumes, containing 0.5 µl of each primer (forward and reverse) at a concentration of 10 nmol, 5 µl of Qiagen 10× PCR buffer, 1.5 µl of $MgCl_2$ (25 mM), 1 µl of dNTPs (2 nmol, Bioline), 0.25 µl of Taq (5 U/µl), and 1 µl of DNA template (~30 ng).

Primers were selected from existing papers or, if no amplification or poor amplification occurred, were designed on the basis of existing sequence data or initial sequence data obtained in this study.

PCR primers. For *Kiwa* n. sp., one mitochondrial gene (16S) and two nuclear genes (18S and 28S) were selected (Table S1), as these genes had previously been shown to be good markers for resolving relationships across broad time scales in the Crustacea [67]. For *Vulcanolepas*, 28S rDNA and the histone gene H3 were selected (Table S2), owing to their use in previous barnacle phylogenetic reconstructions [35,68]. For *Lepetodrilus*, the mitochondrial cytochrome oxidase I was amplified using LCO 1490 and HCO 2198 [69] (Table S3), following the use of this gene to resolve the molecular phylogeny of the Vetigastropoda [70]. PCR cycling protocols were as follows. For *Kiwa* n. sp. 16S rDNA: initial HotStarTaq denaturation at 95°C for 15 min, followed by 40 cycles of 94°C for 45 s, 55°C for 90 s, 72°C for 1 min, and a final extension of 7 min at 72°C. For 18S rDNA: initial HotStarTaq denaturation at 95°C for 15 min, followed by 30 cycles of 94°C for 1 min, 50°C for 90 s, 72°C for 2 min, and a final extension of 7 min at 72°C. For 28S rDNA: initial HotStarTaq denaturation at 95°C for 15 min, followed by 30 cycles of 94°C for 1 min, 55°C for 90 s, 72°C for 2 min, and a final extension of 7 min at 72°C. For *Vulcanolepas* histone gene H3: initial HotStarTaq denaturation at 95°C for 15 min, followed by 50 cycles of 95°C for 1 min, 50°C for 1 min, 72°C for 1 min, and a final extension of 5 min at 72°C. For 28S rDNA: initial HotStarTaq denaturation at 95°C for 15 min, followed by 35 cycles of 94°C for 1 min, 55°C for 1 min, 72°C for 90 s, and a final extension of 7 min at 72°C. For *Lepetodrilus* cytochrome oxidase I: initial HotStarTaq denaturation at 94°C for 15 min, followed by five cycles of 94°C for 1 min, 45°C for 1.5 min, 72°C for 1.5 min, then 30 cycles of 94°C for 1 min, 50°C for 1 min, 72°C for 1 min, and a final extension of 5 min at 72°C.

All PCR reactions and some sequencing reactions were performed on a Bio-Rad C1000 Thermal Cycler. PCR product was purified using QIAquick PCR Purification Kit (catalog number 28106). Where the C1000 Thermal Cycler was used for sequencing reactions, an Applied Biosystems 3100 DNA Analyser was used for sequencing. In all other cases, PCR product was sent to the Macrogen Europe Laboratory, where sequencing was conducted under BigDye terminator cycling conditions; the reacted products were purified using ethanol precipitation and run using an ABI 3730XL Automatic Sequencer. Forward and reverse sequences were assembled and cleaned using the computer program Sequencher 3.0.

Molecular data analyses. Alignments were carried out using MUSCLE [71,72]. For ribosomal genes, gaps were treated as informative events and were added as characters to the end of the sequences using the software FastGap 1.2 [73]. All quoted genetic distances are Tamura-Nei distances calculated using the software MEGA 4.1 [74]. Simple p-distances will tend to underestimate true genetic distances owing to the possibility of multiple nucleotide substitutions ("hits") at the same locus. The Tamura-Nei model corrects for multiple hits, whilst taking into account the differences in substitution rate and nucleotide frequencies.

Divergence dates for *Kiwa* n. sp. versus *K. hirsuta*. There are no substitution rate estimates for anomuran crustaceans for 18S and 28S. For 16S, there is an estimate for porcelain crabs based on divergence of two populations of a species (*Petrolisthes armatus*) isolated from each other by the formation of the Panama Isthmus 3.5 Mya. Stillman and Reeb [31] estimate a divergence rate of 0.53% per million years. The ESR crab has a 6.45% difference to *K. hirsuta*, which would place a divergence date at 12.2 Mya.

There are other substitution rate estimates for crustaceans, such as 0.65% per million years for Jamaican crabs [75], 0.9% per million years for fiddler crabs [76], and 0.67% per million years for a group of North American barnacles [77]. These substitution rates are calculated by dividing the percentage difference of presumed sister or cryptic species from either side of the Panama Isthmus by the estimated date that the Isthmus was formed (3.5 Mya). The 0.53% divergence rate estimate [31] is the preferred estimate as it is the only one for anomurans. Furthermore, it is likely that many populations became isolated from each other before the final closing of the Panama Isthmus, and therefore substitution rate estimates are likely to have been overestimated rather than underestimated, and more conservative rates are likely to be a better reflection of evolution. For these reasons, the tentative 12.2-million-year divergence date calculated for the ESR crab and *K. hirsuta* is likely to be more recent than the real date of divergence. It should be noted also that the 0.53% divergence rate estimated by Stillman and Reeb [31] is based on a tropical shallow-water species of anomuran, and substitution rates for deep-sea crustaceans may be very different.

Phylogenetic analyses. Phylogenetic trees were generated for *Kiwa* n. sp., *Vulcanolepas* n. sp., and *Lepetodrilus* n. sp. in order to reveal their affinity to other vent fauna. Alignments with sequences obtained in this study and sequences from GenBank were constructed using MUSCLE with the software MEGA 4.1 [73]. For ribosomal genes, gaps were treated as informative events and were added as characters to the end of the sequences using the software FastGap 1.2 [74]. Bayesian inference of phylogeny was performed using MrBayes 3.1.2 [78]. Appropriate substitution models for different genes were determined using jModelTest 0.1.1 [79] using the Akaike Information Criterion (AIC). For each of the three species investigated, Metropolis coupled Monte Carlo Markov Chains were run for 5 million generations in two simultaneous runs, each with four differently heated chains. Topologies were sampled every 100 generations, and the first 12,500 trees (25%) were discarded as "burn in".

Species-specific methods. For *Kiwa* n. sp., a 414-bp fragment of the mitochondrial ribosomal gene 16S was used for the phylogenetic analysis (see Table S4). With gaps coded in the final alignment, the length was 495 bp. The substitution model with the best AIC score was the generalised time reversible model with a gamma distribution. For *Vulcanolepas* n. sp., a 296-bp fragment of nuclear protein-coding gene H3 and a 903-bp fragment of the nuclear ribosomal gene 28S were used for the phylogenetic analyses (see Table S5). Gaps in the final 28S

alignment were coded for, and the two separate alignments were concatenated to create a final alignment 1,223 bp long. In the Bayesian analysis using MrBayes 3.1.2, the concatenated dataset was partitioned into the two gene regions, as the substitution models used were different. Based on AIC scores in jModelTest, the Hasegawa, Kishino, and Yano model with gamma distribution and invariable sites was used for the H3 fragment and the Felsenstein 1981 (F81) model was used for the 28S fragment. For *Lepetodrilus* n. sp., a 522-bp fragment of the mitochondrial protein-coding CO1 gene was used for the phylogenetic analysis (see Table S6). Based on AIC scores in jModelTest, the Hasegawa, Kishino, and Yano model with gamma distribution and invariable sites was used in the Bayesian analysis.

Multivariate Analysis

Geographically constrained clustering was performed to investigate the biogeographic placement of the Southern Ocean hydrothermal vents in the global classification scheme proposed by Bachraty et al. [8] using MRT [80]. For this analysis, data were subjected to a Hellinger transformation [81]. Trees were then computed using the ''mvpart'' package [82] in the *R* environment for statistical computing [83]. Optimal tree size was investigated by running 1,000 multiple cross-validations on each dataset.

Supporting Information

Figure S1 Phylogenetic tree for Anomura based on 16S rDNA. Phylogenetic tree showing the relationships of anomurans, including *Kiwa* n.sp., derived from a 495-base-pair sequence of the mitochondrial 16S rDNA gene based on Bayesian inference. Values above nodes are Bayesian posterior probability values. Scale bars indicate percent sequence divergence. All nodes with $p<0.5$ were collapsed into basal polytomies.
(TIF)

Figure S2 Phylogenetic tree for *Lepetodrilus* based on cytochrome oxidase I. Phylogenetic tree showing the relationships of limpets of the genus *Lepetodrilus*, including *Lepetodrilus* n. sp. from the ESR (*Pseudorimula* is used as the outgroup), derived from a 522-base-pair fragment of the mitochondrial cytochrome oxidase I gene based on Bayesian inference. Values above nodes are Bayesian posterior probability values. Scale bars indicate percent sequence divergence. All nodes with $p<0.5$ were collapsed into basal polytomies. CIR, Central Indian Ridge.
(TIF)

Figure S3 Phylogenetic tree for *Vulcanolepas* based on histone H3 and 28S rDNA. Phylogenetic tree showing the relationships of stalked barnacles, including *Vulcanolepas* n. sp., derived from a concatenated sequence of histone H3 and nuclear 28S rDNA gene 1,223 base pairs in length based on Bayesian inference. Values above nodes are Bayesian posterior probability values. Scale bars indicate percent sequence divergence. All nodes with $p<0.5$ were collapsed into basal polytomies.
(TIF)

Figure S4 Multivariate regression trees for seven province models using the Bachraty et al. [8] and combined datasets. (A) Results of geographically constrained clustering using MRTs and a seven province model based on the data from Bachraty et al. [8]. This model recovers all provinces proposed by Bachraty et al. [8], with an additional split in the South East Pacific Rise. (B) Results of geographically constrained clustering using MRTs and a seven-province model based on the data from Bachraty et al. [8] and the Southern Ocean sites described in this study. This model does not recover the North West Pacific province proposed by Bachraty et al. [8]; instead, it supports the additional split in the South East Pacific Rise, as well as a separate province for the Southern Ocean sites.
(TIF)

Figure S5 Results of hierarchical agglomerative cluster analysis of community composition data at species level. The tree is based on the Raup-Crick similarity coefficient, a probabilistic measure for presence/absence data.
(TIF)

Figure S6 Selection of the multivariate regression tree for a global dataset of vent species using different representations of longitude. The dataset is the species data from Bachraty et al. [8], with Southern Ocean vent sites added (combined dataset). Longitude representations are -180° to $+180^\circ$, centred on Greenwich (red/filled circles/solid line), 0° to 360° east of 60°W (blue/open circles/dashed line) and 0 to 360° east of Greenwich (green/open triangles/dotted line). (A) Frequency plot of the optimal tree sizes for 1,000 multiple cross-validations. The most common optimal tree size was five and six provinces for the traditional -180° to 180° representation of longitude, five provinces for eastings from 60°W, and 11 provinces for eastings from Greenwich. (B) The cross-validated relative error indicates that predictive power is similar for a wide range of tree sizes. Vertical bars indicate ± one standard error, and the horizontal lines indicate one standard error above the minimum cross-validated relative error. (C and D) Geographic representation of the effects of different longitude encodings. The world map is shifted accordingly to illustrate the edges introduced by using latitude and longitude like Cartesian coordinates. Note the differing provinces in the East Pacific. (C) A five-province model based on the traditional -180° to 180° representation of longitude. (D) A five-province model based on eastings from 60°W.
(TIF)

Table S1 For *Kiwa* n. sp., primers used for amplification and sequencing of 16S mitochondrial rDNA and 18S and 28S nuclear rDNA genes.
(DOC)

Table S2 For *Vulcanolepas* n. sp., primers used for amplification and sequencing of histone H3 and 28S nuclear rDNA genes.
(DOC)

Table S3 For *Lepetodrilus* n. sp., primers used for amplification and sequencing of cytochrome oxidase I.
(DOC)

Table S4 Sequences used for phylogenetic analysis of 16S rDNA to show the relationship of *Kiwa* n. sp. with other anomuran taxa.
(DOC)

Table S5 Sequences used for phylogenetic analysis of H3 and 28S rDNA to show the relationship of *Vulcanolepas* n. sp. with other stalked barnacles from deep-sea hydrothermal vents.
(DOC)

Table S6 Sequences used for phylogenetic analaysis of cytochrome oxidase I to show the relationship of *Lepetodrilus* n. sp. with other lepetodrilid limpets from deep-sea hydrothermal vents.
(DOC)

Text S1 Supplementary information.
(DOC)

Acknowledgments

The authors thank the masters and crews of the RRS *James Cook* and RRS *James Clark Ross* for their tremendous support during the fieldwork in the Southern Ocean. We also thank the staff of the UK National Marine Facilities at NOC for logistic and shipboard support, especially Jez Evans and Dave Turner and the pilots and technical teams of ROV *Isis*. Dr. Roy Livermore is thanked for his encouragement and support in the early stages of this research.

Author Contributions

The author(s) have made the following declarations about their contributions: Conceived and designed the experiments: NERC consortium PI(PAT); (NERC consortium CoPIs (ADR, JTC, DPC, ANG, RJ, KL, RDL, RAM, RDP, NVCP); JCR224 and JC42 cruise PSOs (RDL, ADR); JCR224 participants (SAB, DPC, JTC, AGCG, AH, ADR, ER-L, PAT); JC42 participants (BA, AA, AC, DPC, JTC, RJJD, AGCG, DG, CRG, JH, LH, VAIH, RJ, KL, LM, WDKR, CNR, CJS, ST, KZ); multivariate analyses PHBS; DAP. Performed the experiments: NERC consortium PI(PAT); (NERC consortium CoPIs (ADR, JTC, DPC, ANG, RJ, KL, RDL, RAM, RDP, NVCP); JCR224 and JC42 cruise PSOs (RDL, ADR); JCR224 participants (SAB, DPC, JTC, AGCG, AH, ADR, ER-L, PAT); JC42 participants (BA, AA, AC, DPC, JTC, RJJD, AGCG, DG, CRG, JH, LH, VAIH, RJ, KL, LM, WDKR, CNR, CJS, ST, KZ); DAP. Analyzed the data: ADR, PAT, JTC, DPC, KL, RDL, CNR, DRHG, PHBS, BA, CRG, KZ, TS, DAP. Contributed reagents/materials/analysis tools: ADR, PAT, JTC, DPC, KL, RDL, CNR, DRHG, BA, CRG, TS, RAM, RJ, VAIH, AGCG, LM. Wrote the paper: ADR, PAT, JTC, DPC, KL, RDL, TS, PHBS. Prepared the figures: VAIH, AGCG, LM, ADR, PHBS, PAT.

References

1. Corliss JB, Dymond J, Gordon LI, Edmond JM, von Herzen RP, et al. (1979) Submarine thermal springs on the Galapagos Rift. Science 203: 1073–1083.
2. Dubilier N, Bergin C, Lott C (2008) Symbiotic diversity in marine animals: the art of harnessing chemosynthesis. Nat Rev Microbiol 6: 725–740.
3. Martin W, Baross J, Kelley D, Russell MJ (2008) Hydrothermal vents and the origin of life. Nat Rev Microbiol 6: 805–814.
4. Van Dover CL (2000) The ecology of deep-sea hydrothermal vents. Princeton (New Jersey): Princeton University Press. 424 p.
5. Ramirez-Llodra E, Shank TM, German CR (2007) Biodiversity and biogeography of hydrothermal vent species. Oceanography 20: 30–41.
6. Vrijenhoek RC (2010) Genetic diversity and connectivity of deep-sea hydrothermal vent metapopulations. Mol Ecol 19: 4391–4411.
7. Van Dover CL, German CR, Speer KL, Parson LM, Vrijenhoek RC (2002) Evolution and biogeography of deep-sea vent and seep invertebrates. Science 295: 1253–1257.
8. Bachraty C, Legrende P, Desbruyères D (2009) Biogeographic relationships among hydrothermal vent faunas on a global scale. Deep Sea Res Part 1 Oceanogr Res Pap 56: 1371–1378.
9. MacPherson E, Jones W, Segonzac M (2005) A new squat lobster family of Galatheoidea (Crustacea, Decapoda, Anomura) from the hydrothermal vents of the Pacific-Antarctic Ridge. Zoosystema 27: 709–723.
10. Edmonds HN, Michael PJ, Baker ET, Connelly DP, Snow JE, et al. (2003) Discovery of abundant hydrothermal venting on the ultraslow-spreading Gakkel Ridge in the Arctic Ocean. Nature 421: 252–256.
11. Schander C, Rapp HT, Kongsrud JA, Bakken T, Berge J, et al. (2010) The fauna of hydrothermal vents on the Mohn Ridge (North Atlantic). Mar Biol Res 6: 155–171.
12. Pedersen RB, Rapp HT, Thorseth RH, Lilley MD, Barriga FJAS, et al. (2010) Discovery of a black smoker vent field and vent fauna at the Arctic Mid-Ocean Ridge. Nat Commun 1: 126. doi:10.1038/ncomms1124.
13. German CR, Livermore RA, Baker ET, Bruguier NI, Connelly DP, et al. (2000) Hydrothermal plumes above the East Scotia Ridge: an isolated high-latitude back-arc spreading centre. Earth Planet Sci Lett 184: 241–250.
14. Klinkhammer GP, Chin CS, Keller RA, Dählmann A, Sahling H, et al. (2001) Discovery of new hydrothermal vent sites in Bransfield Strait, Antarctica. Earth Planet Sci Lett 193: 395–407.
15. Sahling H, Wallmann K, Dählmann A, Schmaljohann R, Petersen S (2005) The physicochemical habitat of *Sclerolinum* sp. at Hook Ridge hydrothermal vent, Bransfield Strait, Antarctica. Limnol Oceanogr 50: 598–606.
16. Winkler G, Newton R, Schlosser P, Crone TJ (2010) Mantle helium reveals Southern Ocean hydrothermal venting. Geophys Res Lett 37: L05601.
17. Smalley R, Dalziel IWD, Bevis MG, Kendrick E, Stamps DS, et al. (2007) Scotia Arc kinematics from GPS geodesy. Geophys Res Lett 34: L21308.
18. Larter RD, Vanneste LE, Morris P, Smythe DK (2003) Structure and tectonic evolution of the South Sandwich Arc. In: Intra-oceanic subduction systems: tectonic and magmatic processes. Geol Soc Spec Pub 219: 255–284.
19. Livermore RA (2003) Back-arc spreading and mantle flow in the East Scotia Sea. In: Intra-oceanic subduction systems: tectonic and magmatic processes. Geol Soc Spec Pub 219: 315–331.
20. Livermore R, Cunningham A, Vanneste L, Larter R (1997) Subduction influence on magma supply at the East Scotia Ridge. Earth Planet Sci Lett 150: 261–275.
21. Bruguier NJ, Livermore RA (2001) Enhanced magma supply at the southern East Scotia Ridge: evidence for mantle flow around the subducting slab? Earth Planet Sci Lett 191: 129–144.
22. InterRidge (2007) InterRidge statement of commitment to responsible research practices at deep-sea hydrothermal vents. Available: http://www.interridge.org/IRStatement. Accessed 2 December 2011.
23. Delaney JR, Robigou V, McDuff RE, Tivey MK (1992) Geology of a vigorous hydrothermal system on the Endeavour segment, Juan de Fuca Ridge. J Geophys Res 97: 19663–19682.
24. Charlou JL, Fouquet Y, Bougault H, Donval JP, Auzende JM (1996) Mineral and gas chemistry of hydrothermal fluids on an ultrafast-spreading ridge: east Pacific Rise, 17° to 19°S (Naudur cruise, 1993) phase separation processes controlled by volcanic and tectonic activity. J Geophys Res 101: 15899–15919.
25. Gamo T, Chiba H, Yamanaka T, Okudaira T, Hashimoto J, et al. (1996) Chemical characteristics of newly discovered black smoker fluids and associated hydrothermal plumes at the Rodriguez Triple Junction, central Indian Ridge. Earth Planet Sci Lett 193: 371–379.
26. Schmidt K, Garbe-Schönberg D, Koschinsky A, Strauss H, Lost CL, et al. (2010) Fluid elemental and stable isotope composition of the Nibelungen hydrothermal field (8°18′S, Mid-Atlantic Ridge): constraints on fluid-rock interaction in heterogeneous lithosphere. Chem Geol 280: 1–18.
27. Fouquet Y, von Stackelberg U, Charlou JL, Donval JP, Foucher JP, et al. (1991) Hydrothermal activity in the Lau back-arc basin: sulfides and water chemistry. Geology 19: 303–306.
28. Craddock PR (2009) Geochemical tracers of processes affecting the formation of seafloor hydrothermal fluids and deposits in the Manus back-arc basin [PhD dissertation]. Cambridge (Massachusetts): Massachusetts Institute of Technology and Woods Hole Oceanographic Institution. 370 p.
29. Butterfield DA, Seyfried WE, Lilley MD (2003) Composition and evolution of hydrothermal fluids. In: Halbach PE, Tunnicliffe V, Hein JR, eds. Energy and mass transfer in marine hydrothermal systems. Dahlem Workshop report 89. Berlin: Dahlem University Press.
30. Machardom A, Macpherson E (2004) Rapid radiation and cryptic speciation in squat lobsters of the genus *Munida* (Crustacea, Decapoda) and related genera in the South West Pacific: molecular and morphological evidence. Mol Phylogenet Evol 33: 259–279.
31. Stillman JH, Reeb CA (2001) Molecular phylogeny of eastern Pacific porcelain crabs, genera *Petrolisthes* and *Pachycheles*, based on the mtDNA 16S rDNA sequence: phylogeographic and systematic implications. Mol Phylogenet Evol 19: 236–245.
32. Goffredi SK, Jones WJ, Ehrlich H, Springer A, Vrijenhoek RC (2008) Epibiotic bacteria associated with the recently discovered yeti crab, *Kiwa hirsuta*. Environ Microbiol 10: 2823–2834.
33. Johnson SB, Warén A, Vrijenhoek RC (2008) DNA barcoding of *Lepetodrilus* limpets reveals cryptic species. J Shellfish Res 27: 43–51.
34. Desbruyères D, Segonzac M, Bright M (2006) Handbook of deep-sea hydrothermal vent fauna, 2nd edition. Linz (Austria): Biologiezentrum der Oberösterreichische Landesmuseen. pp 544.
35. Pérez-Losada M, Harp M, Høeg JT, Achituv Y, Jones D, et al. (2008) The tempo and mode of barnacle evolution. Mol Phylogenet Evol 46: 328–346.
36. Buckeridge JS (2000) *Neolepas osheai* sp. nov., a new deep-sea vent barnacle (Cirripedia: Pedunculata) from the Brothers Caldera, south-west Pacific Ocean. N Z J Mar Freshwater Res 34: 409–418.
37. Van Dover CL, Kaartvedt S, Bollens SM, Wiebe PH, Martin JW, et al. (1992) Deep-sea amphipod swarms. Nature 358: 25–26.
38. Martin JW, France SC, Van Dover CL (1993) *Halice hesmonectes*, a new species of pardaliscid amphipod (Crustacea, Peracarida) from hydrothermal vents in the eastern Pacific. Can J Zool 71: 1724–1732.
39. Sheader M, Van Dover CL, Thurston MH (2004) Reproductive ecology of Bouvierellacurtirama (Amphipoda: Eusiridae) from chemically distinct vents in the Lucky Strike vent field, Mid-Atlantic Ridge. Mar Biol 144: 503–514.
40. Brandt A, Gooday AJ, Brix SB, Brökeland W, Cedhagen T, et al. (2007) First insights into the biodiversity and biogeography of the Southern Ocean deep sea. Nature 447: 307–311.
41. Griffiths HJ, Barnes DKA, Linse K (2009) Towards a generalised biogeography of the Southern Ocean Benthos. J Biogeogr 36: 162–177.
42. Goffredi SK (2010) Indigenous ectosymbiotic bacteria associated with diverse hydrothermal vent invertebrates. Environ Microbiol Rep 2: 479–488.
43. Tunnicliffe V, Fowler CMR (1996) Influence of sea-floor spreading on the global hydrothermal vent fauna. Nature 379: 531–533.

44. Creasey S, Rogers AD (1999) Population genetics of bathyal and abyssal organisms. Adv Mar Biol 35: 1–151.
45. Chevaldonne P, Jollivet D (1993) Videoscopic study of deep-sea alvinellid polychaete populations: biomass estimation and behaviour. Mar Ecol Prog Ser 95: 251–262.
46. Van Dover CL, Fry B, Grassle JF, Humphris S, Rona P (1988) Feeding biology of the shrimp *Rimicaris exoculata* at hydrothermal vents on the Mid-Atlantic Ridge. Mar Biol 98: 209–216.
47. Breiman L, Friedman JH, Olshen RA, Stone CG (1984) Classification and regression trees. Belmont (California): Wadsworth International Group. 358 p.
48. McClain CR, Lundsten L, Ream M, Barry J, DeVogelaere A (2009) Endemicity, biogeography, composition, and community structure on a Northeast Pacific seamount. PLoS ONE 4: e4141. doi:10.1371/journal.pone.0004141.
49. Hurtado LA, Lutz RA, Vrijenhoek RC (2004) Distinct patterns of genetic differentiation among annelids of eastern Pacific hydrothermal vents. Mol Ecol 13: 2603–2615.
50. Audzijonyte A, Vrijenhoek RC (2010) When gaps really are gaps: statistical phylogeography of hydrothermal vent invertebrates. Evolution 64: 2369–2384.
51. McClain CR, Hardy SM (2010) The dynamics of biogeographic ranges in the deep sea. Proc R Soc Lond B Biol Sci 277: 3533–3546.
52. Orsi AH, Whitworth T, 3rd, Nowlin WD (1995) On the meridional extent and fronts of the Antarctic Circumpolar Current. Deep Sea Res Part I Oceanogr Res Pap 42: 641–673.
53. Rogers AD (2012) Evolution and biodiversity of Antarctic organisms: a molecular perspective. In: Rogers AD, Johnston N, Murphy EJ, Clarke A, eds. Antarctic environments: an extreme environment in a changing world. Oxford: Wiley-Blackwell. In press.
54. Potter PE, Szatmari P (2009) Global Miocene tectonics and the modern world. Earth Sci Rev 96: 279–295.
55. Arntz WE, Brey T, Gallardo VA (1997) Antarctic marine biodiversity: an overview. In: Battaglia B, Valencia J, Walton DWH, eds. Antarctic communities: species, structure and survival. Cambridge: Cambridge University Press. pp 3–14.
56. Clarke A, Johnston NM (2003) Antarctic marine benthic biodiversity. Oceanogr Mar Biol Ann Rev 41: 47–114.
57. Frederich M, Sartoris FJ, Pörtner HO (2001) Distribution patterns of decapod crustaceans in polar areas: a result of magnesium regulation? Polar Biol 24: 719–723.
58. Pearse JS, McClintock JB, Bosch I (1991) Reproduction of Antarctic marine benthic invertebrates: tempos, modes and timing. Am Zool 31: 65–80.
59. Well R, Roether W, Stevens DP (2003) An additional deep-water mass in Drake Passage as revealed by ^{3}He data. Deep Sea Res Part I Oceanogr Res Pap 50: 1079–1098.
60. Kinlan BP, Gaines SD (2003) Propagule dispersal in marine and terrestrial environments: a community perspective. Ecology 84: 2007–2020.
61. Cowan RK, Sponaugle S (2010) Larval dispersal and marine population connectivity. Ann Rev Mar Sci 1: 443–466.
62. Newman WA, Ross A (1971) Antarctic Cirripedia. Am Geophys Union Ant Res Ser 14: 257.
63. Fuller NJ, Marie D, Partensky F, Vaulot D, Post AF, et al. (2003) Clade-specific 16S ribosomal DNA oligonucleotides reveal the predominance of a single marine *Synechococcus* clade throughout a stratified water column in the Red Sea. Appl Environ Microbiol 69: 2430–2443.
64. Drummond AJ, Ashton B, Buxton S, Cheung M, Cooper A, et al. (2010) Geneious, version 5.1 [computer progam]. Available: http://www.geneious.com. Accessed 28 November 2011.
65. Pruesse E, Quast C, Knittel K, Fuchs BM, Ludwig W, et al. (2007) SILVA: a comprehensive online resource for quality checked and aligned ribosomal RNA sequence data compatible with ARB. Nucleic Acids Res 35: 7188–7196.
66. Ludwig W, Strunk O, Westram R, Richter L, Meier H, et al. (2004) ARB: a software environment for sequence data. Nucleic Acids Res 32: 1363–1371.
67. Bracken HD, Toon A, Felder DL, Martin JW, Finley M, et al. (2009) The decapod tree of life: compiling the data and moving toward a consensus of decapod evolution. Arthropod Syst Phylogeny 67: 99–116.
68. Pérez-Losada M, Hoeg JT, Crandall KA (2004) Unraveling the evolutionary radiation of the Thoracican barnacles using molecular and morphological evidence: a comparison of several divergence time estimation approaches. Syst Biol 53: 244–264.
69. Folmer O, Black M, Hueh W, Lutz R, Vrijenhoek R (1994) DNA primers for amplification of mitochondrial cytochrome c oxidase subunit I from diverse metazoan invertebrates. Mol Mar Biol Biotechnol 3: 294–299.
70. Geiger DL, Thacker CE (2005) Molecular phylogeny of Vetigastropoda reveals non-monophyletic Scissurellidae, Trochoidea, and Fissurelloidea. Molluscan Res 25: 47–55.
71. Edgar RC (2004a) MUSCLE: multiple sequence alignment with high accuracy and high throughput. Nucleic Acids Res 32: 1792–1797.
72. Edgar RC (2004b) MUSCLE: a multiple sequence alignment method with reduced time and space complexity. BMC Bioinformatics 5: 113. doi:10.1186/1471-2105-5-113.
73. Borchsenius F (2009) FastGap, version 1.2 [computer program]. Aarhus (Denmark): Department of Biological Sciences, University of Aarhus.
74. Tamura K, Dudley J, Nei M, Kumar S (2007) MEGA4: Molecular Evolutionary Genetics Analysis (MEGA) software version 4.0. Mol Biol Evol 24: 1596–1599.
75. Schubart CD, Diesel R, Hedges SB (1998) Rapid evolution to terrestrial life in Jamaican crabs. Nature 393: 363–365.
76. Sturmbauer C, Levinton JS, Christy J (1996) Molecular phylogeny analysis of fiddler crabs: test of the hypothesis of increasing behavioral complexity in evolution. Proc Natl Acad Sci U S A 93: 10855–10857.
77. Wares JP (2001) Patterns of speciation inferred from mitochondrial DNA in North American *Chthamalus* (Cirripedia: Balanomorpha: Chthamaloidea). Mol Phylogenet Evol 18: 104–116.
78. Ronquist F, Huelsenbeck JP (2003) MrBayes 3: Bayesian phylogenetic inference under mixed models. Bioinformatics 19: 1572–1574.
79. Posada D (2008) jModelTest: phylogenetic model averaging. Mol Biol Evol 25: 1253–1256.
80. De'ath G (2002) Multivariate regression trees: a new technique for modelling species-environment relationships. Ecology 83: 1105–1117.
81. Legendre P, Gallagher ED (2001) Ecologically meaningful transformations for ordination of species data. Oecologia 129: 271–280.
82. De'ath G (2011) mvpart: multivariate partitioning. R package version 1.4-0 [computer program]. Available: http://CRAN.R-project.org/package = mvpart. Accessed 28 November 2011.
83. R Development Core Team (2011) R: a language and environment for statistical computing, version 2.13 [computer program]. Vienna: R Foundation for Statistical Computing.

Conservation Genet Resour (2013) 5:835–839
DOI 10.1007/s12686-013-9921-9

TECHNICAL NOTE

Development of polymorphic microsatellite loci for three species of vent-endemic megafauna from deep-sea hydrothermal vents in the Scotia Sea, Southern Ocean

C. N. Roterman · J. T. Copley · K. T. Linse · P. A. Tyler · A. D. Rogers

Received: 22 March 2013 / Accepted: 26 March 2013 / Published online: 12 April 2013

Abstract Microsatellite loci have been developed for three undescribed species discovered at hydrothermal vents on the East Scotia Ridge (ESR) in the Southern Ocean: a yeti crab, *Kiwa* sp. (Kiwaidae), a species of peltospiroid gastropod and a vent limpet, *Lepetodrilus* sp. (Lepetodrilidae). Nine, twelve and fourteen loci were developed for the three species respectively, with two loci deviating significantly from Hardy–Weinberg expectations. Observed heterozygosity ranged from 0.08 to 1 (means of 0.62, 0.44 and 0.63 for the three species respectively). These loci are being used to determine connectivity between vents at the northern and southern end of the ESR and between the ESR and the Kemp Caldera, a submerged part of the South Sandwich Island chain. These data will be crucial in understanding the ecology of the first hydrothermal vent communities discovered in the Southern Ocean.

Keywords Microsatellite · Lepetodrilus · Kiwa · Peltospiridae · Peltospirid · Gigantopelta · Hydrothermal vent · Population genetics

C. N. Roterman (✉) · A. D. Rogers
Department of Zoology, University of Oxford, South Parks Road, Oxford OX1 3PS, UK
e-mail: nicolai@theglide.com

J. T. Copley · P. A. Tyler
School of Ocean and Earth Science, University of Southampton, Waterfront Campus, Southampton SO14 3ZH, UK

K. T. Linse
British Antarctic Survey, High Cross, Madingley Road, Cambridge CB3 0ET, UK

The endemic fauna of deep-sea hydrothermal vents maintain populations along mid-ocean ridges by broadcasting larvae between island-like vent fields (Tyler and Young 1999). To elucidate the factors that determine species ranges, it is necessary to develop genetic markers sufficiently sensitive to reveal connectivity patterns between vent fields. Here we present a suite of microsatellite markers for three species recently discovered at high temperature hydrothermal vents on the East Scotia Ridge (ESR) (Rogers et al. 2012): a yeti crab (Kiwaidae) *Kiwa* sp., a gastropod in the family Peltospiridae and a vent limpet, *Lepetodrilus* sp..

Total genomic DNA was extracted from pereopods in the case of *Kiwa* n. sp. and from foot tissue in the case of the molluscs using the Qiagen DNeasy® Blood and Tissue Kit following the manufacturer's instructions. 5 μg of template DNA from a single individual were sent to either Macrogen Inc (Seoul, South Korea) in the case of *Lepetodrilus* sp., or in the case of the other two species, to Ecogenics GmbH (Switzerland). Microsatellites were isolated broadly in the manner described by Abdelkrim et al. (2009). For *Kiwa* sp. and the peltospirid gastropod, microsatellite enriched libraries were generated, whilst for *Lepetodrilus* sp.a non-enriched library was generated. The libraries for all species were subject to 454 sequencing and fragments containing microsatellites with sufficient flanking regions for primer development were detected using MSATCOMMANDER (Faircloth 2008). Primers were designed on Geneious Pro 5.4.6 (Drummond et al. 2010) using Primer3 (Rozen and Skaletsky 2000) and then manufactured by Eurofins MWG Operon (Ebersberg, Germany).

Initially all loci were tested on four individuals. PCR Reactions were performed in 9 μl volumes, containing 0.6 μl of each primer (forward and reverse) at a

Table 1 Polymorphic loci (GenBank Accessions XXXXXX-XXXXXXXX) from 24 individuals for each of the three species

Species	Locus name	Repeat motif	454 Allele Size	Primer sequence	T_A (°C)	Size range	N_A	H_{obs}	H_{exp}	P
Kiwa n. sp.	KiwESR_01	$(GTT)_8$	166	F: CAAGTAGCTCTGACCAGACAAA R: GTTTGTGTGTTGGTTCACGA	55	148–193	9	0.83	0.76	0.98123
	KiwESR_02	$(TGT)_6$	272	F: CAAGTAAATAACCAGAAACAATAAAAA R: CCTGATTTTATTAAGCTCATTCAG	54	269–275	3	0.75	0.57	0.16174
	KiwESR_03	$(TG)_8$	155	F: TACTCAGATGACACCCGGTAA R: GAGAATCATCGATCTACCTACAAC	57	157–169	5	0.50	0.58	0.7721
	KiwESR_04	$(TGT)_7$	209	F: TAAGGAGGAAGATGGGAGAAA R: ACATCCCTTCCTCGTTCAC	55	200–212	4	0.29	0.49	0.03512
	KiwESR_05	$(AT)_6$	206	F: TGTTTACTGGATTCCGGAGTTA R: GATGGACCGTAGGTATCTGACT	56	204–208	3	0.21	0.26	0.3982
	KiwESR_06	$(TG)_7$	145	F: ACGTCGTATTAGTAGCCACCAC R: CAAATTTAAGGAAATGCATGATAA	52	143–149	4	0.46	0.55	0.1362
	KiwESR_07	$(AT)_5$ $(AC)_{12}$	135	F: GAAGCAAGAAGTTATACACCCAAT R: GGGAACGAGAGGATCAGCTA	56	119–177	21	0.92	0.95	0.70659
	KiwESR_08	$(AC)_{15}$	100	F: CCAAGAGCACGGTCATCAGTA R: ACACGTCTGCCTCGTGTG	57	80–146	23	1.00	0.97	1
	KiwESR_09	$(CAA)_8$	127	F: AATGAGTCCCAGCAAGTGTC R: TAGTGTTCGGGAGGAGAT	53	106–121	6	0.63	0.77	0.06516

Table 1 continued

Species	Locus name	Repeat motif	454 Allele Size	Primer sequence	T_A (°C)	Size range	N_A	H_{obs}	H_{exp}	P
Peltospirid gastropod	PeltESR_01	$(CA)_7$	126	F: TGGGAGAGACAAACAGACAGA R: CGAACTCCTTGTTGGAGATG	58	118–124	4	0.29	0.33	0.60035
	PeltESR_02	$(AC)_9$	137	F: ACATTGGATTAATGTGCGTGT R: TGTCAATTAGCCAGATTTATCCA	58	127–135	4	0.29	0.27	1
	PeltESR_03	$(AC)_{11}$	375	F: AACCGCCGCTAGTGTGAC R: AGCGAAGAGGTTTACCGAAT	58	367–371	2	0.54	0.44	0.35644
	PeltESR_04	$(CTAT)_9$	344	F: TGGGATTATAACCCGCATC R: TTGAGTTGCGTACACCTTTG	57	312–336	5	0.25	0.34	0.1684
	PeltESR_05	$(CATT)_{13}$	235	F: ACTCAATAACCGATGTATGTTTCG R: ATCGCTCGCTAGAGTGGTAA	58	207–255	11	0.83	0.90	0.66916
	PeltESR_06	$(TC)_5$	167	F: AGGGTCCTCTCTAAAGGAAAG R: TTGTTTAACACCACCTCAGC	55	163–165	2	0.33	0.42	0.34444
	PeltESR_07	$(GT)_6$	198	F: CTAAGGTTCAGGCACGTCTC R: GGGTTTCCTCCCTCAATATC	57	198–200	2	0.08	0.08	1
	PeltESR_08	$(GT)_8$ $(GT)_4$ $(GT)_{11}$	303	F: AGTCGTTACACTCGCTCTGG R: TCGTCCGCCATATACACAC	58	271–335	11	0.42	0.55	**0.00191**
	PeltESR_09	$(GT)_6$	158	F: TGGTCGGTGCATGTATATTG R: ACCATACCTCAGTGACAGCAC	58	158–160	2	0.58	0.51	0.67977
	PeltESR_10	$(GTT)_5$ $(GTT)_9$	357	F: GACGTAGCCCAGTGGTAAAG R: CCCAGGATAGTGCTTAAACCAT	57	351–363	6	0.50	0.49	0.26071
	PeltESR_11	$(TA)_5$	146	F: GTCCGACTAATGGCAGTGAG R: CTCCTGCATTTAGAGCCTGTG	59	138–146	4	0.50	0.59	0.1415
	PeltESR_12	$(GT)_{13}$	151	F: CTTACAATTTTGAATCAGTTGC R: TTCTAAATAAGGCATTTACCG	53	137–165	13	0.67	0.87	**0.00015**

Table 1 continued

Species	Locus name	Repeat motif	454 Allele Size	Primer sequence	T_A (°C)	Size range	N_A	H_{obs}	H_{exp}	P
Lepetodrilus n. sp.	LepESR_01	$(AAT)_{14}$	286	F: GTAGCATAATTCCCATGGCG	57	268–292	8	0.79	0.78	0.58051
				R: CAATCGTCTCTCAAACAGGC						
	LepESR_02	$(GT)_{14}$	195	F: CTGACGCCAACTACCTCTTC	57	183–209	13	0.96	0.90	0.34676
				R: CATTCAACCCGACACTAACAC						
	LepESR_03	$(TAA)_7$	179	F: AAATCGATATATTTAGTGCTTTCCA	57	176–227	18	0.83	0.91	0.01775
				R: GAGTTGAGAAGGAATTGAGTGC						
	LepESR_04	$(CATT)_7$	195	F: CTCATGGAAGCTGACATCATTA	57	195–199	2	0.08	0.08	1
				R: ACGAGCCATGCCCATAAA						
	LepESR_05	$(ATT)_{14}$	125	F: GCATGGAGTCCAGCGTATTAT	58	116–161	13	0.67	0.85	0.00865
				R: GGTAAATCTGACCAGTATAGGTTTG						
	LepESR_06	$(ATT)_{13}$	107	F: TGGCGCGCTCTACAAATG	57	86–110	8	0.67	0.81	0.10431
				R: GTTCCATGGTACTTATTGCTGA						
	LepESR_07	$(TTA)_{14}$	129	F: GATTCCAGCGCCTTATACAC	51	114–210	21	0.88	0.96	0.09741
				R: CAGATATCACAGCACATG						
	LepESR_08	$(ACC)_{10}$	357	F: AAGTCGACCTCCTTTGTAGC	58	348–360	5	0.33	0.43	0.05771
				R: CATCTGACTGGATATTGCTGTG						
	LepESR_09	$(AC)_{12}$	117	F: AGTGTCGAGAGTTGTTGGTG	57	101–161	16	0.88	0.92	0.19682
				R: GAGTGACTCCATTGATGCAG						
	LepESR_10	$(TA)_8$	106	F: GGTCATTGTCATGAATATTCTCAAT	58	92–108	8	0.29	0.37	0.11123
				R: CTGGCCCGTAATTACTGTTG						
	LepESR_11	$(ACT)_{20}$	211	F: GTTATGTAAACTACCAACAGTCG	57	187–259	20	1.00	0.95	1
				R: GGTCACTAGCATGCAGAAAG						
	LepESR_12	$(TA)_7$	218	F: GTGACCAAGATAATATGCCAGA	57	198–226	7	0.58	0.67	0.18678
				R: AGATGTGCTGAATGCAGTTTC						
	LepESR_13	$(TAA)_7$	158	F: GATTACAATGGGCCAGTCG	57	149–176	7	0.54	0.69	0.21993
				R: ATTGAGCAGATCCTGTGTCC						
	LepESR_14	$(CT)_7$	115	F: GCTGAGGTATTCTGTTCCATTC	57	107–109	2	0.33	0.28	1
				R: GATGGTCTAGGACATCTTGG						

T_A annealing temperature, size range of alleles (base pairs), N_A number of alleles, H_O observed heterozygocity, H_E expected heterozygocity, P probability of deviation from Hardy–Weinberg Equilibrium (exact test) are reported

Significant P values (after a sequential Bonferroni correction) are highlighted in bold

concentration of 4 pmol/μl, 6.3 μl of Qiagen Taq Master Mix, 1.5 μl of DNA template (~ 10-50 ng/μl). All PCR reactions were performed on a Bio-Rad C1000 Thermal Cycler. The default PCR protocol used was: 95 °C for 5 min, followed by 25 cycles of 94 °C for 35 s, 50 °C for 35 s, 72 °C for 1 min, and a final extension of 72 °C for 1 h. PCR product was visualised on 1 % agarose gel using ethidium bromide. Loci that produced smears, multiple bands or failed to amplify were discarded. Remaining loci were then tested for polymorphism on eight individuals by reordering the forward primers with a 6-FAM fluorescent label and repeating the PCR protocols. Size-fragment analysis of the PCR product was conducted on an ABI 3730xl DNA analyser. Chromatograms were scored using Peak Scanner™ software v1.0.

Polymorphic loci that were easy to score were then tested on 24 individuals from the E2 vent field on the East Scotia Ridge, in order to assess their applicability to population genetics.

Genetic diversity statistics as well as tests for deviation from Hardy–Weinberg Equilibrium (HWE) and linkage disequilibrium were generated with Arlequin 3.5 (Excoffier and Lischer 2010) and corrected for multiple comparisons using the sequential Bonferroni approach (Rice 1989). Presence of null alleles, excessive stutter and large allele dropout were assessed using MicroChecker with 1000 randomizations (van Oosterhout et al. 2004).

For the three species in this study, 454 Roche sequencing yielded 12,453 sequence fragments for *Kiwa* sp., 14,743 sequences for the peltospirid gastropod and 8,707 sequences *Lepetodrilus* sp.. For *Kiwa* sp., 818 sequences (6.57 % of total) contained microsatellites of five or more repeats (excluding mononucleotide repeats), of which 63 loci contained suitable flanking regions for primer design and were initially tested for amplification. Of these 63 loci, 33 were further tested for polymorphism with eight individuals, resulting in nine polymorphic loci. For the peltospirid gastropod, 1,032 sequences contained microsatellites (7 % of total) and of these, 74 contained loci with flanking regions suitable for primer design. 30 loci were tested for polymorphism resulting in 12 polymorphic loci. 1,148 of the 8,707 *Lepetodrilus* sp. sequences contained microsatellites (13.18 %), of which 87 contained loci with flanking regions suitable for primer design. 49 loci were then tested for polymorphism across eight individuals yielding 14 polymorphic loci.

For all three species there was no significant evidence for linkage disequilibrium, however, two loci deviated from HWE after sequential Bonferroni corrections (PeltESR_08 and PeltESR_12, see Table 1). Null alleles were detected for the loci KiwESR_04, PeltESR_12 and LepESR_05.

To our knowledge, this is the first report of the development of microsatellite markers for a kiwaid crab, a lepetodrilid limpet or a peltospirid gastropod. This toolkit will determine the nature of connectivity between individuals collected at the northern and southern end of the ESR as well as between individuals on the ESR and on vents nearby at the Kemp Caldera.

Acknowledgments We'd like to thank the master and crew of the RRS James Cook and the technical crew of ROV ISIS for specimen collection during expedition JC42. Special thanks to Tom Hart, University of Oxford, for crucial input in microsatellite development. Fieldwork and analyses were funded by Natural Environment Research Council (NERC) Consortium Grant (NE/DO1249X/1) and NERC PhD studentship NE/D01429X/1(LH, LM, CNR).

References

Abdelkrim J, Robertson BC, Stanton JAL, Gemmell NJ (2009) Fast, cost-effective development of species-specific microsatellite markers by genomic sequencing. Biotechniques 46(3):185–192

Drummond A, Ashton B, Cheung M, Heled J, Kearse M, Moir R (2010) Geneious pro. Geneious Biomatters Ltd, Auckland

Excoffier L, Lischer HEL (2010) Arlequin suite ver 3.5: a new series of programs to perform population genetics analyses under linux and windows. Mol Ecol Resour 10(3):564–567

Faircloth BC (2008) Msatcommander: detection of microsatellite repeat arrays and automated, locus-specific primer design. Mol Ecol Resour 8(1):92–94

Rice WR (1989) Analyzing tables of statistical tests. Evolution 43(1):223–225

Rogers AD, Tyler PA, Connelly DP, Copley JT, James R, Larter RD, Linse K, Mills RA, Garabato AN, Pancost RD, Pearce DA, Polunin NVC, German CR, Shank T, Boersch-Supan PH, Alker BJ, Aquilina A, Bennett SA, Clarke A, Dinley RJJ, Graham AGC, Green DRH, Hawkes JA, Hepburn L, Hilario A, Huvenne VAI, Marsh L, Ramirez-Llodra E, Reid WDK, Roterman CN, Sweeting CJ, Thatje S, Zwirglmaier K (2012) The discovery of new deep-sea hydrothermal vent communities in the southern ocean and implications for biogeography. PLoS Biol 10(1): e1001234

Rozen S, Skaletsky H (2000) Primer3 on the www for general users and for biologist programmers. Methods Mol Biol 132(3):365–386

Tyler PA, Young C (1999) Reproduction and dispersal at vents and cold seeps. J Mar Biol Assoc U K 79(02):193–208

Van Oosterhout C, Hutchinson WF, Wills DP, Shipley P (2004) Microchecker: software for identifying and correcting genotyping errors in microsatellite data. Mol Ecol Notes 4(3):535–538

PROCEEDINGS OF THE ROYAL SOCIETY B

rspb.royalsocietypublishing.org

Research

Cite this article: Roterman CN, Copley JT, Linse KT, Tyler PA, Rogers AD. 2013 The biogeography of the yeti crabs (Kiwaidae) with notes on the phylogeny of the Chirostyloidea (Decapoda: Anomura). Proc R Soc B 280: 20130718.
http://dx.doi.org/10.1098/rspb.2013.0718

Received: 21 March 2013
Accepted: 23 May 2013

Subject Areas:
evolution, genetics, taxonomy and systematics

Keywords:
Kiwaidae, Chirostyloidea, biogeography, phylogenetics, hydrothermal vents, yeti crab

Author for correspondence:
C. N. Roterman
e-mail: christopher.roterman@zoo.ox.ac.uk

Electronic supplementary material is available at http://dx.doi.org/10.1098/rspb.2013.0718 or via http://rspb.royalsocietypublishing.org.

Royal Society Publishing
Informing the science of the future

The biogeography of the yeti crabs (Kiwaidae) with notes on the phylogeny of the Chirostyloidea (Decapoda: Anomura)

C. N. Roterman[1], J. T. Copley[2], K. T. Linse[3], P. A. Tyler[2] and A. D. Rogers[1]

[1]Department of Zoology, University of Oxford, South Parks Road, Oxford OX1 3PS, UK
[2]Ocean and Earth Science, University of Southampton, Waterfront Campus, Southampton SO14 3ZH, UK
[3]British Antarctic Survey, High Cross, Madingley Road, Cambridge CB3 0ET, UK

The phylogeny of the superfamily Chirostyloidea (Decapoda: Anomura) has been poorly understood owing to limited taxon sampling and discordance between different genes. We present a nine-gene dataset across 15 chirostyloids, including all known yeti crabs (Kiwaidae), to improve the resolution of phylogenetic affinities within and between the different families, and to date key divergences using fossil calibrations. This study supports the monophyly of Chirostyloidea and, within this, a basal split between Eumunididae and a Kiwaidae–Chirostylidae clade. All three families originated in the Mid-Cretaceous, but extant kiwaids and most chirostylids radiated from the Eocene onwards. Within Kiwaidae, the basal split between the seep-endemic *Kiwa puravida* and a vent clade comprising *Kiwa hirsuta* and *Kiwa* spp. found on the East Scotia and Southwest Indian ridges is compatible with a hypothesized seep-to-vent evolutionary trajectory. A divergence date estimate of 13.4–25.9 Ma between the Pacific and non-Pacific lineages is consistent with Kiwaidae spreading into the Atlantic sector of the Southern Ocean via the newly opened Drake Passage. The recent radiation of Kiwaidae adds to the list of chemosynthetic fauna that appear to have diversified after the Palaeocene/Eocene Thermal Maximum, a period of possibly widespread anoxia/dysoxia in deep-sea basins.

1. Introduction

The taxon-rich Anomura, an infraorder of decapod crustaceans, has been subjected to major taxonomic revisions in recent years [1–3]. This is especially true for squat lobsters (anomurans with a proportionally elongated abdomen only partially folded under the thorax), which used to be grouped together with porcelain crabs in the superfamily Galatheoidea [4]. Morphological re-examinations and molecular phylogenetics have revealed that the squat lobster form probably evolved independently at least twice from hermit crab-like forms within Anomura [5,6]. One clade, the Galatheoidea [1], now only comprises the squat lobster families Galatheidae, Munididae and Munidopsidae and the porcelain crabs, Porcellanidae, while the other clade comprises the superfamilies of the freshwater squat lobster Aegloidea, the marine squat lobster Chirostyloidea and the hairy stone crabs (Lomisoidea) [5]. These two groups form larger clades with Paguroidea (hermit crabs), a superfamily now shown to be polyphyletic [5].

The recently described marine squat lobster superfamily Chirostyloidea consists of three families: Chirostylidae, Eumunididae and the chemosynthetic-associated Kiwaidae (yeti crabs). Chirostylidae are divided into five genera (*Chirostylus*, *Gastroptychus*, *Uroptychus*, *Uroptychodes* and *Hapaloptyx*), while Eumunididae contains *Eumunida* and *Pseudomunida*. Kiwaidae are solely represented by the genus *Kiwa* [3]. The phylogenetic relationship among chirostyloid families and their genera is still unclear; analyses of three rRNA ribosomal genes and

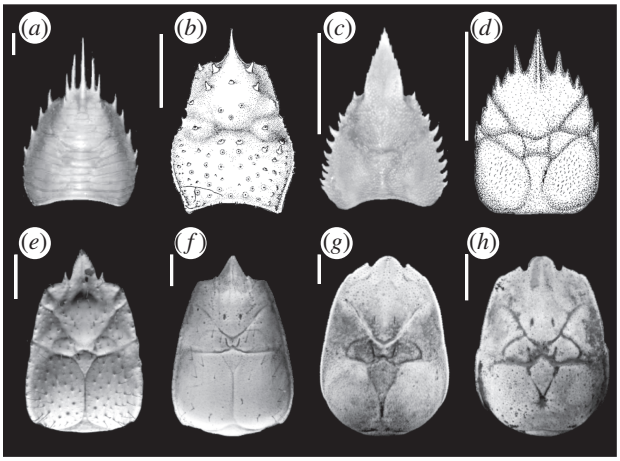

Figure 1. Modified photographs and illustrations of extant and extinct chirostyloid carapaces: (*a*) *Eumunida australis* (Eumunididae) modified from Schnabel & Ahyong [3], (*b*) *Gastroptychus iaspis* (Chirostylidae) from Baba & Haig [8], (*c*) *Uroptychus naso* (Chirostylidae) from Poore & Andreakis [9], (*d*) fossil chirostyloid *Pristinaspina gelasina* from Schweitzer & Feldmann [10], (*e*) *K. puravida* (Kiwaidae) from Thurber *et al.* [11], (*f*) *K. hirsuta* (Kiwaidae) from Macpherson *et al.* [2], (*g*) *Kiwa* n. sp. ESR, original photograph, (*h*) *Kiwa* SWIR, original photograph. Scale bars, 1 cm.

morphological characters by Schnabel *et al.* [6] indicated that *Eumunida* was nested in a clade comprising *Uroptychus*, *Uroptychodes*, *Gastroptychus* and *Chirostylus*, with *Kiwa* and *Pseudomunida* falling out basally, thus challenging the monophyly of Eumunididae. Despite these results, morphological evidence and recent work using the cytochrome oxidase subunit 1 gene (COI) still supports the monophyly of Eumunididae [4]. Comprehensive morphological examination of the sternal plastron in species of *Gastroptychus* [7] suggests two groups: one as *Gastroptychus sensu stricto*, and a second group, superficially similar to *Gastroptychus* s.s, which may have a closer affinity to some species of *Uroptychus* [6].

Using five nuclear protein-coding genes across Anomura, Tsang *et al.* [5] found support for a eumunidid–kiwaid clade as sister to Chirostylidae. This study used three species (*Kiwa hirsuta*, *Eumunida funambulus* and *Uroptychodes grandirostris*) to represent the chirostyloid families. A eumunidid–kiwaid clade is supported by the shared presence of supraocular spines (figure 1), an epipod bearing maxilliped 1 and a distally annulated flagellum on the exopod [3,4].

Kiwaidae, found exclusively in deep-sea chemosynthetic ecosystems, incorporates four species of the genus *Kiwa*, of which two are recently described [2,11]. *Kiwa hirsuta*, the type species for the genus and family, was found adjacent to hydrothermal vents on the Pacific–Antarctic Ridge in 2005 (figure 2). Based on its elongated, setae-covered chelae and a distinctly regionalized carapace, among other characters, a new family was described [2]. The profusion of apparently chemosynthetic filamentous bacteria found among the setae led Macpherson *et al.* [2] to speculate that kiwaids may be partly reliant on these bacteria as a source of nutrition, which was later confirmed [13]. In 2006, a second species, *Kiwa puravida*, was discovered at methane cold seeps on the Pacific continental slope off Costa Rica. Isotope analysis revealed the main diet to be epibiotic bacteria growing on carapace setae, which are scraped off by a specialized third maxilliped 'comb'. *Kiwa puravida* is similar in form to *K. hirsuta*, and molecular characterization based on COI and rRNA 18S sequences confirms their close affinity [11].

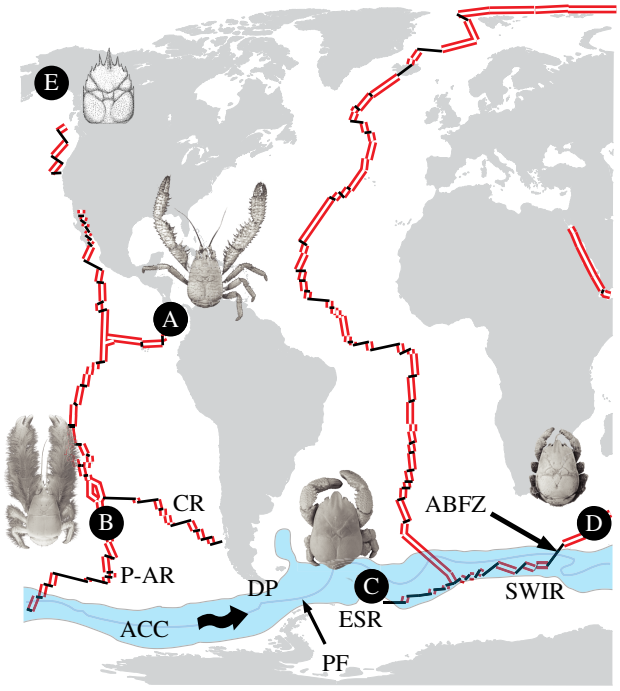

Figure 2. Map showing locations of kiwaids, each with representative image, (A, *K. puravida*; B, *K. hirsuta*; C, *Kiwa* n. sp. ESR; D, *Kiwa* SWIR), as well as the location of the fossil *Pristinaspina gelasina* (E) in relation to mid-ocean ridges (MORs) and the ACC. Double lines denote actively spreading MOR segments; single black lines represent intervening faults and fracture zones. Land shapes and ridge positions are modified from the NASA Digital Tectonic Activity Map [12]. Spreading ridge abbreviations are as follows: P-AR, Pacific–Antarctic Ridge; CR, Chile Rise; ESR, East Scotia Ridge; SWIR, South West Indian Ridge; ABFZ, Andrew Bain Fracture Zone. Shaded area labelled ACC, Antarctic Circumpolar Current as defined by the Subantarctic Front to the north and the Southern ACC front to the south. PF, Polar Front. Wavy arrows illustrate direction of the ACC. DP denotes the Drake Passage. Photographs of *K. puravida* and *K. hirsuta*, courtesy of Shane Ahyong from Thurber *et al.* [11] and Macpherson *et al.* [2], respectively. (Online version in colour.)

A third undescribed species of *Kiwa* was discovered in 2010 in the Atlantic sector of the Southern Ocean at vents on the East Scotia Ridge (ESR) [14]. Compared with the first two species, it has proportionally much shorter chelae, with the majority of the bacteria-growing setae concentrated on the ventral carapace. rRNA sequences confirmed that *Kiwa* n. sp. ESR is closely related to *K. hirsuta* (6.45% divergence for 16S) [14]. In December 2011, a further *Kiwa* species, morphologically similar to *Kiwa* n. sp. ESR, was discovered at the Dragon hydrothermal vent field on the Southwest Indian Ridge (SWIR) [15].

The nature and timing of chirostyloid evolution is still unresolved; the fossil record of Chirostyloidea is poor, in contrast to Galatheoidea, for which there are fossils dating back to the Early Jurassic [4]. Currently, only one fossil has been attributed to Chirostyloidea: *Pristinaspina gelasina*, a fossil recovered from Cenomanian to Maastrichtian deposits in Alaska [10]. The animal was buried in a muddy continental slope environment at present-day latitude (approx. 60° N), which is quite different from either the chemosynthetic environments of extant Kiwaidae or the deep-water coral and sponge habitats with which many Chirostylidae and Eumunididae are believed to be associated [7]. Originally thought to be a chirostylid, the distinctive carapace regionalization characteristic of kiwaids, along with a broad medially

carinate rostrum and supraorbital spines, indicate that this animal is possibly a stem-lineage kiwaid [4] (figure 1). It has been suggested that the northeast Pacific location of the fossil, along with the present-day location of *K. hirsuta* and *K. puravida*, reflect an East Pacific origin for the family [4].

This study aims to resolve phylogenetic uncertainties in the Chirostyloidea, and in particular Kiwaidae, by analysing a concatenated nine-gene ribosomal and protein-coding DNA sequence dataset in order to: (i) confirm the monophyly of Chirostyloidea and test the monophyly of Kiwaidae–Eumunididae; (ii) investigate polyphyly within Chirostylidae; (iii) reveal the internal phylogeny of Kiwaidae; (iv) date the key divergences in Chirostyloidea; and (v) relate divergences in Kiwaidae to past tectonic and oceanographic events.

2. Material and methods

(a) Taxon sample set

Species of *Kiwa*, *Eumunida*, *Uroptychus*, *Gastroptychus*, *Uroptychodes* and *Chirostylus* have been included in this study. Only the monotypic *Pseudomunida* and *Hapaloptyx* genera in Eumunididae and Chirostylidae, respectively, are omitted, owing to tissue rarity. Non-chirostyloid anomurans have been chosen based on the most recent molecular phylogenies of Anomura [5,6] in order to provide fossil calibrations for estimating divergences within Chirostyloidea.

In total, 23 species were included in this study, featuring 15 chirostyloids, six other anomurans and two brachyurans (true crabs) as outgroups. Of the chirostyloids, nine species are chirostylids, two are eumunidids and four are kiwaids (see the electronic supplementary material, table S1 for information on tissue provenance and GenBank accession nos). New sequences have been deposited in GenBank under the nos KF051278–KF051401.

(b) Molecular methods

Total genomic DNA was extracted from pereopods, pleopods or antennae using either Qiagen DNeasy Blood and Tissue Kit following the manufacturer's instructions or, in cases where tissue quantities were very small, a CTAB DNA extraction protocol [16]. Nine gene sequence regions were selected in this study: fragments of the ribosomal rRNA genes 16S (approx. 500 bp), 18S (approx. 1900 bp) and 28S (approx. 300 bp), as well as approximately 500 bp fragments of each of the protein-coding genes COI, arginine kinase (AK), enolase, glyceraldehyde 3-phosphate dehydrogenase (GAPDH), sodium potassium ATPase α subunit (NaK) and phosphoenolpyruvate carboxykinase (PEPCK). Of these genes, two are mitochondrial (16S and COI). Primers for these genes, including 15 newly designed, are listed in the electronic supplementary material, table S2.

PCR reactions were performed in 12 µl volumes, containing 0.8 µl of each primer (forward and reverse) at a concentration of 4 pmol μl^{-1}, 8 µl of Qiagen HotStarTaq Master Mix, 2 µl of DNA template (approx. 10–50 ng μl^{-1}) and 0.4 µl of double-distilled water. All PCR reactions were performed on a Bio-Rad C1000 Thermal Cycler.

General amplification conditions were initial HotStarTaq denaturation at 95°C for 15 min, followed by 35 cycles of 94°C for 1 min, 50°C for 90 s, 72°C for 1 min and a final extension of 72°C for 10 min. PCR product was visualized on 1 per cent agarose gel using ethidium bromide and then purified either using the QIAquick gel purification kits or Diffinity RapidTips. Sequencing reactions were performed in 10 µl volumes, containing 2.5 µl cleaned PCR product, 2 µl H_2O, 2.5 µl of 0.8 pmol μl^{-1} primer, 2.5 µl 6X Buffer and 0.5 µl BigDye. The following sequencing reaction protocol was used: initial denaturation at 96°C for 1 min, followed by 25 cycles of 96°C for 10 s, 50°C for 5 s, 60°C for 4 min and a final cool down to 4°C.

Sequences were resolved using an Applied Biosystems 3100 Genetic Analyzer. Consensus sequences were generated from forward and reverse strands using Geneious Pro v. 5.4.6. [17].

Protein-coding genes (COI, NaK, enolase, AK, GAPDH and PEPCK) were aligned using the geneious alignment tool in Geneious Pro v. 5.4.6, and ribosomal genes (16S, 28S and 18S) were aligned using MAFFT 6 [18] and then adjusted by eye. Difficult-to-align variable regions in the rRNA sequences were excised using Gblocks [19]. The remaining gaps in the alignments were considered to be potentially informative and were coded for, using the FastGaps program [20]. The resulting gap-coding blocks were pasted to the ends of each rRNA sequence in the concatenated alignment to yield the final sequence dataset.

The final concatenated alignment is as follows: 16S (518 bp), 18S (1681 bp), 28S (232 bp), COI (585 bp), NaK (582 bp), enolase (339 bp), AK (600 bp), GAPDH (522 bp) and PEPCK (501 bp), resulting in a concatenated total alignment of 5560 bp, which is available online at TreeBASE (http://purl.org/phylo/treebase/phylows/study/TB2:S14238).

(c) Partitioning and substitution model choice

To avoid multiple phylogenetic analyses on a shortlist of possible partition strategies, PartitionFinder [21] was used to evaluate the best partition scheme and accompanying substitution models according to the Akaike information criterion (see the electronic supplementary material, table S3).

(d) Phylogenetic analyses

Two different methods for determining phylogenies were performed in this study: maximum likelihood (ML) and Bayesian inference (BI). ML analyses were performed using GARLI v. 2.0 [22], with two replicate runs, each with 200 bootstrap pseudo-replicates to determine node support. BI was performed using MrBayes v. 3.2 [23]. Metropolis-coupled Monte Carlo Markov chains (MCMC) were run for 10 million generations in two simultaneous runs, each with four differently heated chains. Convergence of the analyses was validated by the standard deviation of split frequencies and by monitoring of the likelihood values over time using Tracer v. 1.5 [24]. Topologies were sampled every 1000 generations and the first 2500 trees (25%) were discarded as 'burn in'.

(e) Topology hypothesis testing

Given the uncertainty regarding the affinity of Kiwaidae, Eumunididae and Chirostylidae within Chirostyloidea, three alternative *a priori* topological hypotheses were tested using the assessment of the marginal model likelihoods with the stepping-stone method in MrBayes v. 3.2 [25]. The topology hypotheses are as follows: a Kiwaidae–Eumunididae clade, a Kiwaidae–Chirostylidae clade and a Eumunididae–Chirostylidae clade. For each topology constraint, two simultaneous analyses were performed for 2.5 million generations, with default settings.

(f) Divergence estimation using fossil calibration

Bayesian estimation of divergence times was performed with Beast v. 1.7.4 [26] for the entire concatenated dataset. Substitution models and clock models were unlinked across the partitions. Tuning parameters for the MCMC operators were set to auto-optimize and successive runs were tuned accordingly. Each MCMC chain commenced from a starter tree based on the topology of the phylogenetic trees created in §2*e* and run for 50 million generations. Two independent runs were performed; each sampled every 1000 generations, and 10 per cent of samples were removed

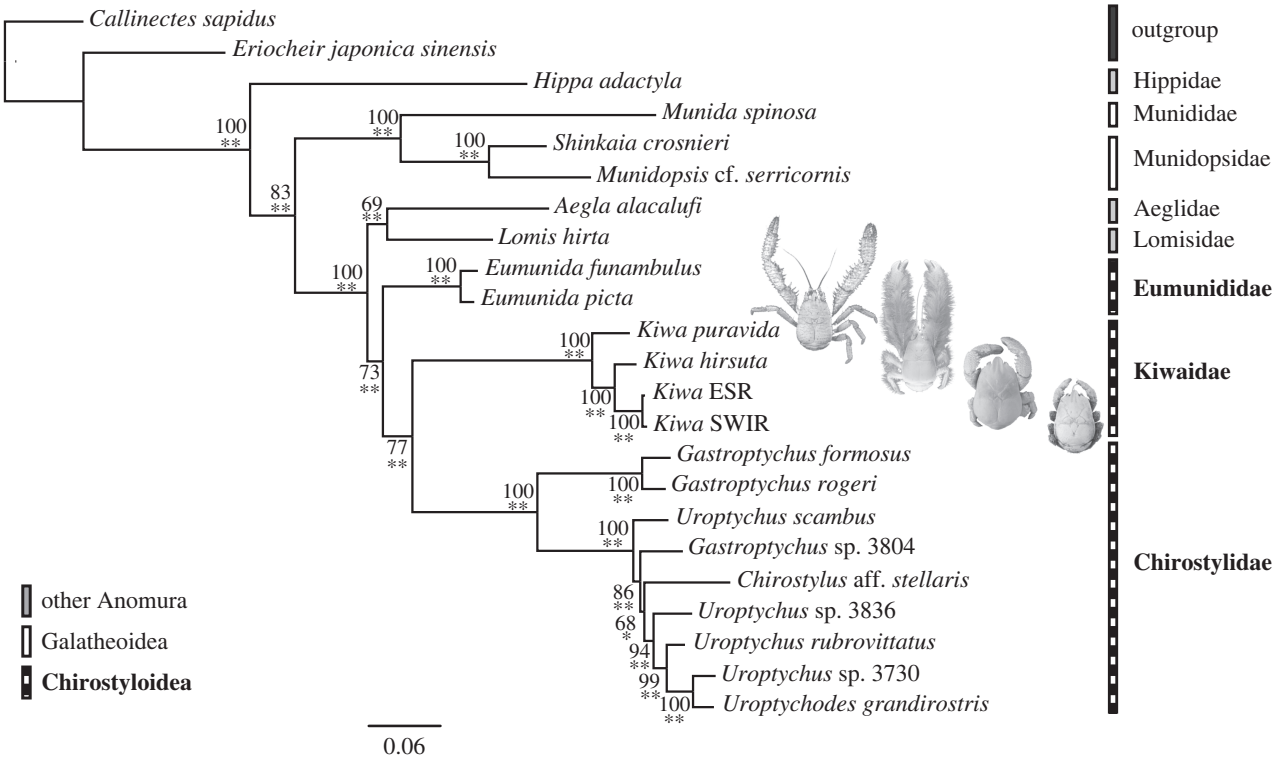

Figure 3. Maximum-likelihood (ML) and Bayesian topology of a nine-gene concatenated dataset with nine partitions. Node support numbers represent ML bootstrap percentages. Bayesian posterior probabilities are summarized as one asterisk for values more than 0.97 and two asterisks for values more than 0.99. Photographs of the four known kiwaids are superimposed next to their names. Photographs of *K. puravida* and *K. hirsuta* courtesy of Shane Ahyong from Thurber *et al*. [11] and Macpherson *et al*. [2], respectively.

as burn-in. Runs were combined using LogCombiner v. 1.7.4. Effective sample size values were greater than 200 for all parameters.

(g) Fossil calibrations

Pristinaspina gelasina was not included as a fossil calibration point for kiwaid divergence, given the lack of any definitive proto-chirostyloid fossils for comparison and its shared features with Eumunididae. However, it may be possible to reveal, based on the inferred divergence dates between Kiwaidae and other chirostyloids, whether the age for this fossil is likely to be a stem-lineage kiwaid or chirostyloid. Three other fossils were identified as calibration points on the basis of being the earliest representative at a particular taxonomical level for that node.

(1) *Platykotta akaina* (Platykottidae) of Norian–Rhaetian age, 199.6–216.5 Ma. Earliest appearance of an anomuran in the fossil record [27].
(2) *Juracrista perculta* (Munididae) of Tithonian age, 145.5–150.8 Ma. Earliest appearance of Munididae in the fossil record [28].
(3) *Protaegla miniscula* (Aeglidae) of Albian age, 99.6–112 Ma. Earliest appearance of Aeglidae in the fossil record [29].

For details regarding the dating scheme and the dating priors in the Beast analyses, see the electronic supplementary material.

3. Results

(a) Data summary and partitions

Of the 23 sequence sets produced, 16 were complete, five were missing a single gene fragment and two (*U. grandirostris* and *Calinectes sapidus*) were missing two gene fragments (see the electronic supplementary material, table S1). A total of 124 new DNA sequences were obtained and 95.7 per cent of the genes were successfully sequenced. Following PartitionFinder, the optimal partition scheme was a nine-partition dataset, with the three ribosomal genes treated separately and the six protein-coding genes split three ways into first, second and third codon positions.

(b) Phylogenetic analyses

Both the ML and BI analyses yielded identical tree topologies (figure 3). In general, node support was stronger in the BI analyses than in ML analyses, with posterior probabilities of greater than or equal to 0.97 for all nodes. In the ML analyses, 13 of the 20 nodes had bootstrap values greater than or equal to 99 per cent. The weakest bootstrap support was recorded for the clade comprising *Chirostylus* and four species of *Uroptychus* (68%). In general, weaker ML bootstrap support values compared with BI posterior probabilities are expected according to comparisons with simulated data [30].

The key features of the tree topology generated in this study are the monophyly of Aegloidea–Lomisoidea–Chirostyloidea, the monophyly of Chirostyloidea and, within it, the monophyly of Kiwaidae–Chirostylidae (figure 3). ML support for the Kiwaidae–Chirostylidae clade is not especially strong (77%), but the BI posterior probability was 1.00, and Bayesian topology hypotheses tests using the stepping-stone method supported this clade over Kiwaidae–Eumunididae (by 17.35 mean log likelihood units) and over Eumunididae–Chirostylidae (23.59 mean log likelihood units; electronic supplementary material, table S4).

Within Chirostylidae, the basal split is between *Gastroptychus* s.s, represented here by *G. formosus* and *G. rogeri*, and the remaining chirostylid taxa, including the second group of *Gastroptychus*, represented by *Gastroptychus* sp. 3804. *Gastroptychus*, as currently defined, is therefore not monophyletic. Likewise, the monophyly

Uroptychus is not supported in this study. *Uroptychus scambus* resides outside a clade comprising the other *Uroptychus* species, *Chirostylus* aff. *stellaris*, *Gastroptychus* sp. 3804 and *U. grandirostris*. The location of *U. grandirostris* in the tree also renders the larger *Uroptychus* group paraphyletic (figure 3). All four species of *Kiwa* cluster together in this study, supporting the monophyly of Kiwaidae. There is a basal split between the seep-endemic *K. puravida* and a vent-endemic clade comprising *K. hirsuta* and the ESR and SWIR *Kiwa* species (figure 3).

(c) Divergence time analyses

For ease of reporting, the median estimated divergence date is given, with the 95 per cent higher posterior density date range in parentheses. According to this study, Chirostyloidea split from sister taxa at 123.4 Ma (111.4–137.5 Ma). The divergences of the chirostyloid families occurred soon afterwards; Eumunididae split off at 114.8 Ma (101.3–129.5 Ma) and the split between Kiwaidae and Chirostylidae occurred at 106.4 Ma (92.8–121.1 Ma). Within Chirostylidae, the basal split between the *Gastroptychus* s.s clade and the other clades occurred at 73.5 Ma (61.2–87.2 Ma). The remaining clade radiated at 38.4 Ma (30.7–47.2 Ma). Extant Kiwaidae radiated at 30.6 Ma (22.7–39.3 Ma), with the split between the Pacific and non-Pacific lineages occurring at 19.1 Ma (13.4–25.9 Ma). The divergence between ESR and SWIR kiwaids was at 1.5 Ma (0.6–2.6 Ma).

4. Discussion

(a) Phylogeny of Chirostyloidea

The higher-level phylogenetic patterns presented here are consistent with previous trees [5,6]. The monophyly of Aegloidea–Lomisoidea–Chirostyloidea supports the suggestion by Ahyong *et al*. [4] that, given the present-day locations of chirostyloids, aegloids and lomisoids (along with the fossil locations of aegloids and *Pristinaspina gelasina*), they all originated in the Pacific. Despite the shared characters between Eumunididae and Kiwaidae mentioned earlier, the monophyly of Kiwaidae–Chirostylidae is conceivable given their shared production of large eggs with highly abbreviated larval development, indicative of lecithotrophy [11,31]. In hydrothermal vent-endemic invertebrates, as well as in squat lobsters in general, mode of larval dispersal appears to be largely taxonomically constrained, rather than determined by habitat [32,33]. This accounts for the many dispersal strategies exhibited by vent-endemic fauna, despite being faced with the same challenges of dispersal from one 'island' to another [33]. Within Chirostylidae, the polyphyly of *Gastroptychus* and *Uroptychus* echoes the findings of Schnabel *et al*. [6], and this discrepancy between morphological taxonomy and molecular phylogenetics will have to be explored in more detail in the future.

The kiwaid phylogeny produced in this study has implications for our understanding of this family's evolutionary history, as well as the evolution of megafauna in chemosynthetic ecosystems in general. The Pacific location of the two basal kiwaids is consistent with a Pacific origin, as previously suggested [4], with a subsequent migration into the Atlantic sector of the Southern Ocean via the Drake Passage and then on to the Indian Ocean (figures 2 and 3). The alternative scenario—that Kiwaidae spread west from the Pacific into the Indian Ocean, and finally to Atlantic Sector of the Southern Ocean—seems unlikely as prevailing currents in the Southern Hemisphere are easterly and kiwaids are apparently absent further east in the Indian Ocean at the Central Indian Ridge. However, the basal split between a Northern Hemisphere kiwaid (*K. puravida*) and the Southern Hemisphere kiwaids, and the Alaskan location for the possible stem-lineage kiwaid fossil *Pristinaspina gelasina*, suggests a North Pacific origin for the family rather than the southern one previously proposed [4]. The tree topology revealed in this study also suggests that the body form with elongated chelae is most likely to be the ancestral state for extant kiwaids, with a trend of decreasing proportional chela length from Pacific species to the Southern and Indian Ocean species.

A noteworthy aspect of the kiwaid tree topology is the basal split between the cold seep lineage and the deeper vent lineages, consistent with the hypothesis that some fauna endemic to deep-sea hydrothermal vents evolved from ancestors that inhabited shallower, more temporally stable and less thermally extreme cold seeps on continental slopes [34]. Molecular phylogenetics shows some limited support for this hypothesis, at least with vestimentiferan tubeworms and mytilid mussels, where seep-endemic species generally fall out basally to the vent clades, as would be expected if vent fauna evolved from seep inhabitants [35,36]. The Pacific location for the seep-endemic *K. puravida* and the vent-endemic *K. hirsuta* suggests this seep-to-vent transition may have occurred along the eastern Pacific plate boundaries. The discovery of more extant kiwaid species, as well as fossils, may help to confirm this in the future. This seep-to-vent trajectory is part of a wider pattern seen in the fossil record whereby coastal lineages have subsequently radiated into offshore, deeper habitats, often with the eventual loss of their shallower relatives [37].

(b) Coenozoic radiations in Chirostyloidea

The Mid-Cretaceous origins (no later than 101.3 Ma) for the chirostyloid families (figure 4) indicate that *Pristinaspina gelasina* (65.5–99.6 Ma) cannot be a stem-lineage chirostyloid. These results are therefore consistent with the suggestion by Ahyong *et al*. [4] that this fossil is a stem-lineage kiwaid, based on its distinctive carapace markings (figure 1), although the possibility of it being a stem-lineage chirostylid–kiwaid cannot be completely ruled out as Kiwaidae and Chirostylidae diverged in 92.8–121.1 Ma. The dates for the formation of the three families are concomitant with a wider global pattern of decapod radiations that occurred during the Late Jurassic and Mid-to-Late Cretaceous, when eustatic sea levels were higher than they are today and there was an expansion of shallow, productive seas [38]. However, with the exception of the split between the *Gastroptychus* s.s clade and the remaining Chirostylidae, the radiations within Kiwaidae and Chirostylidae occur well into the Coenozoic, long after these two families diverged from one another. This pattern is consistent with limited fossil evidence suggesting the end of the Cretaceous was marked by the extinction of many decapod genera, but not families [39], which survived to the Coenozoic and subsequently re-radiated. The time frame for these radiations reported here coincides with a general intensification of global ocean circulation and possible deep-water ventilation from the Late Eocene/Oligocene onwards, following a warmer episode in the deep sea at the Palaeocene/Eocene boundary [40], perhaps allowing the exploitation of new niches in the deep sea.

The Coenozoic radiation of Kiwaidae augments the ever-expanding list of vent- and seep-endemic fauna that are now

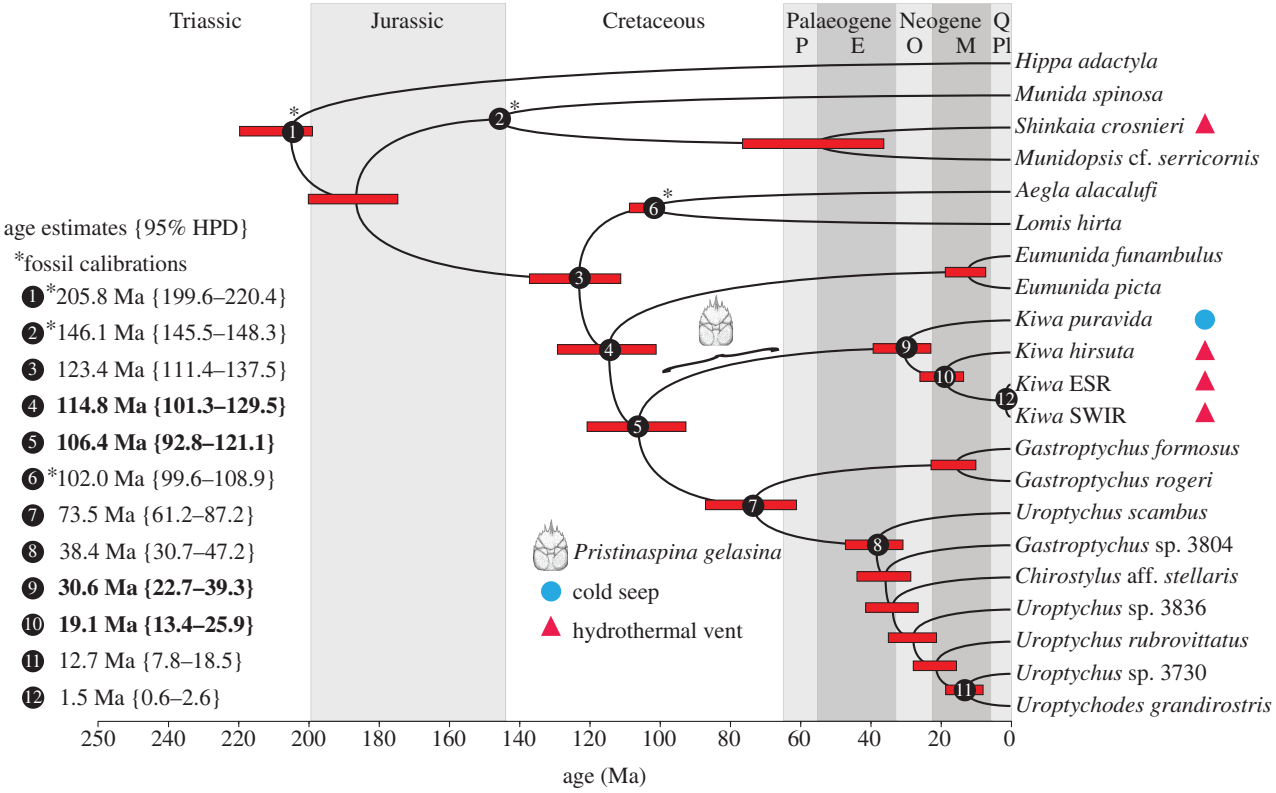

Figure 4. Divergence time estimates for the nine-gene concatenated dataset with nine partitions as calculated with a relaxed lognormal clock on BEAST v. 1.7.4. Node bars represent the 95% highest posterior density (HPD) interval for nodal age. Numbered nodes show dates of interest to this study and quoted age values show median age estimates followed by the 95% HPD ranges in parentheses. Dates highlighted in bold are of particular interest. Nodes marked with an asterisk are fossil calibrated. Carapace illustration of the fossil *Pristinaspina gelasina* shows the date range for the fossil. Geological periods are shown at the top, with recent epochs represented as letters: P, Palaeocene; E, Eocene; O, Oligocene; M, Miocene; Pl, Plio-Pleistocene. Q, Quaternary. (Online version in colour.)

known to have recently evolved, rather than being considered 'living fossils' from the Mesozoic or Palaeozoic [41]. A comprehensive appraisal of the estimated radiation dates for vent and seep taxa suggests that most of them radiated after the Palaeocene/Eocene Thermal Maximum, a warm episode in the deep sea that may have resulted in widespread anoxia/dysoxia [42]. The results therefore reinforce the idea that chemosynthetic fauna may be vulnerable to reduction in oxygen levels in the deep sea as a result of changes to climate and ocean circulation, because they must occupy narrow redox zones at the limit of their physiological tolerance [42]. The fact that Kiwaidae radiated (or re-radiated) recently is reflected by their association with ectosymbiont bacteria, which, in terms of host–symbiont relationships, may be an early evolutionary step towards more intimate symbiotic associations with bacteria [43] (e.g. the housing of chemosynthetic symbionts in specialized internal organs [13]). It is notable that other decapods associated with ectosymbionts, the galatheoid squat lobster genus *Shinkaia* and the shrimp family Bresiliidae, may also have Coenozoic origins, based on fossil and molecular evidence respectively [44,45].

(c) Vicariance in vent-endemic Kiwaidae

Vent-endemic fauna maintain populations along ridges by broadcasting their larvae from vent field to vent field. Species ranges are determined by factors such as larval longevity, current direction and strength distance between vent fields, shelf and ridge topography, and vent field longevity [46]. In general, vent community similarity is determined by along-ridge axis distance between vents rather than the shortest distance along the seafloor [47], because bottom currents are often rectified by ridge topography, thus entraining larvae along ridge axes [46]. In some cases, consequently, the biogeography of hydrothermal vent-endemic fauna can be understood in terms of vicariance caused by past changes in mid-ocean ridge position [48]. Such events may also be responsible for the divergence of vent-endemic Kiwaidae, but explaining present-day biogeographic patterns can be problematic, as tectonic and oceanographic reconstructions become more uncertain with distance into the past.

A key question in the biogeography of Kiwaidae is how they managed to spread from vents in the Pacific to those on the ESR and SWIR. The known present-day locations of Kiwaidae (figure 2) in combination with the phylogeny present here suggest that they entered the Atlantic sector of the Southern Ocean from the Pacific via the Drake Passage. The estimated date range for the split between the Pacific and non-Pacific lineages (13.4–25.9 Ma) is compatible with this scenario, as the deep-water connection in the Drake Passage probably occurred around 33 Ma [49].

Today, the ESR is isolated from the Pacific ridge systems and the means by which kiwaids arrived from the Pacific into the Scotia Sea is not readily apparent. However, at approximately 20 Ma, there was a nearly continuous chain of ridge segments from the Pacific into the widening Scotia Sea via the Chile Rise, Antarctic–Phoenix Ridge and the West Scotia Ridge (WSR) [49] (figure 5*d*). The ESR was forming by approximately 15 Ma [51] at the eastern end of the WSR and by 12 Ma the subducting Chile Rise had left a gap of

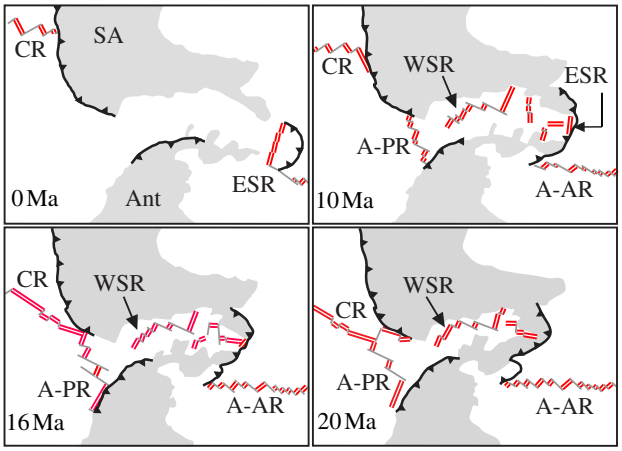

Figure 5. Diagram representing the evolution of ridge positions in the Drake Passage relevant to the divergence of Pacific and non-Pacific kiwaids during the Oligocene and Miocene, modified from Vérard *et al.* [49] and Breitsprecher & Thorkelson [50]. Grey areas represent non-oceanic plate regions. Double lines denote active spreading segments of the ridges. Grey lines represent faults and fracture zones. Solid black lines with triangles denote subduction zones. SA, South America; Ant, Antarctica; CR, Chile Rise; ESR, East Scotia Ridge; A-PR, Antarctic–Phoenix Ridge; WSR, West Scotia Ridge; A-AR, American–Antarctic Ridge. (Online version in colour.)

approximately1000 km between the Pacific Ridges and the WSR–ESR system [49,50] (figure 5*b–d*). This subduction under the South American plate, starting at approximately 16 Ma, coincides with the most recent divergence date estimate for the Pacific and non-Pacific kiwaids (13.4 Ma). This event is not the only candidate, however. On the Chile Rise at approximately 28–26 Ma, there was a nearly 90° realignment in the axis of spreading on the Chile Rise, resulting in the formation and subsequent expansion of large fracture zones [52], which could have isolated vent fauna on the Pacific–Antarctic Ridge from Chile Rise populations. The oldest possible inferred divergence date of 25.9 Ma (figure 4) is close enough to this event for it to be worth considering as a cause of the divergence we see today. Discovering kiwaids on the as-yet-unexplored Chile Rise may resolve this question.

The divergence between the ESR and SWIR kiwaids is very recent compared with the other kiwaids (as recently as 0.6 Ma). During this time, there have been no major changes in ridge configuration between the ESR and SWIR to easily account for such a divergence [53,54]. One possibility is that there has been a recent drop in the number of hydrothermal vent fields along portions of the intervening ridges, which would have reduced the dispersal capability of vent fauna by effectively increasing the distance between adjacent vent fields, leading to isolation and subsequent divergence. Alternatively, changes in current regime may be responsible; large portions of the intervening ridge segments between the ESR and the SWIR are bathed by the Antarctic Circumpolar Current (ACC), which is the dominant force in determining the dispersal direction of larvae throughout the Southern Ocean [55]. Changes to the ACC could have affected the dispersal range of *Kiwa* larvae, and in particular their ability to traverse large potential barriers to gene flow, such as the Andrew Bain Fracture Zone (ABFZ) [56], which effectively splits the SWIR into a lower and an upper portion (figure 2).

Today, the Subantarctic Front and Polar Front of the ACC cut across the ABFZ [57], potentially isolating vent fauna on either side. Changes in the intensity and latitude of the ACC fronts during the Mid-Pleistocene Transition, which occurred between approximately 1.2 Ma and 650 ka, could have transported *Kiwa* larvae across the ABFZ to regions that are now isolated. During this episode, orbitally forced glacial cycles switched in periodicity from 41 to 100 kyr cycles, resulting in colder, extended glacial conditions and northerly shifts in the ACC polar front in the South Atlantic far beyond the northerly extent of recent glacial front migrations [58]. Sediment analyses off the Antarctic Peninsula indicate that there has been a decline in ACC strength since approximately 2.5 Ma [59], which might have cut off the supply of *Kiwa* larvae across fracture zones such as the ABFZ at some point. Exploration of the American–Antarctic Ridge and lower reaches of the SWIR around the Bouvet Triple Junction may elucidate present-day barriers to gene flow between the ESR and SWIR kiwaids, and help in the inference of past changes responsible for their divergence. The investigation of vent fields east of Dragon will aid in determining the extent of this genus on the SWIR, but at a wider scale the discovery of vent communities along the Southeast Indian Ridge and along the Pacific–Antarctic Ridge will help reveal the global extent of vent-endemic Kiwaidae.

5. Conclusion

The nine-gene dataset featured in this study has revealed, in accordance with previous work, that Chirostyloidea are monophyletic. However, in contrast to earlier studies, our results suggest the monophyly of Kiwaidae–Chirostylidae, which is supported morphologically by their similar larvae. Within Chirostylidae, *Uroptychus* and *Gastroptychus* are polyphyletic and need taxonomic re-examination. All three families appear to have Mid-Cretaceous origins, although kiwaids and some chirostylids radiated after the Late Eocene. The basal split in Kiwaidae between the seep-endemic *K. puravida* and a vent-endemic clade is consistent with the seep-to-vent hypothesis, although more evidence is needed to determine this. The vent clade then probably spread via mid-ocean ridges from the East Pacific, through the Drake Passage to the ESR and SWIR within the last 25.9 million years. Similar to many other chemosynthetic taxa, the Coenozoic radiation of Kiwaidae may indicate an inherent vulnerability of chemosynthetic fauna to climatic changes affecting the availability of oxygen in the deep sea, with consequences for their future conservation.

Acknowledgements. We would like to thank Kareen Schnabel (National Institute of Water and Atmospheric Research, New Zealand), Enrique Macpherson (Centro de Estudios Avanzados de Blanes), Tin-Yam Chan (National Taiwan University), Cheryl Morrison (US Geological Survey, Leetown Science Center), Sammy De Grave (Oxford University Museum of Natural History) and Andrew Thurber (Oregon State University) for generously donating tissue for this study. Additional thanks go to Kareen Schnabel, Andrew Thurber, Enrique Macpherson and Heather Bracken-Grissom (Florida International University) for advice and encouragement. Thanks go to the masters and crews of the RRS *James Cook*, and the technical crews of ROV *ISIS* and *KIEL 6000* for collecting squat lobsters from vents and seamounts in the most challenging conditions.

Funding statement. Fieldwork and analyses were funded by NERC Consortium Grant NE/DO1249X/1, NERC Grant NE/F005504/1, Biogeography and Ecology of the First Known Deep-Sea Hydrothermal Vent Site on the Ultraslow-Spreading SWIR NE/H012087/1 and NERC PhD studentship NE/D01429X/1 (C.N.R., J.T.C., K.T.L., P.A.T. and A.D.R.).

References

1. Ahyong ST, Baba K, MacPherson E, Poore G. 2010 A new classification of the Galatheoidea (Crustacea: Decapoda: Anomura). *Zootaxa* **2676**, 57–68.
2. Macpherson E, Jones W, Segonzac M. 2005 A new squat lobster family of Galatheoidea (Crustacea, Decapoda, Anomura) from the hydrothermal vents of the Pacific-Antarctic Ridge. *Zoosystema* **27**, 709–723.
3. Schnabel KE, Ahyong S. 2011 A new classification of the Chirostyloidea (Crustacea: Decapoda: Anomura). *Zootaxa* **2687**, 56–64.
4. Ahyong ST, Schnabel KE, Macpherson E. 2011 Phylogeny and fossil record of marine squat lobsters. *Biol. Squat Lobsters* **20**, 73–104.
5. Tsang LM, Chan T-Y, Ahyong ST, Chu KH. 2011 Hermit to king, or hermit to all: multiple transitions to crab-like forms from hermit crab ancestors. *Syst. Biol.* **60**, 616–629. (doi:10.1093/sysbio/syr063)
6. Schnabel KE, Ahyong S, Maas E. 2011 Galatheoidea is not monophyletic: molecular and morphological phylogeny of the squat lobsters (Decapoda: Anomura) with recognition of a new superfamily. *Mol. Phylogenet. Evol.* **58**, 157–168. (doi:10.1016/j.ympev.2010.11.011)
7. Baba K. 2005 Deep-sea chirostylid and galatheid crustaceans Decapoda: Anomura from the Indo-Pacific, with a list of species. *Galathea Rep.* **20**, 315–317.
8. Baba K, Haig J. 1990 A new species of chirostylid crustacean (Decapoda: Anomura) from off the West Coast of North America. *Proc. Biol. Soc. Wash.* **103**, 854–860.
9. Poore GCB, Andreakis N. 2011 Morphological, molecular and biogeographic evidence support two new species in the *Uroptychus naso* complex (Crustacea: Decapoda: Chirostylidae). *Mol. Phylogenet. Evol.* **60**, 152–169. (doi:10.1016/j.ympev.2011.03.032)
10. Schweitzer CE, Feldmann RM. 2000 First notice of the Chirostylidae (Decapoda) in the fossil record and new Tertiary Galatheidae (Decapoda) from the Americas. *Bull. Mizunami Fossil Museum* **27**, 147–165.
11. Thurber AR, Jones WJ, Schnabel K. 2011 Dancing for food in the deep sea: bacterial farming by a new species of yeti crab. *PLoS ONE* **6**, e26243. (doi:10.1371/journal.pone.0026243)
12. Lowman P, Masuoka P, Montgomery B, OLeary J, Salisbury D, Yates J. 1999 A digital tectonic activity map of the Earth. See http://denali.gsfc.nasa.gov/dtam/gtam.
13. Goffredi SK. 2010 Indigenous ectosymbiotic bacteria associated with diverse hydrothermal vent invertebrates. *Environ. Microbiol. Rep.* **2**, 479–488. (doi:10.1111/j.1758-2229.2010.00136.x)
14. Rogers AD *et al*. 2012 The discovery of new deep-sea hydrothermal vent communities in the southern ocean and implications for biogeography. *PLoS Biol.* **10**, e1001234. (doi:10.1371/journal.pbio.1001234)
15. Copley JT. 2011 RRS James Cook Cruise JC067. Cruise Report JC066 (JC067). See https://www.bodc.ac.uk/data/information_and_inventories/cruise_inventory/report/10593.
16. Doyle JJ, Dickson EE. 1987 Preservation of plant samples for DNA restriction endonuclease analysis. *Taxon* **36**, 715–722. (doi:10.2307/1221122)
17. Drummond A, Ashton B, Cheung M, Heled J, Kearse M, Moir R. 2010 *Geneious Pro*. See http://www.geneious.com.
18. Katoh K, Asimenos G, Toh H. 2009 Multiple alignment of DNA sequences with MAFFT. *Methods Mol. Biol.* **537**, 39–64. (doi:10.1007/978-1-59745-251-9_3)
19. Castresana J. 2000 Selection of conserved blocks from multiple alignments for their use in phylogenetic analysis. *Mol. Biol. Evol.* **17**, 540–552. (doi:10.1093/oxfordjournals.molbev.a026334)
20. Simmons MP, Ochoterena H. 2000 Gaps as characters in sequence-based phylogenetic analyses. *Syst. Biol.* **49**, 369–381. (doi:10.1093/sysbio/49.2.369)
21. Lanfear R, Calcott B, Ho SYW, Guindon S. 2012 PartitionFinder: combined selection of partitioning schemes and substitution models for phylogenetic analyses. *Mol. Biol. Evol.* **29**, 1695–1701. (doi:10.1093/molbev/mss020)
22. Zwickl DJ. 2006 Genetic algorithm approaches for the phylogenetic analysis of large biological sequence datasets under the maximum likelihood criterion. Doctoral thesis, University of Texas at Austin, USA.
23. Ronquist F, Huelsenbeck JP. 2003 MrBayes 3: Bayesian inference under mixed models. *Bioinformatics* **19**, 1572–1574.
24. Rambaut A, Drummond A. 2007 Tracer v. 1. 4. See http://beast.bio.ed.ac.uk/Tracer.
25. Ronquist F *et al*. 2012 MrBayes 3.2: efficient Bayesian phylogenetic inference and model choice across a large model space. *Syst. Biol.* 61, 539–542. (doi:10.1093/sysbio/sys029)
26. Drummond A, Rambaut A. 2007 BEAST: Bayesian evolutionary analysis by sampling trees. *BMC Evol. Biol.* **7**, 214. (doi:10.1186/1471-2148-7-214)
27. Chablais J, Feldmann R, Schweitzer C. 2011 A new Triassic decapod, *Platykotta akaina*, from the Arabian shelf of the northern United Arab Emirates: earliest occurrence of the Anomura. *Paläontologische Zeitschrift* **85**, 93–102. (doi:10.1007/s12542-010-0080-y)
28. Robins CM, Feldmann RM, Schweitzer CE. 2012 The oldest Munididae (Decapoda: Anomura: Galatheoidea) from Ernstbrunn, Austria (Tithonian). *Annalen des Naturhistorischen Museums Wien A* **114**, 289–300.
29. Feldmann RM, Vega FJ, Applegate SP, Bishop GA. 1998 Early Cretaceous arthropods from the Tlayua Formation at Tepexi de Rodriguez, Puebla, Mexico. *J. Paleontol.* **72**, 79–90.
30. Erixon P, Svennblad B, Britton T, Oxelman B. 2003 Reliability of Bayesian posterior probabilities and bootstrap frequencies in phylogenetics. *Syst. Biol.* **52**, 665–673. (doi:10.1080/10635150390235485)
31. Clark PF, Ng PKL. 2008 The lecithotrophic zoea of *Chirostylus ortmanni* Miyake and Baba, 1968 (Crustacea: Anomura: Galatheoidea: Chirostylidae) described from laboratory hatched material. *Raffles Bull. Zool.* **56**, 85–94.
32. Van Dover CL, Williams AB. 1991 Egg size in squat lobsters (Galatheoidea): constraints and freedom. *Crustacean* **7**, 143–156.
33. Tyler PA, Young C. 1999 Reproduction and dispersal at vents and cold seeps. *J. Mar. Biol. Assoc. UK* **79**, 193–208. (doi:10.1017/S0025315499000235)
34. Hecker B. 1985 Fauna from a cold sulfur-seep in the Gulf of Mexico: comparison with hydrothermal vent communities and evolutionary implications. *Bull. Biol. Soc. Wash.* **1985**, 465–473.
35. Halanych KM. 2005 Molecular phylogeny of siboglinid annelids (a.k.a. pogonophorans): a review. *Hydrobiologia* **535**, 297–307. (doi:10.1007/s10750-004-1437-6)
36. Jones WJ, Won Y, Maas P, Smith P, Lutz R, Vrijenhoek R. 2006 Evolution of habitat use by deep-sea mussels. *Mar. Biol.* **148**, 841–851. (doi:10.1007/s00227-005-0115-1)
37. Sepkoski Jr JJ. 1991 A model of onshore–offshore change in faunal diversity. *Paleobiology* **17**, 58–77.
38. Klompmaker AA. 2012 Mesozoic Decapod diversity with an emphasis on the Early Cretaceous (Albian) of Spain. Doctoral thesis, Kent State University, USA.
39. Feldmann RM, Schweitzer CE. 2006 Paleobiogeography of Southern Hemisphere decapod crustacea. *J. Paleontol.* **80**, 83–103. (doi:10.1666/0022-3360(2006)080[0083:POSHDC]2.0.CO;2)
40. McClain CR, Hardy SM. 2010 The dynamics of biogeographic ranges in the deep sea. *Proc. R. Soc. B* **277**, 3533–3546. (doi:10.1098/rspb.2010.1057)
41. Little CTS, Vrijenhoek RC. 2003 Are hydrothermal vent animals living fossils?. *Trends Ecol. Evol.* **18**, 582–588. (doi:10.1016/j.tree.2003.08.009)
42. Vrijenhoek RC. In press. On the instability and evolutionary age of deep-sea chemosynthetic communities. *Deep Sea Res. Part II: Top. Stud. Oceanogr*. (doi:10.1016/j.dsr2.2012.12.004)
43. Smith DC. 1979 From extracellular to intracellular: the establishment of a symbiosis. *Proc. R. Soc. B* **204**, 115–130. (doi:10.1098/rspb.1979.0017)
44. Schweitzer CE, Feldmann RM. 2008 New Eocene hydrocarbon seep decapod crustacean (anomura: galatheidae: shinkaiinae) and its paleobiology. *J. Paleontol.* **82**, 1021–1029. (doi:10.1666/08-007.1)
45. Shank TM, Black MB, Halanych KM, Lutz RA, Vrijenhoek RC. 1999 Miocene radiation of deep-sea hydrothermal vent shrimp (Caridea: Bresiliidae): evidence from mitochondrial cytochrome oxidase subunit I. *Mol. Phylogenet. Evol.* **13**, 244–254. (doi:10.1006/mpev.1999.0642)

46. Vrijenhoek RC. 2010 Genetic diversity and connectivity of deep-sea hydrothermal vent metapopulations. *Mol. Ecol.* **19**, 4391–4411. (doi:10.1111/j.1365-294X.2010.04789.x)
47. Tunnicliffe V, Fowler CMR. 1996 Influence of sea-floor spreading on the global hydrothermal vent fauna. *Nature* **379**, 531–533. (doi:10.1038/379531a0)
48. Tunnicliffe V, McArthur A, McHugh D. 1998 A biogeographical perspective of the deep-sea hydrothermal vent fauna. *Adv. Mar. Biol.* **34**, 353–442. (doi:10.1016/S0065-2881(08)60213-8)
49. Vérard C, Flores K, Stampfli G. 2012 Geodynamic reconstructions of the South America-Antarctica plate system. *J. Geodyn.* **53**, 43–60. (doi:10.1016/j.jog.2011.07.007)
50. Breitsprecher K, Thorkelson DJ. 2009 Neogene kinematic history of Nazca–Antarctic–Phoenix slab windows beneath Patagonia and the Antarctic Peninsula. *Tectonophysics* **464**, 10–20. (doi:10.1016/j.tecto.2008.02.013)
51. Livermore R. 2003 Back-arc spreading and mantle flow in the East Scotia Sea. *Geol. Soc. Lond. Spec. Publ.* **219**, 315–331. (doi:10.1144/GSL.SP.2003.219.01.15)
52. Tebbens S, Cande S. 1997 Southeast Pacific tectonic evolution from Early Oligocene. *J. Geophys. Res.* **102**, 12 061–12 084. (doi:10.1029/96JB02582)
53. Sauter D, Cannat M. 2010 The ultraslow-spreading Southwest Indian Ridge. In *Diversity of hydrothermal systems on slow-spreading ocean ridges*, pp. 153–173. Washington, DC: American Geophysical Union.
54. Schreider A, Schreider AA, Bulychev A, Galindo-Zaldivar J, Maldonado A, Kashintsev G. 2006 Geochronology of the American-Antarctic Ridge. *Oceanology* **46**, 114–122. (doi:10.1134/S0001437006010139)
55. Rogers AD. 2007 Evolution and biodiversity of Antarctic organisms: a molecular perspective. *Phil. Trans. R. Soc. B* **362**, 2191–2214. (doi:10.1098/rstb.2006.1948)
56. Sclater JG, Grindlay NR, Madsen JA, Rommevaux-Jestin C. 2005 Tectonic interpretation of the Andrew Bain transform fault: Southwest Indian Ocean. *Geochem. Geophys. Geosyst.* **6**, Q09K10. (doi:10.1029/2005GC000951)
57. Orsi AH, Whitworth T, Nowlin WD. 1995 On the meridional extent and fronts of the Antarctic Circumpolar Current. *Deep Sea Res. Part I: Oceanogr. Res. Pap.* **42**, 641–673. (doi:10.1016/0967-0637(95)00021-W)
58. Diekmann B, Kuhn G. 2002 Sedimentary record of the Mid-Pleistocene climate transition in the southeastern South Atlantic (ODP Site 1090). *Palaeogeogr. Palaeoclimatol. Palaeoecol.* **182**, 241–258. (doi:10.1016/S0031-0182(01)00498-9)
59. Hassold NJC, Rea DK, van der Pluijm BA, Parés JM. 2009 A physical record of the Antarctic Circumpolar Current: Late Miocene to recent slowing of abyssal circulation. *Palaeogeogr. Palaeoclimatol. Palaeoecol.* **275**, 28–36. (doi:10.1016/j.palaeo.2009.01.011)